W-PM-E7

TWO-DIMENSIONAL STRUCTURE OF THE *NEUROSPORA CRASSA* PLASMA MEMBRANE H^+-ATPASE AS DETERMINED BY ELECTRON CRYO-MICROSCOPY. ((M. Cyrklaff[1], M. Auer[1], W. Kühlbrandt[1], and G. A. Scarborough[2])) [1]European Molecular Biology Laboratory, Heidelberg, Germany, and [2]University of North Carolina, Chapel Hill, NC, 27599.

Large, well-ordered two-dimensional crystals of the dodecylmaltoside complex of the *Neurospora crassa* plasma membrane H^+-ATPase grow rapidly on the surface of a polyethylene glycol-containing mixture similar to that originally developed for growing three-dimensional crystals of this integral membrane transport protein. Negative stain electron microscopy of the crystals shows that many are single layers. Cryoelectron microscopy of unstained specimens indicates that the crystals have a hexagonal layer group (p6) with unit cell dimensions of a=b=167 Å. Image processing of selected electron micrographs has yielded a projection map at 10.3 Å resolution. The repeating unit of the ATPase crystals comprises six 100 kDa ATPase monomers arranged in a symmetrical ring. The individual monomers in projection are shaped like a boot. These results provide the first indications of the molecular structure of the H^+-ATPase molecule. They also establish the feasibility of precipitant-induced surface growth as a rapid, simple, alternative to conventional methods for obtaining two-dimensional crystals of integral membrane proteins.

W-PM-E8

MODELING THE MEMBRANE DOMAINS OF ION-TRANSPORTING ATPases. ((K.B. Munson and G. Sachs)) UCLA Department of Medicine, VMAC/ West L.A., L.A., CA. 90073.

We have built molecular models for the membrane domains of the catalytic polypeptides from several phosphorylating (P-type) ion-transporting ATPases. The purpose is to identify residues that may affect ion binding and inhibitor specificity. The models include only the first six transmembrane segments and their connecting loops (M1/M2, M3/M4, M5/M6) for two reasons; first, because several members of the class terminate after M6 and second, because the sites for specific inhibitors are known to be luminally exposed. A novel procedure was used to build the models. Multiple alignments using more than 20 sequences were constructed for the regions around each membrane pair and the species with the shortest loops identified. Their canonical nature allowed modeling the 'minimal loops' from similar helix-loop-helix structures found in the Brookhaven Data Base (transmembrane segments were assumed to be helical). Thus the short loops identified the helix orientations for each membrane pair in the P-type family (a 'homology modeling' assumption borne out by the alignments). Two models were built based on these results, K-ATPase of S. feacalis and hog gastric HK-ATPase. Larger loops were inserted while maintaining helix orientations. Assembly of the transmembrane pairs was influenced by factors such as potential charge and hydrogen bond interactions and the apparent position of the lipid. Comparison of the models identifies potential ion binding sites and suggests a mode of inhibitor action for clinically important inhibitors of acid secretion.

W-PM-E9

THE MITOCHONDRIAL ATP SYNTHASE OF *TRYPANOSOMA BRUCEI*: REGULATION AND GENETIC MAPPING ((S.V. Brown, T.B. Chi, M. Tanaka, and N. Williams)) SUNY at Buffalo, Buffalo, NY 14214

The mitochondrial ATP synthase of the parasitic protozoan, *Trypanosoma brucei* has been the focus of study in this laboratory. The F_1 component has a typical $\alpha_3\beta_3\gamma\delta\epsilon$ structure with polypsptide molecular weights of 55, 42, 32, 22, and 17 kD. The F_0 has been less well characterized but appears to be comprised of at least 4-5 subunits. An endogenous inhibitor peptide has recently been shown to be associated with the complex. Regulation of the ATP synthase occurs on a number of levels. Both the F_1 and F_0 components are present at the highest levels in the procyclic [insect] stage of the *Trypanosoma brucei* which is most active in oxidative phosphorylation and at the lowest level in the early bloodstream form which is highly glycolytic. In contrast, the inhibitor peptide is at highest levels in the early bloodstream form and in the lowest levels in the procyclic stage. This suggests a tight regulation of the ATP synthase both in terms of the amount of enzyme present and in the activity that the enzyme may express in the cell. We are currently trying to determine whether regulation occurs at the level of transcription for several of the ATP synthase components [α, β, and the inhibitor peptide]. We are also mapping the genes for these proteins to the *Trypanosoma brucei* chromosomes to determine whether they are physically linked.

Ca^{2+} CHANNEL MODULATION

W-Pos1

CYCLIC AMP-MEDIATED PHOSPHORYLATION OF THE L-TYPE CALCIUM CHANNEL BETA-SUBUNIT IN INTACT MYOCARDIUM: ((H. Haase, P. Karczewski and E.G. Krause)) Max Delbrück Center for Molecular Medicine, 13122 Berlin, Germany. (Spon. by I. Morano)

Interaction between the α_1- and ß-subunits determines basic properties of L-type Ca^{2+} channels. We studied whether the ß-subunit undergoes cAMP-mediated phosphorylation in intact dog hearts and may thereby regulate channel activity. ß-subunits were phosphorylated in native membranes, solubilized, and subsequently immunoprecipitated with a polyclonal antibody generated against the deduced carboxy terminal sequence of the cardiac ß-subunit. In preparations from dog hearts which were depleted from endogenous catecholamines by reserpine treatment (0.5 mg/kg, 2 days), the cyclic AMP-dependent protein kinase induced substantial [$^{32}P_i$]-phosphate incorporation into the ß-subunit (0.7 mol P_i per mol dihydropyridine receptor). Using the back-phosphorylation technique (1), we found that in intact myocardium the ß-subunit was fully phosphorylated *in-vivo* in response to cAMP elevating agents (isoprenaline, 10 µg/kg; noradrenaline, 10µg/kg). Since the *in-vivo* phosphorylation is inversely related to the *in-vitro* [$^{32}P_i$]-incorporation, a close correlation was found among the rise in cAMP and ß-subunit phosphorylation as well as positive inotropic and chronotropic responses. We suggest that in canine myocardium phosphorylation of the Ca^{2+} channel ß-subunit is involved the cAMP-mediated control of channel opening.

(1) Mundina-Weilemann et al. (1991) J Biol Chem 266, 4067-4073.

W-Pos2

DIFFERENTIAL EFFECT OF BRAIN/CARDIAC BETA-SUBUNIT ($ß_{2a}$) ON CLONED FULL LENGTH CARDIAC ALPHA-SUBUNIT (α_{1C}) AND CARDIAC (α_{1C})-SKELETAL (α_{1S}) CHIMERIC ($\alpha_{1C[156-422S]}$) CALCIUM CHANNELS. (María Laura Messi, Murali Gopalakrishnan and Osvaldo Delbono). Bowman Gray School of Medicine. Wake Forest University, Dept. of Physiology and Internal Medicine, Winston-Salem, NC 27157.

A conserved motif in α_{1S}, α_{1A}, α_{1B} and α_{1C-a} I-II cytoplasmic linker plays an important role in channel modulation by the ß-subunit (Pragnell *et al.*, Nature 368: 67-70, 1994). Recent studies on cardiac (α_{1C}) and cardiac (α_{1C})-skeletal (α_{1S}) chimeric calcium channel construct suggest that changes in α_{1C} amino terminus and Domain I sequences modify the interaction with beta subunit ($ß_{2A}$) (Delbono *et al.*, Biophys. J. 66: A88, 1994). In this work, gating and ionic currents in *Xenopus* oocytes expressing cRNA encoding α_{1C} and $\alpha_{1C[156-422S]}$ alone or in association with $ß_{2a}$, were recorded. α_{1C} and $\alpha_{1C[156-422S]}$ share the same I-II linker. An small area of the oocytes were voltage-clamped at V_h=-90 mV and recorded in 10 mM Ba^{2+}. Gating currents were measured in a solution containing 2 mM $CoCl_2$. Oocytes were permeabilized with 0.1% saponin and equilibrated with 110 mM potassium glutamate. Maximal membrane conductance (G_{max}) in cardiac (α_{1C}) was increased five fold by coexpressing $ß_{2A}$. G_{max} (nS/nF) were 40±11 (n=17) and 207±24 (n=20), in α_{1C} and α_{1C} plus $ß_{2A}$, respectively. G_{max} (nS/nF) in $\alpha_{1C[156-422S]}$ alone and plus $ß_{2A}$ were 57±14 and 954±66 (n=15), respectively. Beta subunit promoted 15-16 fold increase in G_{max}. Maximum gating currents (Q_{max}) in α_{1C} were barely modified by $ß_{2A}$ coexpression (1.52±0.28 and 1.64±0.17 pC/nF, respectively, n= 12). Gating currents were undetectable in oocytes injectected with $\alpha_{1C[156-422S]}$ alone (n=10). When the chimeric α_1 was coinjected with $ß_{2A}$, Q_{max} (8.5 pC/nF) was five fold the maximum charge measured in α_{1C} plus $ß_{2A}$ (1.66±0.37, n=12). These results suggest that, in addition to I-II linker of α_1, Domain I plays an important role in the interaction with beta-subunit.

W-Pos3

β SUBUNIT COEXPRESSION INDUCES LONG CHANNEL OPENINGS IN THE α_{1C} CARDIAC CALCIUM CHANNEL. ((James Costantin[#], Ning Qin, Lutz Birnbaumer[#], Enrico Stefani[#], and Alan Neely*. Dept. of Anesthesiology[#], UCLA School of Medicine, Los Angeles CA 90024; Dept. of Physiology*, Texas Tech Univ. School of Medicine, Lubbock TX 79430))

Three gating modes have been reported for native cardiac calcium channels. These modes can be categorized as a low open probability (Po) mode (mode I), a higher Po mode (mode II), and null sweeps that contain no single channel openings (mode 0). We report here that the α_{1C} pore forming subunit, when expressed alone, is capable of gating in all three modes. Recordings were performed in cell attached mode with 80 mM Ba^{2+} and 10 μm (-)Bay K 8644 [10 uM] in the pipette. Mode 1 sweeps have a Po of less then 0.3 while mode 2 sweeps have a Po above 0.6. We found that mode I openings are not affected by the coexpression of the β subunit. Open time histograms, constructed from sweeps containing only mode I openings, can be fit by two exponentials with time constants near 1 and 3 ms, whether or not the β subunit is present. Coexpression of the β subunit does, however, affect mode II gating. When the β subunit is absent, the high Po mode is interrupted more frequently by channel closures. Open time histograms constructed from mode II sweeps without the β subunit can be fit with a third exponential centered near 10 ms. The α_1 subunit open time distributions, when coexpressed with the β subunit, can be fit by a third exponential centered near 20 ms. We conclude that coexpression of the β subunit affects mode II gating by increasing the number of long openings. We have also found that the β subunit causes the channel to remain in a particular mode for a longer period of time with less switching between modes. Supported by NIH grants AR 38970 to ES and AR 43411 to LB.

W-Pos4

THE AMINO TERMINUS OF A CALCIUM CHANNEL β SUBUNIT SETS RATES OF CHANNEL INACTIVATION INDEPENDENTLY OF THE SUBUNIT'S EFFECT ON ACTIVATION. ((Riccardo Olcese, Ning Qin, Toni Schneider[#], Alan Neely*, Xiangyang Wei[‡], Lutz Birnbaumer and Enrico Stefani. Dept. Anesthesiology, UCLA School of Medicine Los Angeles, CA, [#]Inst. Neurophysiology, Univ.of Cologne,Germany,*Texas Tech Univ. School of Medicine,Lubbock,TX,[‡]Center for Molecular Medicine, Medical College of Georgia,Augusta GE))

We recently reported that regulatory β subunit coexpressed with the pore forming cardiac Ca^{++} channel α_{1C} improves the coupling of voltage sensing to pore opening (Neely et al. Science 292:575-578,1993). Using the cut open oocyte voltage clamp technique (Taglialatela et al.,Biophys. J 61, 78-82,1992), we now studied the effect of type-1 and type-2 β subunits on both activation and inactivation of human E-type α1 calcium channel expressed in Xenopus oocytes. We found that the effect on the activation was practically identical for all the β subunits tested (β_{1a}, β_{1b}, β_{2a}, β_{2b}, β_3), resulting in ~ 80% increase of the low-voltage activated component of the G-V curves fitted with the sum of two Boltzmann distributions without significant changes in the effective valence (z ~3.5). The remaining small second component (z ~1.5) of the G-V curve was shifted to more negative potentials. Half activation ($V_{1/2}$) was 27.7 ± 8 mV more negative for the α_{1E} + β_{2a} compared to α_{1E} subunit expressed alone ($V_{1/2}$= 52.4 ± 3.3 mV (n=10)). On the other hand the same β subtypes affected the voltage dependent inactivation properties differently, even in opposite directions. Unsubtracted Ba^{2+} currents evoked at +20 mV were measured at the peak after a 10 s inactivating prepulses ranging from -120 to 27 mV and data were fitted with a Boltzmann distribution. $V_{1/2}$ inactivation were -35.4 ± 1.2 mV (n=5) for α_{1E} alone; -54.8 ± 0.8 mV (n=5) for α_{1E} + β_{1b}, -42.0 ± 3.6 mV (n=3) for α_{1E} + β_{1a}, -26.1 ± 1.1 mV (n=5) for α_{1E} + β_{2a}, -43.4 ± 2.0 mV (n= 6) for α_{1E} + β_{2a}, -52.4 ± 2.2 mV (n=3) for α_{1E} + β_3 N-terminal chimeras between β_{2a} and β_{1b}, having opposing effect on inactivation, resulted in the reciprocal transfer of their effects. $V_{1/2}$ inactivation was = -22.1 ± 2.2 mV (n=11) for the chimeric β_{1b} with N terminus of β_{2a} and -47.1 ± 2.2 mV (n = 4) for the reversed chimera. These results allow us to conclude that regulation of activation and inactivation are separable functions for which the N terminus of the β subunits is an important structural determinant. (Supported by NIH grants AR38970 and AR43195).

W-Pos5

CLONING AND FUNCTIONAL EXPRESSION OF A CALCIUM CHANNEL β SUBUNIT FROM *DROSOPHILA MELANOGASTER*. ((D. Ren, M. Chopra, C.T. Kousky and L.M. Hall)) Dept. of Biochemical Pharmacology, SUNY at Buffalo, Buffalo, NY 14260

In vertebrates, voltage-gated calcium channels are composed of α_1, α_2, β, γ and δ subunits. While the α_1 subunit is the main pore-forming peptide, other auxiliary subunits play important roles in the regulation of α_1. The β subunit is of special importance because its coexpression with α_1 subunits dramatically changes the biophysical properties of these channels. Despite the demonstrated *in vitro* importance of the β subunit, its *in vivo* role is little understood. As a first step toward a genetic dissection of the *in vivo* function of β subunits we cloned, sequenced and functionally expressed a cDNA encoding a β subunit from *Drosophila*. The gene encoding this subunit maps to the left arm of the second chromosome. The deduced amino acid sequence shows high similarity to the vertebrate counterparts and reveals two highly conserved domains likely to define functionally important regions. Alternative splicing occurs in at least three regions in this gene: the amino terminal, the middle region and the carboxy terminal. This alternative splicing in the *Drosophila* β subunit generates isoforms which have both domains (full length), the first domain only or the second domain only. Coexpression with a rabbit cardiac α_1 subunit in *Xenopus* oocytes shows that the full length β and some of the alternatively spliced truncated forms can stimulate the expressed current from a mammalian α_1 subunit. Supported by grants from NIH (HL39369) and Rhone Poulenc AG to L.M.H. and a Howard Hughes Predoctoral Fellowship to C.T.K.

W-Pos6

FUNCTIONAL STUDIES OF CALCIUM CHANNEL β-SUBUNIT BY ANTISENSE OLIGONUCLEOTIDE INJECTION IN CULTURED SENSORY NEURONES. ((V. Campbell, H.A. Pearson, N.S. Berrow, E.G. Fitzgerald, K. Brickley and A.C. Dolphin)) Department of Pharmacology, Royal Free Hospital School of Medicine, London, NW3 2PF, UK (Sponsor: D. Eisner).

The role of voltage-dependent calcium channel (VDCC) β-subunits has been examined in cultured rat dorsal root ganglion (DRG) neurones by depletion following microinjection of an antisense oligonucleotide. There was a marked reduction in whole cell I_{Ba} compared to nonsense-injected cells consistent with studies in which β-subunit has been co-expressed with VDCC α_1 subunits (Campbell *et al.*, J.Physiol. in press). Preliminary data indicate a reduction in density of L type single channels. Effects on N channels are currently under investigation. (-)-Baclofen inhibits I_{Ba} in these neurones via the G protein G_o.

A maximal concentration of (-)-baclofen (50 μM) produced a greater inhibition of the residual current in β-subunit depleted cells, of 44.4±5.0% (n=14) compared to 26.9±5.3% (n=12) in nonsense-injected and 27.9±5.1% (n=12) in control cells. A similar effect was observed with 100μM (-)-baclofen. There is no difference in the inhibition of whole cell I_{Ba} by ω-CTX GVIA between these three conditions.

A model is proposed whereby activated G_o-GTP competes either directly or indirectly for binding to VDCC α_1 subunits with VDCC β-subunits, and is thus more effective when the stoichiometry between the VDCC α_1 and β-subunits is altered by depletion of the β-subunit. We also propose that VDCCs normally act as GTPase activating proteins or GAPs but this is impaired following depletion of the β-subunit, since (1) depletion of β-subunit did not affect the maximum response to G-GTPγS; (2) an antibody to the β subunit inhibits the (-)-BayK8644 stimulated GTPase, thought to be due to interaction of G_o with L type VDCCs (Sweeney and Dolphin (1992) Febs.Letts 310, 66-70).

This work was supported by the Wellcome Trust.

W-Pos7

THE BENZOTHIAZEPINE BINDING DOMAIN OF L-TYPE CALCIUM CHANNELS: EVIDENCE FOR A LOCALIZATION ADJACENT TO THE DIHYDROPYRIDINE BINDING DOMAIN ((T. Brauns, J. Striessnig, H. Prinz*, Z.-W. Cai[+], S.D. Kimball[+], H.-C. Kang[§], R.P. Haugland[§], S. Berjukov, S. Hering, H. Glossmann)). *Institut für Biochemische Pharmakologie, Universität Innsbruck, Austria; *Max-Planck-Institut für Molekulare Physiologie, Dortmund, Germany; [+]Bristol-Myers Squibb Pharmaceutical Research Institute, Princeton, NJ; [§]Molecular Probes, Eugene, OR.*

We synthesized a new series of N-propylamino-substituted benzazepinone-analogues (NPSBs) that are potent blockers of L-type calcium channels (LTCCs) in intact muscle cells and bind to the benzothiazepinone (BTZ) binding domain of skeletal muscle calcium channels. In contrast to (+)-cis-diltiazem, their affinity increases upon channel purification. A fluorescent NPSB, DMBODIPY-BAZ, reversibly labels partially purified L-type calcium channels with high affinity (K_d=25 nM, B_{max}=580 pmol/mg). Its kinetic and equilibrium binding properties are consistent with the labeling of a BTZ binding domain on the channel. It was used to develop a fluorescent binding assay exploiting fluorescent resonance energy transfer (FRET) allowing on-line detection of drug binding. DMBODIPY-BAZ binding is partially blocked by preincubation of the channel with nanomolar concentrations of the dihydropyridine (DHP) (+)-isradipine. Addition of (+)-isradipine to DMBODIPY-BAZ-calcium channel complexes caused extremely slow dissociation. Preincubation of the channel with (-)-isradipine concentration-dependently decreased the apparent association and dissociation rate constants for DMBODIPY-BAZ but did not decrease equilibrium binding. These data can be explained by steric hindrance, where isradipine inhibits access of DMBODIPY-BAZ to an adjacent or partially overlapping binding domain. This is further supported by our observation that both isradipine enantiomers stereospecifically increased DMBODIPY-BAZ fluorescence when added after DMBODIPY-BAZ equilibrium binding was reached. This phenomenon was not observed with other DHPs suggesting the presence of a direct isradipine-specific drug-drug interaction.

Taken together our data indicate that the DHP and BTZ binding domain are located on adjacent or overlapping sites on the extracellular surface of muscle LTCCs.

This work was supported by grants from the Fonds zur Förderung der Wissenschaftlichen Forschung, Austria (S56601, S56602, S56603).

W-Pos8

LOCALIZATION OF A REGION IN THE CARDIAC L-TYPE CALCIUM CHANNEL IMPORTANT FOR DIVALENT-DEPENDENT INACTIVATION. ((A. Gonzalez, J. Nakai and K. Beam)) Dept. of Physiology, Colorado State University, Fort Collins, CO 80523.

Cardiac L-type calcium channels display voltage and calcium-dependent inactivation. To identify regions important for calcium-dependent inactivation, cDNAs encoding chimeras of the skeletal and cardiac L-type channels were expressed in dysgenic myotubes and currents were measured with the whole-cell patch clamp technique. Inactivation was characterized both by the time constant of current decay as a function of test potential (τ_h) and by the normalized amplitude of the current during a constant test pulse as a function of a preceding 10 s prepulse (h_∞). With 10 mM Ca^{2+} as charge carrier, τ_h for the skeletal L-type channel of normal myotubes decreased monotonically with test potential (2.33 ± 0.47 and 1.64 ± 0.13 s at +20 and +40 mV, respectively; n=13) and h_∞ decreased monotonically to zero as a function of prepulse potential. By contrast for the cardiac channel (CARD1) expressed in dysgenic myotubes, τ_h and h_∞ showed a "U-shaped" dependence on potential, consistent with a contribution of calcium to inactivation (although τ_h was several-fold larger than for L-type channels in cardiac cells). Inactivation was cardiac-like for CSk9, a chimera in which the intracellular loops are skeletal but all four repeats are cardiac (in 10 mM Ca^{2+}, τ_h = 3.56 ± 0.53 and 5.07 ± 0.87 s at +20 and +40 mV, respectively; n=8). For both CARD1 and CSk9, τ_h and h_∞ showed a monotonic dependence on potential when the charge carrier was 150 mM Na^+. Inactivation behavior of SkC15, which is identical to CSk9, except that repeat I is skeletal, was like that of the purely skeletal channel. Further, SkC50, in which the SS1-SS2 and S6 segments of the first repeat of CSk9 were converted from cardiac to skeletal sequence, also showed skeletal-like inactivation (in 10 mM Ca^{2+}, τ = 3.41 ± 0.37 and 2.10 ± 0.26 s at +20 and +40 mV, respectively; n=6). Thus, the SS1-SS2 and S6 segments of the first repeat appear to be involved in divalent-dependent inactivation. Supported by NIH grant NS24444 to KB.

W-Pos9

NO SYNTHASE IS UNNECESSARY FOR ACh INHIBITION OF Ca CURRENT IN FROG VENTRICULAR MYOCYTES. ((P.F. Méry, L. Hove-Madsen, C. Hartzell, & R. Fischmeister)) Université de Paris-SUD, Châtenay-Malabry, France. Emory Univ., Atlanta, GA.. (Spon: R.L. DeHaan).

In mammalian sino-atrial node, inhibition of L-type Ca current (I_{Ca}) by ACh seems to involve nitric oxide (NO) production by NO synthase (NOS). In contrast, studies by us in frog ventricular myocytes suggest that inhibition of I_{Ca} by ACh can be explained entirely by inhibition of adenylyl cyclase. We have re-examined this conclusion by testing the hypothesis that NO also plays a role in ACh inhibition of I_{Ca} in frog myocytes. In whole-cell patch clamp, NOS substrates (arginine, ARG) or NOS inhibitors (N_G-monomethyl-L-arginine {NMMA} or N_G-nitro-L-arginine {NNA}) applied extracellularly or intracellularly at 500 μM had no effect on basal I_{Ca} or on I_{Ca} stimulated by isoproterenol (ISO). These agents also had no effect on the ability of ACh to inhibit ISO-stimulated I_{Ca}. The response to ACh was the same under control conditions or in the presence of internal 500 μM NNA or 500 μM ARG (I_{Ca} was reduced to 29±3% (n=3), 27±2% (n=4); and 24±7%, (n=3), respectively). In the nystatin perforated patch configuration, exposure to external 500 μM NMMA for 15 to 90 min also had no effect on the response to ACh (ACh decreased I_{Ca} to 17±7%, n=4). Thus, NOS does not participate in the cholinergic inhibition of I_{Ca} in frog ventricular myocytes. Furthermore, NOS does not appear to modulate the stimulatory effect of ISO.

W-Pos10

PROTEIN PHOSPHATASES CONTROL SLOW AND FAST GATING OF SMOOTH MUSCLE L-TYPE Ca^{2+} CHANNELS

K. Groschner and K. Schuhmann,
Dept. of Pharmacology and Toxicology, Univ. of Graz, Austria.

The role of protein phosphatases (PP) in cellular regulation of smooth muscle Ca^{2+} channels was investigated in cells isolated from the media of human umbilical veins. Currents through single L-type Ca^{2+} channels were recorded in cell-attached mode using 10 mM Ba^{2+} as charge carrier, and the effects of inhibition of basal dephosphorylation were studied using okadaic acid or tautomycin as inhibitors of PP1 and PP2A, and cyclosporin A as an inhibitor of PP2B. Both okadaic acid and tautomycin induced a dual change in L-type Ca^{2+} channel function. Low concentrations of either phosphatase inhibitor (<100 nM okadaic acid and <10 nM tautomycin) induced predominantly a reduction in the availability of Ca^{2+} channels while high concentrations favored the occurrence of long channel openings. Although both inhibitors of PP1 and 2A exerted a similar dual action, the stimulatory component of action which was based on promotion of long channel openings was prominent with okadaic acid, while the inhibitory component due to suppression of channel availability was prominent with tautomycin. Cyclosporin A did not affect Ca^{2+} channel function up to a concentration of 1 μg/ml.
It is concluded that cellular activities of PP1 and PP2A may represent important determinants of L-type Ca^{2+} channel function in smooth muscle. Our results support the hypothesis of multiple regulatory phosphorylation-dephosphorylation processes, one of which controls slow cycling of Ca^{2+} channels between available and unavailable states while another process controls fast gating behavior.

Supported by the Austrian Research Funds (S6605)

W-Pos11

PROTEIN PHOSPHORYLATION MODULATES L-TYPE CALCIUM CHANNEL ACTIVITY IN THE A7R5 SMOOTH MUSCLE CELL LINE. C. Obejero-Paz. M. Auslender, and A. Scarpa. Department of Physiology and Biophysics.Case Western Reserve University, Cleveland, OH 44106.

We have perviously show that L-type calcium channels have a variable response to 1-oleoyl-2-acetylglycerol (OAG) in A7r5 depending on the previous resting calcium channel activity. One interesting possibility is that different phosphorylation of the channel may determine different kinetic characteristics and cause opposite responses to OAG. In order to test this hypothesis we studied the effect of 50-100 nM staurosporine and 0.1- 1 μM calphostin C, an specific Protein Kinase C (PKC) inhibitor, on single channel currents carried by 110 mM Ba^{2+} in cell attached patches. Three patches showing high percentage of sweeps with long open events (4.6 $\pm$ 1.3 %), and relatively high NPo values (4.5 $\pm$ 2.5 %) were strongly inhibited after 5.6 min of exposure to staurosporine. By contrast, channel activity from two patches showing in control sweeps low NP_O values (< 1%) , and absence of long open events, were not affected. The main effect of staurosporine was to decrease the fraction of active sweeps. Calphostin C decreased channel availability in 4 out of 12 patches, but any interpretation is made difficult by the light requirements necessary for calphostin C inhibition. Taken together, these experiments support the existence in A7r5 cells, under non stimulated conditions, of a resting level of channel phosphorylation due to PKC. Supported by NIH HL41618. C.O-P and M.A were recipients of Research Fellowships sponsored by the American Heart Association, Northeast Ohio Affiliate, Inc.

W-Pos12

EXPRESSION OF CARDIAC AND SKELETAL L-TYPE CA CHANNELS IS DIFFERENTIALLY REGULATED BY RETINOIC ACID ANALOGS IN EMBRYONIC CARDIAC CELLS. ((P. Lory, S. Pupier, C. Goudet, and J. Nargeot))-CRBM CNRS, BP 5051 , 34033 Montpellier cedex (Spon. by P. Charnet).

In adult cardiac and skeletal tissues, there are specific L-type Ca channels with distinct functional properties related to specific expression of CARDα1 (α1-C) and SKMα1 (α1-S) isoforms, respectively. In contrast, at embryonic stage, cardiac and skeletal tissues both express α1-C and α1-S isoforms. We have characterized the electrophysiological properties of L-type Ca currents expressed in the myoblast cell line H9C2, that derives from embryonic rat ventricule. The data indicated that H9C2 cells present properties of embryonic or non differentiated cardiac cells. Thus, freshly plated cells (myoblasts) expressed exclusively cardiac L-type Ca currents (3.1±0.8 pA/pF). When H9C2 cultures were confluent several multinucleated, Troponine T-, MyoD- and myogenin-positive myotubes appeared (5% of the cells), which expressed skeletal L-type Ca current. In large myotubes, skeletal Ca current was 8.1±1.5 pA/pF and no cardiac Ca current was then detected. RT-PCR experiments indicated that the appearence of skeletal Ca channels in these cells was primary associated with the presence of α1-S transcript. A change in the β subunit isoform expression was further characterized. H9C2 cells were then used to identify factors that regulate muscle Ca channel expression. In that respect, we have characterized the effect of retinoic acid (RA) analogs on muscle Ca channels. After 5-7 days of chronic treatment with 10 nM *all trans* RA, cardiac Ca current was up-regulated (2-3 fold) in multinucleated cells, compared to moyblasts. In addition, skeletal Ca current was completely abolished in RA treated cells. RT-PCR experiments were conducted to determine the Ca channel subunit composition. We conclude that RA plays an important role in the regulation of cardiac Ca channel expression.

W-Pos13

CONSTITUTIVE REGULATION OF CALCIUM CHANNEL CURRENTS IN PHEOCHROMOCYTOMA CELLS: ROLE OF *c-fos* AND *c-jun*.

((David E. García[1], Adolfo Cavalié[2], and Hans D. Lux[2])). [1]Fac. de Medicina UNAM, Depto. de Fisiología, Apdo. Post. 70250, Mexico 04510 DF and [2]Max-Planck-Institut für Psychiatrie, Abt. Neurophysiologie, D-82152 Martinsried, FRG.

The role of immediate early genes in the functional expression of calcium channels was studied in pheochromocytoma (PC12) cells that were stimulated transiently one hour every day, either with NGF or by KCl induced membrane depolarization. The component of high-voltage-activated calcium currents sensitive to w-conotoxin was preferentially induced by NGF and not by membrane depolarization. Concomitantly, the transient peaks in the mRNA levels of *c-fos* and *c-jun* increased every day with each exposure to NGF and, only the mRNA level of *c-fos* with repetitive membrane depolarization. Transient cotransfection of *c-fos* and *c-jun* resulted in a differential increase of calcium channel currents. Thus, AP1 transcription factors, like Fos-Jun, could mediate the functional expression of calcium channels sensitive to w-conotoxin, when they are transiently induced by external stimuli.

Supported by DGAPA-UNAM IN203293 and Alexander von Humboldt Stiftung.

W-Pos14

REGULATION OF Ca^{2+} CHANNEL EXPRESSION IN CULTURED ADULT RAT VENTRICULAR MYOCYTES ((Amy J. Davidoff, Tiina M. Maki[1], James D. Marsh)) Wayne State University School of Medicine, Detroit, MI, [1]University of Helsinki, Finland

The mechanisms regulating Ca^{2+} channel expression are not well understood. Elevated intracellular Ca^{2+} ($[Ca^{2+}]_i$) has been shown to alter mRNA for early response genes as well as some late genes for membrane proteins (e.g., Na^+ channel and possibly Na/Ca exchanger). We determined the effects of elevating $[Ca^{2+}]_i$ on levels of mRNA and protein for the Ca^{2+} channel, and on whole-cell Ca^{2+} current (I_{Ca}) in isolated cardiac myocytes. Adult rat ventricular myocytes were cultured for 1-3 days in serum-free medium containing either normal (1.8 mM) or high (4.8 mM) Ca^{2+}. Exposing myocytes to high Ca^{2+} elevates $[Ca^{2+}]_i$ as determined by fura-2. After 3 days in culture under either condition, myocytes maintained adult-like phenotype. Northern blot analysis using an α_1 subunit cDNA probe revealed that culturing in high Ca^{2+} produced greater mRNA levels at day 2 (202±80% of control) and day 3 (146±12%, n= 3). The abundance of α_1 subunit protein (determined by DHP ligand binding) increased 2-fold in myocytes after 3 days in high Ca^{2+}. Whole-cell I_{Ca} density in cells cultured in high Ca^{2+} (but recorded in normal Ca^{2+} buffer) paralleled the binding data. Peak I_{Ca} (pA/pF) was larger in cells cultured in high Ca^{2+} (-17.8±1.5, n=26) than in controls (-11.0±1.0, n=23; $p<0.05$). Voltage-dependent activation and inactivation, rates of I_{Ca} decay, and % increases in I_{Ca} elicited by Bay K8644 were characteristic of L-type channels and remained unchanged regardless of days in culture or Ca^{2+} exposure. Therefore, the larger I_{Ca} likely represents a greater number of channels. Since I_{Ca} exhibits typical L-type kinetics, the other channel subunits must be either co-regulated with α_1 subunits or expressed in excess. These results show that changes in $[Ca^{2+}]_i$ can alter Ca^{2+} channel mRNA, protein abundance and number of functional Ca^{2+} channels in adult ventricular myocytes.

W-Pos15

SINGLE CHANNEL STUDIES IN NATIVE AND SYNTHETIC MEMBRANE OF NE1-115 NEUROBLASTOMA CELLS. ((L. Shajenko and R.M. Davidson)) University of Connecticut Health Center, Farmington, CT 06030.

In whole cell recordings, we have shown that Amyloid β-Peptide (AβP) increases the amplitude of an L-type calcium current in N1E-115 Neuroblastoma (NB) cells (Davidson et al., 1994). We hypothesized that AβP might alter the activity or number of endogenous calcium channels and/or form calcium channels *de novo*. To further understand the underlying mechanism of AβP's effect on calcium current in the N1E-115 cell, we have begun to characterize it's L-type calcium conductance at the single channel level. To study AβP's effects in the absence of endogenous ion channels, we have also developed a synthetic, liposomal model of the NB membrane.

All recordings were obtained in excised patches. With 100 mM barium aspartate in the patch pipette, analysis of the NB nimodipine-sensitive, L-type calcium channel revealed a voltage-gated, 12 Ps conductance, with mean Popen ranging from 0.08±0.07 (Mean;±SD) at -40 mV to 0.35±0.20 at 10 mV (n=10). Channel activity typically occurred in bursts, and was voltage dependent; mean burst duration was 50±16 ms at -40mV, and increased to 96±57 ms at 10 mV. For the liposomal model, NB cell membrane was isolated and analyzed by thin layer chromatography. Inorganic phosphate and cholesterol levels were determined using colorimetric assays. To form vesicles, a thin lipid film with the following composition: 53% PtdChol(brain), 26% PtdEtn(heart), 21% PtdSer(brain) ±0.50 mole ratio cholesterol:PL was incubated at 70 deg. C in physiological saline for 2-4 hrs. The liposomes were typically 20 μ in diameter and appeared unilamellar under EM. In excised patch recordings made in symmetric solutions of standard ECS, Alamethicin (1 ug/ml) added to the bath, produced a characteristic pattern of cation channel activity. In addition, channel activity differed in cholesterol-containing liposomes when compared to cholesterol-free preparations.

W-Pos16

RUNDOWN OF THE L-TYPE Ca CHANNEL IN EXCISED PATCH REVEALS MULTIPLE STEPS OF CONDUCTANCE. ((J.L. Bossu, R. Lambert and A. Feltz)) Laboratoire de Neurobiologie Cellulaire, CNRS, 5 rue Blaise Pascal, 67084 Strasbourg, France

Transition between the closed and open states of the Ca channel is usually schematically described as a single step. This model corresponds to the assumption that on channel activation the pore lining transmembrane segments ensue such a synchronized conformation change so as to yield a single conductance level. This characteristic of opening is usually maintained after patch excision. Albeit a rundown then takes place, it corresponds to a progressive reduction of the opening frequency with no change in the elementary event amplitude. We report here about exceptions to the above observation. We run a series of experiments where L-type Ca channel activity was recorded from cerebellar granule cells maintained in culture. Patches containing one type of channel amplitude in cell-attached condition eventually displayed a progressive step by step decrease of the unitary currents following patch excision. Four to five levels of conductance could be therefore identified. These data can be interpreted in terms of a hypothesis according to which different parts of the channel forming protein could act independently and so yield a channel with distinct conducting properties.

W-Pos17

EXPRESSION OF L-TYPE CA^{2+} CHANNEL ISOFORMS IN NEONATAL RAT VENTRICULAR MYOCYTES WITH PHENYLEPHRINE INDUCED HYPERTROPHY. ((Beth A. Bailey, Julian A. Mattiello, Colleen A. Hefner and Steven R. Houser)) Temple University School of Medicine, Phila. PA 19140.

The membrane density of L-type Ca^{2+} channel current changes with development and in certain diseases; these changes have important functional consequences. We are studying the role of Ca^{2+} channel α_1 subunit isoform switching in these changes. Previous studies with heart tissue suggest the existence of two distinct L-type Ca^{2+} channel isoforms with different third membrane spanning regions of the fourth motif (IVS3). RT-PCR using primers flanking this region was performed using neonatal myocyte (NM) RNA. cDNA fragments were cloned into pBS and sequenced. Two distinct isoforms, the normal adult cardiac isoform(AI) and a fetal isoform (FI), were found. Isoform mRNA levels were examined in control NM and NM with hypertrophy secondary to 48hr treatment with the α-adrenergic agonist phenylephrine (20μM)(PHE). RNAse protection assay (RPA) using riboprobes specific for each isoform showed a reduction in the relative expression of FI mRNA levels with chronic PHE treatment. In parallel experiments RT-PCR was performed using NM RNA from control and PHE treated cells and primers flanking the IVS3 region. Southern blot analysis was performed on RT-PCR products using labeled oligonucleotides specific for each isoform. These data confirmed the RPA results, suggesting that the relative expression of the FI mRNA of the L-type Ca^{2+} channel is reduced in NM with PHE-induced hypertrophy.

W-Pos18

PROPERTIES OF CALCIUM CHANNEL BLOCK BY ω-AGATOXIN IVA IN SQUID NEURONS. ((MB McFarlane and WF Gilly)) Departments of Biology and Molecular & Cellular Physiology; Hopkins Marine Station of Stanford University, Pacific Grove, CA 93950.

We have studied the block of voltage-activated Ca channels by ω-Aga IVA in squid giant fiber lobe (GFL) neurons using whole cell voltage clamp. Two Ca channel populations exist in GFL neurons which are distinguishable by their fast and slow deactivation rates (FD and SD; Llano and Bookman, 1986). Here, we describe the properties of ω-Aga IVA block of FD Ca channels; SD channels are insensitive to this toxin at doses up to 750 nM. ω-Aga IVA blocks FD channels in a dose-dependent manner with an IC_{50} of 250-450 nM (50 mM Ca, 10 mM Mg). Block is independent of holding potential, and activation and deactivation kinetics of the residual FD currents are unaffected. Relief of block occurs during prolonged depolarizations but only at positive voltages. This process can be rapid and complete (τ = 180 ms and 65% unblock at +40 mV; τ = 64 ms and 100% at +80 mV). 2 mM $NiCl_2$ reduces FD current amplitude by roughly 50%, slows activation kinetics, and block is not significantly relieved by depolarization. Ni also interferes with the depolarization-induced unblocking of ω-Aga IVA. 100 μM $CuCl_2$ similarly reduces FD current amplitude but without a change in activation kinetics. Also in contrast to Ni, depolarization-induced unblocking occurs in Cu in the absence or presence of ω-Aga IVA. These results point to complex state-dependent interactions between ω-Aga IVA, transition metal divalents and the squid FD calcium channel.

[ω-Aga IVA was kindly provided by Pfizer, Inc. (Bachem)]

W-Pos19

USE-DEPENDENT BLOCK OF DIVERSE TYPES OF VOLTAGE-GATED CALCIUM CHANNELS EXPRESSED IN *XENOPUS* OOCYTES BY THE NOVEL NON-DIHYDROPYRIDINE DRUG RO 40-5967. ((Ilya Bezprozvanny and Richard W. Tsien)) Dept of Mol and Cell Physiol, Beckman Ctr, Stanford Univ Med Ctr, Stanford, CA

Several small organic compounds are known to block L-type Ca^{2+} channels but little is known about non-peptide agents that block other major classes of voltage-gated Ca^{2+} channels. Here we report effects of the new nondihydropyridine calcium antagonist Ro 40-5967 (Hoffmann-La Roche) on class A (P/Q-type), B (N-type), C (L-type) and E (most likely R-type) α_1 subunits, expressed in *Xenopus* oocytes in combination with auxiliary subunits. Ro 40-5967 inhibited all four Ca^{2+} channel types with apparent dissociation constants of 8 μM (α_{1A}), 3 μM (α_{1B}), 22 μM (α_{1C}), and 7 μM (α_{1E}). The blocking effect of the drug was significantly potentiated as the holding potential was displaced toward positive voltages, suggesting a higher affinity binding of the drug to the inactivated state of the channels. The rate of inactivation was accelerated in the presence of Ro 40-5967 for all four channel types, suggesting that the drug also binds to the open state of the channels. The ability of Ro 40-5967 to inhibit L-type channels was increased with an elevated frequency of stimulation. These features of Ro 40-5967 action are relevant to its favorable pharmacological profile in animal tests and clinical trials (Clozel at al, 1991, Cardiovas Drug Rev, 9:4-17).

W-Pos20

DIFFERENTIAL MODULATION OF CLASS A AND C RECOMBINANT CALCIUM CHANNELS IN *XENOPUS* OOCYTES BY GTPγS. ((J.P. Roche, V. Anantharam, and S.N. Treistman)) University of Massachusetts Medical School, Worcester, MA 01655. (Spon. by S.N. Treistman)

The α_1 subunits of the class A and C Ca^{++} channels were independently expressed in combination with the α_{2b} subunit in *Xenopus* oocytes and tested for modulation by endogenous G-proteins. The α_{1C-a} showed an 87% reduction of peak current after 30 minutes when the oocyte was injected with 4.6 nL of 50mM GTPγS. To rule out the possibility of the α_{2b} subunit mediating this effect, we tested the α_{1C} subunit alone. Furthermore, to eliminate Ca^{++} induced inactivation of the channels via G-protein mediated Ca^{++} release, we injected the Ca^{++} chelator BAPTA. These conditions did not change the degree of inhibition produced by injection of GTPγS. In contrast to this result, the α_{1A} (when expressed with the α_{2b}) showed only a 33% decrease after 30 minutes when injected with GTPγS. GDPβS injection, which had no effect on the C-type channel, caused an almost 2-fold increase in current levels when injected into oocytes expressing the $\alpha_{1A}\alpha_{2b}$ subunit combination. The effects of GDPβS indicate that the two classes of α_1 subunit may be under different levels of tonic control by G-proteins. The difference in inhibition may be solely due to this difference in tonic control, or alternatively, may be due to a difference in the ability of the two α_1 subunits to interact with the activated G-proteins. Supported by NIH grant AA05542.

W-Pos21

PREPULSE DEPOLARIZATION PROMOTES HIGH OPEN PROBABILITY ACTIVITY OF NEURONAL L-TYPE CALCIUM CHANNELS ((R.A. Craig and N.V. Marrion)). Vollum Institute, O.H.S.U, Portland, OR 97201.

Voltage pulses to depolarized levels can promote high open probability (Po) behavior of L-type calcium channels in cardiac muscle (Pietrobon & Hess, 1992; *Nature*, 346, 578). The effect of voltage prepulses on single L-type calcium channel activity in cultured hippocampal neurons was studied using the 'cell-attached' patch configuration. Cells were bathed in an equimolar potassium solution and single channel currents were recorded using 110 mM Ba^{2+} as the charge carrier. Patches were held at -40 mV, with test pulses to +10 mV (200 ms duration) being preceded by a 200 ms voltage step ranging from +20 to +110 mV. L-type channels were characterized by their conductance (25 pS) and their sensitivity to BAYK 8644 (5 μM).

At prepulse voltages below +60mV, open duration histograms of channel activity during the test pulse were best fit by one exponential (τ_1~0.35ms). Open duration histograms with prepulses from +60mV to +110mV, however, were best fit by the sum of two exponentials (τ_1~0.35ms; τ_2~5ms). This resulted in an increase in channel Po from approximately 0.05 (prepulse to +20mV) to 0.5 (prepulse to +110mv). It is to be determined if this effect results from a switch from short open time events to long open time activity, or from a recruitment of long open time activity. In separate experiments, application of the membrane permeant analog of cAMP, 8-CPT cAMP, promoted long open time behavior at lower prepulse voltages (30% of patches). This effect is being studied further. Supported by NS29806.

W-Pos22

TRYPSIN-MODIFICATION OF SINGLE L-TYPE Ca^{2+} CHANNEL ACTIVITY IN EXCISED INSIDE-OUT PATCHES. ((R. Schmid, K. Seydl, W. Baumgartner and C. Romanin)) Institute for Biophysics, University of Linz, Austria.

The patch-clamp technique was employed to investigate effects of the protease trypsin applied to the intracellular face of excised membrane patches from guinea-pig ventricular myocytes. Run-down of L-type Ca^{2+} channels was prevented by calpastatin and ATP. Ca^{2+} channel activity was monitored employing 96 mM Ba^{2+} in the presence of 2.5 μM (-) BAYK 8644. Upon application of trypsin (0.1 mg/ml) Ca^{2+} channel activity determined as Np increased by a factor of 6.1±2.9 (n=18, mean±S.D.). Channel activity remained elevated upon removal of trypsin as expected by an irreversible, proteolytic modification. Trypsin-modified Ca^{2+} channels still exhibited a run-down upon wash-out of calpastatin and ATP. Single channel unitary conductance and reversal potential were not different to those of untreated Ca^{2+} channels. However, Ca^{2+} channel availability was ~3-fold enhanced after trypsin treatment concomitant to a reduction in voltage-dependent inactivation. Specifically, inactivation rate during a depolarizing voltage pulse (0 mV, 1500 ms) was diminished from 54±18% in control to 15±12% in trypsin-modified Ca^{2+} channels. Yet, Ca^{2+}-induced inactivation of trypsin-modified Ca^{2+} channels remained unaffected as found by an unchanged reduction in channel activity upon elevation of intracellular Ca^{2+} to ~15 μM. Similarly, drug sensitivity to phenylalkylamine derivatives such as D600 and D890 was still observed in trypsin-treated Ca^{2+} channels.
(Supported by Austrian Research Funds S6606)

W-Pos23

MANIPULATORS OF THE ACTIN CYTOSKELETON REGULATE SINGLE CARDIAC L-TYPE CALCIUM CHANNELS. ((Aaron Kitzmiller and Robert L. Rosenberg)) Curriculum in Neurobiology and Dept. of Pharmacology, Univ. of North Carolina, Chapel Hill, NC 27599

The gradual reduction (rundown) in open probability (P_O) of Ca^{2+} currents from macropatches in *Lymnea* neurons has been shown to be sensitive to intracellular Ca^{2+}, ATP, and the cytoskeleton-specific manipulators, phalloidin and cytochalasin B (Johnson and Byerly, Neuron 10:797). To determine whether agents affecting cytoskeletal elements affect the activity of mammalian L-type Ca^{2+} channels, porcine cardiac membrane preparations were used in conjunction with the planar lipid bilayer technique and manipulation of the cytoskeleton with Ca^{2+}, ATP, and the actin filament stabilizer, phalloidin. Reconstituted L-type Ca^{2+} channels were studied in the presence of dihydropyridine agonist (+)202-791 and the stimulatory G-protein, $G_{S\alpha}$. Under these conditions, rundown is slowed, but not completely eliminated by, $G_{S\alpha}$. This remaining rundown was delayed by addition of HEDTA to chelate Ca^{2+} in the intracellular solution. Actin filament involvement was more specifically indicated in experiments in which sarcolemmal membranes were incubated with 20μM phalloidin, 10mM $MgCl_2$, and 1mM ATP. Channel activity from phalloidin-treated membranes (5 of 10 channels) persisted longer (16 ± 2 minutes; n = 5) than did that of untreated membranes, or of membranes incubated with Mg^{2+}, ATP, and the methanol vehicle (9 ± 1 minutes; n = 7). Unlike currents in *Lymnea* neurons, inactivation rates were not affected. These results are consistent with a role for the actin cytoskeleton in the regulation of cardiac L-type Ca^{2+} channels.

W-Pos24

EFFECT OF ARACHIDONIC ACID ON THE L-TYPE CALCIUM CURRENT IN FROG HEART MYOCYTES.

((J.Petit-Jacques and H.C. Hartzell)) Department of Anatomy and Cell Biology, Emory University School of Medicine, Atlanta, GA 30322.

The whole-cell configuration of the patch-clamp technique was used to investigate the effects of arachidonic acid and other fatty acids on the L-type calcium current in ventricular cells of the frog heart. Arachidonic acid (AA) has no effect on the basal I_{Ca}, but has a potent inhibitory effect on the Isoprenaline stimulated current. 10μM of AA inhibited the Iso stimulated current 86.8 ± 2.3 % (mean ± S.E.M, n=11). 5 μM AA inhibited the current about the same amount (88 ± 1.7 % , n=13). A saturated fatty acid, myristic acid (MA) has no effect on the Iso stimulated calcium current (the Iso stimulated current increases 7 ± 2.1 % with 10 μM MA, and decreases 84.4 ± 2.6 % with 10 μM AA in the same cells, n=5). When the cells were internally dialyzed with cAMP, AA (5 μM) inhibited 81.6 ± 3.1 % of the cAMP stimulated I_{Ca} (n=5), suggesting that the target of AA effect is beyond adenylyl cyclase. The inhibitory effect of AA is also observed in the presence of non-hydrolyzable analogs of cAMP in the internal perfusion (88.9 ± 0.3 % inhibition of 8Bromo-cAMP stimulated current (n=2) and 85± 3.6 % inhibition of CPT-cAMP stimulated current (n=2). Thus the AA effect seems not linked to activation of guanylate cyclase or activation of phosphodiesterase. When the cells were internally perfused with a non-hydrolyzable analog of ATP, ATP-γ-S (2.5 mM), the inhibitory effect of AA (5 μM) on the Iso (or cAMP) stimulated I_{Ca} was diminished from 88% to 39± 2.4 % (n=4), suggesting that AA affects phosphorylation-dephosphorylation mechanisms of the L-type calcium channels. When AA is internally perfused, the I_{Ca} is unaffected, indicating that the inhibitory effect on I_{Ca} is triggered by a metabolite of AA rather by AA itself. These results suggest that AA and other fatty acids involved in inflammatory processes can potently affect the cardiac Ca channel.

W-Pos25

DOES NITRIC OXIDE AFFECT I_{Ba2+} IN VASCULAR SMOOTH MUSCLE? ((M.L. Earle*, M.F. Wilkinson & C.R. Triggle*)). Dept. Pharmacology & Therapeutics* & Dept. Medical Physiology, University of Calgary, Calgary, Alberta, CANADA. T2N 1R4. (Spon. by W.C. Cole).

Nitric oxide (NO) has been implicated in many diverse physiological functions, NO is synthesized from l-arginine by the enzyme nitric oxide synthase (NOS) and freely diffuses to produce a wide variety of effects including smooth muscle relaxation, via activation of soluble guanylate cyclase. The action of NO on ion channel activity is however, still an area of controversy. In the present study we present evidence to suggest that the widely used NOS inhibitor L-NAME, and its isomer D-NAME may depress calcium ion channel activity and that this inhibition may be via an NO-independent pathway. Barium currents (I_{Ba2+}) were recorded from isolated vascular myocytes from the rat tail artery by nystatin perforated patch whole-cell voltage clamp in the presence and absence of NOS inhibitors and NO donors. All experiments were performed in the absence of calcium, in an EGTA-containing bath solution. In the presence of L-NAME (10uM, n=3) and D-NAME (10uM, n=4) a reversible inhibition of I_{Ba2+} was apparent (9.4±2.9 to 3.0±1.8 pA/pF, L-NAME & 7.4±2.2 to 2.1±0.4 pA/pF, D-NAME), however inhibition was not observed in the presence of 100uM L-NMMA (6.9±2.1 to 8.6±2.8 pA/pF, n=4). In addition, the inhibitory effect of L/D-NAME could not be reversed by l-arginine (5mM), suggesting that NO was not directly involved in these inhibitory responses. No effect of the NO donor SNC (200uM, n=2) on I_{Ba2+} was observed. These results suggest that the widely used NOS inhibitor L-NAME and its isomer D-NAME may inhibit calcium ion channel activity in a NO-independent manner.
(Supported by A.H.F.M.R., A.H.S.F. & M.R.C.)

W-Pos26

MUTATIONAL ANALYSIS AND FUNCTIONAL IMPORTANCE OF α_1-β INTERACTION SITES IN VOLTAGE-DEPENDENT Ca^{2+} CHANNELS. ((M. De Waard, D.R. Witcher, M. Pragnell and K.P. Campbell)) Howard Hughes Medical Institute, Dept. of Physiology and Biophysics, University of Iowa College of Medicine, Iowa City, IA 52242.

Voltage-sensitive Ca^{2+} channels are multimeric protein complexes consisting of at least α_1, $\alpha_2\delta$ and β subunits. Despite the molecular diversity of α_1 and β subunits, the functional and structural features of α_1-β interaction sites are well conserved. The amplitudes, kinetics and voltage-dependencies of all α_1 subunit Ca^{2+} currents are modified by β subunits. The α_1 subunit interaction domain (AID) which binds the β subunit was identified as an 18 amino-acid motif of which 9 are conserved among all α_1 subunits (Pragnell *et al.*, Nature 368, 67-70, 1994). Also, the β subunit interaction domain (BID) which binds the α_1 subunit was localized to a 30 amino-acid sequence in the second conserved region of all β subunits (De Waard *et al.*, Neuron 13, 495-503, 1994). To further analyse the structural properties of these two interacting domains, mutants were generated in both the AID and BID sites. Two consensus protein kinase C phosphorylation sites were also mutated in the BID site. The ability of the mutated forms to bind to the wild-type β subunit or the wild-type α_1 epitope was assessed by an *in vitro* binding assay using Glutathione-S-Transferase fusion proteins bound to Sepharose beads. We have identified a total of 3 amino-acids in the AID site and 5 amino-acids in the BID site that are critical for the α_1-β interaction. The functional importance of AID and BID was also analysed by expressing the mutant forms of α_1 and β subunits in *Xenopus* oocytes. To further analyse the molecular mechanisms of β-induced current stimulation of α_1 Ca^{2+} currents, we have correlated the affinities of the mutant β subunits for AID and their abilities to stimulate currents.

W-Pos27

FACTORS DETERMINING Ca^{2+}-DEPENDENT INACTIVATION OF HETEROLOGOUSLY EXPRESSED L-TYPE Ca^{2+} CHANNELS.

((R.Shirokov, A.Chien, X.-L.Zhao, M.Hosey & E.Ríos))
Rush Univ., Northwestern Univ., Chicago, IL 60612

Inactivation properties of Ca^{2+} currents through cardiac $\alpha 1$-$\beta 2A$ channels expressed in HEK (tSA) cells were studied using whole-cell patch clamp. After electrophysiological experiments, the same dish of cells was fixed and stained with anti-beta antibody. Immunofluorescence micrographs were taken of the individual cells that had been patched.

In different cells the fraction of the Ca current that inactivated rapidly and in a Ca-dependent manner (CDI) was variable over a wide range. CDI did not correlate with peak current density. In most cells the rates of inactivation were fastest at voltages more negative than those eliciting maximal current. Both observations indicate that unitary, rather than total current determines inactivation, which in turn is consistent with a Ca-inactivation site close to the channel mouth. CDI was little in some cells that showed β in immunomicrographs. Therefore cellular factors other than β must participate in CDI.

One possibility is phosphorylation, which slows CDI (Chad & Eckert, JP 378, 1986). In this view, the variable CDI observed would correspond to variable phosphorylation in different cells. A gating model (Shirokov et al., JGP 102, 1993) explains the effects assuming that phosphorylation stabilizes the open state and lowers the affinity of the Ca-inactivation site.

Supported by NIH, AHA and AHA-Chicago.

W-Pos28

FACILITATION OF L-TYPE CALCIUM CHANNEL CURRENT IN ROD PHOTORECEPTORS

((D.E. Kurenny and S. Barnes)) Neuroscience Research Group, University of Calgary, Calgary, Alberta, Canada T2N 4N1.

Non-inactivating Ca channel currents in vertebrate photoreceptors provide for the sustained synaptic release of glutamate in darkness. Several reports show that these channels share features with other high voltage activated Ca channels, and in cones, the presence of at least L-type Ca channels is pharmacologically indicated. Our work shows that Ca channels in tiger salamander rod photoreceptors seem to be entirely of the L-type and that activation of these channels can be facilitated by strong prepulse depolarizations. Permeabilized patch clamp recordings revealed that cadmium-sensitive inward barium current, elicited positive to −40 mV, was blocked by nifedipine (1 μM) but not by ω-conotoxin GVIA (500 nM). Current magnitude increased many times in the presence of Bay K 8644 (1 μM), while both Bay K and nifedipine prominently slowed tail currents. Prepulses to 100 mV for 50 ms facilitated the activation of Ca channels at subsequently-applied lower potentials, increasing current magnitude. Facilitation was not observed in the presence of cadmium or nifedipine and was enhanced in the presence of Bay K. Application of ω-conotoxin had no effect on facilitation. These results show that the L-type Ca channels of rod photoreceptors can be facilitated by strong depolarization in the same manner reported in other cell types.

Supported by the Alberta Heritage Foundation and the Medical Research Council of Canada.

W-Pos29

TIME COURSE OF ONSET AND RECOVERY FROM STATE-DEPENDENT PHOSPHORYLATION OF NEURONAL CALCIUM CHANNEL CURRENTS.

((A. Sculptoreanu)) Lady Davis Institute for Medical Research of SMBD-Jewish General Hospital. Depts. of Surgery and Experimental Medicine, McGill University, Montreal. Quebec.

Calcium channel currents are an essential link in coupling electrical signals integrated in the neuron to release of neurotransmitters at axon terminals. Several types of Ca^{2+} channels are co-expressed in neurons and are modulated by neurotransmitters, second messengers and G-proteins. There is growing evidence that specificity of release of neurotransmitters dependents on coupling to unique types of Ca^{2+} channels and is sensitive to patterns of neuronal activity. The presynaptic mechanism controlling transmitter release specificity and its dependence on neuronal electrical activity is not presently understood. Here, we present data which suggests that state-dependent phosphorylation of neuronal L-type Ca^{2+} channel currents may account in part for synaptic facilitation at major pelvic ganglion neurons. Whole-cell patch clamp techniques were used to record Ca^{2+} currents in cultured neurons isolated from major pelvic ganglia of rats. A three square pulse protocol was applied every 5 s as follows: a control test pulse to -20 mV, 50 ms in duration, was followed by a conditioning pulse of increasing duration to either 0, +50 or +100 mV and a second test pulse identical to the first following a brief (5 ms) hyperpolarization to -60 mV. Potentiation, defined as an increase in current in the second test pulse relative to the first test pulse in the sequence increases for conditioning pulses 5 to 20 ms in duration. For conditioning pulses longer than 20 ms, potentiation declines slowly. The currents recover fully to control magnitude in the 5 seconds separating each sequence. The rapid raise of potentiation is due to recruitment of state-dependent phosphorylated channels as suggested by the blocking action of PKI and Rp-cAMP. The subsequent decline in potentiation may be due to voltage-dependent inactivation of the Ca^{2+} channels. Alternatively, phosphorylated channels may be trapped in a slowly inactivated state. The rapid onset of state-dependent potentiation may account for the facilitation of synaptic release by burst of electrical activity in major pelvic ganglia neurons.

W-Pos30

VOLTAGE-DEPENDENT POTENTIATION OF SKELETAL MUSCLE L-TYPE Ca^{2+} CHANNELS REQUIRES ANCHORED PKA.

((B.D. Johnson, T. Scheuer and W.A. Catterall)) Dept. of Pharmacology, University of Washington School of Medicine, Seattle, WA 98195. (Spon. by T. Hinds)

Skeletal muscle L-type Ca^{2+} channels respond to trains of brief depolarizations with a strong shift of the voltage dependence of channel activation toward more negative membrane potentials and slowing of channel deactivation. This voltage-dependent Ca^{2+} channel potentiation requires rapid phosphorylation by cAMP-dependent protein kinase (PKA), suggesting that kinase and channel might be maintained in close proximity through kinase anchoring. Type II PKA regulatory subunits are anchored by PKA anchoring proteins (AKAPs) and peptides derived from the conserved kinase binding domain in AKAPs have been shown to prevent anchoring. Whole-cell recordings from a mouse skeletal muscle cell line ($129CB_3$) and rabbit skeletal muscle myoballs reveal that such peptides block voltage-dependent Ca^{2+} channel potentiation by endogenous PKA as effectively as inhibition of PKA by a specific peptide inhibitor or by omission of ATP from the intracellular solution. In contrast, a proline-substituted AKAP peptide has no effect. Potentiation in the presence of 2 μM exogenous catalytic subunit of PKA is unaffected, indicating that kinase anchoring is specifically blocked by the AKAP peptide. No effects of these agents were observed on the level or voltage dependence of basal Ca^{2+} channel activity before potentiation, suggesting that close physical proximity between the skeletal muscle Ca^{2+} channel and PKA is critical for voltage-dependent potentiation of Ca^{2+} channel activity but not for basal activity.

(Supported by NIH grant NS22625, the MDA, and a postdoctoral fellowship from Training Grant DK07441)

W-Pos31

MODULATION OF CARDIAC Ca^{2+} CURRENT BY PHOTO-RELEASE OF Ca^{2+} FROM DIFFERENT CAGED COMPOUNDS.

((A.M. Gurney and R.E. Davies)) Dept. Pharmacology, UMDS, St. Thomas's Hospital, London, U.K. SE1 7EH

The Ca^{2+} current (I_{Ca}) recorded from guinea-pig ventricular myocytes is influenced by the cytoplasmic $[Ca^{2+}]$. Photo-induced release of Ca^{2+} from the caged compounds nitr-5 and DM-nitrophen modulates I_{Ca}, but different effects are seen with the two probes. While nitr-5 photolysis results in transient inhibition of I_{Ca} followed by pronounced facilitation, inhibition is the only response with DM-nitrophen. To investigate the reasons for this discrepancy, we compared photo-induced modulation of I_{Ca} under various conditions, using nitr-5, nitr-7, DM-nitrophen or nitrophenyl-EGTA (NPE) as the Ca^{2+} donor. Nitr-7 resembles nitr-5 in its photochemistry and Ca^{2+} selectivity, but has a higher affinity. NPE has photochemical properties similar to DM-nitrophen, but is more like nitr-5 in its ability to discriminate between Ca^{2+} and Mg^{2+}. Ventricular cells were bathed in physiological saline and I_{Ca} recorded with the whole-cell technique, using the following pipette solution (mM): CsCl 130; Hepes 15; ATP 2; $MgCl_2$ 1; caged Ca^{2+} 2; pH 7.2. Under these conditions, a single light flash augmented I_{Ca} amplitude when the pipette contained nitr-5 (by 117±10%; n=5), nitr-7 (77±24%; n=3) or NPE (7±2%; n=3). When $CaCl_2$ was added to the pipette to set the free $[Ca^{2+}]$ at 50 nM, the augmentation caused by photolysis of NPE was larger (96±52%; n=4). Omitting Mg^{2+} from the pipette and extracellular solutions enhanced the response to nitr-5 photolysis (168±32%; n=6). Furthermore, in Mg^{2+}-free conditions, photolysis of DM-nitrophen enhanced I_{Ca} (39±29%; n=3). Thus Mg^{2+} influences the response to photo-released Ca^{2+}, but does not mediate the response. NPE, presumably due to its Ca^{2+} selectivity, behaves more like nitr-5 than DM-nitrophen. (Supp. by the Wellcome Trust. We are grateful to G. Ellis-Davies for providing NPE).

W-Pos32

INFLUENCE OF INTRACELLULAR PH ON CALCIUM AND CALCIUM-DEPENDENT CURRENTS IN CHICK DORSAL ROOT GANGLION NEURONS.

((M.J. Callahan, C.M. Witkowski and S.J. Korn)) Physiol. and Neurobiol., Univ. Connecticut, Storrs, CT 06269

Calcium (Ca) channels, intracellular Ca binding proteins and Ca transporters are all sensitive to pH. We are investigating whether cellular mechanisms that regulate intracellular pH influence Ca channel function or intracellular Ca levels. Ca and Ca-dependent chloride currents ($I_{Cl(Ca)}$)were studied in chick dorsal root ganglion neurons (DRGs) with both standard whole cell and perforated patch recording techniques. Intracellular [Ca] and pH were monitored with the fluorescent dyes, Fura-2 and BCECF, respectively. Extracellular application of 20 mM NH_4^+ to isolated DRGs resulted in alkalinization of the cytoplasm and an increase in intracellular free [Ca], as measured with Fura-2. Subsequent removal of extracellular NH_4^+ resulted in a rebound acidification, with no change in intracellular [Ca]. When studied with standard whole cell patch clamp techniques, NH_4^+ application potentiated voltage-gated Ca currents and prolonged Ca-dependent Cl currents. In contrast, currents were not influenced when NH_4^+ was applied during perforated patch clamp recordings. Combined perforated patch clamp recordings with photometric observation of Fura-2 fluorescence suggest that following influx, [Ca] declines much faster adjacent to the membrane than on average in the cell interior. The rate of reduction of [Ca], whether measured with Fura-2 (cell-averaged) or by the decay rate of $I_{Cl(Ca)}$, was unaffected by removal of extracellular Na^+. Taken together, these data suggest that a Na^+-independent Ca or pH buffering mechanism was active in perforated patch recordings but not in standard whole cell recordings. *Supported by the Whitaker Foundation, and the UCONN Research Foundation.*

W-Pos33

DIADENOSINE POLYPHOSPHATES SELECTIVELY POTENTIATE N-TYPE OF Ca++ CHANNELS IN THE RAT CENTRAL NEURONES.

V.A.Panchenko, J.Pintor*, A.Ya.Tsyndrenko, M.T.Miras-Portugal* and O.A.Krishtal.
A.A.Bogomoletz Institute of Physiology, Ukrainian Academy of Science, Bogomoletz str.4, Kiev-24, Ukraine.
* Departamento de Bioquimica Facultad de Veterinaria Universidad Complutense. 28040 Madrid. Spain.

ABSTRACT
The action of diadenosine polyphosphates on Ca++ channels was studied in two preparations: isolated hippocampal neurons and synaptosomes both from the rat brain.
High voltage activated Ca++ channels were studied in freshly isolated CA3 neurons using whole-cell patch-clamp technique. Current-voltage relationships were measured in control and after incubation in 5 uM Ap4A or Ap5A. The latter procedure led to the 15%+-3 of reversible increase of current through Ca++ channels when measured at the holding potential of -100 mV but not at -40 mV. In the experiments on synaptosomes from the whole brain Ap4A and Ap5A in the concentration of 100 uM increased intrasynaptosomal calcium level by 26+- 1.8 nM measured by means of spectrofluorimetry. Nifedipine failed to block this effect in synaptosomes. In isolated neurones nifedipine-sensitive current trough L-type Ca++ channels didn't demonstrate the increase under diadenosine polyphosphates. Both potentiation of current trough Ca++ channels in hippocampal neurons and an increase in intrasynaptosomal Ca++ were irreversibly blocked by 5 uM w-Conotoxin, but not by 200 nM w-Aga-IVA.
These data indicate that diadenosine polyphosphates enhance activity of N-type Ca++ channels in the central neurons of rat.

W-Pos34

THAPSIGARGIN REGULATION OF *DROSOPHILA TRP* CHANNELS REQUIRES THE COOH-TERMINAL DOMAIN. ((W.G. Sinkins, L. Vaca, D.L. Kunze, and W.P. Schilling)) Dept. of Molecular Physiology and Biophysics, Baylor College of Medicine, Houston, TX 77030.

Our previous studies have shown that the *Drosophila* proteins *trp* and *trpl* can be functionally expressed using the baculovirus/Sf9 insect cell system. Studies with the fluorescent Ca^{2+} indicator fura-2 demonstrate that expression of *trpl* promotes an increase in the basal level of intracellular calcium ($[Ca^{2+}]_i$), and also leads to an increase in the plasmalemmal permeability to Ca^{2+} and Ba^{2+}. Electrophysiological measurements have revealed that those effects coincide with the appearance of nonselective, Ca^{2+}-permeable cation channels that are not blocked by 10 μM Gd^{3+} and are not activated by thapsigargin (TG). Similar experiments with *trp* indicate that expression of the latter promotes at most a small increase in $[Ca^{2+}]_i$ and does not lead to an increase in Ba^{2+} permeability. However, *trp*-infected cells respond to TG with an increase in plasmalemmal Ca^{2+} permeability and an increase in whole-cell membrane current. Both of those responses are blocked by 10 μM Gd^{3+}. Since both *trp* and *trpl* appear to form channels, we have sought to determine which regions of each protein are responsible for channel activity and regulation. Inspection of the amino acid sequences reveals that the two proteins are most similar in the NH_2-terminal and putative transmembrane regions: 53% of the first 700 aa in each are identical, but of the remainder only 24% are identical. A chimeric protein therefore was created in which the NH_2-terminal and putative transmembrane domains of *trp* (693 aa) were combined with the COOH-terminal domain of *trpl* (423 aa). Like *trpl*, expression of the chimera in Sf9 cells produces a large increase in $[Ca^{2+}]_i$ as determined by fura-2 fluorescence, and also coincides with the appearance of constitutively active, TG-insensitive cation currents. However, chimera-infected cells also resemble *trp*-infected cells: whole-cell currents are highly Ca^{2+}-selective, Ca^{2+} influx is completely blocked by 10 μM Gd^{3+}, and there is no increase in Ba^{2+} permeability. It therefore is likely that the NH_2-terminal and transmembrane regions contain the residues responsible for ionic selectivity of *trp* and *trpl* channels, and that TG regulation of *trp* is conferred by residues in the COOH-terminal domain. (Supported by HL44119, HL45880, and HL47876)

W-Pos35

PROPERTIES OF THE *DROSOPHILA trpl* CHANNEL EXPRESSED IN Sf9 INSECT CELLS. ((D.L. Kunze, W.G. Sinkins, L. Vaca and W.P. Schilling)) Dept. Molecular Physiology and Biophysics. Baylor College of Medicine, Houston, TX 77030.

The *trpl* protein is thought to form ion channels activated during *Drosophila* phototransduction. To determine if *trpl* forms channels, currents were recorded in cell-attached and outside-out patches from Sf9 cells infected with recombinant baculovirus containing *trpl* cDNA under control of the polyhedrin promoter. Both the bath and the pipette contained (in mM) 100 NaGluconate, 10 MES and 150 mannitol. Single channel activity was evident at 24-48 hrs (n=43) but not at 12 hrs (n=10) postinfection as expected from whole cell recordings. After 24 hrs the density of the channels per patch increased with time postinfection with at least 90% of the patches containing multiple channels by 36 hrs. This channel was not observed in patches from non-infected Sf9 cells (n=10) or from cells infected with baculovirus containing the bradykinin receptor cDNA (n=52) used as controls and studied at 12-48 hrs. Channel mean open time was generally brief (< 0.2ms) although a second open state was occasionally observed with open times of 5-20 ms. Single channel conductance calculated from long openings in symmetrical sodium was 51 pS at positive potentials. The probability of opening was lower at negative potentials than at positive potentials, consistent with the outward rectification displayed by the whole cell currents (*Am.J.Physiol.* 267 (Cell Physiol. 36), In press, 1994). Furthermore, channel activity was blocked by 1 mM but not 10 μM Gd^{3+} consistent with the sensitivity of *trpl* whole cell currents. We conclude that the channel described here can be attributed to expression of the *trpl* protein. (Supported by HL44119, HL47876 and HL45880)

W-Pos36

NOVEL HYDROPHOBIC ω-CONOTOXINS FROM MOLLUSCIVOROUS CONIDAE TARGET L-TYPE CALCIUM CHANNELS

Karel S. Kits, Johannes C. Lodder, and Michael Fainzilber
Graduate School Neurosciences Amsterdam, Research Institute Neurosciences Vrije Universiteit, Faculty of Biology, De Boelelaan 1087, 1081 HV Amsterdam, The Netherlands.

Five novel conopeptides have been purified from three molluscivorous *Conus* venoms, using a direct bioassay on voltage-clamped Ca^{2+} currents in caudodorsal neurons (CDC) of the snail *Lymnaea stagnalis*. The amino acid sequences of the new toxins differ markedly from those of previously described ω-conotoxins, especially in their high content of hydrophobic and negatively charged residues. The only aspect in common with the primary sequences of classical ω-conotoxins is their cysteine framework. The primary sequences exhibit marked variability within the subgroup.

Two of the new toxins act as selective blockers of transient L-type Ca^{2+} currents in the CDC. A third blocker is selective for a second L-type current, with delayed and sustained opening kinetics. Dose response curves for all these blockers are extremely steep, suggesting a cooperative mode of action. The other two toxins (MrVIA and B) affect both voltage gated sodium and calcium currents in *Lymnaea*. The toxins completely block the sodium current (ED_{50}~0.2 μM); the block is only slowly and parially reversible. The block of the calcium current (ED_{50}~8 μM) is selective for the fast-inactivating subtype and rapidly reversible. Intriguingly, at low doses MrVIA acts as a calcium channel agonist. MrVIA/B have the same cysteine framework as the ω and δ conotoxins, and a high content of hydrophobic residues, in common with the δ conotoxins.

The cooperative mode of action of all these toxins suggests that their binding sites may be located on external surfaces of the channel that are not actually in the ion pore. The unusual cross-channel activity of MrVIA/B suggests they may represent an "intermediate" variant of conotoxin, in the diversification of one conotoxin structural family that selectively targets either sodium or calcium channels.

CHANNEL SELECTIVITY

W-Pos37

NA AND CA CURRENTS IN NMDA CHANNELS. ((M.Iino, S.Ciani, K.Tsuzuki, S.Ozawa and Y.Kidokoro)). Gunma Univ.,Maebashi,371,Japan; UCLA,Los Angeles,CA.90024.

The I-V relations of NMDA receptor channels expressed in Xenopous oocytes were studied in outside-out patches either with only Na in the solutions, or with Na inside and Na-Ca mixtures outside. All the data could be fitted with a three-barrier model similar to one described in detail elsewhere [*]. The rate constants, in units of s^{-1} or $s^{-1}M^{-1}$, divided by 10^9, and listed in the same "left-to-right" sequence as in eq.10 of [*], are: 1.68,.128, .031, 1.98,.064,.053 for Na, and 19.19, .0051,.008, 12.71,.034, .002 for Ca. Using these numbers to estimate Km and Gmax (eqs.14 and 15 of [*]) gives 10.8mM and 49pS for Na, and 0.085mM and 14.5pS for Ca. The low Km for Ca accounts for its blocking effect on the conductance. Substituting those values for Km and Gmax in the equation for P_{Ca}/P_{Na} (eq.12 of [*]) yields 9.4, in fair agreement with previous estimates from reversal potential and the GHK equation. The "electric" distances of the energy wells from the inner interface were found to be .29 and .79.
[*] "Chang et al."; J. Physiol. (1994), 476, 1.
(Supp. by Jap. Min. Ed. Sci. Cult. and by J.S.P.S).

W-Pos38

TWO EXTERNAL BARIUM BLOCKING SITES IN *SHAKER* POTASSIUM CHANNELS EXPRESSED IN *XENOPUS* OOCYTES. ((R. S. Hurst, R. Latorre[#], L. Toro and E. Stefani)) Dept. of Anesthesiology, UCLA, 90024 and [#]Centro de Estudios Cientificos, Santiago, Chile.

External barium inhibits potassium current in *Xenopus* oocytes injected with mRNA encoding the non-inactivating deletion of *Shaker* (ShH4 Δ6-46). We investigated this block at the macroscopic and single channel level using the cut-open oocyte and patch clamp techniques. Barium can block the closed state of the channel as evidenced by the instantaneous reduction in current amplitude at the onset of a depolarizing command. Installation of this block was assayed by a brief (8 ms) test pulse to 30 mV every 5 s. The block has a fast and slow component. The fast component is quasi instantaneous and has an apparent dissociation constant (K_d) of 23.7 ± 5.7 mM (n=3). This is not a non-specific effect of charge screening; the level of block by 20 mM barium was not different when compared to control solutions containing either 2 mM calcium (46.8 ± 3.7 %, n=4) or 20 mM calcium (40.9 ± 5.5 %, n=5). This fast component is evidenced at the single channel level as a reduction in the unitary current amplitude.

The slow component of barium block has a single exponential time course with a time constant (τ) of 159 ± 31 s (2.0 mM Ba, HP -90 mV, n=4). The apparent affinity of this component is dependent on the holding potential giving an electrical distance (δ) of 0.25; at -90 mV the K_d is 1.4 ± 0.2 mM (n=4). This slow component may correspond to the reduction in channel open probability, observed as long closed times in single channel records. External barium (2 mM) reduces the open probability ~60 % (control, n=5; Ba, n=3), similar to the decrease in macroscopic current by the slow component at this concentration (64.7 ± 3.1%, n=4). These observations can be explained by a model with two classes of barium binding sites. One site resides within the permeation pathway which, when occupied, blocks potassium conduction. The occupancy of a second more external site(s) by barium reduces the flux of potassium probably by raising an energy barrier experienced by the permeant ions.
(Supported by NIH grant GM50550 to ES and LT)

W-Pos39

THE MECHANISM OF THE RECTIFICATION OF THE IRK1 GENE-EXPRESSED CURRENTS. ((K. Ishihara, M. Hiraoka* and R. Ochi)) Dept. of Physiology, Juntendo Univ. School of Medicine, Tokyo, Japan, *Dept. of Cardiovascular Diseases, M.R.I., Tokyo Medical and Dental Univ., Tokyo, Japan

The gene encoding the inward rectifier K^+ channel, IRK1, was stably expressed in the mouse fibroblast cell line, and the mechanism of the rectification of expressed channels was studied using the whole-cell patch-clamp method by testing intracellular solutions containing different Mg^{2+} concentrations ($[Mg^{2+}]_i$). When the membrane was depolarized from the hyperpolarized potential, at which the IRK1-expressed channels are fully activated, outward currents were suppressed by the combination of two mechanisms, the Mg^{2+}-independent gating mechanism and the opened-channel block by intracellular Mg^{2+}, as shown for the inward rectifier K^+ channel in cardiac myocytes. With higher $[Mg^{2+}]_i$, the increase in the number of channels that transit between the Mg^{2+}-blocked state and the opened state led to the increase in the outward current amplitude at depolarized membrane potentials.

W-Pos40

PERMEATION OF SODIUM THROUGH A CLONED POTASSIUM CHANNEL (Kv2.1) ELIMINATES TEA SENSITIVITY. ((S.J. Korn*, Y. Zhu, D.L. Lewis and S.R. Ikeda)) *Physiol. and Neurobiol. Univ. Connecticut, Storrs, CT 06269 and Pharmacol. and Toxicol., Medical College of Georgia, Augusta, GA 30912.

We have previously demonstrated that in chick dorsal root ganglion neurons (DRGs) and rat superior cervical ganglion neurons, removal of both intracellular and extracellular K^+ permits Na^+ to pass through a delayed rectifier K^+ channel (*J. Physiol.*, **468**: 1993; *J. Gen. Physiol.*, **104**: 1994). We report here that K^+ channel clone Kv2.1 possesses identical properties to the neuronal K^+ channels. cRNA for Kv2.1 was injected into either L-cells (mouse fibroblast) or RBL-1 cells (rat basophilic leukemia cells) and expressed. Patch clamp recordings were made to record currents through this channel under voltage-clamp conditions. When K^+ was the dominant intracellular cation and Na^+ the dominant extracellular cation, delayed rectifier K^+ currents, and associated small outward tail currents, were recorded.When K^+ was removed from both intracellular and extracellular solutions (Na^+ or NMG^+ used as intracellular replacements), a large inward current appeared during the voltage step and tail that was carried by Na^+. When extracellular Na^+ was replaced by K^+, a similar but larger inward tail current was observed. When carried by K^+, both inward and outward currents were inhibited approximately 90% by 30 mM extracellular TEA. Currents carried by Na^+ were completely insensitive to TEA. These data confirm our previous observations that one or more delayed rectifiers will pass Na^+ in the absence of K^+. Furthermore, these data indicate that the sensitivity of the channel to external TEA depends on the permeant cation. *Supported by The Whitaker Found. and the UCONN Res. Found. (SJK).*

W-Pos41

A NEGATIVE CHARGE IN M2 REGULATES SENSITIVITY OF INWARD RECTIFIER K CHANNELS TO EXTERNAL CATION BLOCK ((P. Henry*, A.N. Lopatin, E.N. Makhina & C.G. Nichols). Dept. Cell Biol. and Physiol. Washington U. Sch. Med., 660 So. Euclid, St. Louis, MO 63110 and Lab. de Physiol. Cellulaire, U. Paris XI, Orsay, France

Cloned inward rectifying potassium channels were expressed in *Xenopus* oocytes and macroscopic currents were measured in two micro-electrode voltage-clamp experiments. Strong inward rectifier HRK1 channels were blocked by both external Cs^+ ($K_{1/2,-100}$ = 50 μM) and Ba^{2+} ($K_{1/2,-100}$ = 60 μM). ROMK1 channels were also blocked by Ba^{2+} ($K_{1/2,-100}$ = 50 μM), but were almost insensitive to Cs^+ ($K_{1/2,-100}$ ~ 3 mM). Mutation of the aspartate residue in the M2 domain of HRK1 to asparagine (D164N) *reduced* Cs^+ and Ba^{2+} sensitivity ($K_{1/2,-100}$ = 200 μM and 300 μM, respectively). Mutation of the asparagine at the corrresponding site in ROMK1 to aspartate (N171D) *inreased* both Cs^+ and Ba^{2+} sensitivity ($K_{1/2,-100}$ = 10 μM and 1 mM, respectively). As well as increasing sensitivity to block by external cations, a negative charge at this site causes high affinity block by internal Mg^{2+} (Stanfield et al., 1994 *J. Physiol.* **478**, 1-6; Wible et al. 1994 *Nature* **371**, 246-249; Lu & MacKinnon, 1994 *Nature* **371**, 243-246 and polyamines (Lopatin et al. 1994 *Nature*, in press). The results may imply that D164 lines the pore of the channel and contributes to the binding site for both internal and external cations. Conversely, internal cations might enhance the block of external cations, by limiting access of intracellular K^+ ions to binding sites within the long pore of the channel.

W-Pos42

A STRUCTURAL MODEL OF THE K^+ CHANNEL PORE ((G. Lipkind, H. Fozzard, and D. Hanck)) The University of Chicago, Chicago, IL 60637

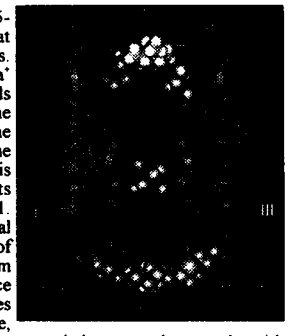

Mutation studies identify a region of the S5-S6 loop of the Shaker-type K^+ channel that confers both TEA block and pore properties. We have modelled a similar region of the Na^+ channel as β-hairpins with the C-end strands from each of the 4 domains forming the external vestibule and charged residues at the β-turns comprising the selectivity filter. The K^+ channel amino acid composition is markedly different, and we have modelled its pore using the following postulates: 1. External TEA binding site is Tyr380; internal TEA site is Met371 and Thr372 (Kv2.1) of the four P regions. 2. P regions form extended hairpins with β-turns in sequence ITMT. 3. Only C-ends of hairpins (residues 371-380) form the inner walls of the pore, while N-ends are outside. 4. The C-ends are extended non-regular strands, with backbone carbonyl oxygens of segments VGYGD facing the pore with the conformation BRLRL. 5. Juxtaposition of P loops of 4 subunits form the 27Å-long pore. Fitting outside and inside TEA sites to TEA molecules determines the pore size. Its narrowest point (GYG) has a diameter about 5.5Å, and this may be the selectivity filter; other less selective K^+ binding sites also exist. Selectivity is achieved by carbonyl interactions with K^+ including its first hydration shell

W-Pos43

STATE DEPENDENT ACCESSIBILITY OF THE AMINO ACID RESIDUES LINING THE PORE OF A CYCLIC NUCLEOTIDE-GATED CHANNEL. ((Z-P. Sun, E. H. Goulding, M. Akabas, A. Karlin, and S. A. Siegelbaum)) (Spon.by G. Tseng) Depts. Pharmacol., Physiol., Ctr. Neuro. & Behav., & Ctr. Molec. Recog., Columbia University, NYC, NY10032

We combined site-directed cysteine substitution and subsequent covalent modification to study the state dependent accessibility of residues lining the ion permeation pathway (H5 or P domain) of the cloned bovine retinal cyclic nucleotide-gated (CNG) channel (RET). The positively charged methanethiosulfonate derivative MTSEA ($CH_3SO_2SCH_2CH_2NH_3^+$) specifically modifies cysteine residues by adding the $-SCH_2CH_2NH_3^+$ moiety to free -SH groups to form mixed disulfides. We mutated, one at a time, consecutive residues in the H5 domain of RET to cysteine and expressed the mutants in *Xenopus* oocytes. Using MTSEA as a probe, we investigated the accessibility of each cysteine residue to MTSEA in both closed and open channels. We located 2 residues (V348 and V368) accessible only when the channel was closed. We identified 4 residues (T360, I361, T364 and P366) accessible from the intracellular side whether the channel was closed or open. T364 and P366 were also accessible to extracellular MTSEA in the open state. These results suggest the conformational changes of the H5 domain during channel gating and also raise questions about the current view of the topology of the H5 domain.

W-Pos44

ASPARTATE RESIDUE D737 IN PORE II OF THE CARDIAC CALCIUM CHANNEL α_{1C} SUBUNIT CONTRIBUTES TO HIGH-AFFINITY CALCIUM AND CADMIUM BINDING. ((L. Parent, D.D. Davila, M. Gopalakrishnan, A.M. Brown)) Dept. Molecular Physiology and Biophysics, Baylor College of Medicine, Houston, TX 77030.

Voltage-dependent L-type calcium channels select for Ca^{2+} ions and other divalent cations by high-affinity calcium binding and ion-ion interactions in the permeation pathway. A series of highly conserved glutamate residues within the SS2 segment of each of the four repeats of the rabbit α_{1C} subunit was recently identified as a major determinant of divalent cation selectivity in calcium channels (Yang et al., Nature 366: 158, 1993). We further investigated the role of the neighboring aspartate residues in the SS2 segment of Repeats I, II and IV in α_{1C}. Wild-type and mutant calcium channels were co-expressed with subunits α_{2b} and β_2 in *Xenopus* oocytes. Calcium affinity was assessed from the calcium block of whole-cell currents in 120 mM LiMeS. In Repeats I and IV, neutralization of the aspartate residues, D397N and D1450N, did not significantly alter the channel affinity for calcium ions with IC_{50}'s = 0.12μM and 0.11μM respectively. In Repeat II, the aspartate residue D737 is present in all calcium channel α_1 subunits but absent in Na^+ channels. Deletion of D737 in α_{1C} decreased the calcium affinity (IC_{50} = 6μM) similarly to mutations E1145Q (IC_{50} = 2μM) and E1446Q (IC_{50} = 1.4μM) and significantly different from E736Q (IC_{50} = 0.2μM) and wild-type α_{1C} (IC_{50} = 0.1μM). Furthermore, D737Δ was 10 times less sensitive to cadmium block in BaMeS solutions (IC_{50} = 12μM), than were E736Q (IC_{50} = 1.4μM) and wild-type α_{1C} (IC_{50} = 1.2μM). Nickel, cobalt and magnesium blocks in BaMeS, and the single-channel conductance of 23 pS measured with 115 mM $BaCl_2$ were not affected in D737Δ. These results suggest that, in the rabbit L-type calcium channel, the aspartate residue D737 in pore II contributes to high-affinity calcium binding in concert with the glutamate residues E1145 in pore III and E1446 in pore IV. Supported by AHA-Texas Affiliate grant 94G-196 and NIH grant HL37044.

W-Pos45

SODIUM SELECTIVITY EXHIBITED BY SYNTHETIC FRAGMENTS DERIVED FROM THE P-REGIONS OF DOMAINS I AND III OF THE *eel* SODIUM CHANNEL. ((H. Duclohier, P. Cosette, Y. Pouny, Y. Shai)) URA 500-Université de Rouen, 76821 Mont- Saint-Aignan, France; Department of Membrane Research and Biophysics, Weizmann Institute of Science, Rehovot, 76100, Israel.

The peptide strategy [Grove et al. (1992) Methods in Enzymol. 207, 510] has been implemented to contribute solving the structure-function of the presumed selectivity-filter of ion channels. In the case of the voltage-dependent sodium channel, it has been shown that a synthetic peptide derived from the P-region of eel domain IV is rich in β structure and can also form essentially non voltage-dependent channels, but unselective for Na^+ [Cosette et al. (1994) Biophys. J. 66, A281]. In addition, spectroscopic studies revealed that segments from the P-regions of domains I and III could preferentially self- or co-assemble in their membrane-bound state, and to partially adopt α-helical structures [Pouny & Shai (1994) Biophys. J. 66, A103]. To support a role for the P-regions as structural elements lining the pore, herein using single-channel experiments ('tip-dip' method) we assayed the ability of the later two segments to form conducting bundles in DOPE/POPC (8/2) planar lipid bilayers. The peptide sequences reproduce positions 340-370 for H5-1L and positions 1187-1221 for H5-3L from the eel sodium channel. In 0.5 M NaCl, the main single-channel conductance level induced by H5-1L and H5-3L was 40 pS and 30 pS, respectively. Mean lifetime of the open state was 10-20 ms. The permeability ratio PNa/PK was about 3 for both peptides and is interesting given the opposite charges carried by the assumed β bends. It is not clear yet what is the structure of the bundle formed by these H5 segments and what other segments participate in the pore. However, with the selectivity previously reported for a S4-S45 peptide [Brullemans et al. (1994) Eur. Biophys. J. 23, 39], it seems that an appreciable selectivity can be achieved with bundles of short fragments selected from large ion channels.

W-Pos46

AMINO ACID SPECIFICITY FOR BLOCK BY DIVALENT CATIONS AT A RESIDUE WHICH DETERMINES ZINC SENSITIVITY OF SODIUM CHANNEL SUBTYPES. ((Isabelle Favre, Edward Moczydlowski and Laurent Schild)) Institut de Pharmacologie et Toxicologie, 1005 Lausanne, Switzerland.

In mammalian heart Na channels Cys 374 has previously been found to be an important determinant of high-affinity block by Zn^{2+} and Cd^{2+}. The corresponding residue of the μ1 rat muscle Na channel is Tyr 401. We have investigated the chemical basis for high-affinity block of Na channels by divalent cations by measuring inhibition of macroscopic Na^+ current for a series of point mutations at residue 401 of rat μ1 Na channels expressed in X. laevis oocytes. Substitutions of Tyr 401 by Gly, Ala, Ser, Cys, Asp and His produced functional Na^+ currents without major effects on gating or ionic selectivity. High-affinity block by Zn^{2+} (K_i=8-23μM) required Cys, His or Asp, three residues that are commonly found to coordinate directly with Zn^{2+} in metalloproteins. For the μ1 Cys mutant, inhibition of macroscopic Na^+ conductance by Zn^{2+} saturated at 85%-90%, suggesting the presence of a Zn^{2+}-dependent substate current. Ca^{2+} titration of the Asp mutant revealed enhanced affinity for inhibition by Ca^{2+} (K_i=0.3mM vs. 40mM in wild type) and incomplete block saturating at 69% inhibition. The Asp mutant exhibited no change of selectivity. In contrast to Zn^{2+} and Ca^{2+}, Cd^{2+} completely blocked macroscopic current in the Cys mutant, implying that the magnitude of substate current depends on the species of divalent cation and the particular residue at position 401. Substitution with His also resulted in enhanced sensitivity to block by H^+ with a pKa of 7.5 for the introduced imidazole group. These results provide futher evidence for the notion that residue 401 is located in the external vestibule of the Na channel and that divalent cations binding at that position interferes with Na^+ permeation. Functional groups of Cys, His or Asp at this location apparently provide a coordination site which determines the ionic selectivity for external block by various inorganic cations.

W-Pos47

AMINO ACID SPECIFICITY FOR BLOCK BY DIVALENT CATIONS AT A RESIDUE WHICH DETERMINES ZINC SENSITIVITY OF SODIUM CHANNEL SUBTYPES. ((Isabelle Favre, Edward Moczydlowski and Laurent Schild)) Institut de Pharmacologie et Toxicologie, 1005 Lausanne, Switzerland.

In mammalian heart Na channels Cys 374 has previously been found to be an important determinant of high-affinity block by Zn^{2+} and Cd^{2+}. The corresponding residue of the μ1 rat muscle Na channel is Tyr 401. We have investigated the chemical basis for high-affinity block of Na channels by divalent cations by measuring inhibition of macroscopic Na^+ current for a series of point mutations at residue 401 of rat μ1 Na channels expressed in X. laevis oocytes. Substitutions of Tyr 401 by Gly, Ala, Ser, Cys, Asp and His produced functional Na^+ currents without major effects on gating or ionic selectivity. High-affinity block by Zn^{2+} (K_i=8-23μM) required Cys, His or Asp, three residues that are commonly found to coordinate directly with Zn^{2+} in metalloproteins. For the μ1 Cys mutant, inhibition of macroscopic Na^+ conductance by Zn^{2+} saturated at 85%-90%, suggesting the presence of a Zn^{2+}-dependent substate current. Ca^{2+} titration of the Asp mutant revealed enhanced affinity for inhibition by Ca^{2+} (K_i=0.3mM vs. 40mM in wild type) and incomplete block saturating at 69% inhibition. The Asp mutant exhibited no change of selectivity. In contrast to Zn^{2+} and Ca^{2+}, Cd^{2+} completely blocked macroscopic current in the Cys mutant, implying that the magnitude of substate current depends on the species of divalent cation and the particular residue at position 401. Substitution with His also resulted in enhanced sensitivity to block by H^+ with a pKa of 7.5 for the introduced imidazole group. These results provide futher evidence for the notion that residue 401 is located in the external vestibule of the Na channel and that divalent cations binding at that position interferes with Na^+ permeation. Functional groups of Cys, His or Asp at this location apparently provide a coordination site which determines the ionic selectivity for external block by various inorganic cations.

W-Pos48

μ-CONOTOXIN BLOCK IN THE Na CHANNEL VESTIBULE ((S. Dudley, G. Lipkind, and H. Fozzard)). Cardiac Electrophysiology Laboratories. The University of Chicago, Chicago, IL 60637.

The conus snail toxin, μ-conotoxin GIIIA (μ-CTX), blocks the adult rat skeletal muscle Na^+ channel (μI) with nanomolar affinity yet apparently does not bind to or block cardiac or brain isoforms. μ-CTX competes with saxitoxin (STX) for a common binding site which is thought to be at the outer vestibule of the ion permeation pathway. Identification of the binding interactions of μ-CTX could refine models of this region. Mutagenesis of the channel has failed to clearly elucidate the binding site, however [Chen et al., 1992. *FEBS Lett* **309**:253]. We predicted a binding site for μ-CTX based on the NMR structure for the toxin and on our model of the tetrodotoxin (TTX)/STX binding site [Lipkind and Fozzard, 1994. *Biophys. J.* **66**:1], but this proposal was challenged by the observation that elimination of a glutamate-403 critical for TTX and STX binding results in minor changes in μ-CTX affinity [Stephan et al., 1992. *J. Membrane Biol.* **137**:1]. Our model was tested by mutating two residues of μ1 to their cardiac analogs. E1524Q (domain IV, S5-6) and D1375N (domain IV, S1-2) had no effect on blocking efficacy. The affinity of μ-CTX for μI, E1524Q, and D1375N at 0 mV was 17 ± 10 nM, 34 ± 10 nM, and 27 ± 14 nM respectively. Nevertheless, reducing the external Na^+ from 90 to 10 mM at a constant ionic strength resulted in an increase in the μ-CTX affinity of E1524Q from 38 to 4 nM consistent with the idea of competition at the channel vestibule. A revised model of the vestibule is consistent with the all of the current mutational results.

W-Pos49

α7 ACETYLCHOLINE RECEPTOR PORE REGION PROBED WITH NONCOMPETITIVE ANTAGONISTS.
((C.D.Patten*, A.V.Ferrer-Montiel°, and M.Montal°))
Depts. of *Physics and °Biology, Univ. of California, San Diego
La Jolla, CA 92093-0357 (Sponsored by John M. Ward)

The M2 transmembrane segment of ligand gated ion channels, a major component of the ionic pore, determines the selectivity for permeant ions and the susceptibility to open channel blockers. However, the specific topology of M2 residues is still unknown. Here we have used three noncompetitive cholinergic antagonists QX-222, MK-801, and PCP together with site-directed mutagenesis to probe the structure of the α7 neuronal acetylcholine receptor (α7AChR) pore region. Threonine 244 on M2 of the α7AChR was mutated to aspartic acid. Homomeric wild type and T244D mutant α7AChR channels were expressed in *Xenopus* oocytes and challenged with the three antagonists in the presence of 50μM acetylcholine. These blockers inhibit wild type α7AChR channel activity with μM inhibition constants in a voltage dependent manner. A ring of negatively charged residues at position 244 increases the efficacy of blockade from 2 to 10 fold at -80mV. This mutant also potentiates the voltage dependence of blockade increasing the fraction of the transmembrane potential felt at the binding site up to 4 fold. These drugs appear, therefore, to penetrate into the pore and interact with pore lining residues. Specifically, the blocker interaction with residue 244 indicates the exposure of this site to the pore lumen. These results substantiate the suitability of pharmacological probes as tools to elucidate pore structure.

(supported by N.I.H. and O.N.R.)

W-Pos50

ARE MOST TRANSPORTERS AND CHANNELS BETA BARRELS? ((J. Fischbarg*^+, M. Cheung^, J. Li^, P. Iserovich^, F. Czegledy#, K. Kuang^, and M. Garner@)). Depts of Physiol.& Cellular Biophysics*, Ophthalmol.^, and Med.#, Coll. of P. & S., Columbia Univ., New York, NY 10032, and Dept. of Ophthalmol.@, Southwestern Health Sci. Ctr., Univ. of Texas, Dallas, TX 75235.

Given the sequence of transporters or channels of unknown secondary structure, it is usual to predict their putative transmembrane regions as alpha-helical. However, recent evidence for a facilitative glucose transporter (GLUT1) has led us to propose an alternative folding model for GLUTs based on the 16-stranded antiparallel β-barrel of porins. We have now extended the predictive algorithms used for GLUTs to several other membrane proteins. Some with known structure (beta barrels: Rhodobacter capsulatus and Escherichia coli porins; multihelical: colicin A, bacteriorhodopsin, and reaction center L chain) were used to test the prediction procedures. The other proteins analyzed (CHIP28, acetylcholine receptor alpha subunit, lac permease, Na^+-glucose cotransporter, shaker K^+ channel, sarcoplasmic reticulum Ca^{2+}-ATPase) represent classes of similar membrane proteins. As with GLUTs, we find that the predicted transmembrane segments of these proteins are consistently shorter than expected for transmembrane spanning α-helices, but are of the correct length and number for the proteins to fold instead as porin-like β-barrels.

W-Pos51

DOMINANT-NEGATIVE SUPPRESSION OF MAMMALIAN DELAYED RECTIFIER K+ CHANNELS BY CO-EXPRESSION OF A TRUNCATED AND TAGGED CHANNEL ((A. Kuznetsov, G.H. Ma , J. Mao, D.J. Ren, J.F. Worley III, M.E. Lancaster, I.D. Dukes and L.H. Philipson)) Univ. of Chicago, Chicago, IL 60637; and Glaxo Research Institute, RTP, NC 27709

We have constructed an epitope-tagged and truncated K^+ channel, termed H1S1myc, derived from the amino terminal and first membrane spanning domain of the delayed rectifier hKv1.5. This sequence includes the recently defined amino terminal recognition sequence for *Shaker*-like K^+ channel subunit assembly and terminates with an octapeptide *c-myc* epitope oriented in the extracellular space. The H1S1 peptide was tested for its ability to suppress the expression of functional hKv1.5 channels in *Xenopus* oocytes and mammalian cells. *Xenopus* oocytes were co-injected with cRNAs encoding hKv1.5 or hKv1.4 and H1S1myc in various combinations and currents determined by the two microelectrode voltage clamp technique. No currents were observed in oocytes injected with only H1S1myc. The large outward currents seen in oocytes injected with hKv1.5 or hKv1.4 alone were suppressed when the oocytes were co-injected with H1S1myc. A representative experiment, at two days after injection, showed the average maximal amplitude of currents in control oocytes was 7.0±1.5 μA, whereas that in the co-injected oocytes was 1.8±0.5 μA, for a suppression of 75%. By five days after injection, four out of five co-injected oocytes had only background levels of maximal current (0.4-0.8 μA). The epitope attached to the H1S1myc peptide will allow immunohistochemical studies of transfected cells. Suppression of functional K^+ currents demonstrates the utility of this system for further studies on the interaction of truncated subunits with functional channel complexes, and for the use of this construct to suppress endogenous currents in mammalian cells.

W-Pos52

SUBUNIT INTERACTIONS IN SHAKER K+ CHANNEL PROBED BY OXIDATION OF ENDOGENOUS CYSTEINE RESIDUES. ((C.T. Schulteis, S.A. John, L. Santacruz-Toloza, A.F. Mock, and D.M. Papazian)) Department of Physiology and IDP Neuroscience, UCLA School of Medicine, Los Angeles, CA 90024 (Spon. by S. Tiwari-Woodruff).

We have previously demonstrated that there are no intrasubunit or intersubunit disulfide bonds linking endogenous cysteine residues in Shaker K^+ channels (Schulteis et al., *Biophys. J. 66*, A107). Exposure of intact, Shaker-expressing, HEK293T cells to oxidizing conditions, however, results in the formation of intersubunit disulfide bonds. Similar results have been obtained by lysing cells without protecting free sulfhydryls. We propose that intracellular cysteine residues are in close enough proximity in the native Shaker channel to form intersubunit disulfide bonds upon exposure to oxidizing conditions. We tested this hypothesis by oxidizing both wild type and mutant Shaker protein in intact cells where native tertiary and quaternary structure is maintained. Transfected and mock transfected HEK293T cells were exposed to 1 mM I_2 for 10-20 min. The reaction was quenched with 5 mM NEM to block remaining free sulfhydryls. Protein was subjected to electrophoresis under reducing and non-reducing conditions, and immunoblot analysis. Disulfide cross-linking was detected by the presence of high molecular weight adducts under non-reducing conditions. Cross-linking was eliminated upon serine substitution of either C96 in the N-terminus or C505 in the C-terminus. In contrast, substitution of both C301 and C308 in the S2-S3 cytoplasmic loop did not eliminate intersubunit disulfide formation. These results indicate that disulfide bonds form between C96 and C505 in adjacent subunits, suggesting that these residues are in close proximity in the native quaternary structure of the channel.

W-Pos53

BIOCHEMICAL EVIDENCE THAT PURIFIED Kv1.3 K+ CHANNEL PROTEIN IS A FUNCTIONAL HOMOTETRAMER.
((R.H. Spencer*, B.K. Takenaka, M. Bruns+, D. Hanson+, G.A. Gutman*, and K.G. Chandy)) Dept. of Physiol. & Biophys. and *Dept. of Micro. & Mol. Genetics, UC Irvine, CA 92717 and +Pfizer Central Research, Groton, CT.

Significant quantities (40-50μg) of nearly homogeneous mKv1.3 K+ channel protein have been previously purified from as few as 10^7 mammalian cells using vaccinia virus (Biophys. J. A343, 1994). Although preliminary evidence from gel filtration experiments suggested that the purified protein was maintained as a tetrameric complex, we have sought to confirm the subunit stoichiometry using sucrose density centrifugation analysis. Based upon the relative sedimentation rate of Kv1.3 protein to 3 different molecular weight standards, we have estimated the molecular mass of Kv1.3 to be approximately 227kDa which is within 8.5% of the expected value for a tetramer of Kv1.3 (monomer=62kDa). To address whether this protein has maintained its functional integrity, a toxin binding assay was performed using [^{125}I]ChTX. Purified protein demonstrated specific ChTX binding using either unlabeled ChTX or MgTX as competitive inhibitors. However, similar to results reported by Sun *et al* (Biochem. 33:9992, 1994), this binding activity appears to degenerate with time. (Supported by grants from Pfizer, Inc. and AI24783)

W-Pos54

USE OF HYDROPHILIC AMINO ACID EPITOPE INSERTIONS TO PROBE THE TOPOLOGY OF THE SHAKER H4 POTASSIUM CHANNEL. ((T.M. Shih and A.L. Goldin)) Department of Microbiology and Molecular Genetics, University of California, Irvine, CA 92717.

The structure of the Shaker H4 potassium channel has been modeled as passing through the cellular membrane eight times with both the N-and C-termini on the cytoplasmic side (Durell and Guy, Biophys.J., 1992, 62:238-250). To test the validity of this structural model, we have inserted an epitope consisting of eight hydrophilic amino acids (DYKDDDDK) in regions throughout the channel. The channels containing the synthetic epitope were expressed in *Xenopus* oocytes, and function was examined by two electrode voltage-clamping. Immunofluorescent staining was used to determine the membrane location of the epitope in each of the insertion mutants. Extracellular epitopes were identified by incubating whole oocytes with the antibody before fixation and fluorescent labeling. Intracellular epitopes were identified by injecting the antibody before fixation and fluorescent labeling. The localization of epitope insertions in the N-terminus, S3-S4 loop, and C-terminus have proved to be consistent with the Durell and Guy model. However, at least one insertion in a proposed transmembrane segment results in functional channels, suggesting that the model is not completely correct in this region. Data concerning the electrophysiological properties of the mutants and localization of the epitopes will be presented.

W-Pos55

FUNCTIONAL CELLULAR EXPRESSION AND *IN VITRO* MULTIMERIZATION OF A KV1.3 DELETION MUTANT. ((L. Tu, Z. F. Sheng, G. Panyi, V. Santarelli, D. Pain and C. Deutsch)) Depts. of Physiology, University of Pennsylvania and Jefferson Medical College, Phila., PA 19104-6085.

Recent work suggests that K^+ channel inter-subunit recognition is mediated by a sequence of amino acids in the cytoplasmic N-terminal region, referred to as the "tetramerization 1" (T1) domain[1-3]. In some cases T1 is essential for assembly and functional expression (e.g. Shaker B[1] and Kv1.1[2,4]). For other isoforms, extensive N-terminal deletion does not abolish functional expression in oocytes (e.g., Kv1.3[5]; Kv1.4[3]; Kv2.1[6]). We have tested a (T1-)-mutant of Kv1.3 (lacking the first 141 amino acids). In oocytes, Kv1.3 (T1-) forms channels with electrophysiological characteristics similar to those of wild-type Kv1.3. These results show that sites in the central core of the homotetrameric human Kv1.3 channel polypeptide are sufficient to permit correct subunit assembly. Unlike the wild-type Kv1.3, Kv1.3(T1-) cannot be suppressed by a truncated Kv1.3 containing only the amino terminus and S1, nor by a truncated Kv1.3 containing only S5, H5, S6, and the C-terminus. Kv1.3(T1-) can form functional channels in mammalian cells, e.g., mouse cytotoxic T cells (CTLL-2) and in human embryonic kidney cells (tsA201). These currents are similar to wild-type Kv1.3, however, the efficiency of Kv1.3 (T1-) expression is lower and recovery from inactivation faster, vis-a-vis wild-type Kv1.3. *In vitro* translation and sucrose gradient analysis of wild-type Kv1.3 and Kv1.3 (T1-) cRNA show that while both form tetramers, Kv1.3(T1-) forms mainly monomers. Wild-type Kv1.3 forms mainly tetramers. These results are consistent with the decreased expression of the Kv1.3(T1-) mutant in mammalian cells. (Supp. GM41467,FOS TWO5079)

References: [1]Li *et al.*, 1992; [2]Shen *et al.*, 1993; [3]Lee *et al.*, 1994; [4]Hopkins *et al.*, 1994; [5]Aiyar *et al.*, 1993; [6]VanDongen *et al.*, 1990

W-Pos56

[^{125}I]MARGATOXIN, AN EXTRAORDINARY HIGH-AFFINITY LIGAND FOR VOLTAGE-GATED K+ CHANNELS IN MAMMALIAN BRAIN.
((R.O.A. Koch, A. Eberhart, C.V. Seidl#, A. Saria#, G.J.Kaczorowski*, R.S. Slaughter*, M.L. Garcia* and H.G. Knaus)). Inst. Biochem. Pharmacol., University Innsbruck, Austria, #Neurochem. Res. Unit, Dept. of Psychiatry, Innsbruck, Austria and *Dept. Membrane Biochem. & Biophys, Merck Res. Lab., Rahway, NJ 07065.

Margatoxin (MgTX) is a 39 amino acid peptide isolated from *C. margaritatus* venom that blocks with high affinity the voltage-gated K^+ channel, $K_v1.3$. [^{125}I]MgTX specifically and reversibly labels a maximum of 0.8 pmol of sites/mg protein in purified rat brain synaptic plasma membrane vesicles with a dissociation constant of 0.1 pM as determined by either equilibrium binding or kinetic binding experiments. Thus, this toxin represents the highest affinity, reversible radioligand for any membrane-bound receptor or ion channel described to date. [^{125}I]MgTX binding is modulated by mono- and divalent cations in a complex manner. Moreover, binding is inhibited by charybdotoxin, α-dendrotoxin, kaliotoxin and the agitoxins I and II, but not by iberiotoxin, suggesting that the receptor site is likely to be associated with a voltage-gated K^+ channel complex, of which the *Shaker*-like K^+ channel, $K_v1.3$, is a prominent component. In the presence of the bifunctional cross-linking reagent, disuccinimidyl suberate, [^{125}I]MgTX is specifically and covalently incorporated into a polypeptide of M_r 75,000 in rat membranes. In rat striatal slices, MgTX evokes a dose-dependent, tetrodotoxin-sensitive dopamine release suggesting that this MgTX-sensitive, voltage-dependent K^+ channel can provide an important repolarization pathway in certain neurons.

W-Pos57

CROSSLINKING OF [^{125}I]CHARYBDOTOXIN TO THE HIGH-CONDUCTANCE Ca^{2+}-ACTIVATED K^+ CHANNEL FROM TRACHEAL SMOOTH MUSCLE.

((P. Munujos, H.-G. Knaus*, A. Eberhart*, G.J. Kaczorowski, and M.L. Garcia)). Dept. Membrane Biochem. & Biophys, Merck Res. Lab., Rahway, NJ 07065 and *Inst. Biochem. Pharmacol., University of Innsbruck, Austria.

Purified high-conductance Ca^{2+}-activated K^+ (maxi-K) channels from tracheal smooth muscle consist of two subunits, α encoded by *mSlo*, and a 31 kDa β-subunit. The β subunit has been cloned and represents the protein to which [^{125}I]charybdotoxin (ChTX) is specifically and covalently incorporated in the presence of a bifunctional crosslinking reagent. Proteolytic digestion of the [^{125}I]ChTX-crosslinked β subunit in conjunction with immunostaining and deglycosylation studies have identified Lys_{69} in the β subunit as the acceptor residue for the crosslinking reaction. These studies have also confirmed the postulated transmembrane topology of the β subunit. To determine which residue in ChTX is involved in the crosslinking reaction and therefore estimate the distance between the extracellular loop of β and the outer vestibule of the maxi-K channel, ChTX mutants in which individual Lys residues had been neutralized were radiolabeled and employed in crosslinking experiments. All these ChTX mutants bind to maxi-K channels with the same characteristics as ChTX. However, the mutant in which Lys_{32} had been neutralized failed to incorporate into the β subunit upon addition of several crosslinking reagents. Since Lys_{32} in ChTX appears to be located above the wall of the outer vestibule that is formed by the α subunit (Stampe et al., Biochemistry 33, 443-450 (1994)), these data place at least a region of the extracellular loop of β at a maximum distance of 7.7 Å from the outer vestibule and they are consistent with the finding that β does not contribute to the receptor site for ChTX.

W-Pos58

BINDING OF MONO- AND DI-IODINATED MARGATOXIN TO HUMAN PERIPHERAL T LYMPHOCYTES AND TO JURKAT PLASMA MEMBRANES.

((J.P. Felix, R.M. Bugianesi, A.A. Abramson and R.S. Slaughter)) Merck Research Laboratories, Rahway, NJ 07065

Margatoxin (MgTX) is a potent, selective inhibitor of lymphocyte voltage-gated potassium channels (K_v1.3). This 39 amino acid peptide has now been iodinated by a lactoperoxidase-glucose oxidase (Enzymobeads™) treatment. By varying concentrations of reagents, MgTX can selectively be mono- or di-iodinated. For resting human T lymphocytes and for plasma membranes prepared from Jurkat cells, binding parameters at physiological monovalent salt concentrations (106 mM NaCl, 4.6 mM KCl and 10 mM HEPES, pH 7.4) are, respectively: [^{125}I]$_2$MgTX, K_d, 8 pM, 7 pM; [^{125}I]MgTX, K_d, 30 pM, 42 pM; B_{max}, both forms, 400 sites/cell, 100 fmol/mg protein. These data define a surprising inverse relationship for binding to lymphocytes where [^{125}I]MgTX is less potent than [^{125}I]$_2$MgTX. External KCl (3 - 10 mM) is required for binding to Jurkat plasma membranes and enhances binding to intact, resting T cells. Higher concentrations of KCl are inhibitory. Reduction of NaCl concentration from standard conditions results in increased potency of Jurkat membrane binding to K_d's of 1 pM for [^{125}I]$_2$MgTX and 5 pM for [^{125}I]MgTX. Ca^{2+} and Mg^{2+} inhibit binding with IC_{50}'s of 0.5 mM and 1 mM, respectively, at high salt. The binding data for Jurkat membranes contrasts with that for rat brain synaptic membranes where [^{125}I]MgTX binds in high salt with an affinity of 1 pM and [^{125}I]$_2$MgTX has a K_d of about 5 pM (cf Koch, et al).

W-Pos59

ANALYSIS OF IRK1 USING AN *IN-VITRO* TRANSLATION SYSTEM

((Deborah L. Laidlaw, K. George Chandy and George A. Gutman*)) Department of Physiology and Biophysics, and *Department of Microbiology and Molecular Genetics, University of California, Irvine, California 92717

IRK1 is an inwardly rectifying potassium channel cDNA clone from the J774.1 macrophage cell line. The 47 kDa protein contains two putative transmembrane regions and a pore region homologous to other K^+ selective ion channels. Previous studies of voltage gated K+ channels have shown that the channels function as tetramers and it is reasonable to hypothesize that IRK1 may also funciton as a multimer. Determination of the multimeric nature of the IRK1 channel could be accomplished if small quantities of the protein could be obtained in relatively pure form. We have previously shown that substantial amounts of Kv1.3 channel protein can be obtained using a vaccinia virus expression system and this method is also being pursued for purification of the IRK1 protein (Laidlaw et al Biophysical Abstracts, 1993 and Spencer et al, Biophysical Abstracts, 1994). Presently, a rabbit reticulocyte *in-vitro* translation system has allowed us to obtain nanogram quantities of relatively pure radiolabeled (^{35}S-methionine) IRK1 protein. While the yield of protein from the *in-vitro* translation system is not enough for extensive structural studies, preliminary studies on subunit association are possible. The native IRK1 clone and an engineered IRK1 clone containing the antigenic Gene10 site will be used in conjunction with this translation system to study the association of subunits into functional channels. The relative molecular weight of the functional channel will be estimated using sucrose gradient and Western blot techniques. (Supported by grants from the NIH [AI-24783] and Pfizer Inc.)

W-Pos60

SPLICE VARIANTS OF ROMK1, A HUMAN INWARDLY RECTIFYING K^+ CHANNEL

((R.L. Martin, H. Yano, J. Takeda, and D.A. Hanck)) The Univ. of Chicago, Chicago, IL.

ROMK1 was cloned from an adult human kidney cDNA library. The gene has 5 exons and 3 ATG sites. Alternative splicing produces 4 variants, and translation can be initiated at each of 3 ATG's resulting in the occurrence of 3 coding sequences with different N-termini (B&C make same protein). These ROMK1 variants were studied in *Xenopus* oocytes with either two microelectrode voltage clamp or single electrode voltage clamp in the cell-attached patch configuration. In 2.5 mM external K^+, the resting potentials of the oocytes expressing each splice variant were -87.3 ± 1.7, -84.2 ± 1.1, -86.0 ± 2.7. Although not significantly different from each other, these values were different from uninjected oocytes (-40 mV). Expressed channels from the 3 splice variants were stable during 120 min recording periods, and all displayed weak inward rectification. Inward currents, elicited during a 300 ms voltage step, were blocked completely by 200 μM external Ba^{2+}, whereas outward currents displayed more interesting block behavior. The current was initially blocked by Ba^{2+} in a concentration dependent manner, but with continued depolarization, the outward currents showed relief from block. Because all variants expressed well in oocytes and no electrophysiological differences were found between them, we suggest splice variants may be used for controlling expression of the channel rather than modifying its function.

	Liver	Kidney	Heart	Spleen	Islets
A	++	+++	+++	+	++
B	—	+	—	—	—
C	—	++	—	—	—
D	++	+++	+	+	++

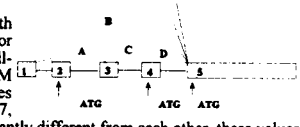

W-Pos61

CHARACTERIZATION OF THE α-SUBUNIT OF THE HIGH-CONDUCTANCE Ca^{2+}-ACTIVATED K^+ CHANNEL FROM TRACHEAL SMOOTH MUSCLE.

((H.-G. Knaus, A. Eberhart, P. Munujos*, G.J. Kaczorowski* W.A. Schmalhofer*, J.W. Warmke#, and M.L. Garcia*)). Inst. Biochem. Pharmacol., University Innsbruck, Austria & Depts. Membrane Biochem. & Biophys* and Animal Biochem. & Molec. Biology#, Merck Res.Lab., Rahway, NJ 07065.

Purified high-conductance Ca^{2+}-activated K^+ (maxi-K) channels from tracheal smooth muscle have been shown to consist of a 60 - 70 kDa α-subunit, encoded by *mSlo*, and a 31 kDa β-subunit. The size of the α-subunit is smaller than that predicted from the *mSlo* coding region. To determine the basis for this discrepancy, sequence-directed antibodies against *mSlo* have been raised. Immunostaining experiments employing tracheal smooth muscle membranes and these antibodies reveal that the α-subunit possesses an apparent molecular weight of 120 kDa. The difference between the size of the α-subunit in membranes and in the purified preparation is due to a highly reproducible proteolytic decay that occurs at an advanced stage of the maxi-K channel purification. In some purified maxi-K channel preparations, the full length α-subunit, an intermediate form of 85-90 kDa, and the 60-70 kDa polypeptide, as well as smaller size fragments can be detected. Proteolysis occurs exclusively at two distinct positions within the long carboxyterminal tail of *mSlo*. *In-vitro* translation or expression of *mSlo* in *COS-7* cells yields an α-subunit of 135 kDa which is of significantly higher M_r than the membrane-expressed *mSlo* product. This finding could be due to either post-translational processing, proteolysis during membrane preparation, or the existence of some as yet unidentified splice variants in tracheal smooth muscle.

W-Pos62

Heterologous Expression of a Potassium Channel in Clonal Mammalian Cells by Direct Microinjection of cDNA.

((J. Ashot Kozak, Kim W. Chan, Jinliang Sui and Diomedes E. Logothetis)) Department of Physiology and Biophysics, Mount Sinai School of Medicine, CUNY, New York, NY. 10029.

Efficient heterologous expression of ion channels in clonal mammalian cells is highly desirable for structure-function studies. Current techniques have mainly employed traditional transient or stable transfection protocols. These methods are rather impractical due to the length of time required to obtain cells expressing the transfected DNA. Direct microinjection of either cRNA of voltage-gated K channels or cDNA of a voltage-gated Na channel into clonal cells has been shown to be successful (Ikeda *et al.*, 1992; West et al., 1992). We have compared the efficiency of heterologous expression of a human pancreatic ATP-sensitive non voltage-dependent K channel (hpK_{ATPI}) in clonal mammalian cells both by stable transfection methods and by direct microinjection of cDNA. We subcloned hpK_{ATPI} in the eucaryotic expression vector pMT2. Chinese hamster ovary (CHO) clonal cells were microinjected with hpK_{ATPI} using an Eppendorf microinjection system. DNA was injected at a concentration of 0.06 μg/μl with micropipettes fabricated with a Flaming-Brown puller (Sutter Instruments). Patch recordings 20-30 hours following injection showed multiple single channel activity from most injected cells. The conductance and bursting kinetics of hpK_{ATPI} channels were identical to those obtained from stably transfected CHO cells (see abstract by Chan *et al*) and matched those reported for native K_{ATP} channels from pancreatic β cells . HeLa cells have also successfully expressed hpK_{ATPI} following cDNA microinjection. We are currently, testing a number of recombinant channels and clonal cell lines to compare the efficiency and time course of expression.

W-Pos63

CLONING AND FUNCTIONAL EXPRESSION OF A HUMAN HEART INWARD RECTIFIER, hIRK1.((LS Wood, TD Tsai, KS Lee and G Vogeli)) Cardiovascular Pharmacology, Upjohn Laboratories, Kalamazoo, MI 49007

We have isolated a cDNA clone from a human fetal heart library for the human inward rectifying potassium channel (hIRK1). The nucleotide sequence of the coding region is 88% similar to the mouse clone with only 7 amino acid changes. The human clone was modified for expression of its mRNA in Xenopus oocytes. The initial human construct expressed very low levels of protein, but the addition of a SmaI site 3' of the poly(A) tail increased the level of protein expression at least 10 fold. *Xenopus* oocytes injected with 45 nl of 30 to 100 ng/µl of hIKK1 cRNA developed resting membrane potential averaged -96.4 ± 1.3 mV. Currents recorded by the two microelectrode voltage clamp technique from hIKR1 injected oocytes bathed in 50 mM external K^+ solution displayed large inward current of 50 µA at -120 mV, but decreased linearly with voltage towards E_K. Positive to E_K, the outward current rectified strongly inward. Complete blockade of hIRK1 channel at -100 mV required 10 mM Cs^+ but only 0.3 mM Ba^{2+}. Both ions produced voltage and time dependent channel block. The relationship of E_K per decade external K^+ concentration $[K]_o$ had a slope of 54.6, and that for channel conductance can be approximated by a square root function, with exponent factor of 0.3. Cell attached single channel conductance in 140 mM K^+ pipette solution averaged about 29.3 ± 0.8 pS (n=10). We conclude that hIRK1 can be expressed in *Xenopus* oocytes and the channel shares typical characteristics of cloned inward rectifiers reported earlier.

W-Pos64

HEIGHTENED EXPRESSION OF A NOVEL K^+ *SHAKER*-RELATED CHANNEL (KV1.7) IN DIABETIC β-CELLS: POTENTIAL ROLE IN IMPAIRED INSULIN SECRETION IN DIABETES. ((Katalin Kalman, Julie Tseng-Crank*, Iain D. Dukes*, Grischa Chandy, Mary E. Lancaster*, Robert H. Spencer, Jayashree Aiyar, George A. Gutman, K. George Chandy)) Dept. Physiology and Biophysics, UC Irvine, CA 92717; *Glaxo Res. Inst., Research Triangle Park, NC 27709

Non-insulin-dependent diabetes mellitus (NIDDM) is a metabolic disease of unknown etiology, typified by defects in both insulin secretion and insulin action. Ion channels in pancreatic islet β-cells are the primary elements coupling nutrient signals to the regulation of insulin secretion; although drugs affecting these channels are used for the therapeutic management of NIDDM, the genes encoding them have not yet been identified. We have previously reported the cloning of a novel, *Shaker*-related voltage-gated K^+ channel gene, Kv1.7, that is expressed in β-cells. *In-situ* hybridization demonstrated the presence of Kv1.7 mRNA in islet cells of normal mice, and increased expression in islet cells from diabetic C57BL/KsJ(*db/db*) mice, a model for NIDDM. Whole-cell current recordings showed a parallel increase in a TEA-resistant K^+ current in diabetic *db/db* β-cells. TEA caused increased *in vitro* insulin secretion in control *db/+* and pre-diabetic *db/db* mice, but not from diabetic, hyperglycemic *db/db* mice. Our results are consistent with the idea that the transition to the diabetic state in NIDDM is associated with overexpression of Kv1.7, and that delayed rectifier K^+ channels play an important role in the regulation of β-cell glucose signaling.

W-Pos65

INACTIVATION KINETICS OF A CLONED CARDIAC K^+ CHANNEL COEXPRESSED WITH A ß-SUBUNIT CLONED FROM FERRET VENTRICLE ((R.C. Castellino, M.J. Morales, D.L. Campbell, H.C. Strauss and R.L. Rasmusson)) Duke University Medical Center, Durham, NC 27710.

We have recently isolated a K^+ channel ß-subunit (Kvß3) from ferret ventricle which alters inactivation rate when coexpressed with the ferret ventricular Kv1.4 channel (FK1). It shares some similarity to a ß-subunit (Kvß1), isolated from rat brain, which increases the rate of inactivation of Kv1.1 and Kv1.4 channels (Rettig et al. 1994. Nature 369, 289.). The inactivation properties of this subunit were conferred by its amino terminal, and were shown to operate via a "ball and chain" mechanism similar to that which mediates N-type or fast inactivation intrinsic to the α-subunit of some K^+ channels. However, Kvß3 displays no sequence similarity in the first 80 NH_2-terminal amino acids to Kvß1. Inactivation of FK1 has been previously shown to be biexponential with two closely spaced time constants at +50 mV. The time constant of the fast component of inactivation decreased from 42±3 msec (n=20) for FK1 alone to 6.2±0.2 msec (n=28) for the coinjected oocytes. The time constant of the slow component (313±94 msec) was decreased to 101±2 msec when FK1 was coexpressed with Kvß3. Steady-state voltage dependence of inactivation of FK1 was relatively unaltered by coexpression with Kvß3. The voltage dependence of time constants of fast inactivation of FK1 was altered by coexpression with Kvß3. The fast time constant of inactivation in FK1 was voltage insensitive in the range 0 to +60 but became strongly voltage dependent when coexpressed with Kvß3 changing from 59±8 msec at 0 mV to 5.1±0.3 msec at +60 mV. In conclusion, Kvß3 alters both the time and voltage dependence of inactivation of Kv1.4.

W-Pos66

MOLECULAR CHARACTERIZATION OF A VOLTAGE INDEPENDENT $K(Ca^{2+})$ CHANNEL OF SMALL CONDUCTANCE IN HeLa CELLS. ((R. Sauvé, L. Garneau, S. Cai and H. Klein)) Membrane Transport Research Group, Dept. of Physiology, Univ. Montréal, Montréal, Canada H3C 3J7. (Spon. by G. Roy)

Our previous works on HeLa cells have provided evidence for a voltage independent 50 pS $K(Ca^{2+})$ channel characterized by an inward rectifying I/V curve. The present study was aimed at establishing 1) how the pharmacological and phosphorylation properties of this channel differed from those reported for the putative Maxi $K(Ca^{2+})$, and 2) to what extent the amino acid sequence for the 50 pS $K(Ca^{2+})$ is homologous to that obtained for the human $K(Ca^{2+})$ channel of large conductance. Our results essentially indicate 1) that the $K(Ca^{2+})$ in HeLa channel is insensitive to ChTx(40 nM), apamin (1 µM), 4-AP (10 mM) and TEA (20 mM), but can be blocked by d-tubocurarine (2 mM); 2) that cytosolic addition of NaF (10 mM) in the presence of 500 µM deferoxamine (Al^{3+} chelator) increases channel activity (11/20) whereas phosphatase alkaline (300 U/ml) inhibits channel activation and 3) that the open channel probability is not modified by PKA. In addition, RT-PCR carried out on $polyA^+$ mRNA from HeLa cells with primers derived from the Maxi $K(Ca^{2+})$ S3 and S6 sequences yielded a single band of expected size. DNA sequence analysis indicated that the resulting PCR product was identical to the human Maxi $K(Ca^{2+})$ channel. This observation does not therefore support the electrophysiological data obtained on HeLa cells where no $K(Ca^{2+})$ channels other than the 50 pS $K(Ca^{2+})$ were observed. Supported by the Medical Research Council of Canada.

W-Pos67

ON THE ORIGIN AND ROLE OF CLONED INWARDLY RECTIFYING K^+ CHANNELS IN MOUSE BONE MARROW OSTEOCLAST / OSTEOBLAST COCULTURES. ((D.L. Ypey, K. Folander, G. Weselowsky, H. Tanaka, R. Nagy, G. Rodan, R. Swanson, and L. Duong)) Merck Research Laboratories, West Point, PA 19486.

We have previously reported the cloning of a cDNA encoding a sequence variant of IRK1 from a co-culture of mouse bone marrow cells and the osteoblastic cell line, MB1.8. In the presence of $1,25(OH)_2D_3$, osteoclast (OCL) formation is observed after 7 days in this co-culture. We further demonstrated the presence of an inwardly rectifying K^+ conductance (G_{IRK}) in the co-culture derived OCLs. We have now investigated the cellular origin of this co-culture IRK channel and its possible role in osteoclast formation. Whole-cell patch-clamp experiments were carried out on the isolated MB1.8 cells. The Na^+, K^+, and Ca^{2+} concentration gradients across the membrane were of normal asymmetry. Under these conditions, a G_{IRK} was found in at least 25% of the cells, whether they were maintained in the presence (n=15) or absence (n=8) of $1,25(OH)_2D_3$. The observed inwardly rectifying K^+ conductance shifted its voltage activation range with external $[K^+]$ and was reversibly blocked by 5 mM external Cs^+ or Ba^{2+}. Furthermore, OCL formation in the co-culture, estimated by the number of tartrate resistant acid phosphatase positive multinucleated cells, was inhibited by extracellular Cs^+ with an IC_{50} = 1-3 mM (n=4). These results suggest the possible origin of the coculture IRK1 clone from either MB1.8 cells or OCLs and suggest a role for inwardly rectifying K^+ channels in osteoclast formation.

W-Pos68

REGULATION OF RAT EAG POTASSIUM CHANNELS ((J. Ludwig, J. Roeper, C. Stansfeld, R. Weseloh and O. Pongs)) ZMNH, Martinistraße 52, D-20251 Hamburg, FRG. (Spon. by C. Methfessel)

The protein encoded by the *Drosophila eag* locus defines a new class of voltage dependent potassium channels that share sequence and structural similarities with cyclic nucleotide-gated channels. We recently described the cloning of a rat homologue (rat *eag*) of *Drosophila eag* and electrophysiological properties of this channel expressed in *Xenopus* oocytes. To study the regulation of rat eag, we constructed a mammalian cell line from human embryonic kidney 293 cells stably expressing rat *eag* protein. Depolarisation of the membrane of this cells gives rise to a non-inactivating, potassium selective outward current. In whole-cell patch clamp recordings, this current exhibits a rapid 'rundown' during dialysis of the cell. Rundown can be prevented by adding reducing agents (DTT or glutathione) and ATP to the pipette solution. Non hydrolyzable analogues of ATP, cAMP and cGMP have no effect. The phosphatase inhibitor, okadaic acid, is capable of decreasing the rate of rundown in the absence of ATP. Therefore proper phosphorylation of rat *eag* seems to be necessary for channel activity. This phosphorylation is probably not mediated by CaM-kinase II, since addition of the calmodulin antagonist trifluoperazine to the intracellular solution does not increase rundown in the presence of ATP. Calcium on the other hand regulates rat *eag* activity via another pathway: Increasing free Ca2+ in the pipette solution from 20 to 200 nM markedly increases the rat *eag* mediated current and accelerates activation kinetics.

W-Pos69

FUNCTIONAL PROPERTIES OF A CLONED INWARD RECTIFIER K+ CHANNEL FROM THE CHICK COCHLEA. ((D.S. Navaratnam, L. Escobar*, M. Covarrubias* and J.C. Oberholtzer)) Dept. Path. & Lab Med., Univ. Penna. Sch. Med., Phila., PA. 19104; *Dept. Path. & Cell Biol., Jefferson Med. Col., Phila., PA. 19107. (Spon. by Zu-Fang Sheng).

We have isolated a cDNA clone encoding an inward rectifier K^+ channel from the chick cochlea (cIRK-1). As suggested from electrophysiological studies *in vivo* (Fuchs & Evans, *J Physiol* **429**: 529, 1990), we have found that transcripts encoding this channel appear to be expressed preferentially in the apical region of the basilar papilla (the chick auditory receptor epithelium). Functional expression in *Xenopus* oocytes revealed currents that exhibit pronounced inward rectification at membrane potentials above E_K, and a single channel conductance of ~20 pS. Structurally and functionally, cIRK-1 is highly homologous to mIRK-1 (Kubo et al, *Nature* **362**: 127, 1993). However, cIRK-1 was found to be less sensitive to external Ba^{2+} and Cs^{2+} block (K_{app}~20 and 30 μM, respectively). We have identified a single amino acid residue (glutamine 125 in cIRK-1) which is responsible for this difference. Glutamate occupies the corresponding position in both mIRK-1 and ROMK-1 (Ho et al, *Nature* **362**: 31, 1993). Mutation of Gln^{125} to Glu resulted in an approximately five-fold increase in sensitivity to both Ba^{2+} and Cs^{2+}. This mutation did not affect either the current kinetics or inward rectification.

This work supported by the NIDCD and the Pennsylvania Lions Hearing Research Foundation (JCO) and the NINDS (MC).

W-Pos70

CHARACTERIZATION OF A CLONED HUMAN 'MAXI' K_{Ca} (*hSlo*) CHANNEL USING PATCH CLAMP AND BILAYER TECHNIQUES. ((*M. Ottolia, *P. Meera, *M. Wallner, §R. Latorre, *E. Stefani, and *L. Toro)) *UCLA, Los Angeles, CA 90024. §CECS and Univ. Chile, Santiago 9, Chile.

cDNA encoding functional maxi K_{Ca} channel α subunit cloned from human myometrium (*hSlo*) were expressed in *Xenopus laevis* oocytes. The cloned channel displayed characteristics typical of native maxi K_{Ca} channel, including calcium sensitivity, kinetics and pharmacology. Single channel conductance was 289 ± 13 pS (n=9) in patches and 279 ± 5 pS in lipid bilayers (110 mM KCl). *hSlo* K_{Ca} channels were blocked by external charybdotoxin and iberiotoxin with a K_d of 20 nM and 1.9 nM (20 mV), respectively. TEA was effective in blocking channel opening. For external TEA the K_d was 248 ± 15 μM and for internal TEA was 50 ± 3 mM, (40 mV). Glibenclamide, pinacidil, lemakalim (10 μM), apamin (100 nM) and 4-aminopyridine (10 mM) were unable to evoke an effect, while external niflumic acid (100 μM) activated *hSlo* K_{Ca} channels. No significant differences were found in the voltage- and calcium-sensitivities using either of these techniques. Single channel activation curves gave an effective valence of 2.4 ± 0.5 (n=18) in lipid bilayers and 1.8 ± 0.7 (n=25) in patches; whereas analysis of steady-state macroscopic currents gave a value of 1.8 ± 0.35 (n=17). The apparent calcium affinity ($K_{1/2}$) at constant voltage (-10 mV) ranged from 10-20 μM with a Hill coefficient of 1.9 ± 0.28, either in patch or in bilayers. Finally, we found a linear relationship in semi-log plot between $V_{1/2}$ and $[Ca^{2+}]i$ in the range of 20 nM to 5 mM. Channels with similar characteristics as those from *hSlo* have been recorded in myometrium. Supported by NIH HL47382, GM50550, and FNI 1940227.

W-Pos71

CHARACTERIZATION OF CLONED SQUID KV2 K^+ CHANNELS EXPRESSED IN *XENOPUS* OOCYTES.((D.E. Patton, E. Perozo* and F. Bezanilla)), Dept. of Physiology, UCLA. School of Medicine, Los Angeles, CA 90024;*Centro de Biofisca y Bioquimica, IVIC, Caracas, Venezuela.

We have electrophysiologically characterized 2 Kv2 family K^+ channels (sqKv2a and sqKv2b) assembled from cDNA clones isolated from the brains and optic lobes of the squid *Loligo pealei* (Silva and Bezanilla 1994, *Biophys J.*,66:A105). These 2 channels have different carboxy termini which are likely due to alternative splicing. The channels also differ from one another by single amino acid substitutions at 3 other positions. Macroscopic and gating currents were recorded using the cut-open oocyte vaseline-gap technique and single channel currents were recorded using cell attached patches. G(V) relationships were determined isochronally from peak tail currents recorded in 60 mM external K^+ and the data were fit with 2 Boltzmann functions in parallel. The voltage dependent parameters for the 2 channels were similar except that sqKv2b had a midpoint voltage for the high valence component that was about 7 mV positive to sqKv2a (-34 mV vs -41 mV). The deactivation rate for sqKv2b was twice that measured for sqKv2a at -100 mV. Gating currents were recorded from oocytes expressing sqKv2a by replacing both internal and external K^+ with TEA. The Q(V) relationship had a midpoint at -55 mV. As expected, sqKv2b is approximately 40 fold more sensitive to external block by TEA as compared to sqKv2a (sqKv2a contains cysteine at a position in the P region equivalent to 449 in *Shaker*, whereas sqKv2b contains tyrosine at this position). Single channel currents were recorded using symmetrical 120 mM K^+. The single channel current-voltage relationships and conductances for the two channels were similar with both channels showing inward rectification and conductances of about 30 pS at 0 mV. Supported by USPHS grants GM30376 and NS07101.

W-Pos72

ALTERNATIVE UTILIZATION OF TWO POLY-A SIGNALS GENERATES THE 3.5 AND 4.5 kb Kv1.4 mRNAs. ((R.S. Wymore, K. Kalman, A. Nguyen, P. Joson, S. Grissmer, K.D. Kinoshita, S.S. Lin, G.A. Gutman*, and K.G. Chandy)) Dept. of Physiology and Biophysics, and *Dept of Microbiology and Molecular Genetics, UC Irvine, 92717.

Kv1.4 is expressed in the brain and the heart as 3.5 or 4.5 kb mRNAs. Genomic probes corresponding to exon 1, the coding region, and the 3'-NCR (Wymore *et al.*, Genomics 20:191, 1993), hybridize to both transcripts in the Northern blot assays. The 3' NCR contains two polyadenylation signals: the first lies 0.5 kb from the end of the coding region while the second is approximately 1 kb further downstream. A genomic probe 30 bp downstream to the signal-1 hybridized only to the 4.5 kb mRNA. A probe immediately downstream to signal-2 did not hybridize to either transcript, although it hybridized to the Kv1.4 genomic clone. These results suggest that the 3.5 kb mRNA ends at signal-1 while the 4.5 kb transcript ends at signal-2. The 5'-NCR contains numerous AUGs which could alter translation. Experiments are in progress to examine their role. Using the vaccinia transfection-infection expression system, we have characterized the biophysical and pharmacological properties of Kv1.4 expressed in mammalian cells. (Supported by AI24783 and Pfizer Inc.)

W-Pos73

MAPPING THE 5'NCR OF MKV1.3 AND LOCALIZATION OF ITS PROMOTER WITHIN A GC-RICH ISLAND. ((Mariella T. Simon, Edward E. Conley, George A. Gutman, George K. Chandy)). Depts. of Phys. & Biophys. and Micro. & Mol. Gen., UC Irvine, CA 92717-4560.

Kv1.3, a Shaker-related gene, encodes the biophysically well characterized type *n* channel in T lymphocytes. Although several distinct Kv1.3 transcripts have been described, none have been mapped, and little is known about the cis-acting elements that control transcription. As a first step, a 4.1 kb EcoRI/HindIII genomic fragment of Kv1.3, containing the entire intronless coding region, was cloned into the MEL vector (containing a hemoglobin locus control region which can activate putative promoters). Transcription of the Kv1.3 gene and expression of Kv1.3 currents followed transfection into murine erythroleukemia cells, suggesting the promoter lay within the 4.1 kb fragment. In further studies we engineered 5' flanking fragments into Promega pLuciferase-enhancer vectors (containing a SV40 enhancer which can activate putative promoters). Transcription of the luciferase gene by the mKv1.3 promoter followed transfection into cultured NIH-3T3 cells, and the subsequent production of the luciferase enzyme was determined by a fluorimetric assay. Deletion analysis indicate that the promoter lies within a GC-rich 120 bp SmaI/SacI fragment lacking a TATA box, a feature characteristic of promoters of housekeeping genes, growth-related genes, and oncogenes, and contains the motif GGGCGG (which forms part of the HMG-CoA reductase promoter) repeated three times along with a SP1 site. The "promoter" region is positioned 150 bp upstream of the coding region. Comparison of the genomic and cDNA sequences indicates that this region is intronless like the coding region. (Supported by grants from Pfizer, Inc. and the NIH [AI24783])

W-Pos74

THE TRANSCRIPTIONAL REGULATORY ELEMENTS OF MOUSE Kv1.4 LIE WITHIN A CpG-RICH ISLAND. ((Keith D. Kinoshita, Randy S. Wymore, George A. Gutman*, K. George Chandy)) Department of Physiology and Biophysics, and *Department of Microbiology and Molecular Genetics, University of California Irvine, Irvine, CA 92717-4560. (Spon. by M. Estacion)

The voltage-gated K^+ channel gene, mKv1.4, is expressed in the heart and brain. To identify the mKv1.4 promoter, 5'-flanking regions upstream of exon 1 (Wymore et al., *Genomics*, 20, 191, 1993) were engineered into Promega pLuciferase-enhancer vectors (containing a SV40 enhancer which can activate putative promoters). Transfection of the enhancer constructs either into cultured NIH-3T3 cells or African green monkey kidney cells, CV-1, followed by transcription of the luciferase gene by the mKv1.4 promoter , and the subsequent production of the luciferase enzyme was determined by a fluorimetric assay. Initial deletion analysis indicated that the promoter lay within a 480 bp CpG-rich PstI fragment lacking a TATA box, a feature characteristic of promoters of housekeeping genes, growth-related genes, and oncogenes. Since two smaller sub-fragments of this PstI fragment, generated by PCR, were found to lack promoter activity, we focused our attention on the 125 bp located at the 3'-end of the PstI fragment. This region contained the motif CCCGCC (which forms part of the HMG-CoA reductace promoter) repeated three times (two being in tandem), along with SP1 and AP2 sites and a CCAAT-enhancer binding motif. Further studies are ongoing to precisely delineate the promoter/enhancer complex of this gene. (Supported by grants from the NIH [AI-24783] and Pfizer Inc.)

W-Pos75

CLONING, EXPRESSION AND DISTRIBUTION OF HUMAN Ca^{2+}-ACTIVATED K^+ CHANNEL α- AND β-SUBUNITS. ((Peter H. Reinhart[1], Julie Tseng-Crank[2], Jeffrey D. Krause[1], Robert Mertz[2], Nathalie Godinot[2], Timothy J. DiChiara[1] and Christine D. Foster[2].)) [1]Dept. of Neurobiology, DUMC, P.O. Box 3209, Durham, NC 27710.and [2]Dept. of Cell Physiology, Glaxo Research Institute, RTP, NC 27709

Large conductance Ca^{2+}-activated K^+ channels couple chemical signaling to electrical signaling, and are found in virtually every cell type examined. To define the distribution of functionally different Ca^{2+}-activated K^+ channels we have cloned and expressed cDNA encoding nine Ca^{2+}-activated K^+ channel isoforms from human brain. All isoforms possess significant identity with the *slowpoke* gene products of *Drosophila* (*dslo*) and mouse (*mslo*). Isoforms are generated by alternate splicing of a single gene located on chromosome 10 at band q22.3 (*hslo*). The *hslo* gene encodes proteins ranging in size from 1154 to 1195 amino acids. RNA splicing of *hslo* occurs at 4 sites in the carboxy-terminal portion of the protein. Two of these splice sites are unique to the human gene, while the other 2 are conserved between mouse and human. The splice variants differ dramatically in their expression pattern and in their sensitivity to Ca^{2+}. Most notably 2 variants differing in only 4 amino acids demonstrate a 4-fold difference in Ca^{2+} sensitivity. Cloning of the human Ca^{2+}-activated K^+ channel β-subunit has shown significantly higher expression levels in human smooth muscle than in human brain. We are currently determining the role of β-subunits in regulating the activity of α-subunits. Work supported in part by NIH grant # NS31253 to PHR.

W-Pos76

AN INWARD RECTIFIER CLONED FROM A HAMSTER INSULINOMA CELL LINE; COMPARISON WITH IRK1. ((Collins, A., Zhao, B., Jan, Y.N. and Jan, L.Y.)). HHMI and Dept. of Physiology, UCSF, CA 94143-0724

An inwardly rectifying potassium channel with 60% amino acid sequence identity to IRK1, designated IRK3(HIT), was cloned from the hamster insulinoma-derived HIT T15 cell line. Expression of IRK3(HIT) in Xenopus oocytes induced a strongly-rectifying potassium current with a single channel conductance of 10 pS and a sensitivity to voltage-dependent block by 300 μM external Ba^{2+}. In cell-attached giant patches (inner tip diameter 15-40 μm), inward current activated with an instantaneous component followed by a rising phase described by a single exponential. The magnitude of the instantaneous component was 90% of the maximum current upon repolarization from a prepulse potential of -25 mV (V_m-E_k); this decreased to 30% as the prepulse potential was increased to +35 mV, according to a Boltzmann function. As the duration of the depolarising prepulse was increased incrementally between 0.1 and 1 ms, the instantaneous component decreased with a time constant of ~700 μs for prepulses of +15 mV and ~270 μs for +45 mV. The activation time constant increased from 0.3 ms at -75 mV to 1.4 ms at -25 mV. In the same preparation, the activation rates of IRK1 currents had a similar voltage dependence, but were faster than IRK3(HIT) currents at a given membrane potential. This work was done during the tenure of a research Fellowship from the American Heart Association, California Affiliate to A. Collins.

W-Pos77

EXPRESSION OF TWO K CHANNEL mRNAS FROM CLONED SQUID SEQUENCES. ((JC Rosenthal, MA Perri, and WF Gilly)) Department of Biology; Hopkins Marine Station of Stanford University, Pacific Grove, CA 93950.

Squid giant fiber lobe (GFL) neurons express two Shaker-type (Kv1) mRNAs, KZ4 and KZ18. The predicted proteins differ only in that KZ18 lacks the first 11 amino acids of KZ4 (excluding the initial met) and shows 8 other differences, all but one of which occur near the amino terminal. None of the differences occur in regions known to determine functional attributes. We report the expression of both K channel types by microinjection of cRNA into Xenopus oocytes and detection of resultant K currents (I_k) by 2-electrode voltage clamp. I_k from both cRNAs thus far have proven indistinguishable. Steady-state voltage dependence matches that of Ik in GFL neurons studied with whole cell patch clamp, and activation kinetics of the cloned channels are similar to but slightly slower than, those seen with GFL neurons at the same temperature. Very similar I_k also exist in large non-GFL neurons in the stellate ganglion that express KZ18 but not KZ4, as demonstrated by in situ hybridizations. Properties of activation gating of the cloned K channels thus appear to match those in the cell types which express these mRNAs. Inactivation properties are more complex however, and differences in rate and extent of Ik inactivation exist between axonal and somatic domains of GFL neurons and between each of these and oocytes.

W-Pos78

CLONING AND CHARACTERIZATION OF GIRK ISOFORMS FROM RAT ATRIA. ((Liangxue Zhu, Michael Bin Wu, Xiaying Wu, Jinliang Sui, Diomedes E. Logothetis, and William B. Thornhill)). Department of Physiology and Biophysics, Mount Sinai School of Medicine, New York, NY 10029.

Parasympathetic stimulation causes a decrease in heart rate via activation of a muscarinic G-protein-coupled K^+ channel (I_{KACh}) in atria tissue, presumably through direct coupling of G-proteins to the channel. A muscarinic G-protein-coupled inward rectified K^+ channel (GIRK1) was recently cloned from rat atria and brain (Kubo Y. et al., (1993) Nature 364: 802-806 and Dascal N. et al., (1993) PNAS 90:10235-10239).

We screened a rat atrial cDNA library with a cDNA probe that spans the M1-H5-M2 region of GIRK1 and have isolated three distinct isoforms of GIRK1, termed GIRK2, 3, and 4. The GIRK isoforms appear to be generated by alternative splicing since the cDNA sequences are essentially identical in the coding regions of the clones. The isoforms have nearly identical amino acid sequences to GIRK1 but are truncated at the C-termini. Northern analysis suggests that the isoforms are expressed to different levels in atrial tissue. The co-expression of the m2 muscarinic receptor and each of the GIRK isoform mRNAs in *Xenopus* oocytes has demonstrated that they exhibit distinct kinetic properties. Our novel isoforms provide a new aspect to the understanding of the ACh-induced current in native atrial cells. Moreover, they provide structural relevance to the regulation of this current by specific G-protein subunits. (Supported by NIH grants to D.E.L and W.B.T).

W-Pos79

MOLECULAR CLONING AND EXPRESSION OF A HUMAN HEART INWARD RECTIFIER POTASSIUM CHANNEL. ((K. F. Raab-Graham, C. M. Radeke, and C. A. Vandenberg)) Dept. of Biological Sciences and Neuroscience Research Institute, University of California, Santa Barbara, CA 93106.

We have isolated a cDNA encoding an inwardly rectifying K^+ channel (HH-IRK1) from human heart. The cDNA codes for a 427-amino acid protein, with two putative transmembrane domains and an H5 region. The primary structure of HH-IRK1 is homologous to that of the IRK1 channel cloned from a mouse macrophage-like cell line. Functional expression in *Xenopus* oocytes showed that HH-IRK1 is a K^+ channel with strong inward rectification, blocked by extracellular Ba^{2+} and Cs^+, and with a single-channel conductance of 30pS. Cs^+ block of HH-IRK1 produced rapid flickery interruptions of the single-channel currents and nearly instantaneous block in whole cell recordings upon hyperpolarization. Northern analysis showed HH-IRK1 transcripts in human heart, brain, skeletal muscle, placenta, lung and kidney. HH-IRK1 was assigned to human chromosome 17 using PCR amplification of somatic cell hybrid DNA.

W-Pos80

EXPRESSION OF mRNA FROM THE KV1 POTASSIUM CHANNEL GENE FAMILY IN AIRWAY SMOOTH MUSCLE CELLS. ((S. Adda, B.D. Freedman, and M.I. Kotlikoff)) Depts. of Animal Biology and Pathology, University of Pennsylvania, Philadelphia, PA 19104. (Spon. by J. Rosenbloom)

We have previously shown that voltage-dependent potassium channels regulate resting membrane potential and passive electrical behavior in airway smooth muscle cells, and that inhibition of these channels produces contraction in resting tissue (Fleischmann et al, J. Physiol. 469, 625, 1993). In order to identify the specific potassium channels responsible for this action, we have performed RT PCR and northern blot analysis on RNA from airway smooth muscle tissue and cultured airway myocytes. Using unique probes, transcripts for KV1.1 (9.5 Kb), KV1.2 (~ 11 Kb), and KV1.5 (3.5 and 4.4 Kb) were identified on Northern blots prepared from equine tracheal tissues. RT-PCR analysis of RNA from cultured cells provided confirmation that the identified transcripts were expressed by smooth muscle cells. In further experiments using cultured human tracheobronchial myocytes, two transcripts for KV1.5 (6.5 and 3.3 Kb) were identified in Northern blots, and KV1.1 expression was confirmed by RT-PCR. Thus airway myocytes express mRNA from several members of the KV1 gene family, and the previously described functional actions of voltage-dependent potassium channels in this tissue may result from the activity of several distinct potassium channel subtypes. (Supported by NIH HL-41084 and NIH HD-01056).

W-Pos81

MODULATION OF RAT *EAG* CHANNEL BY MAGNESIUM AND REDUCING AGENTS. ((H. Terlau, J. Ludwig[1], O. Pongs[1] and W. Stühmer)) Max-Planck-Institut für experimentelle Medizin, 37075 Göttingen, Germany. [1]ZMNH, Institut für neurale Signalverarbeitung, 20251 Hamburg, Germany.

Recently we described the cloning and functional expression of a rat homologue of *Drosophila eag* cDNA, encoding a distinct type of voltage-activated potassium channels. The kinetics of rat *eag* channel activation depend strongly on the holding membrane potential. Addition of Mg^{2+} to the extracellular solution leads to a dramatic slowing of the activation in a voltage dependent manner. The more negative the holding potential is the more profound this effect is, indicating an interaction of Mg^{2+} with an early closed state of the channel. The evoked currents of rat *eag* channels measured in excised patches decrease upon excision of the patch within different time scales from seconds up to minutes. After this "run-down" phenomenon the evoked currents can be at least partially restored by addition of the reducing agents glutathione or dithiothreitol to the cytoplasmic site of the patch. This indicates that for rat *eag* channels reducing conditions at the cytoplasmic site are essential for a completely functional channel.

W-Pos82

OUTWARD CURRENT THROUGH A SOMATOSTATIN (SRIH)-ACTIVATED INWARD RECTIFIER IS BLOCKED BY TETRABUTYLAMMONIUM (TBA^+) BUT NOT BY Cs^+. ((P. Thomas and D.W. Waring)) Department of Human Physiology, University of California, Davis, CA 95616.

SRIH, an inhibitor of ACTH secretion, inhibits spontaneous plasma membrane electrical activity and intracellular [Ca^{2+}] (Ca_i) spiking in individual AtT-20/D16v-F2 corticotroph tumor cells. Measurements of Ca_i combined with perforated-patch, current-clamp recordings revealed that this inhibition was due to an SRIH-induced plasma membrane hyperpolarization (membrane polarity increased by 12 ± 1.9 mV, n = 18). Perforated-patch, voltage-clamp recordings using a ramp protocol revealed an SRIH-induced current (I_s). The inward I_s grew larger at increasingly negative potentials (-22 ± 5.4 pA at -120 mV, n = 5), and at more positive potentials the outward I_s was small (5.5 ± 1.7 pA at -45 mV, n = 5), *i.e.*, the current inwardly rectifies. The inward I_s was markedly inhibited by both 5 mM Cs^+ (I_s = -1.5 ± 1.0 pA at -120 mV, n = 4) and 5 mM TBA^+ (I_s = -6.0 ± 3.1 pA at -120 mV, n = 5). On the other hand, the small outward I_s was differentially inhibited by these two cations. TBA^+, 5 mM, reduced outward I_s by approximately 75% (1.4 ± 1.2 pA at -45 mV, n = 5); whereas, 5 mM Cs^+ had no effect on outward I_s (8.7 ± 3.1 pA at -45 mV, n = 4). Consistent with these results, TBA^+, but not Cs^+ (n = 7), was able to reverse the SRIH-induced inhibition of Ca_i spiking (12 of 13 cells); and in combined Ca_i/current-clamp recordings 5 mM TBA^+ completely counteracted the SRIH-induced hyperpolarization (n = 5). In summary, an outward TBA^+-sensitive I_s through an inwardly rectifying K^+ channel is responsible for the SRIH-induced membrane hyperpolarization and resultant inhibition of Ca_i spiking in AtT-20 cells. (Supported by the American Cancer Society, BE-150; NIH-HL07682.)

ANIONIC CHANNELS

W-Pos83

CONTRIBUTION OF PROLINE RESIDUES LOCATED IN THE MEMBRANE-SPANNING DOMAINS OF CFTR TO Cl^- CHANNEL FUNCTION. ((D.N. Sheppard, S.M. Travis, and M.J. Welsh.)) Howard Hughes Medial Institute, University of Iowa, Iowa City, IA 52242. (Spon. by R.H. Ashley).

Proline residues located in the membrane-spanning domains (MSDs) of transport proteins are suggested to have a key role by kinking α-helices. In CFTR four prolines are found in the MSDs: P99, P205, P324 and P1021. These residues are conserved across species and two are associated with CF mutations (P99L and P2055). We mutated each proline either individually to alanine (A) or glycine (G) or mutated all four simultaneously to alanine (P-Quad-A) and examined the processing and function of these constructs in HeLa cells. Mutations at P99, P324 and P1021 produced mature protein (band C). However, band C was much reduced with the P205 mutants, and P-Quad-A made no band C. cAMP agonists activated whole-cell Cl^- currents resembling wild-type in cells expressing each construct except P-Quad-A, although the amount of current generated by the P99 and P205 constructs was reduced. The anion-selectivity sequence of the mutants (Br ≥ Cl > I) resembled wild-type except for P99L (Br > Cl = I). Because the P99 constructs produced band C but had altered whole-cell currents, we studied their single-channel characteristics. Mutant channels had normal regulation by PKA and ATP, however single-channel conductance was decreased in the rank order: wild-type > P99G > P99L ≥ P99A. These data suggest that P205, which lies in the middle of a putative α-helix, is critical for correct protein processing while P99, which is near the external surface of the channel, may contribute to the pore of the CFTR Cl^- channel.

W-Pos84

USE OF HUMAN-*XENOPUS* CHIMERIC PROTEINS TO ANALYZE THE ANION PERMEABILITY OF CFTR Cl^- CHANNELS. ((Hiroshi Ishihara, Margaret P. Price, David N. Sheppard, and Michael J. Welsh.)) Howard Hughes Medical Institute, University of Iowa, Iowa City, Iowa 52242. (Spons. by M.J. Welsh)

We found that the anion permeability sequence of cAMP-activated current in the apical membrane of *Xenopus* A6 epithelia was I > Br > Cl. This result suggested that the anion permeability sequence of *Xenopus* CFTR (*X*CFTR) may differ from that of human CFTR (hCFTR) which is Br > Cl > I. To test this possibility, we closed and sequenced *X*CFTR and expressed it in HeLa cells. *X*CFTR generated cAMP-activated whole-cell currents with an anion permeability sequence of Br ≥ I ≥ Cl. To better understand the structure and function of CFTR we constructed chimeric proteins by replacing either M1-M6 or M7-M12 of hCFTR with the equivalent sequences from *X*CFTR (hX1-6 and hX7-12). hX7-12 had an anion permeability like hCFTR but hX1-6 had a sequence (Br ≥ I ≥ Cl) like that of *X*CFTR, suggesting that the difference in anion permeability is conferred by M1-M6. Because previous studies have shown that charged residues near the extracellular surface of hCFTR alter relative anion permeability, we mutated specific charged residues in this region that differ in hCFTR and *X*CFTR, but they did not alter anion selectivity, suggesting that uncharged residues are involved. An hX1-2 and an hX1-4 chimera manifested anion permeability half way between hCFTR and *X*CFTR. These data indicate that residues in M5 and/or M6 are important in determining the anion permeability sequence and that additional residues in M1 and/or M2 may contribute to the conduction mechanism of CFTR.

W-Pos85

NITRIC OXIDE-DEPENDENT REGULATION OF THE CARDIAC CFTR CHLORIDE CURRENT IN GUINEA-PIG VENTRICULAR MYOCYTES. ((S.I. Zakharov and R.D. Harvey)) Department of Physiology and Biophysics, Case Western Reserve University, Cleveland, OH 44106-4970

The potential role of nitric oxide in regulation of the cardiac CFTR Cl^- current was studied in isolated guinea-pig ventricular myocytes using the conventional whole-cell patch-clamp technique. When the Cl^- current was activated by submaximally effective concentrations of the ß-adrenergic receptor agonist isoproterenol (ISO), subsequent exposure to the nitric oxide (NO) donors SIN-1 and sodium nitroprusside (SNP) reversed activation of the current in a concentration dependent manner. Furthermore, the effects of SIN-1 and SNP were blocked by the NO inhibitors LY83583 (LY) and methylene blue (MB). LY and MB also suppressed antagonism of the ISO activated Cl^- current by the muscarinic receptor agonist acetylcholine (ACh). In fact, LY not only reversed the effect of ACh, at higher concentrations LY actually caused a rebound of the ISO-activated Cl^- current to a level beyond that observed prior to ACh inhibition. This enhancement of the Cl^- current in the presence of LY was probably not a direct effect, because LY alone did not activate the Cl^- current. However, it was possible to activate the Cl^- current with subthreshold concentrations of ISO in the presence of LY, indicating that LY can increase the sensitivity of the Cl^- current to activation by ISO. These results suggest that NO is involved in muscarinic regulation of the Cl^- current in mammalian ventricular myocytes and that basal levels of NO production may modulate the sensitivity to ß-adrenergic regulation, even in the absence of muscarinic agonists. Supported by NIH grant HL 45141.

W-Pos86

ALTERED BETA-ADRENERGIC AND MUSCARINIC SENSITIVITY OF THE CARDIAC CFTR CHLORIDE CURRENT IN DIALYZED VENTRICULAR MYOCYTES. ((S.I. Zakharov and R.D. Harvey)) Department of Physiology and Biophysics, Case Western Reserve University, Cleveland, OH 44106-4970

Autonomic regulation of the cardiac CFTR Cl^- current was studied in isolated guinea-pig ventricular myocytes using various configurations of the whole-cell patch-clamp technique. When currents were recorded using the conventional patch-clamp technique, it was possible to continue to activate the Cl^- current upon repeated exposure to isoproterenol (ISO) for up to 60 minutes after initiating dialysis. However, there was significant run-down of the magnitude of the Cl^- current response to the maximally stimulating concentrations of ISO. In addition, the concentration of ISO that produced half-maximal activation of the Cl^- current ($K_{1/2}$) increased with time. Conversely, the $K_{1/2}$ for acetylcholine (ACh) inhibition of the ISO activated current decreased with time. When currents were recorded using the perforated patch-clamp technique, the sensitivity to both ß-adrenergic and muscarinic receptor stimulation was stable. Immediately after initiating dialysis with the conventional patch-clamp technique, the sensitivity to ISO was nearly identical to that determined using the perforated patch-clamp technique. However, the initial sensitivity to muscarinic receptor activation was significantly greater. These results indicate that cell dialysis associated with conventional patch-clamp techniques not only results in a time-dependent run-down of current amplitude, but it also significantly alters the concentration dependence of ß-adrenergic and muscarinic receptor regulation of ion channel function. Supported by NIH grant HL 45141.

W-Pos87

COMPARISON OF DRUG TRANSPORT PROPERTIES FOR MDR AND CFTR TRANSFECTANTS ((P.D. Roepe, L.J. Robinson & M.M. Hoffman)) Laboratory of Membrane Biophysics, Memorial Sloan-Kettering Cancer Center, 1275 York Ave. New York, NY 10021.

3T3 fibroblasts transfected with hu CFTR cDNA that were not previously exposed to chemotherapeutics exhibit a multidrug resistance phenotype as defined by drug resistance to doxorubicin,,vincristine and colchicine; reduced electrical membrane potential; altered pH_i homeostasis; reduced ^3H - vinblastine accumulation; and the ability to select rapidly expanding colonies exhibiting increased resistance to a variety of drugs via continuous exposure to one chemotherapeutic. We have thus examined doxorubicin transport for cells transfected with either mu MDR 1 or hu CFTR cDNA, using sensitive continuous monitoring of fluorescence (CMF) techniques. Transfectants not previously exposed to chemotherapeutic exhibit reduced doxorubicin accumulation. Accumulation rates for the CFTR transfectants are similar to those for MDR transfectants, but retention of the drug (as measured in zero - trans efflux experiments) is different. Since both MDR and CFTR overexpressors exhibit decreased $\Delta\Psi$ but steady state pH_i perturbations in opposite directions, we conclude that lowered rates of accumulation are at least in part a consequence of lowered electrical membrane potential in these cells, and that pH_i perturbations play a more important role in determining intracellular binding efficiency. Uptake experiments with parental cells performed in the presence of various concentrations of K^+ support this conclusion, as does comparison to CFTR clones expressing lower levels of the anion channel. These data support a model for the MDR protein wherein overexpression of the protein alters the character and / or magnitude of plasma membrane electrochemical potential and thus indirectly alters intracellular drug retention over time.

We thank Drs. Phillipe Gros (McGill University) and M. Jackson Stutts (U.N.C. Chapel Hill) for generously providing MDR and CFTR transfectants, respectively. This work was supported by grants from the Raymond & Beverly Sackler Foundation and the Wendy Will Case Fund. P.D.R. is a Sackler Scholar at MSKCC.

W-Pos88

EXPRESSION OF INSECT P-GLYCOPROTEIN HOMOLOGS IS ASSOCIATED WITH ATP-PERMEABLE CHANNELS. ((I. Bosch, J. Croop, and H. F. Cantiello)) Harvard School of Public Health, Dana Farber Cancer Institute, and Department of Medicine, Harvard Medical School, and Renal Unit, Massachusetts General Hospital East, Charlestown, Massachusetts.

Recently we demonstrated that a mouse P-glycoprotein (*mdr1*, Pgp) is an ATP-permeable channel (PNAS, 90:312, 1993). To assess whether this novel function of Pgp is shared by other members of the Pgp family, the whole-cell clamp technique was used to determine ATP channel activity the in the Pgp homologs, MDR65 and MDR49 recently cloned from *Drosophila melanogaster*. Pgp-baculoviral expression was determined by immunoblotting of membrane-enriched fractions of infected Sf9 cells. Whole-cell currents were assessed under asymmetrical, ATP_i/Cl_o, or symmetrical, ATP_i/ATP_o conditions. The whole-cell conductance (ATP_i/Cl_o) of MDR65-expressing Sf9 cells was 1891% higher than either uninfected or mock-infected Sf9 cells (0.24 ± 0.05 nS/cell, n=5, vs. 4.78 ± 0.80, n= 8, $p<0.001$), and did not rectify between ±100 mV. A 0.34 ATP/Cl permselectivity ratio was determined, similar to CFTR but not murine Pgp. The whole-cell conductance of MDR49-expressing cells, in contrast, was 1.41 ± 0.45 nS/cell, n=6 (488% vs Sf9, $p<0.025$). The permselectivity ratio for MDR49 was 2.77, instead. The molecular nature of the ATP currents of MDR65 and MDR49-expressing cells was further investigated under excised inside-out conditions. The data indicate that although both insect Pgp homologs share functional ATP channel properties, their voltage gating properties and their permeability to ATP differ.

W-Pos89

ANTIVIRAL DRUGS FROM THE NUCLEOSIDE - ANALOGUE FAMILY BLOCK VOLUME - ACTIVATED CHLORIDE CHANNELS

((Martin Gschwentner, Alex Susanna, Ewald Wöll#, Markus Ritter#, Ulrich O. Nagl, Andreas Schmarda, Andreas Laich, Germar M. Pinggera, Helmut Ellemunter+ and Markus Paulmichl)) Department of Physiology, Fritz-Pregl-Str. 3, # Department of Internal Medicine, +Department of Pediatrics, Anich-Str. 35, University of Innsbruck, A-6020 Innsbruck, Austria, Europe

Antiviral drugs like AZT or acyclovir are generally used in the therapy of viral infections like human immunodeficiency virus (HIV) or herpes virus. These substances are known to impede virus replication by premature nucleic acid chain termination. It is not yet clear, however, if this is the solely responsible effect for the antiviral impact and/or for the numerous side effects observed in patients treated with these agents. Here we show a novel mechanism by which this class of drugs could possibly restrict virus growth. We show that AZT as well as acyclovir are able to block the swelling-induced chloride current in fibroblasts and in human T-cell lymphoma cells at micromolar concentrations. The block is effective on both current directions and instantaneously after drug application. The nucleotide CTP is able to block I_{Cln} at one order of magnitude higher concentration than the nucleoside analogues. The nucleotide TDP is unable to affect I_{Cln} up to 0.1 mM added to the extracellular solution. Most important is the finding that TDP competitively blocks the blocking by AZT indicating that TDP is binding to the nucleotide 'receptor' of the channel protein thus impairing the binding and consecutive blocking of I_{Cln} by AZT. Blockage of this current reduces the ability of the cells to counterbalance a lethal cell volume increase observed during active viral replication.

W-Pos90

FLUORESCENCE - OPTICAL MEASUREMENTS OF CHLORIDE IN CELLS UNDER HYPOTONIC STRESS.

((Ewald Wöll#, Martin Gschwentner, Gabriele Buemberger, Peter Deetjen and Markus Paulmichl)) Department of Physiology, University of Innsbruck, Fritz-Pregl-Str. 3, # Department of Internal Medicine, University of Innsbruck, Anich-Str. 35, A-6020 Innsbruck Austria, Europe

I_{Cln}, a chloride channel cloned from epithelial cells (1-3), is paramount in regulatory volume decrease. Using antisense oligonucleotides complementary to the first 30 coding nucleotides of I_{Cln} we could annihilate the swelling induced chloride current (I_{Cl}) in NIH 3T3 fibroblasts. A unique feature of I_{Cl} is its sensitivity to different nucleotides added to the extracellular fluid. Nucleoside-analogues are able to block I_{Cl} at one to two orders of magnitude lower concentrations than nucleotides. I_{Cl} can also be blocked by NPPB, a known chloride channel blocker. Phenol-derivatives like NDGA or gossypol which are structurally related to NPPB are similarly able to impede I_{Cl}. Using MEQ, a fluorescence dye sensing the cellular chloride, we can show that the employed antisense oligonucleotides sensing the I_{Cln} protein selectively reduce the swelling activated chloride flux across the cell membrane of fibroblasts thus demonstrating the unambiguous involvement of I_{Cln} as the major swelling dependent chloride channel in these cells. In addition nucleoside-analogues and the phenol derivatives tested are able to significantly reduce the chloride 'flux'. In conclusion, the nucleoside-analogues, the phenol-derivatives NDGA and gossypol and the selective reduction of the I_{Cln} protein are able to reduce the chloride flux across the cell membrane of NIH 3T3 fibroblasts.1 Paulmichl et al., *Nature* 356: 238-241, 1992; 2 Paulmichl et al., *Cellular Physiol. Biochem.* 3: 374-387, 1993; 3 Gschwentner et al., *Renal Physiol. Biochem.* 17: 148-152, 1994

W-Pos91

MDR/P-GLYCOPROTEIN EXPRESSION IS ASSOCIATED WITH REDUCED SWELLING-ACTIVATED K+ AND CL- EFFLUX IN MESSA AND DX5 CELLS ((D.B. Luckie, KL Harper, M.E. Krouse, T.C. Law, B. Sikic, and J.J. Wine)) Cystic Fibrosis Research Laboratory, Stanford University, Stanford, CA 94305-2130 (Spon. by H. Kutchai)

To test the association between P-glycoprotein (P-gp) and swelling currents, a human uterine carcinoma cell line (Mes-sa) and its doxorubicin selected/P-gp upregulated (DX5) counterpart were studied. Western blots identified a broad ~160kD band (P-gp) in the DX5 cells while low/no expression in the control (Mes-sa). In whole cell patch clamp experiments with 50% hypotonic stimulus, MDR expressing cells and control cells produced chloride current densities of the same magnitude (~200pA/pF@100mV). Outside-out patches from both cell lines revealed transiently active outwardly rectifying chloride channels. These experiments were repeated using Iodide-125 efflux. Unexpectedly, Iodide-125 efflux was smaller in the DX5 (high P-gp) cells than in control cells. At 50% hypotonicity, Iodide-125 efflux from the DX5 cells was one half that of the Messa (control) cell line (n=4). A smaller K+ efflux (Rb-86) response to hypotonicity was also observed in the DX5 cells. At 50% hypotonicity, Rb-86 efflux of the DX5 (high P-gp) cell line was one third that of the Messa (low P-gp) line (n=4). Thus in this cell line, MDR/P-gp expression is associated with reduced swelling-stimulated Cl- and K+ efflux. While previous results (Luckie et al. AJP 267 C650, 1994) made it clear that P-gp was not a swelling-activated Cl- channel, they left open the possibility that P-gp expression might upregulate a step in the pathway from hypotonic challenge to K+ and Cl- efflux. These data suggest that such a relation is not universal. *Supported by DK45913, HL42368, & CFRI.*

W-Pos92

EPITHELIAL CELLS EXPRESSING WILD TYPE CFTR HAVE LOWER STEADY STATE AND STIMULATED ACID EFFLUX RATES THAN CELLS EXPRESSING MUTANT CFTR ((D.B. Luckie, and J.J. Wine)) Cystic Fibrosis Research Lab, Stanford University, Stanford, CA 94305

A new biosensor, the silicon microphysiometer, that can detect small changes (~0.005 pH unit) in the proton efflux of cultured living cells was used to exploit pH differences to differentiate between CFTR+ and CFTR- cells *in vitro*. The steady state acid efflux rates of control and mutant 508CFTR-transfected c127 mouse mammary epithelial cells were 74 +/- 9.6 uV/s (n=6)(uV=~millipH) and 48.7 +/- 11.2 uV/s (n=4) respectively, while that of wild-type CFTR transfected cells was 26 +/- 3.1 uV/s (n=8). The cAMP elevating agent, forskolin (10 uM), increased the acid efflux rates of parental, vector-transfected, and dF508 CFTR-transfected epithelial cells by 30 +/- 12 uV/s (n=8). On the other hand, 10 uM forskolin stimulus decreased the acid efflux rate of wild-type CFTR-transfected cells by 16 +/- 4 uV/s (n=7). This inhibition is observed only in cells expressing wild-type CFTR. In control experiments, dideoxyforskolin (10 uM) was shown to have no effect (a 0.0 uV/s (n=3)) on the acidification rates in all cell lines, and hypotonic solutions were shown to equally stimulate acidification rates in all cell lines (30% hypo = +20 uV/s). The Ca-elevating agent, ionomycin, was found to mimic the effects seen with forskolin: control (+29 uV/s), 508CFTR (+14 uV/s), and wtCFTR (-14 uV/s). Like forskolin, ionomycin is known to be both a good metabolic stimulant and a CFTR activator. These results raise the possibility that CFTR's function may alter extracellular pH, and that the microphysiometer may have the capacity to differentiate CFTR+ cells from CFTR- cells through pH. *Supported by DK45913, HL42368, & CFRI.*

W-Pos93

MASS SPECTROMETRIC ANALYSIS OF RECOMBINANT R-DOMAIN PHOSPHORYLATION SITES OF THE CYSTIC FIBROSIS CHLORIDE CHANNEL. P. Lipniunas, B. Tulk, J. Biwersi, M. Wiener, A.S. Verkman, and R.R. Townsend, Cystic Fibrosis Research Center, and the Mass Spectrometry Facility, University of California, San Francisco, CA

The regulatory (R)-domain of CFTR contains nine potential sites (8 Ser, 1 Thr) for phosphorylation by PKA. Mutation of all of these sites to Ala did not abolish cAMP-dependent chloride conductance (Chang, *et al.*, J. Biol. Chem. 268: 11304-11311, 1993), indicating that phosphorylation at other sites plays a role in the regulation of CFTR activity. Toward identifying these cryptic sites, we have used a method which does not depend on the availability of standard phosphopeptides or deduction of phosphorylation sites from consensus sequences. Microbore reversed-phase HPLC-electrospray ionization mass spectrometry was used to determine the precise mass of tryptic peptides of recombinant R-domain. Using the pGEX-KG expression vector, the R-domain was expressed in fusion with glutathione-S-transferase (GST). Following induction with 1 mM IPTG, inclusion bodies were purified from *E. coli* cultures overexpressing GST-R-domain, and solubilized in 6 M guanidine-HCl. After 6-fold dilution, GST-R-domain was treated with trypsin for 16 hrs. at 37°C. Using ~1 pmol of the tryptic digest, we obtained masses within 0.5 atomic mass unit of those predicted for peptides containing Ser residues 660, 700, 712, 737, 768, 795, and 813. This new approach is being used to define phosphorylation sites in native CFTR which cannot be determined from consensus sequence approaches.

This work supported by CFF and NIH.

W-Pos94

NORMAL AND ΔF508 CFTRs ARE FUNCTIONAL Cl^- CHANNELS IN THE OUTER MEMBRANE OF THE NUCLEAR ENVELOPE. ((E. Pasyk and J.K. Foskett)) Division of Cell Biology, Hospital for Sick Children, Toronto, Ontario, Canada. (Spon. by E. Pasyk)

Cystic fibrosis (CF) is associated with defective plasma membrane Cl^- channel activity. Some mutant CFTRs, including ΔF508-CFTR, are retained in the endoplasmic reticulum (ER) and fail to reach the plasma membrane. The objective of this study was to determine whether CFTR functions as a Cl^- channel when it is localized in the ER membrane. Because the outer membrane of the nuclear envelope is continuous with the ER, we patch clamped isolated nuclei from transfected CHO cells. In excised patches from nuclei isolated from cells expressing ΔF508-CFTR, we recorded single channel activities that satisfy criteria for CFTR: (i) Cl^- selectivity, (ii) single channel conductance 6-10 pS (39/49 patches), (iii) linear I-V relationship, (iv) open probability (P_o) 0.3-1, (v) PKA (90 nM) sensitivity (50/61 patches), (vi) DIDS (0.1-0.5 mM) insensitivity (7/7 patches), and (vii) detection usually as multi-channels with apparent cooperative activity. Similar Cl^- channel activities were also observed in excised nuclear membrane patches from cells expressing wild type CFTR (14/18 patches). Additionally, wild type CFTR was present and functional in the plasma membrane, as revealed by Western blot and patch clamp (6/7 patches). In nuclear membrane of control cells (vector only), either there were no channel activities (24 patches) or an endogenous Cl^- channel was present (32 patches) with low conductance (5-8 pS), linear I-V relation, no multi-levels, low P_o (<0.05), and DIDS (0.1-0.3 mM) sensitivity (10/10 patches). We conclude that normal and ΔF508 CFTRs function as Cl^- channels in the ER, demonstrating that protein conformational changes which are recognized by ER-retention mechanisms do not necessarily affect channel activity. Such Cl^- channel activity in the ER may contribute to the pathophysiology of CF. *Supported by the Canadian Cystic Fibrosis Foundation.*

W-Pos95

DIFFERENT PROPERTIES OF SWELLING-ACTIVATED Cl^- CURRENTS IN P-GLYCOPROTEIN (Pgp) EXPRESSING AND CONTROL CELLS. ((E.S. Han, C. Vanoye-Treviño, G. A. Altenberg and L. Reuss)) Dept. of Physiology and Biophysics, University of Texas Medical Branch, Galveston, Texas 0641-77555.

There is disagreement as to whether Pgp expression is associated to cell-swelling-activated Cl^- currents (I_{Cl}) directly, indirectly, or not at all. The negative conclusion is to some extent based on the assumption that all outwardly-rectifying I_{Cl} are accounted for by the same channel. Here we report differences in the characteristics of I_{Cl} between the human breast cancer cell lines MCF-7 (wild-type, drug-sensitive) and BC19/3 (Pgp-expressing, multidrug resistant), and others. First, shortly after detachment (EDTA exposure) MCF-7 cells did not exhibit I_{Cl} (by 25% dilution of the bath solution), whereas BC19/3 cells did; I_{Cl} were the same in glass-attached MCF-7 and BC19/3 cells. Second, mAb C219 (10 or 50 μg/ml in the pipette solution) prevented I_{Cl} in BC19/3, but not in cells that do not express Pgp in the plasma membrane (MCF-7, BALBc-3T3, rat hepatocytes). Rat IgG and other anti-Pgp mAbs (C494, JSB-1) did not block I_{Cl}. Further, swelling of BC19/3 cells also activates a K^+ current (I_K), which was not affected by C219, although the mAb blocked I_{Cl} in the same cells. We conclude that there is a specific relationship between Pgp expression and I_{Cl}, i.e., that Pgp is either a Cl^- channel or a regulator thereof. If Pgp is a regulator, it acts within the signaling pathway connecting cell swelling to Cl^-current activation, but not in that connecting cell swelling to K^+-current activation. [Supported by Searle Research and Development.]

W-Pos96

MUSCLE CHLORIDE CHANNEL MUTATIONS IN MYOTONIA CONGENITA ALTER CHANNEL GATING PROPERTIES. ((Ch. Fahlke, R. Rüdel, F. Lehmann-Horn, and A.L. George)) Dept. of Medicine, Vanderbilt University, Nashville, TN 37232, USA, Dept. of General Physiology University of Ulm, D-89069 Ulm, Germany

Myotonia congenita is a hereditary disease characterized by stiffness of voluntary muscles occuring upon sudden contraction. The condition is caused by mutations in the muscle Cl^- channel gene and may be either autosomal dominant or recessive. Two mutations that cause either dominant (R894X) or recessive (D136G) myotonia were characterized by heterologous expression of mutant human muscle Cl^- channels (hClC-1) in *Xenopus* oocytes. The D136G mutation (glycine for aspartic acid) occurs in the first transmembrane domain of hClC-1 (D1), R894X truncates hClC-1 by 95 amino acids via introduction of a premature in-frame termination codon. Two-electrode voltage clamp recordings were made of oocytes expressing either wild-type hClC-1 (WT), D136G, or R894X. Both mutations exhibit reduced peak current amplitudes at -145 mV (D136G 1.2 ± 0.9 μA vs WT 5.0 ± 2.1 μA, S.D.), have slower deactivation kinetics, and exhibit less inward rectification than WT channels. These results suggest that altered gating properties of mutant Cl^- channel may play an important role in the pathogenesis of myotonia, and that regions within D1 and the C terminus contribute to gating.

W-Pos97

THE MYOTONIC MOUSE EXHIBITS ABNORMAL MYELINATION. ((R. Hahin)) Northern Illinois University, DeKalb, IL 60115

The myotonic mouse (SWR/J-*adr^{mto}*/*adr^{mto}*) is a model for the study of the human diseases myotonia congenita and dystrophia myotonica which exhibit involuntary muscle after-contractions caused by a presumed reduction in chloride current. In the myotonic mouse, muscle chloride channels are not expressed because a transposon has been inserted into the chloride channel (Clc-1) structural gene. The genetic defect has been described to be a simple recessive trait. Light and transmission electron microscopic studies of sciatic nerves obtained from *adr^{mto}*/*adr^{mto}* and *adr^{mto}*/+ mice showed abnormalities in myelination when compared to wild-type, +/+, controls. Mice with two abnormal Clc-1 genes (*adr^{mto}*/*adr^{mto}*) showed the most extensive loss of myelin. Analysis of sciatic nerves from myotonic (*adr^{mto}*/*adr^{mto}*) mice (≥ 12 weeks old) from collages of photographs showed 20 ± 3% (8) of the fibers exhibited a major loss of myelin, while no significant loss of myelin was observed in normal wild-type animals of similar age. An analysis of heterozygotes (*adr^{mto}*/+) showed 1 ± .02% (5) of the fibers exhibited a major loss in myelin, but 8 ± 2% (5) of the fibers exhibited myelin abnormalities, observed most often as myelin loss and/or a disruption in myelin compactness. These results show that heterozygotes are not completely normal when compared to their wild-type littermates, and further suggest that the wild-type allele is incompletely dominant to *adr^{mto}*.

W-Pos98

MOLECULAR CLONING OF THE MYOTONIC GOAT SKELETAL MUSCLE CHLORIDE CHANNEL. ((C.L. Beck and A.L. George, Jr.)) Departments of Medicine and Pharmacology, Vanderbilt University School of Medicine, Nashville, TN, 37232 USA.

The skeletal muscle chloride channel (ClC-1) gene is the genetic locus for autosomal dominant human myotonia congenita (Thomsen's disease) and autosomal recessive myotonia in both human and mouse. A myotonic syndrome with autosomal dominant transmission also occurs in goats and much of the early knowledge about the electrophysiology of myotonia in general was based on studies of this animal model. We obtained skeletal muscle from myotonic and electromyographically normal goats to investigate the possible role of the ClC-1 channel in the pathophysiology of myotonia in this animal. To evaluate expression of ClC-1 mRNA in goat muscle, we performed Northern blot analysis of total RNA from normal and myotonic muscle (quadriceps) using a human ClC-1 probe (nt 1-1415) under moderately high stringency conditions. A prominent ~4 kb transcript of near equal intensity was seen in both normal and myotonic muscle, but not in brain, heart, liver, or kidney, indicating a ClC-1 homologue is present and selectively expressed in the muscle. To clone the myotonic goat ClC-1 we constructed a cDNA library and screened it with human ClC-1 under moderately high stringency conditions. One cDNA (B8; 2.4 kb) isolated from this library has been partially sequenced and encodes a protein with >90% amino acid identity with human and rat ClC-1. These results are consistent with the cloning of a partial length goat ClC-1 cDNA. Work is in progress to identify the mutation responsible for myotonia in goats. This work may reveal structure-function information about the ClC-1 channel.

W-Pos99

CALPAIN ACTIVATES CHLORIDE CHANNELS IN CULTURED MOUSE MYOTUBES. ((Gordon C. McCarter and Richard A. Steinhardt)) Dept. of Molecular and Cell Biology, Univ. of California, Berkeley, CA 94720

Single channel patch-clamp recordings were made from cultured mouse myotubes using the inside-out excised configuration. Bath application of 0.25 μM calpain, a calcium dependent cysteine protease, activated one or more chloride channels in roughly half of previously silent patches. Most of the activated channels had characteristics of the fast chloride channel in rat described by Blatz and Magleby (1985). These channels had a mean conductance of 35 pS, a mean open time of 1-2 ms, and usually opened in long bursts. Channels with slower kinetics but similar conductance were also sometimes seen, in addition to very large conductance channels (>300 pS). Protease-triggered activity was seen at resting and hyperpolarized potentials, unlike the previously described channels which opened more often with depolarization. Papain, another cysteine protease, activated chloride channels in a similar fraction of patches. This calcium dependent activation of a chloride conductance may provide a mechanism for muscle cells to limit excitability when intracellular calcium levels are excessive.

W-Pos100

MODULATION OF CA^{2+}-ACTIVATED CHLORIDE CHANNEL BY EXTERNAL PROTON IN CARDIAC VENTRICULAR MYOCYTE. ((S. KAWANO, Y. HIRAYAMA and M. HIRAOKA))
Department of Cardiovascular Disease, Medical Research Institute. Tokyo Medical and Dental University, Tokyo , Japan.

We have reported that Ca^{2+}-activated chloride current, $I_{Cl(Ca)}$, could be activated by Ca^{2+}-induced Ca^{2+} release mechanism (CICR) in the physiological concentration of internal Ca^{2+}; $[Ca^{2+}]_i$. The purpose of this study is to understand the regulation of this current in the pathological conditions. We examined the effects of external proton on $I_{Cl(Ca)}$ in rabbit ventricular myocytes by patch clamp method. $I_{Cl(Ca)}$ was activated by perfusing the cells with 0.1 ~ 1 μM Ca^{2+} in the pipette solution. $I_{Cl(Ca)}$ was markedly enhanced at low pH (6.4 ~ 5.5) in spite of strongly decreasing Ca^{2+} current (I_{Ca}) and was depressed at high pH (8.4 ~ 9.1) with increasing I_{Ca}. Under the low pH conditions, dihydropiridine failed to block $I_{Cl(Ca)}$, indicating that I_{Ca} did not contribute to the activation process of $I_{Cl(Ca)}$. However, the application of tetrodotoxin or Ni, or elimination of Na^+ or Ca^{2+} from the bath solution caused complete block of $I_{Cl(Ca)}$, suggesting the contributions of Na-Ca exchange. $I_{Cl(Ca)}$ at low pH was also blocked by the bath application of caffeine, ryanodine or thapsigargin but not by amiloride. These results indicate that for activation of $I_{Cl(Ca)}$ the contribution of I_{Ca}-dependent CICR is diminished at low pH, while the CICR triggered by Ca-entry through Na-Ca exchange or via other unknown mechanisms may play a predominant role for its activation.

W-Pos101

F-ACTIN INTEGRITY IS NOT REQUIRED FOR ACTIVATION OF VOLUME-REGULATED Cl^- CURRENT IN B-LYMPHOCYTES. ((I. Levitan[1], C. Almonte[1], P. Mollard[2] and S.S. Garber[1])) Departments of [1]Physiology and [2]Anatomy /Neurobiology, Medical College of Pennsylvania, Philadelphia, PA 19129.

We address whether F-actin integrity is involved in activation of a volume-regulated Cl^- current (VRCC) in B-lymphocytes. VRCC activation was initiated in response to establishing a whole cell recording in the presence of an hypo-osmotic gradient. Parallel confocal experiments using Phalloidin-Rhodamine as a specific marker of F-actin showed that the sub-membrane actin ring is reversibly disrupted in response to an hypo-osmotic gradient. Pre-incubation of cells with VRCC blockers (200 μM DIDS or 200 μM NPPB) did not alter the effect of an osmotic gradient on F-actin. F-actin integrity, however, could be disrupted by incubating cells in 50 μM cytocholasin B (CB). This condition is not sufficient to trigger activation of VRCC under iso-osmotic conditions or to potentiate the rate of activation in response to a 75% hypo-osmotic gradient (39.6 (pA/pF)/min. (n = 10), 75% gradient; 40.2 (pA/pF)/min. (n = 9), 50 μM CB+75% gradient). In contrast, incubation with CB increased the rate of VRCC activation in response to a 90% hypo-osmotic gradient from 6.6 (pA/pF)/min. (n = 8), 90% gradient alone, to 15.6 (pA/pF)/min. (n = 10), 90% gradient+CB. Thus, CB enhances a low rate of activation when there is little disassembly of F-actin due to an osmotic gradient. VRCC is still activated when F-actin is stabilized by phalloidin. These observations suggest that disassembly is not critical for VRCC activation in B-lymphocytes. Disassembly of F-actin, however, exerts a synergistic effect on the rate of VRCC activation in the presence of an hypo-osmotic gradient. (NIH DK46672 & AHA 94002340)

W-Pos102

CHLORIDE CONDUCTANCE IS OPPOSITELY AFFECTED IN EXTENSOR DIGITORUM LONGUS AND DIAPHRAGM MUSCLES FROM MDX MICE. ((A. De Luca, S. Pierno, A. Roselli and D. Conte Camerino)) Unit of Pharmacology, Dept. of Pharmacobiology, University of Bari, Italy.

We previously recorded an increase of macroscopic chloride conductance (G_{Cl}) in extensor digitorum longus (EDL) muscle fibers from 8-week-old mdx mice with respect to controls (De Luca et al., Biophys. J. 64: A97, 1993). To evaluate whether this increase is due to the lack of dystrophin or rather to the regeneration process, we recorded *in vitro*, with the computerized two intracellular microelectrode technique, the G_{Cl} value and excitability characteristics of the EDL muscle and of the non-regenerating diaphragm (DIA) muscle from mdx mice aging 4 weeks up to 4 months. In EDL muscle from 4- and 6-week-old mdx mice, G_{Cl} was not different with respect to controls. Again, a significant increase of G_{Cl} from a control value of 2132±91μS/cm² (n=43) to 2813±95μS/cm² (n=37) was found at 8 weeks of age and higher values of G_{Cl} were recorded up to 13 weeks. The high G_{Cl} accounted for the increase of threshold current, the shorter latency of action potential and the less firing capability of EDL muscle from mdx with respect to controls from 8 up to 13 weeks of age. However, the EDL muscles from 4-month-old mdx mice showed a 20% lower G_{Cl} with respect of age-matched controls. In DIA muscles from control mice, G_{Cl} increased from 1399±93μS/cm² (n=14) at 4 weeks to 2135± 120μS/cm² (n=15) at 10 weeks of age. Afterwards, G_{Cl} remained constant up to 4 months of age. In DIA muscle from mdx mice, G_{Cl} was slightly higher (by 12%) than controls at 4 and 6 weeks of age. In 8-week-old mdx mice we recorded significantly lower values of G_{Cl} (1597±71μS/cm²; n=23) and such a decrease of G_{Cl} was observed up to 4 months of age. Concomitantly, the DIA fibers from mdx mice tended to be more excitable with respect to controls. Our results suggest that the increase of G_{Cl} in EDL muscle of mdx mice is due to the regeneration process, since this parameter is oppositely affected in the non-regenerating DIA muscle (Supports of Telethon-Italy to De Luca's project # 322, 1992 and CNR 93-263 are acknowledged).

W-Pos103

PROPERTIES OF UNITARY CHLORIDE CHANNELS ACTIVATED BY PROTEIN KINASE C AND PROTEIN KINASE A IN GUINEA-PIG HEART. (M.L. Collier and J. R. Hume) Department of Physiology, University of Nevada, Reno, NV 89557-0046.

Protein kinase A (PKA)-activated chloride channels in heart are encoded by an isoform of the epithelial cystic fibrosis transmembrane conductance regulator gene (CFTR). From macroscopic current studies, it is not clear whether PKC activates the same population of channels as PKA, or a separate class of chloride channels, although the regulatory (R) domain of CFTR in epithelia and heart, contain phosphorylation sites for both PKA and PKC. Here we show evidence of PKC-activated chloride channels and directly compare the properties of these channels with those activated by PKA in cell-attached patches of guinea-pig ventricular myocytes. Pipette and bath solutions contained N-methyl-D-glucamine and Cs^+ or tetraethylammonium as substitutes for Na^+ or K^+ respectively, and chloride concentration in the pipette was either 155mM or 45 mM. Bath application of phorbol 12,13-dibutyrate (PDBu, 50nM), an activator of PKC, activated single chloride channels with a mean conductance of 9.31 ± 0.94 pS (n = 8) which had reversal potentials close to predicted E_{Cl}. Addition of staurosporine (500 nM), an inhibitor of PKC, reduced open probability (P_o) of channels activated by PDBu. Bath application of the phosphodiesterase inhibitor, 3-isobutyl-1-methyl-xanthine (IBMX; 500 μM), activated chloride channels with a similar mean conductance of 8.76 ± 0.67 pS (n = 3) as those activated by PDBu. PKA- and PKC-activated chloride channels exhibited voltage independence, had similar kinetics and were insensitive to block by 4,4'-diisothiocyanatostilbene-2,2'-disulphonic acid. Moreover, the addition of IBMX increased P_o of PKC-activated channels without any change in unitary conductance. We conclude that PKC can activate unitary cardiac chloride channels with similar conductance and kinetic properties as those activated by PKA (supported by NIH HL30143 and AHA Nevada Affiliate).

W-Pos104

ISOLATION AND PORE-FORMING PROPERTIES OF A 32 kDa PROTEIN FROM EPIDERMIC MUCUS OF CARP (*Cyprinus carpus*). ((C. Lemaître, S. Julien, E Dé, P. Saglio, and G. Molle)) URA 500 CNRS, Université de Rouen, 76821 Mont-Saint-Aignan, France and Unité d'Eco-toxicologie Aquatique, INRA, 35042 Rennes, France. (Spon. by J. Dufourcq)

Nine g of crude epidermic mucus has been collected by scraping from 90 young carps and lyophilized. Detergent solubilized fraction of this mucus was shown to form ion channels into POPC-DOPE (7:3) planar lipid bilayer by the Montal Muller technique. In order to determine the component responsible of this ionophore activity, purification by detergent (Octyl-POE) differential extraction allowed to isolate two highly hydrophobic proteins about 55 and 32 kDa. These both proteins have been separated by preparative SDS-PAGE electrophoresis followed by electroelution and reconstituted into planar lipid bilayers. The 32 kDa protein by itself restores the same ion channel properties than the crude mucus. This protein does not show any voltage-dependence and displays a main unit conductance level of 450 pS in 1 M KCl The ionic specificity experiments have been performed with 1 M potassium gluconate allowing to determine a strong anionic selectivity (P_{Cl}/P_K = 5). Thus, a pore forming-activity has been observed with an epidermic mucus of fish and one can speculate about the defensive role of this protein in fish.
Supported by GDR 1153 CNRS.

W-Pos105

ACIDITY AFFECTS THE RECTIFICATION OF AN OUTWARDLY RECTIFYING EPITHELIAL CHLORIDE CHANNEL. ((M. Duszyk, D. Liu, A.S. French and S.F.P. Man)) Departments of Medicine and Physiology, University of Alberta, Edmonton, Canada

Apical membrane proteins from cultured CFPAC-1 cells, were separated from basolateral membrane proteins by the magnesium precipitation method, and were incorporated into liposomes for patch clamp studies. Liposomes were formed from L-α-lecithin by a dehydration-hydration method. Ion channels were characterized using the excised inside-out patch clamp configuration. One commonly-seen group of anion channels had a non-ohmic single-channel conductance and were similar to the outwardly rectifying Cl^- channels described previously in several epithelia. The degree of rectification was strongly dependent on the bath pH, showing least rectification at acidic values (~3.5), and the strongest rectification at alkaline values (~9.5). These results indicate that the channel protein contains titratable chemical groups on the cytoplasmic side, which control the passage of ions through the channel. The channel open probability was voltage-dependent, opening more at depolarizing voltages. It could be blocked by the stilbene derivative DNDS (10 μM), in a pH-dependent manner. DNDS had no effect on channel activity in acidic environment, but was effective at neutral and alkaline pH values. We conclude that the surface charge from titratable groups present at the cytoplasmic side of the channel controls the rectification of these epithelial chloride channels.

W-Pos106

CHARACTERIZATION OF THE CALCIUM-DEPENDENT CHLORIDE CONDUCTANCE OF CFPAC-1 CELLS. ((M.W.Y. Ho, M. Duszyk, and A.S. French)) Departments of Physiology & Medicine, University of Alberta, Edmonton, Alberta, Canada.

Activation of purinergic receptors by 10^{-6}M ATP induces a calcium-dependent chloride conductance (I_{Cl}) in CFPAC-1 cells. Whole-cell Ca^{2+}-I_{Cl} showed strong outward rectification. It reached a peak value within one minute after the application of ATP and then declined to a lower value. Intracellular fura2 experiments indicated that the increase in $[Ca^{2+}]_i$ was also biphasic, transiently increasing to a peak value and then decreasing to a plateau level within 2 minutes. When extracellular Ca^{2+} was removed from the bath solution, both the peak and the plateau values were reduced proportionally. This Ca^{2+}-I_{Cl} could be blocked by 10^{-5}-10^{-4}M DIDS. Noise analysis of individual whole-cell currents suggested that two Lorentzian components are involved in the development of Ca^{2+}-I_{Cl}, with one of the Lorentzian component becoming more prominent as the whole-cell current develops.

Supported by the Medical Research Council of Canada, the Alberta Heritage Foundation for Medical Research, and the Canadian Cystic Fibrosis Foundation.

W-Pos107

CHLORIDE CHANNELS STUDIED IN EXCISED MEMBRANE PATCHES FROM HUMAN PLATELETS. ((A.B.MacKenzie and M.P.Mahaut-Smith)) Physiological Laboratory, Downing Street, Cambridge. CB2 3EG. (Spon. by C.L.H.Huang)

Previous evidence for anion channels in human platelet surface membranes comes from studies of single channels reconstituted into lipid bilayers and whole-cell patch clamp recordings. We have now detected anion-selective channels in excised, inside-out patches from human platelets. Following formation of an on-cell patch recording from a platelet in suspension, the attached platelet was impaled into silicone grease on the base of the recording chamber. Upon removal, the outer vesicle of the platelet remained in the grease yielding a stable excised, inside-out patch recording. When the pipette and bath solutions contained (in mM) 150 NaCl, 10 HEPES, 1 $MgCl_2$, 1 EGTA, pH 7.35 (20°C), spontaneous channel openings were rarely observed. Depolarized potentials (+60mV to +100mV) elicited channel activity, after 30 seconds to 5 minutes, in 38% of patches. The unitary conductance at +80mV (outward current) was 53.5±1.5pS decreasing to 20.9±2.7pS at -80mV (inward current), E_{rev} approximately 0mV. Replacement of Na^+ in the bath with N-methyl D-glucamine did not significantly affect the I-V relationship, whereas replacement of Cl^- in the bath with gluconate shifted E_{rev} by 40mV/10 fold change of $[Cl^-]$. From the average number of channels (0.45) in all the patches we estimate each platelet has at least 29 Cl^- channels. Kinetic analysis of current traces suggested the presence of at least two open states (133ms and 0.34ms) and two closed states (31.7ms and 0.24ms). 5-nitro-2-(3-phenylpropylamino) benzoate (10^{-4}M) induced a 'flickery-type' block of the Cl^- currents. This study represents the first recordings of ionic currents in excised membrane patches from human platelets and provides further evidence for the existence of an intermediate conductance Cl^--permeable channel. The role of anion channels in platelet responses remains uncertain. Ongoing studies are aimed at determining the dependence of this Cl^- channel on second messengers known to be important in platelet function. *Funded by the BHF*

W-Pos108

ANION PERMEABILITY OF PHOSPHOLEMMAN - THE PORE IS LARGE. ((Gopal C. Kowdley, Gabor Szabo, Larry R. Jones, J. Randall Moorman)) University of Virginia and Indiana University.

We have reported that phospholemman (PLM) forms anion-selective ion channels in lipid bilayers. A novel feature was voltage-dependent switching between anion - and cation-selective states. To explore further this channel's unusual selectivity properties, we have studied the channel's permeability to 15 anions. Relative permeabilities were determined from reversal potential measurements under bi-ionic conditions with 150 mM salt solutions on both sides of the membrane. We find that the PLM channel continues to show voltage-dependent switching between states, and that the channel's selectivity for anions differs in these states. For some anions, an interesting feature of the channel is a permeability switch from less to more permeant than chloride. The pore of the channel, in any state, appears to be large (> 4.5Å x >7Å, at least), as determined by the size of benzoic acid, the largest anion we have tested. We have not found an impermeant anion. As might be expected for a large pore, the permeability of halide ions is in the order $I^- > Br^- > Cl^- > F^-$, at pH 7.4, which corresponds to the free solution mobilities for these ions, and indicates a weak strength anionic site. However, the permeability of larger anions does not always follow their free solution mobilities. This suggests that the channel is not so large that it allows anions of larger size to permeate freely. We conclude that the PLM channel does not select solely on the basis of anion size, as a molecular sieve would, but instead appears to use additional properties of the anion to determine selectivity.

W-Pos109

VOLTAGE DEPENDENT CLOSING OF PHOSPHOLEMMAN CHANNELS - ROLE OF THE C-TERMINUS ((Zhen-hui Chen, Steven E.Cala, J. Randall Moorman, Larry R. Jones)) Indiana University and University of Virginia.

Phospholemman (PLM), a 72 amino acid sarcolemmal protein which is the major substrate for PK-A and PK-C in heart, forms Cl^- selective, voltage dependent ion channels when expressed in *Xenopus* oocytes and when reconstituted into planar lipid bilayers. In oocytes, the induced Cl current is activated by hyperpolarization. We now find voltage-dependent gating of PLM currents in lipid bilayers. As shown in the plot of probability of closing as a function of voltage, channel closures were frequent over the voltage range 75 to 100 mV in 8 bilayers, and over -50 to -100 mV in 15 other bilayers. This suggests that the PLM voltage sensor is asymmetric, and that purified PLM can insert in either direction in synthetic lipid bilayers. We have shown that PLM channels make transitions between anion- and cation-selective states. In these experiments in 200:50 mM KCl, a 350 pS three-fold cation-selective conformation predominated. To study the role of the C-terminus in voltage-dependent gating and in ion selectivity, we used trypsin to cleave the last 29 amino acids (residues 44-72) from the extramembranous C-terminus. The truncated protein (residues 1-43) still exhibited channel activity, but did not show voltage dependent closing, and the cation-selective state no longer predominated. The C-terminus of PLM, containing the phosphorylation sites, may function as part of the selectivity filter and voltage sensor of the channel.

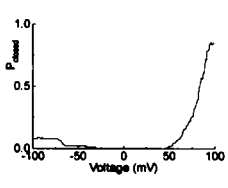

W-Pos110

RECONSTITUTION OF A VOLTAGE-DEPENDENT ANION CHANNEL FROM THE INNER ENVELOPE MEMBRANE OF PLANT CHLOROPLASTS. **((B. Fuks and F. Homblé)) Laboratory of Plant Physiology, CP 206/2, Université Libre de Bruxelles, Boulevard du Triomphe, B-1050 Brussels, Belgium.**

The reconstitution of the inner envelope membrane of chloroplasts into planar lipid bilayers has revealed a main single-channel conductance of 525 ± 12 pS in 150 mM KCl. The values of the reversal potential measured in the presence of different KCl gradients indicate that this channel is weakly anion selective (P_{Cl}/P_K=1.6 ± 0.2). The gating of the pore is voltage-dependent. The channel is closed at negative electrical potentials and the open conductance shifts to a substate at positive electrical potentials. Succynilation of the protein increases the open probability and reverses the selectivity of the channel. Analysis of the single channel conductance as a function of the salt concentration and of the open probability at various voltages suggest that this chloroplastic channel is a new membrane porin not previously identified in other membranes.

W-Pos111

MODULATION OF MYOPLASMIC CALCIUM RESPONSES BY THE TYROSINE KINASE INHIBITOR, GENISTEIN, IN PORCINE CORONARY SMOOTH MUSCLE CELLS.((Y.Liu and M.Sturek)) Dalton Cardiovascular Research Center and Dept. of Physiology, Univ. of Missouri, Columbia, MO 65211. (Spon. by V.Huxley)

Although tyrosine kinase is well known to play an important role in mediating cell growth in various tissue types, it is not clear whether it is involved in short-term responses, especially in vascular smooth muscles. Recent studies have indicated that tyrosine kinase activation may cause contraction of certain smooth muscle preparations. Thus, we examined the effect of genistein, a tyrosine kinase inhibitor, on myoplasmic Ca ($[Ca]_m$) responses (measured with fura-2 ratios) in freshly isolated smooth muscle cells. Genistein (GEN, 30 μM) caused a 15-30% inhibition of the $[Ca]_m$ response induced by depolarization with 80 mM KCl (n = 8 cells). Also, it reversibly reduced the sustained phase of $[Ca]_m$ response to endothelin (ET, 10 nM) to near basal level in 70% of the cells (14/20). The initial transient $[Ca]_m$ response to ET, however, was not affected by GEN added 4 min prior to ET exposure. The caffeine (5 mM)-induced $[Ca]_i$ transient resulting from Ca release from the sarcoplasmic reticulum was also not affected by GEN. These results suggest a role of a genistein-sensitive tyrosine kinase in $[Ca]_m$ regulation in vascular smooth muscle. The cellular mechanisms for the effect of genistein on $[Ca]_m$ remain to be elucidated. (Supported by NIH grants, HL41033, RCDA HL02872 and AHA grant, 93011900 and a postdoctoral fellowship from AHA, Missouri Affiliate)

W-Pos112

MECHANISMS FOR CALCIUM SIGNALING IN VASCULAR SMOOTH MUSCLE RESOLVED FROM ^{45}CA UPTAKE AND EFFLUX EXPERIMENTS. ((S.A. Lapidot, B.K. Huang, and R.D. Phair)) Dept. Biomedical Eng., Johns Hopkins School of Medicine, Baltimore, MD 21205. (Spon. by L. Tung)

Established cell lines are now widely used in experiments concerning vascular smooth muscle(VSM) function; however, considerable evidence suggests that cultured VSM cells are functionally different from VSM cells in intact blood vessels. Ion efflux experiments using ^{45}Ca are widely used to obtain kinetic information on intracellular signaling and membrane transport. In order to determine if the kinetics of Ca^{2+} stores are comparable in the two preparations, we developed a new method for high resolution efflux studies in A7r5 cells. Using both uptake and efflux experiments, combined with a detailed mathematical model allows estimation of the rate constants for release and uptake of Ca^{2+} from intracellular stores (sarcoplasmic reticulum and mitochondria) with a high degree of confidence (C.V.<18%) as well as the Ca^{2+} contents and transmembrane fluxes associated with these stores. Quantitative comparison of results obtained from A7r5 cells with those we previously obtained for rabbit aortic segments reveals marked similarities, and suggests that, A7r5 cells serve as an excellent model for experiments on VSM cell Ca2+ homeostasis.

W-Pos113

THE DIFFERENTIAL ROLE OF SMALL G PROTEIN RHO IN THE CONTRACTION OF ARTERIAL SMOOTH MUSCLE. ((M. J. Jiang, S. H. Huang and Y. Chern)) Institute of Biomedical Sciences, Academia Sinica, Taipei 11529, Taiwan, R.O.C.

We examined the effects of the small G protein rho and GTPγS on isometric contractions of rat tail artery strips. Rho protein was purified from the fusion protein rho-glutathione S-transferase expressed by *E. coli*. Both molecules were introduced into tail artery strips by electroporation. GTPγS, at a maximally effective concentration of 0.1 mM, enhanced contractions elicited by 24 mM KCl but not those by 36 mM KCl, 51 mM KCl or different concentrations of α_1-adrenergic agonist phenylephrine. Electroporation of 10 μM rho-GTPγS had no significant effect on contractions activated by either KCl or phenylephrine. However, electroporation of ADP-ribosyltransferase C3 (2.5 μg/ml), which preferentially ADP-ribosylates rho and renders it inactive, inhibited phenylephrine- but not KCl-induced contractions. Co-introduction of rho-GTPγS and C3 diminished the inhibitory effects of C3 on phenylephrine-activated contractions. $[Ca^{2+}]_i$ measurements using aequorin as the indicator showed that C3 did not change the $[Ca^{2+}]_i$-force relationship for phenylephrine-induced contractions. These results suggest that rho is involved in signaling pathways mediating phenylephrine- but not KCl-activated contractions and that inactivation of rho by C3 did not seem to change calcium sensitivity of the contractile apparatus during phenylephrine-activated contractions of rat tail artery smooth muscle. Supported by NSC and Academia Sinica, R.O.C..

W-Pos114

TYROSINE PHOSPHORYLATION AND CONTRACTION OF SWINE CAROTID ARTERY. ((Christopher M. Rembold and Barbara A. Weaver)). Cardiovascular Division, Internal Medicine, University of Virginia, Charlottesville, Virginia 22908 USA

Regulation of $[Ca^{2+}]_i$ and modulation of Ca^{2+} sensitivity in smooth muscle were recently hypothesized to involve phosphorylation of one or more proteins on tyrosine residues. We tested this hypothesis by measuring the relative amounts of tyrosine phosphorylation on four proteins extracted from swine carotid artery homogenates. We found that histamine stimulation increased phosphorylation of a number of proteins on tyrosine residues. However, during both histamine induced contraction and relaxation after washout of histamine, changes in tyrosine phosphorylation on the four major phosphoproteins studied occurred at a rate slower than changes in contractile force. Phosphorylation of these four proteins on tyrosine residues did not correlate with Ca^{2+} sensitivity following agonist or high $[K^+]_o$ stimulation. Phorbol dibutyrate stimulation also increased tyrosine phosphorylation levels of these four proteins but the pattern of tyrosine phosphorylation differed from that observed with histamine stimulation. Tyrosine phosphorylation levels of phosphoprotein 2 correlated with phorbol dibutyrate induced contraction and changes in Ca^{2+} sensitivity. These data suggest that histamine and phorbol dibutyrate may differentially activate tyrosine phosphorylation and contractile mechanisms in the swine carotid artery. Histamine increased both force and tyrosine phosphorylation, however, these appeared to be parallel pathways: phosphorylation of these four proteins studied was not substantially involved in either the initial or sustained phase of histamine-induced contraction. In the swine carotid artery, histamine-dependent increases in phosphorylation of these four proteins on tyrosine residues may be either 1) permissive in the regulation of sustained contraction or 2) involved in other smooth muscle function such as growth, differentiation, and/or secretion. In contrast, phorbol dibutyrate dependent contraction could potentially involve tyrosine phosphorylation of some of these four proteins.

W-Pos115

PHOSPHOLIPASE C β2 IS THE MOST ABUNDANT FORM OF PHOSPHOLIPASE Cβ IN VASCULAR SMOOTH MUSCLE ((E.F. LaBelle and E. Polyak)) Bockus Res. Inst., Graduate Hospital, Philadelphia, PA , 19146. (Spon. by E. Murer)

This study was performed in order to identify the isoforms of phospholipase C (PLC) that are involved in force development and maintenance in vascular smooth muscle. Proteins extracted from rat tail artery were transferred to nitrocellulose filters by Western blotting, and the filters probed with antibodies to either PLC γ1, PLC β1, PLC β2, or PLC δ1. PLC γ1, PLCβ 2, and PLC δ1 were detected as strong bands in rat tail artery cytosol, and as faint bands in pellet fractions (containing membranes and perhaps nuclei). The MWs of PLC γ1 and PLC δ1 were the same as we observed using cytosol from calf brain as standards: 145kD for PLC γ1 and 85kD for PLC δ1. PLC β1 was detected by this procedure in cytosol from rat tail artery, but the band was very faint. The MW of PLC β2 was determined to be 132kD in the cytosol while in the pellet two bands were detected, one of 132kD and the other 101kD. The concentration of PLC β2 observed in rat tail artery was about the same as the concentration of PLC γ1 and much greater than the concentration of PLC δ1. PLC β2 has not been reported previously in smooth muscle or in any normal (non-transformed tissues). Since PLC β2 has been shown by other investigators to be activated by the same G proteins that are activated by the α1 adrenergic receptor, it seems likely that this isoform of PLC is responsible for norepinephrine-induced IP_3 production in vascular smooth muscle that precedes the generation of force. (Supported by NIH Grant HL 37413).

W-Pos116

cGMP INHIBITS RECEPTOR-LINKED SECOND MESSENGER SYSTEMS THAT REGULATE Ca^{2+} SENSITIVITY IN CANINE TRACHEAL SMOOTH MUSCLE (CTSM). ((K.A. Jones, G.Y. Wong, and D.O. Warner)) Dept. of Anesthesiology, Mayo Clinic and Foundation, Rochester, MN 55905. (Spon. by P.R. Housmans)

This study tested the hypothesis that cGMP reduces the amount of force produced for a given cytosolic Ca^{2+} concentration ($[Ca^{2+}]_i$) (i.e., myofilament "Ca^{2+} sensitivity") in CTSM EXCLUSIVELY by inhibiting receptor-linked second messenger systems that regulate Ca^{2+} sensitivity. CTSM strips were permeabilized with 100 μM β-escin, which allows free Ca^{2+} to diffuse across the cell membrane while preserving receptor/G-protein coupling to second messenger systems that regulate Ca^{2+} sensitivity. Sarcoplasmic reticulum Ca^{2+} stores were depleted with 10 μM A23187. Acetylcholine (ACh) caused an increase in force at constant $[Ca^{2+}]_i$, indicating an increase in Ca^{2+} sensitivity, which was dependent on GTP and was attenuated by the protein kinase C inhibitor, staurosporin. Concentration-response curves were generated with ACh (0.01 to 100 μM) in the presence and absence of 8-bromo cGMP at a constant $[Ca^{2+}]_i$ of 0.1 μM. In a second protocol, concentration-response curves were generated with free Ca^{2+} (0.01 to 100 μM) alone or during exposure to 100 μM ACh, in the presence and absence of 100 μM 8-bromo cGMP. 8-Bromo cGMP (1, 10, and 100 μM) decreased maximal force produced by ACh at constant $[Ca^{2+}]_i$ by 50 ± 12, 75 ± 8, and 82 ± 10%, respectively. In the absence of ACh, 8-bromo cGMP had no effect on the Ca^{2+}-force relationship. In the presence of ACh, 8-bromo cGMP caused a rightward shift of the Ca^{2+}-force relationship (changed the ED_{50} $[Ca^{2+}]_i$ from 7.4 μM to 3.4 μM) and reduced maximal force produced by 100 μM free Ca^{2+} (by 32 ± 11%). These findings indicate direct actions of cGMP on receptor-linked pathways controlling Ca^{2+} sensitivity, suggesting an important mechanism for nitric oxide-induced relaxation of CTSM.

W-Pos117

ARACHIDONIC ACID (AA) AND DIACYLGLYCEROL AS POTENTIAL CA^{2+}-SENSITIZING MESSENGERS IN SMOOTH MUSCLE ((M. C. Gong, P. Gailly, M. Kinter, A. V. Somlyo and A.P. Somlyo)) Department of Molecular Physiology and Biological Physics, UVa, Charlottesville, VA 22908

Arachidonic acid (AA) sensitizes the contractile response of smooth muscle to Ca^{2+} by inhibiting the 20 kDa myosin light chain (MLC_{20}) phosphatase(1). Futhermore, both AA and diacylglycerol (DAG) are increased by phenylephrine, an α_1 agonist, and by GTPγS, at constant free Ca^{2+}(2). The purpose of the present study was to determine in permeabilized femoral artery smooth muscle whether the time course and mass of the GTPγS-induced increases in AA and DAG, at constant free Ca^{2+}, are compatible with the putative role of AA and/or DAG (and kinase C) as Ca^{2+}-sensitizing messengers. We show that the increase in AA and DAG preceeded contraction and, within the limits of the time resolution of the method, MLC_{20} phosphorylation. The absolute mass of AA reached was 61 to 88 μM in tissue stimulated with GTPγS (50 μM, 30 min). Exogenous short fatty acid chain DAG (DiC_8) left-shifted the force-dose response curves of high K^+ in intact and of Ca^{2+} in α-toxin permeabilized rabbit femoral artery. DiC_8 (10 μM for 30 min) increased the MLC_{20} phosphorylation evoked by pCa 6.7 within 5 min from 34±3.1% (n=5) to 61±2.3% (n=5, p<0.001) and prolonged the $t_{1/2}$ of relaxation, in the presence of ML-9, a kinase inhibitor, from 2.4±0.29 (n=4) to 4.6±0.26 min (n=5, p<0.001). The results are consistent with a possible second messenger role of both AA and DAG mediating G-protein coupled inhibition of MLC_{20} phosphatase and, consequently, Ca^{2+}-sensitization. The relative contributions of, respectively, kinase C-mediated and/or direct inhibition of MLC_{20} phosphatase (3) pathways to this process remain to be determined. 1. Gong et al, J. Biol. Chem. 267: 21492-21498, 1992; 2.Gong et al, Biophys. J. 66:A409, 1994; 3. Somlyo et al, Adv. Prot. Phosphatase 5: 181-195, 1989

W-Pos118

EXTRACELLULAR CA^{2+} ENTRY THROUGH VOLTAGE-GATED CA CHANNELS, ACH-GATED CHANNELS, AND CA^{2+}-INDUCED RELEASE OF INTRACELLULAR CA^{2+} ALL CONTRIBUTE TO CONTRACTIONS OF A MOLLUSCAN SMOOTH MUSCLE. ((V. Brezina and K. R. Weiss)) Dept. of Physiology and Biophysics, Mt. Sinai School of Medicine, CUNY, New York, NY.

We have studied single, functionally intact fibers dissociated from the accessory radula closer (ARC) muscle of *Aplysia californica*, using a technique that combines current or voltage clamp with continuous on-line measurement of contractions (Brezina 1995, *Pflügers Arch.*, in press). Application of the physiological contraction-inducing transmitter ACh rapidly depolarizes unclamped fibers by opening voltage-independent, cation-permeable channels. Contraction begins when the fiber is depolarized (by the ACh or indeed simply by current injection) above about -40 mV, where its voltage-gated 'L'-type Ca channels begin to open. These rapid contractions immediately fail in Ca^{2+}-free solution, when the Ca channels are blocked by low nifedipine, or when the depolarization is prevented under voltage clamp. In this last case, however, ACh can still often slowly contract the fiber. These contractions are also blocked in Ca^{2+}-free solution, but not by low nifedipine, and increase with hyperpolarization rather than depolarization. They are most likely due to Ca^{2+} entering through the ACh-gated channels themselves. Finally, the fibers clearly contain intracellular Ca^{2+} stores, as they contract massively (in Ca^{2+}-free solution) in response to caffeine or the Ca^{2+}-ionophore A23187. It is likely that, during most normal contractions, entering extracellular Ca^{2+} triggers further release of this stored Ca^{2+}. Most contractions are partially or completely blocked by ryanodine, and are accompanied by transients of Ca^{2+}-activated K current that probably reflect 'quantal' units of Ca^{2+} release. We are now adding fluorescence Ca^{2+} measurements to our technique in order to evaluate to what extent each of the three sources of Ca^{2+} contributes to contractions under different physiological conditions.

W-Pos119

NITROVASODILATORS INDUCE PHOSPHORYLATION OF MYOSIN LIGHT CHAIN KINASE IN SWINE CAROTID ARTERY. ((D.A.Van Riper, N. L. McDaniel, and C. M. Rembold)) Cardiovascular Division (Internal Medicine & Pediatrics), University of Virginia, Charlottesville, VA USA

Nitrovasodilators are hypothesized to induce smooth muscle relaxation by the following pathway: the locally produced nitric oxide activates guanylyl cyclase which produces cGMP. The increase in [cGMP] then activates cGMP dependent protein kinase(s) which then phosphorylates unknown proteins involved both in regulation of $[Ca^{2+}]$ and $[Ca^{2+}]_i$ sensitivity. Recent studies suggest increases in [cGMP] can also activate cAMP dependent protein kinase. cAMP dependent protein kinase, but not cGMP dependent protein kinase, can phosphorylate myosin light chain kinase on site A, a reaction that decreases the sensitivity of myosin light chain kinase to Ca^{2+}-calmodulin. We investigated the role of myosin light chain kinase phosphorylation (at site A) in nitrovasodilator induced relaxation of swine carotid artery. In tissues stimulated with 10 μM histamine, addition of 100 μM nitroglycerin or 100 μM nitroprusside for 4 min decreased both myosin light chain (MLC) phosphorylation and force but did not significantly change $[Ca^{2+}]_i$. This indicated a nitrovasodilator-dependent decrease in the $[Ca^{2+}]_i$ sensitivity of MLC phosphorylation. Histamine alone and histamine plus either nitroglycerin or nitroprusside increased myosin light chain kinase phosphorylation to similar extents. In unstimulated tissues, addition of 100 μM nitroglycerin or 100 μM nitroprusside also increased myosin light chain kinase phosphorylation but did not significantly alter aequorin estimated $[Ca^{2+}]_i$ or force. These data suggest that the nitrovasodilator induced decrease in the $[Ca^{2+}]_i$ sensitivity of MLC phosphorylation was not caused by myosin light chain kinase phosphorylation. Nitrovasodilators can, however, induce phosphorylation of myosin light chain kinase in unstimulated swine carotid, a reaction that could slow subsequent contraction. Support: NIH HL38918 & VA AHA.

W-Pos120

TRACHEAL SMOOTH MUSCLE CONTRACTION IS ASSOCIATED WITH TYROSINE PHOSPHORYLATION OF THE MEMBRANE-ASSOCIATED DENSE PLAQUE PROTEIN PAXILLIN. ((S.J. Gunst, Z. Wang and F.M. Pavalko)) Department of Physiology and Biophysics, Indiana University, School of Medicine, Indianapolis, IN, 46202.

We have previously shown that talin, a protein localized to the membrane attachment sites of the actin cytoskeleton, is phosphorylated during contractile activation of tracheal smooth muscle (Pavalko, et al. AJP Cell: 1995). Tyrosine phosphorylation of another membrane-associated dense plaque protein, paxillin, has been associated with remodelling of the actin cytoskeleton during embryonic development and fibroblast transformation. In the present study, we investigated the role of tyrosine phosphorylation of paxillin to assess a possible role for cytoskeletal remodelling during smooth muscle contraction. Canine tracheal smooth muscle strips were contracted isometrically with acetylcholine (Ach 10^{-4} M), and then freeze-clamped at various time points after stimulation. Paxillin was extracted, electrophoresed and transferred to nitrocellulose. Tyrosine phosphorylation of paxillin was detected using anti-phosphotyrosine antibody and the paxillin protein band was confirmed using anti-paxillin antibody. As an index of contractile protein activation, myosin light chain phosphorylation (MLCP) was assayed in the same strips. Tyrosine phosphorylation of paxillin increased significantly during contraction but with a much slower time course than MLCP. Results suggest that tyrosine phosphorylation of paxillin plays a role in excitation-contraction coupling. Paxillin phosphorylation may be associated with cytoskeletal remodelling during the contractile activation of smooth muscle cells.

Supported by HL29289 and Amer. Lung Assoc.

W-Pos121

TRANSIENT INCREASE IN MYOSIN LIGHT CHAIN (MLC) PHOSPHORYLATION AT CONSTANT CA^{2+} IN PERMEABILIZED SMOOTH MUSCLE. ((*T. Murahashi, A. Fujita and T. Kitazawa)) Dept. Physiol. & Biophys., Georgetown Univ., Washington, D.C. 20007

Time courses of MLC phosphorylation (P) and contraction (F) induced by Ca^{2+} alone or agonist/GTPγS were examined in α-toxin permeabilized, A23187-treated smooth muscles. A step increase in Ca^{2+} to pCa 6.3 in phasic (portal vein) smooth muscle produced a rapid rise in P and F due to activation of MLC kinase, followed by a spontaneous decline to low steady-state levels. There was no significant change in F/P ratio with time (except early phase of activation) in phasic (portal vein) and tonic (femoral artery) smooth muscles, respectively, suggesting tight coupling between P and F during Ca^{2+}-activated contraction. Cytochalasin D completely abolished F, but did not affect the transient time course of P, suggesting that the transient property of F is due to the intrinsic nature of P process. Application of α_1 agonist or GTPγS markedly increased both P and F due to inhibition of MLC phosphatase. While F levels were maintained, P levels declined significantly with time even in the continuous presence of either agonist or GTPγS. These results suggest that 1) the spontaneous decline of P during agonist stimulation is not due to the receptor desensitization, but due to desensitization/inactivation of G protein or other process(es), and 2) the late phase of agonist/GTPγS-induced contraction in α-toxin-permeabilized smooth muscle at constant Ca^{2+} may be partly caused by "latch state" of cross-bridge. This work was supported by NIH HL51824.

W-Pos122

ROLE OF PKC ACTIVATION IN AGONIST-G PROTEIN MEDIATED CA^{2+} SENSITIZATION OF SMOOTH MUSCLE CONTRACTION. ((A.K.M. Gaznabi, *A. Fujita, T. Murahashi and T. Kitazawa)) Dept. Physiol. & Biophys., Georgetown Univ., Washington, D.C. 20007

We have reported that DAG and phorbol ester, like agonist or GTPγS, inhibit MLC phosphatase to increase both MLC phosphorylation at Ser-19 and force development at constant Ca^{2+} (J. Gen. Physiol. 104, 265-286, 1994). Here we examine whether force and phosphorylation induced by PKC activators are sensitive to MLC kinase inhibitors and whether PKC activation is involved in agonist-induced Ca^{2+} sensitization of contraction in permeabilized smooth muscle. MLC kinase inhibitors (wortmannin and ML-9) inhibited either Ca^{2+}-, GTPγS- and PDBu-induced MLC phosphorylation and contraction in femoral artery, supporting the above hypothesis. A selective PKC inhibitor peptide (IP) inhibited PDBu- and DAG (diC_8)-induced contractions, but not Ca^{2+}-activated contraction, indicating its selectiveness. PKC-IP 30 μM reduced histamine-induced potentiation of contraction in rabbit femoral artery by 51 % ± 4.5 and phenylephrine-induced enhancement of contraction in portal vein by 42 % ± 2.6. On the other hand, 100 μM IP failed to reduce endothelin-induced contraction in femoral artery. GTPγS-induced potentiation of contraction was decreased by 25 % in the presence of 30 μM IP. These results suggest that PKC activation significantly, but not totally regulates the agonist-induced Ca^{2+} sensitization of the regulatory/contractile apparatus, but the degree of its regulation may vary depending on agonist. This work was supported by NIH HL51824.

W-Pos123

LYSOPHOSPHATIDYLCHOLINE CAUSE INCREASE IN Ca-SENSITIVITY OF CONTRACTILE PROTEINS IN α-TOXIN PERMEABILIZED RAT MESENTERIC SMALL ARTERY SMOOTH MUSCLE. ((P.E. Jensen, J. Ohanian* and C. Aalkjaer)) Dep of Pharmacology, Univ of Aarhus, 8000 Aarhus C, DK and *Dep of Medicine, Univ of Manchester, UK. (Spon. by M.J. Mulvany)

Agonists can increase the Ca-sensitivity of smooth muscles, but the cellular signalling pathways have not been clarified yet. In *in vitro* experiments lysophosphatidylcholines (LPC), lipid metabolites released when PLA_2 act on phosphatidylcholine (PC), can activate protein kinase C (PKC) [K. Oishi et al., J Biol Chem, 263:6865-5871, 1988]. PKC is a potential messenger involved in increasing the Ca-sensitivity in smooth muscles [A.L. Ruzycky and K.G. Morgan, Br J Pharmacol, 97:391-400, 1989; J. Nishimura et al., Am J Physiol, 259:H2-H8, 1990]. Thus, to investigate if LPC may be a second messenger causing increase in Ca-sensitivity, the effect of LPC on the Ca-sensitivity of isometric force development in small segments of α-toxin permeabilized rat mesenteric small arteries was assessed and in larger quantities of unmounted arteries, the levels of LPC and PC during stimulation with norepinephrine (NE) were measured. LPC (1-myristoyl and 1-palmitoyl, 100μM) increased tone induced by 1μM free Ca by 93% (mean, n=4) and 143% (n=6), respectively. LPC with other fatty acids in position 1 had smaller or no effects. Furthermore, PC, myristic and palmic acid, choline and L-α-glycerophosphorylcholine, possible metabolites of LPC, had no effects. EC_{50} values for 1-myristoyl and 1-palmitoyl LPC were 3μM (n=3) and 24μM (n=6), respectively, and maximal effects were obtained with 100μM. Ca-EC_{50} was 794nM (n=4) before 30 min treatment with LPC. After, Ca-EC_{50} was significantly decreased to 470nM (n=4, 1-myristoyl) and 314nM (n=4, 1-palmitoyl). To measure the levels of LPC and PC, arteries were incubated with ^{3}H-myristate, lipids extracted followed by separation using HPLC and finally quantitated by liquid scintillation. The levels of ^{3}H labelled PC and LPC could be measured, however, there were no changes in these levels after 30 sec (n=3) or 5 min (n=3) presence of 100μM NE. In summary, contractile studies indicated that LPC could increase the Ca-sensitivity of rat mesenteric small artery smooth muscle, but the level of LPC was not changed during stimulation with NE. Thus, there is a potential role for LPC as a second messenger increasing Ca-sensitivity but it remains controversial because no changes in the levels of LPC could be measured under the conditions in the present study.

W-Pos124

INCREASED TROPONIN I PHOSPHORYLATION IN RESPONSE TO β-ADRENERGIC STIMULATION IN CARDIAC MYOCYTES FROM THE SPONTANEOUSLY HYPERTENSIVE RAT ((Bradley K. McConnell, Christine S. Moravec and Meredith Bond)) Dept. of Physiology and Biophysics, CWRU and Dept. of Molecular Cardiology, CCF, Cleveland, Ohio 44195

Cardiac myocytes from hypertrophied hearts of the spontaneously hypertensive rat (SHR) are characterized by a diminished inotropic response to sympathetic stimulation in spite of normal baseline contractile function (Moravec and Bond, in preparation). Inotropic responses to β-adrenergic stimulation have been shown to result from both increased availability of Ca^{2+} for activation of contraction and increased phosphorylation of contractile proteins. In this study, we have used suspensions of isolated, $^{32}P_i$-labelled, left ventricular cardiac myocytes from the SHR with stable hypertrophy (26 weeks) and age-matched, normotensive WKY controls, to compare protein kinase A (PKA) dependent phosphorylation of the contractile proteins, troponin I (TnI) and myosin light chain 2 (MLC_2). Following a 10 min incubation of the labelled cells with activators of the β-adrenergic pathway, myofibrillar proteins were separated by polyacrylamide gel electrophoresis and then subsequently quantified using a PhosphorImager. TnI phosphorylation in response to isoproterenol, over its own unstimulated control, was approximately 75% greater in SHR than in WKY myocytes. This enhanced TnI labelling in the SHR was also observed when the myocytes were stimulated with norepinephrine plus prazosin, forskolin, or Cl-cAMP, indicating that the reason for the differing responses of the two strains is downstream of cAMP production. In contrast, we did not observe a significant change in MLC_2 phosphorylation, over its own control, in response to β-adrenergic stimulation in the SHR or in the WKY. This increased PKA-dependent phosphorylation of TnI may result in a rightward shift of the force/pCa curve in the SHR, resulting in a decreased sensitivity of troponin C, for Ca^{2+}. Thus, the depressed inotropic response to sympathetic stimulation in hypertensive hypertrophy may be due, in part, to alterations in the sensitivity of the myofibrillar apparatus to Ca^{2+}.

W-Pos125

ACTIN FILAMENTS MODULATE CHOLINERGIC RECEPTOR-MEDIATED INTRACELLULAR [CA^{2+}], MYOSIN LIGHT CHAIN PHOSPHORYLATION, AND CONTRACTION IN AIRWAY SMOOTH MUSCLE. ((B. Kowalski, R. Kim and C.-M. Hai)) Brown University, Providence, RI 02912.

Cholinergic receptor-mediated intracellular [Ca^{2+}], myosin light chain phosphorylation, and contraction in airway smooth muscle have been found to be length-dependent (Yoo et al., Am. J. Physiol., in press), suggesting that cytoskeletal filaments may modulate smooth muscle activation. This hypothesis was tested by investigating the effect of actin filament disruption by cytochalasin B on airway smooth muscle activation and contraction. Cytochalasin B (10 uM) significantly lowered force generation, intracellular [Ca^{2+}], and myosin phosphorylation induced by 1 uM carbachol. The observed effect of cytochalasin B was not due to inhibition of glucose transport because removal of glucose had no effect on carbachol-induced intracellular [Ca^{2+}] and contraction. Filamentous actin in fixed sections of smooth muscle was labelled and observed by fluorescence microscopy. The fluorescence of cytochalasin-treated tissues were not apparently different from control, suggesting that actin filaments were interrupted but not severely depolymerized. This suggestion will be confirmed by experiments on single smooth muscle cells. In summary, these results suggest that actin filaments modulate cholinergic receptor-mediated intracellular [Ca^{2+}] and myosin phosphorylation in airway smooth muscle (Supported by AHA).

W-Pos126

POLYAMINES SENSITIZE SMOOTH MUSCLE TO Ca^{2+} BY SELECTIVE INHIBITION OF A MYOSIN PHOSPHATASE. ((P. Hellstrand, K. Swärd, I. Nordström, B.-O. Nilsson, and M. D. Pato*)) Dept of Physiol & Biophys, Univ of Lund, Sweden, and *Dept of Biochemistry, Univ of Saskatchewan, Canada

Polyamines increase Ca^{2+}sensitive force in permeabilized guinea-pig ileum, in potency order spermine>spermidine>putrescine (Swärd et al., AJP 266:C1754, 1994). This is associated with increased myosin LC_{20} phosphorylation and with reduced rate of dephosphorylation. Force increase is slower in α-toxin than in β-escin permeabilized preparations. Phosphatase inhibitors (okadaic acid, microcystin-LR) potentiate force and concomitantly reduce the additional effect of spermine. Sensitization by spermine (1 mM) has been demonstrated in permeabilized guinea-pig ileum, taenia coli, portal vein and mesotubarium, and in rat femoral artery and portal vein. Tonic muscles are sensitized at lower [Ca^{2+}] than are phasic, resembling the pattern of GTPγS induced sensitization. However, sensitization to Ca^{2+} produced by GTPγS has an optimum at lower β-escin concentration than that by spermine, suggesting that G-proteins are not involved. The effects of polyamines on smooth muscle phosphatases (SMP-) I-IV, isolated from turkey gizzard, were investigated *in vitro*. These are all active against phosphorylated LC_{20}, but only SMP-III and IV dephosphorylate HMM. With both substrates, spermine inhibits SMP-IV but stimulates SMP-I and II, whereas SMP-III activity against PLC_{20} is inhibited and that against HMM stimulated. Addition of SMP-IV to Triton X-100 permeabilized ileum induced relaxation, an effect that was antagonized by spermine. Spermine did not affect binding of SMP-IV to myosin and did not dissociate the phosphatase into subunits. The results indicate that polyamines sensitize smooth muscle by inhibiting SMP-IV activity in organized fibers.

W-Pos127

CALPONIN PHOSPHORYLATION IN SWINE CAROTID ARTERIAL HOMOGENATE. ((A. Rokolya, M.P. Walsh, and R.S. Moreland)) Bockus Research Institute, Graduate Hospital, Philadelphia, PA 19146, and Department of Medical Biochemistry, University of Calgary, Alberta, Canada, T2N 4N1.

Phosphorylation of calponin, a smooth muscle specific, thin filament-associated protein, reverses its inhibitory effect on myosin ATPase activity in reconstituted filament systems; studies using intact smooth muscle have not however consistently supported this result. The goal of this study was to determine if vascular smooth muscle contains all of the necessary biochemical machinery to catalyze calponin phosphorylation and if so what kinase(s) is involved. We used as a model the swine carotid arterial homogenate which allows direct access to the intracellular components and contains all endogenous proteins and enzymes at physiological relative concentrations. Calponin phosphorylation increased in response to Ca^{2+} from a basal value of 0.01±0.01 to 0.07±0.01 and 0.25±0.02 mol P_i/mol calponin in the absence and presence of okadaic acid, respectively. Phorbol 12-13-dibutyrate (PDBu) in the absence of Ca^{2+} increased calponin phosphorylation to 0.23±0.06 and 0.40±0.09 mol P_i/mol calponin in the absence and presence of okadaic acid, respectively. PDBu-induced calponin phosphorylation was not increased by the addition of Ca^{2+}. 1-Oleoyl-2-acetyl-3-*sn*-glycerol (OAG) induced significant increases in calponin phosphorylation levels in the absence and presence of okadaic acid; 0.42±0.03 and 1.37±0.01 mol P_i/mol calponin, respectively. All increases in calponin phosphorylation, both Ca^{2+}-dependent and Ca^{2+}-independent, were inhibited by the PKC inhibitors staurosporine and PSSI. Our data suggest that although a Ca^{2+}-dependent kinase can induce calponin phosphorylation, the primary kinase involved is a Ca^{2+}-independent isoform of PKC. Supported in part by NIH HL37956 and HL46704 (RSM) and a SEPA AHA Fellowship (AR).

W-Pos128

ROLE OF PHOSPHODIESTERASES IN REGULATION OF COLONIC MOTILITY. ((S.R. Brave., M.E. Bradley and I.L.O. Buxton)) Dept. Pharmacology, Univ. Nevada, Reno, NV 89557. (Spon. by John Peacock)

Recently PDE IV was demonstrated to be the important PDE in canine colonic smooth muscle. We have evidence that PDE II (cGMP-stimulated) and cross-talk between the cAMP/cGMP pathways are also of importance. Strips of circular canine proximal colon were set up for the recording of isometric tension responses. Phasic contractions were induced by 1 or 10 μM histamine. Concentration-response curves for relaxation to ISO, FSK, VIP, SNP, and S-nitrosocysteine were unchanged. In control tissues the IC_{50} for VIP was 20 nM and following incubation with 5 nM SNP, was 1 mM. In similar experiments, the maximal response for relaxation to ISO was reduced by 40%. This suggests the involvement of PDE II, which under these conditions is activated by SNP. Rolipram, a specific PDE IV inhibitor, at 0.1 and 1 μM, increased the relaxant effects of VIP and FSK. Paradoxically, 10 μM rolipram either had no effect or shifted the relaxant curves rightwards. This suggests that a negative feedback pathway is activated or the high [cAMP] may activate cGMP-protein kinase, resulting in a concomitant activation of PDE II. Concentration-response curves for relaxation to rolipram revealed that this PDE IV inhibitor was more potent as a relaxant agent on 10 than 1 μM histamine-induced phasic contraction (IC_{50}: 0.3 μM and 30 μM for 10 and 1 μM histamine, respectively). This suggests the involvement of a calcium-sensitive adenylyl cyclase which is activated by 10 μM histamine-induced calcium changes. Basal and 1 μM-induced [cAMP] were doubled by 10 μM histamine. Hence it is clear that a novel calcium-sensitive adenylyl cyclase is present in the canine colon; PDE II and the activation of protein kinases by cAMP may play important roles in the regulation of colonic motility.

W-Pos129

INHIBITION OF FORCE AND WHOLE CELL L-TYPE Ca CURRENT BY NEOMYCIN IN RAT ARTERIAL SMOOTH MUSCLE. ((P.D. Langton)) Ion Channel Group, Dept. Cell Physiology and Pharmacology, University of Leicester, LE1 9HN, U.K.

Neomycin and other aminoglycoside antibiotics block neuromuscular transmission and inhibit high $[K^+]_o$-induced elevation of $[Ca]_i$ effects which can be partially relieved by increasing $[Ca]_o$. It has been suggested that these compounds may act as blockers of Ca conductance. The effects of neomycin on Ca-dependent force and voltage-gated Ca current in rat arterial smooth muscle have been examined. **Results:** In rat mesenteric artery, high (40 mM) K^+-induced force was abolished in the absence of Ca_o and was blocked by the dihydropyridine (DHP) antagonist (-)202-791 (EC_{50} 1.9 nM). Neomycin relaxed K^+-induced force with EC_{50} of 70 μM and a slope close to 1. Doubling extracellular [Ca] to 3.6 mM shifted the concentration-effect curve for neomycin to the right, increasing the EC_{50} to 180 μM. Whole-cell patch clamp recordings of caesium-dialysed rat isolated basilar arterial myocytes showed voltage-gated inward current carried by Ba which exhibited DHP-sensitivity typical of L-type current. Neomycin inhibited this inward current with EC_{50}s of 34 μM and 134 μM in 1.8 and 10 mM Ba, respectively (fig. 1.).

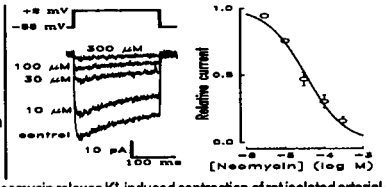

Figure 1.
Left: Voltage clamp traces showing neomycin block of inward current in 1.8 mM Ba.
Right: Concentration-effect curve for neomycin block of inward current for n = 3 cells.

These data suggest that neomycin relaxes K^+-induced contraction of rat isolated arterial smooth muscle by inhibition of DHP-sensitive Ca channels.

Supported by the British Heart Foundation.

W-Pos130

EFFECTS OF SODIUM NITROPRUSSIDE (SNP) ON TENSION, INTRACELLULAR $^{\wedge}$CALCIUM AND CALCIUM CURRENT IN COLONIC SMOOTH MUSCLE ((J.D. Campbell, S.C. Kwon, N.G. Publicover and K.M. Sanders)) Department of Physiology, University of Nevada School of Medicine, Reno, NV 89557.

Nitric oxide (NO) is an inhibitory neurotransmitter in visceral smooth muscles, inducing both hyperpolarization and inhibition of contraction. Hyperpolarization caused by NO appears to be due to activation of K^+ currents (*Biophys.J.* 64:A386, 1993). NO also causes a decrease in intracellular calcium ($[Ca^{2+}]_i$; PNAS 90:2087-2091, 1993) which may be partially due to its effects on membrane potential, and also due to direct effects on Ca^{2+} influx through voltage-dependent Ca^{2+} channels. We compared the effects of the NO donor, SNP, on tension, $[Ca^{2+}]_i$, and whole cell Ca^{2+} current (I_{Ca}) in intact muscles and freshly dispersed smooth muscle cells from the circular layer of the canine proximal colon. SNP (10 μM) reduced both tension and phasic changes in $[Ca^{2+}]_i$ (as measured by INDO-1/AM fluorescence) by 61% (n=2), but SNP had little effect on resting $[Ca^{2+}]_i$. Using the patch clamp technique, SNP at 1 and 10 μM did not affect peak I_{Ca} elicited when voltage was stepped from -80 mV to 0 mV (n=10). SNP at 100 μM, however, decreased peak I_{Ca} by 19 ± 5.7% (n=3). The time course of this inhibition occurred rapidly, within 1 minute of treatment, unlike SNP's activation of K^+ currents. The decrease in I_{Ca} could not be mimicked by 8-bromo cGMP treatment (100 mM; n=4). These data suggest that a minor component of the decrease in $[Ca^{2+}]_i$ caused by NO involves a reduction in I_{Ca} which is not mediated by cGMP.

(Supported by NIDDK 08811 and 32176.)

W-Pos131

A MODEL FOR EXTRACELLULAR LIPID LIPOSOME INITIATION AND GROWTH IN ARTERIAL INTIMA. ((Y. Yin, K.-H. Lim, S. Weinbaum, S. Chien and D. Rumschitzki)) City College, CUNY, NYC 10031 & UCSD, San Diego, Ca. (Spon. by R. Callender)

Hypercholesterolemic rabbits develop (Simionescu *et al*, 1986) localized extracellular cholesterol packets (liposomes) comprised of the lipid from one or more LDL bound to subendothelial matrix and circulating monocytes stick to nearby endothelial regions. Since these monocytes can enter the intima and devour lipid to become foam cells, their formation and growth is critical in early atherogenesis. Frank and Fogelman (1989) clearly visualize such liposomes with rapid freeze etching and give their size distribution for both WHHL hypercholesterolemic rabbits and cholesterol-fed normal rabbits. These distributions differed markedly.

We have shown that much LDL crosses the endothelium through short-lived, infrequent leaks associated with cells in turnover. LDL-bearing fluid then encounters a nearly impermeable internal elastic laminar (IEL), convectively spreading *parallel* to the endotheluim through the loose intimal matrix before seeping through the IEL. We suggest that the high LDL concentration regions of these leakage spots supply the LDL that binds to matrix to nucleate liposomes; overlapping spots of subsequent leaks furnish LDL to polymerize the liposomes. We construct a hierarchy of models for intimal lipid liposome nucleation and growth/polymerization to characterize the observed size distributions as a response to multiple, overlapping leaks. Coupling these to artery the wall transport models explains both distributions and links their difference to the focal nature of the endothelial leaks. More intricate models include liposome crowding, decay, size-dependent reactivity and merging.

W-Pos132

MEMBRANE POTENTIAL DEPENDENCE OF CEREBRAL ARTERIAL DIAMETER REFLECTS ACTIVATION OF VOLTAGE- DEPENDENT CALCIUM CHANNELS. ((Harry J. Knot, Michael Rubart and Mark T. Nelson)) University of Vermont, Dept. of Pharmacology, CMRF, 55A South Park Drive, Colchester VT 05446-2500.

Intravascular pressure causes resistance arteries to contract (myogenic tone) from which they can constrict or dilate by modulating substances. We tested the hypothesese that (1) pressure induced depolarization in myogenic cerebral arteries is sufficient to account for the change in vascular diameter and (2) that the membrane-potential dependence of diameter reflects the steady-state voltage-dependence of Ca^{2+}-channels in the smooth muscle myocytes in the arterial wall. The following observations are consistent with the first hypothesis; (1) Pressure causes graded depolarization (from about -65 mV (at 10 mm Hg) to about -30 mV (at 90 mm Hg)) and associated constriction in these arteries. (2) At constant pressure, depolarization (by K^+ channel blockers) leads to vasoconstriction, and hyperpolarization (by K^+ channel openers) leads to vasodilation. (3) Keeping the membrane potential constant (by opening K_{ATP} or K_{Ca} channels) prevents the pressure-induced vasoconstriction. The following observations are consistent with the second hypothesis; (1) The calcium channel antagonists nisoldipine (100 nM) or nimodipine (100 nM) abolished all active tone in these arteries at any pressure. (2) The steady-state voltage-dependence of Ca^{2+} channels (see Rubart, Patlak & Nelson this meeting) is similar to the membrane potential sensitivity of arterial diameter. We propose that an important mechanism by which pressure constricts myogenic cerebral arteries is through membrane depolarization which activates voltage-dependent Ca^{2+} channels.

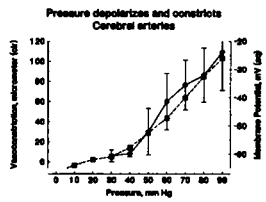

HJK is a Fellow of the AHA Vermont affiliate. Supported by the NSF and NIH.

W-Pos133

DIMINISHED VASCULAR RESPONSE TO K_{ATP} CHANNEL OPENERS IN RESISTANCE SIZE CEREBRAL ARTERIES FROM DIABETIC RATS.

((Paul A. Zimmermann* and Mark T. Nelson)) University of Vermont, Dept. of Cardiology* and Pharmacology, CMRF, 55A South Park Drive, Colchester VT 05446-2500.

Diabetes mellitus has long been considered a risk factor for cerebrovascular disease. Studies have linked altered vasodilation capability with the onset of diabetes. Recent *in vivo* evidence has suggested that part of this impaired function may be related to K_{ATP} channel activity. To test the hypothesis that K_{ATP} channel activity might be altered in diabetes, we examined response of pressurized mid-cerebral arteries to K_{ATP} channel openers, lemakalim and pinacidil, in diabetic and non-diabetic rats.

Twelve week old female rats were injected with saline or streptozocin(STZ)(60mg/kg). Rats were studied at 16 weeks; STZ injected rats having had uncontrolled diabetes for four weeks. Control rats had a blood sugar level of 75±18 mg/dl, and diabetic rats had a blood sugar level of 356±64 mg/dl. Mid-cerebral arteries were pressurized to 60mmHg (approximate to physiologic pressure). Diabetic arteries developed 30.8±1.4% tone (constricted 30.8% from diameter in calcium-free buffer), and control arteries developed 26.7±1.4% tone (p=.07). Both diabetic and control arteries dilated to 85% maximum diameter in response to lemakalim and pinacidil. However, there was a tenfold shift in the EC_{50} of the lemakalim dilator response between diabetic, 500nM, and non-diabetic, 50nM, arteries(p<.05). In addition, there was a similar shift in the EC_{50} of the pinacidil dilator response.Dilation response to acetylcholine and nipride were similar to control.These *in vitro* experiments suggest that alterations in vascular dilator activity between diabetic and non-diabetic animals occurs, in part, to altered K_{ATP} channel number and/or sensitivity to K_{ATP} channel openers. Ongoing patch clamp studies are aimed at elucidating the basis for this difference. Supported by the NIH.

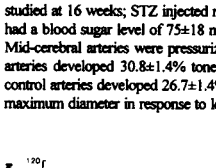

W-Pos134

PACAP MODULATES THE L-TYPE CALCIUM CURRENT IN VASCULAR SMOOTH MUSCLE CELLS. ((B. Li, C.L. Chik, A.K. Ho and E. Karpinski)) Department of Physiology, University of Alberta, T6G 2H7

Pituitary adenylate-cyclase activating polypeptide (PACAP) receptors have been localized in many tissues (including vascular smooth muscle cells) and PACAP has also been shown to reduce blood pressure. In this study, the effect of PACAP was investigated in vascular smooth muscle cells prepared from the rat tail artery. PACAP ($1x10^{-10}$M to $1x10^{-6}$M) increased cAMP accumulation up to 20-fold. Since cAMP is a known modulator of the L-type calcium current, the effect of PACAP on this current was compared with that of 8-bromo-cAMP. PACAP ($5x10^{-10}$M to $1x10^{-7}$M) increased the L-type calcium current; the maximum increase in current (50 ± 5%) occurred at a concentration of 10^{-8}M. In contrast, 8-bromo-cAMP ($1x10^{-7}$M to $1x10^{-3}$M) decreased this current. Taken together, these observations suggest that the effect of PACAP on the L-type calcium current in these cells was independent of cAMP. Since PACAP has been shown to stimulate phospholipase C in other cells, the effect of protein kinase C (PKC) on this current was examined. PMA ($1x10^{-6}$M), a PKC activator, increased the L type calcium current 52±4%. The intracellular application of calphostin, a PKC inhibitor, blocked the effects of PACAP and PMA on the L-type calcium currents. Pretreatment with PMA also blocked the effect of PACAP on this current. Based on these results, it is concluded that although PACAP probably activates both the PKA and PKC signal pathways in this cell preparation, the effect of PACAP on the L-type calcium current appears to be PKC dependent.

W-Pos135

P_2 RECEPTOR AGONISTS ACTIVATE Ca^{2+}-DEPENDENT K^+ AND Cl^- CURRENTS IN HUMAN CORONARY ARTERY SMOOTH MUSCLE CELLS VIA PRODUCTION OF INOSITOL PHOSPHATES AND RELEASE OF Ca^{2+} FROM INTERNAL STORES.

((D. Mathiasen[1,2], P. Christophersen[1], S. Dissing[2], S.-P. Olesen[1])). [1]NeuroSearch, DK-2600 Glostrup; [2]Dept. Med. Physiol., U. of Copenhagen, DK-2200, Denmark.

Coronary arteries are innervated by ATP-containing nerves, and large amounts of this transmitter may also be released in the vascular wall during pathological aggregation of thrombocytes. ATP can mediate very different functional effects via a diversity of P_2 purinoceptors, and we here report the major signal transduction pathway activated by ATP in cultured human coronary artery smooth muscle cells.

The ATP-induced changes in the cytosolic Ca^{2+} concentration was measured in single muscle cells using a digital imaging system. ATP (0.1-500 μM) increased $[Ca^{2+}]_i$ dose-dependently (EC_{50} = 5 μM) up to a maximum of 600 nM. Oscillations in $[Ca^{2+}]_i$ were sometimes induced by ATP at concentrations of 3 to 30 μM, whereas ATP at higher concentrations induced a single transient response. The effects were independent of external Ca^{2+}, but they could be blocked by the phospholipase C inhibitor U 73122. The formation of inositol phosphates was determined, and stimulation with 100 μM of ATP or UTP increased the levels of $InsP_2$, Ins(1,3,4), Ins(1,4,5)P_3 and Ins(1,3,4,5)P_4 with characteristic time courses. Whole-cell patch clamp recordings confirmed that ATP did not activate a significant Ca^{2+} current through the cell membrane. At resting membrane potential, ATP did, however, activate a transient outward K^+ current and an inward Cl^- current with a time course comparable to that of the Ca^{2+} spike. Inclusion of 10 mM EGTA in the pipette solution blocked both currents. The K^+ current was studied further at the single channel level, and it showed the characteristics of a BK current.

In conclusion, external ATP at physiological concentrations stimulated the formation of inositol phosphates and subsequent release of Ca^{2+} from internal stores in human coronary artery smooth muscle cells. Surprisingly, the Ca^{2+} concentration just below the cell membrane increased sufficiently to activate Ca^{2+}-dependent BK channels at resting membrane potential.

W-Pos136

VOLTAGE-DEPENDENT NON-SPECIFIC CATION CHANNEL IN BASILAR ARTERY AND CEREBRAL PRECAPILLARY ARTERIOLAR SMOOTH MUSCLE CELLS.

((Y. Song and J. M. Simard)) Division of Neurological Surgery and Department of Physiology, University of Maryland, Baltimore, M.D. 21201

It is well known that membrane potential is important in regulating vascular smooth muscle tone by controlling Ca^{2+} entry through Ca^{2+} channels. We have identified a cation channel that might participate in regulating membrane potential in cerebral arteries. We studied smooth muscle cells isolated from guinea pig basilar artery and from cerebral precapillary arterioles using conventional patch clamp techniques. In whole-cell recordings of macroscopic current with CsCl inside and NaCl with no Ca^{2+} outside, the channel gave an inward current at negative potentials and an outward current at positive potentials, with a reversal potential of +5 to +10 mV. The current did not inactivate during 10-sec test pulses to potentials up to +80 mV and had extremely slow on-time and off-time kinetics. It was voltage-dependent with a threshold for activation of -50 mV. It was carried by a number of monovalant cations with the permeability sequence of $Na^+ = K^+ > Cs^+ > TEA^+ >$ N-methyl-glucamine. It was not permeable to Ca^{2+} or Cl^-, was blocked by Ba^{2+} and partially blocked by external H^+ and appeared to be unaffected by internal Ca^{2+}. Whole-cell recordings of single channel currents revealed a slope conductance of 69 pS. The function of this channel has not been identified, but some of its features resemble those described for gap junction channels.

W-Pos137

LOCALIZED Ca^{2+} EFFLUX FROM CORONARY SMOOTH MUSCLE CELLS

((M. Sturek)) Vascular Cell Biophysics Laboratory, Dalton Cardiovascular Res. Center and Dept. of Physiol., Univ. of Missouri, Columbia, MO 65211.

The morphological association of sarcoplasmic reticulum (SR) with the sarcolemma and extracellular free Ca^{2+} (Ca_e) gradients was studied with confocal microscopy. Coronary artery cells were loaded by incubation with $2.5x10^{-7}$ M of the SR marker 3,3'-dihexyloxacarbocyanine iodide ($DiOC_6$). Optical sections were obtained at 1 μm intervals in the z-axis to observe SR morphology while measuring Ca_e simultaneously with $5x10^{-5}$ M of the fluorescent indicator Ca^{2+} crimson in Ca^{2+}-free extracellular solution. At rest there were minimal localized Ca_e sites. Release of Ca^{2+} from the SR with $5x10^{-3}$ M caffeine was associated with localized areas of high Ca_e, which comprised < 10% of the sarcolemmal surface area and were abolished after depletion of SR Ca^{2+} by >4 min exposure to caffeine. Localized fluorescence sites were not the result of artifactual localization of Ca^{2+} crimson because saturating the dye with extracellular Ca^{2+} abolished the localized sites. Three-dimensional reconstruction of optical sections revealed large infoldings of the sarcolemma 1-2 μm wide and 1-6 μm deep into the interior of the cell clearly defined by Ca^{2+} crimson which was removed immediately by rinsing the cell with dye-free solution. Sarcolemmal infoldings were associated with SR and Ca_e sites. These data strongly indicate functional and structural colocalization of the SR and sarcolemmal Ca efflux sites. (Support: NIH HL41033, RCDA HL02872, AHA 93011900)

W-Pos138

GLUCOSE DECREASES INTRACELLULAR CALCIUM ($[Ca^{2+}]_i$ AND pH_i IN CULTURED VASCULAR SMOOTH MUSCLE (VSM) CELLS.

((X. Wang[1], Y.-H.H. Lien[1], R.J. Gillies[2], and R. Martinez-Zaguilan[2]))Dept. Medicine[1] and Physiol[2]. U. Arizona. Tucson, AZ 85724.

Diabetes mellitus in both animals and man is associated with impaired blood flow autoregulation. Strict control of $[Ca^{2+}]_i$ is necessary for phasic contraction and maintenance of vascular tone in smooth muscle. We have recently shown that glucose decreases pH_i and $[Ca^{2+}]_i$ in both non-tumor and tumor cells[3]. The present study investigates the effect of elevated extracellular glucose concentrations on $[Ca^{2+}]_i$ and pH_i in cultured rat aortic VSM cells. The VSM cells were co-loaded with Fura-2 and SNARF-1 for simultaneous $[Ca^{2+}]_i$ and pH_i measurements, respectively. VSM cells were treated with glucose concentrations from 0 to 23mM. The results indicate that glucose induces decreases in both $[Ca^{2+}]_i$ and pH_i in a concentration dependent manner. These effects were fully reversible. To investigate whether the $[Ca^{2+}]_i$ decreases were due to activation of Ca^{2+}-ATPase by glucose, we used Ca^{2+}-ATPase inhibitors: thapsigargin (TG), cyclopiazonic acid (CPA) and 2,5-di-(tert-butyl)-1,4-benzohydroquinone (BHQ). Pretreatment with either TG, CPA, or BHQ abolished the glucose-induced $[Ca^{2+}]_i$. The effect of drugs on $[Ca^{2+}]_i$ and pH_i following glucose was drug-dependent. These data suggest that glycolysis and ion transport are linked. The alterations in pH_i and $[Ca^{2+}]_i$ induced by glucose may be relevant for the decrease in vascular tone observed in early diabetes mellitus.

[3]Martinez, G.M., Martinez-Zaguilan, R., and Gillies, R.J. 1994. J.Cell.Physiol., 161:129-141.

W-Pos139

CALCIUM SIGNALLING IN ARTERIAL SMOOTH MUSCLE

((T. Kamishima and J.G. McCarron)) Institute of Biomedical and Life Sciences, University of Glasgow, Glasgow G12 8QQ, Scotland.

We investigated the cytosolic Ca^{2+} buffer power of arterial smooth muscle by simultaneously measuring Ca^{2+} currents (I_{Ca}) and cytosolic free Ca^{2+} concentration ($[Ca^{2+}]$). Smooth muscle cells were dissociated from the rat superior cerebral artery (o.d. ~150 μm) and from the rat basilar artery (~300 μm). Single smooth muscle cells were voltage clamped in the whole cell configuration and $[Ca^{2+}]$ was measured using fura-2. Depolarization to 0 mV from a holding potential of -70 mV for 1.2 s evoked I_{Ca} and an increase in $[Ca^{2+}]$. The increased $[Ca^{2+}]$ returned to resting level upon repolarization. The total cell Ca^{2+} change was calculated from the integral of I_{Ca} and its time course was closely related to the increase in $[Ca^{2+}]$. Indeed I_{Ca} alone was more than sufficient to account for the elevation in $[Ca^{2+}]$. Cytosolic Ca^{2+} buffering power was determined over the first 240 ms of the voltage clamp pulse with the assumption that the rate of Ca^{2+} removal has not changed over this time. During the first 240 ms of the depolarization $[Ca^{2+}]$ increases from 251 ± 26 nM to 523 ± 74 nM. Ca^{2+} buffer power, calculated from the total cell Ca^{2+} divided by the measured increase in $[Ca^{2+}]$, increased from about 64 ± 17 at the lowest $[Ca^{2+}]$ to plateau around 170 above 400 nM $[Ca^{2+}]$. We found essentially similar results using rat basilar artery smooth muscle cells. The estimated maximum contribution of fura-2 to the total buffer power was 28% at the lowest $[Ca^{2+}]$ and this decreased as $[Ca^{2+}]$ increased. Thus about 85 μmoles/liter Ca^{2+} is required to increase $[Ca^{2+}]$ to around 500 nM from about 200 nM. *Supported by The Wellcome Trust*

W-Pos140

MECHANISMS REGULATING FORCE DEVELOPMENT AND AGONIST SENSITIVITY FOLLOWING CONTROLLED LENGTH CHANGES IN CANINE TRACHEAL SMOOTH MUSCLE.

((D. Mehta, M.F. Wu, L.P. Adam and S.J. Gunst.)) Dept. Physiology, Indiana Univ, Sch. Med., Indianapolis, IN 46202.

Changes in muscle length either prior to or during active contraction have a profound effect on airway smooth muscle tone; however, the cellular mechanisms underlying these effects are not clear. The effects of muscle length on intracellular Ca^{2+} $[(Ca^{2+})]_i$ and myosin light chain phosphorylation (MLCP) were determined either during isometric contraction with 10^{-5}M acetylcholine (ACh) or following a 30% length step imposed during isometric contraction at Lo. At all time points from 1 to 10 min after contraction, $(Ca^{2+})_i$ and MLCP were lower when the muscles were contracted isometrically at shorter lengths. This length-dependent reduction in MLCP was also observed at all concentrations of ACh from 10^{-7} and 10^{-4}M; however the effect of length on MLCP was not sufficient to account for the length-dependent reduction in isometric force. A length step imposed on the contracted muscle resulted in large depression of force redevelopment; however MLCP was not correspondingly reduced. Decreased isometric force and agonist sensitivity at shorter muscle lengths may be partially caused by reduced Ca^{2+}-calmodulin dependent MLCP. However, the depression of contractility caused by shortening actively contracted muscle cannot be explained by a reduction in MLCP. These observations are consistent with the hypothesis that the cytostructural organization of the smooth muscle cell is determined by its length at the time of contractile activation. Changes in muscle length following activation may result in a distortion of cell structure thereby impairing contractility.

Supported by PHS HL 29289 and Am. Heart. Assoc. Fellowship to Mehta.

W-Pos141

ALTERATIONS IN RAT RENAL ARTERIAL MEMBRANE POTENTIAL, K^+ AND Ca^{2+} CHANNELS IN HYPERTENSION. ((Craig H. Gelband)) Department of Physiology, University of Florida College of Medicine, Gainesville, FL 32610.

In renal vascular beds which control blood pressure, little data is available on ion channel function in hypertension. The patch clamp technique and contractile assays were used to examine the differences in Wistar-Kyoto (WKY) and spontaneously hypertensive rat (SHR) interlobar arteries. KCl (80 mM), angiotensin II (Ang II, 100 nM), caffeine (10 mM), phenylephrine (1 μM) and 4-aminopyridine (4-AP, 1-10 mM) caused contraction of isolated rings. When contraction was normalized to muscle stress, the SHR segments produced significantly more force than the WKY (n = 6). In current clamp experiments, SHR cells were 20.2 ± 3.4 mV more depolarized than the WKY (n = 5). Application of charybdotoxin (ChTX, 100 nM) and niflumic acid (100 μM) caused little change in resting membrane potential or $[Ca^{2+}]_i$. Subsequent application of Ang II (100 nM) or 4-AP (10 mM) caused a 26 ± 2.9 and 22 ± 1.5 mV depolarization and increased $[Ca^{2+}]_i$ in WKY cells while having little effect in the SHR. In voltage clamp experiments, SHR Ca^{2+} current exhibited an increased peak current and rate of inactivation compared to the WKY (n = 5). With 4-AP (10 mM) and niflumic acid (100 μM) present to inhibit $I_{K(dr)}$ and $I_{Cl(Ca)}$, SHR $I_{K(Ca)}$ was significantly larger and activated at more negative potentials than the WKY (n = 5). Conversely, with ChTX (100 nM) and niflumic acid (100 μM) present to inhibit $I_{K(Ca)}$ and $I_{Cl(Ca)}$, SHR $I_{K(dr)}$ was significantly smaller than the WKY (n = 5). Finally, in inside-out patches (h.p. +30 mV; pCa 8-6), SHR Ca^{2+}-activated K^+ (BK) channels exhibited a greater Ca^{2+} sensitivity than the WKY (n = 4). These results suggest that membrane potential as well as K^+ and Ca^{2+} channels are altered in hypertensive rat renal interlobar arteries. (Supported by NKF YIG-33).

CELL MOTILITY AND THE CYTOSKELETON

W-Pos142

FIBROBLAST CONTRACTILITY IS NOT REGULATED BY PHOSPHORYLATION OF MYOSIN LIGHT CHAINS. ((R.J. Paul[1], K. Obara[1], G. Nikcevic[2], G. Nowak[2], L. Pestic[2], V. Guerriero, Jr.[3] and P. de Lanerolle[2])) Depts. of Physiology and Biophysics, [1]Univ. of Cincinnati, [2]Univ. of Illinois at Chicago, and [3]Dept. of Biochemistry, Univ. of Arizona.

Phosphorylation of the 20 kDa myosin light chain (LC_{20}-P_i) is the major pathway for activation of smooth muscle contraction and is postulated to regulate non-muscle contractility. We tested this hypothesis by measuring the mechanical properties of fibers made from fibroblasts grown in a collagen matrix. We compared wild type NIH fibroblasts to fibroblasts expressing the constituitively active, catalytic domain of myosin light chain kinase (tMK), which show a 5.7-fold increase in LC_{20}-P_i relative to the wild type. Serum elicited a dose-dependent response in which maximum force (~1 mN/mm², 30% serum) and ED50 were similar in both types. LC_{20}-P_i was not increased above basal levels by serum in either preparation. Cytochalasin D decreased force in both preparations to a similar degree below their initial force baselines. Moreover, maximum velocity, force-velocity relationships and stiffness were also similar, despite the higher level of LC_{20}-P_i in the tMK fibroblasts. Our results indicate that 1) force generation in serum-stimulated fibroblasts, in contrast to smooth muscle, can occur without an increase in LC_{20}-P_i, and 2) high levels of LC_{20}-P_i do not alter contractile parameters. Thus phosphorylation of LC_{20} does not appear to be a major mechanism for regulating contractility in fibroblasts. Supported in part by NIH HL23240 (RJP) and HL35808 (PdL).

W-Pos143

REGULATION OF T CELL SHAPE AND MOTILITY BY CA^{2+} AND ANTIGEN PRESENTATION. ((Paul A. Negulescu and Michael D. Cahalan)) Dept. of Physiology and Biophysics, UC Irvine, CA 92717.

We employed a $[Ca^{2+}]_i$-clamp protocol using the microsomal Ca^{2+}-ATPase inhibitor, thapsigargin (TG) to produce a sustained $[Ca^{2+}]_i$ elevation in an antigen-specific T cell line (1E5). By altering the driving force for Ca^{2+} influx (e.g. depolarization with high $[K^+]$ solutions), we maintained $[Ca^{2+}]_i$ at various levels in TG-treated cells and determined the $[Ca^{2+}]_i$ dependence of both T cell shape and motility using simultaneous DIC and fluorescence microscopy. Raising $[Ca^{2+}]_i$ caused reversible rounding of the cell and inhibited crawling on glass (*see Figure*). These changes were steeply $[Ca^{2+}]_i$-sensitive (1/2 maximal effect at 200 nM). We compared these findings to the physiological stimulus of T cell contact with antigen presenting B cells and found that the interaction is impaired by interfering with the $[Ca^{2+}]_i$ signal. Taken together, these results indicate an important role for $[Ca^{2+}]_i$ in stabilizing early T cell-B cell contact and in immobilizing activated T cells. PKA activation by cAMP inhibits T cell motility without changes in $[Ca^{2+}]_i$. Since PKA suppresses T cell activity we conclude that both stimulatory (i.e. Ca^{2+}) and inhibitory (cAMP) pathways converge on the machinery controlling T cell shape and locomotion. Supported by NIH grant GM41514.

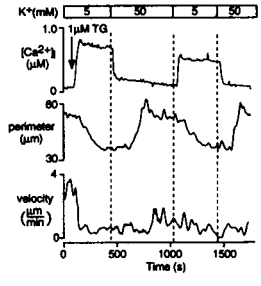

W-Pos144

TRACTION FORCES DURING CYTOKINESIS. ((K. Burton & D.L. Taylor)). Center for Light Microscope Imaging and Biotechnology and Department of Biological Sciences, Carnegie Mellon University, Pittsburgh, PA, 15213.

We have studied patterns of traction forces applied by fibroblasts to highly compliant substrata during cytokinesis, which is defined here to include both cleavage and subsequent separation of the daughter cells. Nomarski DIC microscopy was used to image Swiss 3T3 fibroblasts at intervals of 12-30 sec. at two focal planes, one at the substratum and a second approximately at the level of the chromosomes during mitosis. Traction forces were monitored using a technique based on that of Harris et al. (*Science* 208:177, 1980) in which strain in transparent silicone rubber substrata is visualized. We found that there was a significant reduction in traction force as cells rounded up prior to division and this necessitated the production of very compliant silicone sheets which could be distorted by these small forces. During cytokinesis, wrinkles formed in the silicone sheet on either side of the cleavage furrow where the presumptive daughter cells adhered to the substratum. The two sets of wrinkles were curved with their convex side facing the furrow, thus indicating that traction forces, probably due to conventional myosin, were centered on the furrow. Cells occasionally divided with the cleavage plane oriented approximately parallel to the substratum. In these cases, one pole of the cell was adherent to the silicone sheet and wrinkles present under the pole moved towards the center of the polar region during cleavage. This result suggests that contraction and force generation can occur simultaneously at the pole and at the equator of a dividing cell and hence simple "polar relaxation" is not a requirement for formation of a cleavage furrow (White & Borisy, *J. Theor. Bidl.*, 101:289, 1983). Blebs and filopodia which formed following cleavage occasionally adhered to the substratum and produced wrinkles, suggesting that these locomotory organelles contribute to traction forces required for daughter cells to spread and migrate apart prior to separation. Myosin I has been observed in filopodia of interphase cells (Conrad et al, *J.Cell Biol.* 120:1381, 1993) and so may contribute to these forces. (Support: NIH #BIK-8920118, NSF #AR32461).

W-Pos145

GTPγS INHIBITS CELL TRANSLOCATION BUT NOT ACTIN NUCLEATION AND RETROGRADE FLOW IN PERMEABILIZED EPIDERMAL CELLS. ((S. Ray and M. S. Cooper)) Department of Zoology, University of Washington, Seattle, WA 98195. (Spon. by S. Ray)

In order to control the ionic milieu and nucleotide concentrations within migrating epidermal cells, we porated their plasma membranes with Staph-α-toxin. After permeabilization with Staph-α-toxin, fish epidermal cells still translocate for over one hour. Staph-α-toxin pores limit the entry of molecules >1000 MW. Within 15 min. after the addition of Staph-α-toxin, a fluorescent analog of ADP, TNP-ADP (681 MW), can enter these cells as confirmed by confocal microscopy. Lamellipodial activity can be maintained in a buffer with 2 mM ATP and 0.5 mM GTP. In GTP, the cells move at ~0.5 μm/sec. These moving cells were fixed and stained with BODIPY-FL-phallacidin to visualize actin. The lamellipodia of GTP-treated cells have a uniform meshwork of fine actin filaments extending 10 μm from the lamellipodial leading edge. When we exchange GTP with GTPγS, the cells stop translocating. These cells engage in ruffling activity within ~2 μm from the border and this region does not appear attached to the cell substratum. The cells appear attached posterior to this region where retrograde flow or 'treadmilling' of actin filaments takes place. The actin-staining-patterns of GTPγS-treated cells show finer filaments within ~2 μm from the border. Posterior to the leading edge, actin filaments are thicker and more radial. On the whole, the entire actin pattern of a GTPγS-treated cell resembles slower migrating cells such as fibroblasts. GTPγS-treatment may activate a rho-like, small GTPase that promotes stress-fiber formation. After washing out GTPγS with GTP, the lamellipodia begin to detach and ruffle again. We conclude that GTP-hydrolysis is involved in attachment and detachment to its substratum. The stability of cell-subtratum attachment may serve to indirectly control actin-filament turnover.

W-Pos146

MECHANICALLY STIMULATED POLYMERIZATION AND MASS FLOW IN HUMAN NEUTROPHILS. ((D. V. Zhelev and R. M. Hochmuth)) Department of Mechanical Engineering and Materials Science, Duke University, Durham, NC 27708-0300.

Cell crawling is an important feature for some of the immune cells. The human neutrophil, being one example, is found to roll over the endothelial cells of postcapillary venules, after its activation. With an increase of the inflamantory response the cell stops, spreads on the cells lining the venule and than crawls through the endothelial cell junctions. Crawling through the junctions requires the exertion of a sufficient force. This force has been measured recently and is on the order of 10-20 nN (Evans et al., 1993 J. Cell Biol. 122:1295). We have found that after subjecting a portion of a neutrophil to high stresses, the cell responds in a similar way as it does after its activation with chemotactic factors. It produces significant amount of F-actin in the prestressed region and its body starts to contract. A mechanical test with micropipets is used to characterize these events. The initial polymerization is followed by mass transfer from the main cell body into the prestressed region and 30 to 50 s later the cell body starts to contract. The pressure driving the initial mass flow is generated in the prestressed region and most probably is due to the "swelling" and the "contraction" of the cytoskeletal network in this region. The contraction of the main cell body is very similar (in its time dependence and magnitude) to the contraction during phagocytosis. The measured maximum cortical tension is on the order of 0.3 to 0.5 mN/m which corresponds to a maximum contraction force of 7 to 11 nN.
This work is supported by grant 5 RO1 HL23728 from NIH.

W-Pos147

SPATIAL ORGANIZATION OF FIBRONECTIN RECEPTORS IN LOCOMOTING FIBROBLASTS. ((M.J. Brown and L.M. Loew)) Department of Physiology, University of Connecticut Health Center, Farmington, CT 06030.

The degree of lateral mobility of the fibronectin receptor has been previously correlated to the migratory state of cultured fibroblasts (Duband et al., 1988, JCB 107:1385). We have examined the subcellular distribution of fibronectin and its integrin receptor ($\alpha_5\beta_1$) in migrating murine fibroblasts. NIH 3T3 fibroblasts were exposed to a uniform DC electric field to induce directional locomotion. Following cell fixation, fibronectin and the fibronectin receptor were labeled via indirect immunofluorescence. The fibronectin receptor was found to be more highly aggregated toward the trailing edge of cells and more diffuse across extending lamellipodia. The distribution of extracellular fibronectin was similar, with extensively cross-linked fibronectin concentrated toward the trailing edge and deposited as a trail behind cells. Our results suggest that subcellular differences of integrin and fibronectin aggregation are involved in the regulation of localized cellular extensile activity and may determine the direction of cell locomotion. (Supported by NIEHS grant no. ES05973).

W-Pos148

CALCIUM HETEROGENEITIES IN FISH KERATOCYTES TURNING IN ELECTRIC FIELDS. ((Ingrid Brust-Mascher†, Rebecca M. Williams*, and Watt W. Webb†)) †Applied & Eng. Physics and *Physics, Cornell University, Ithaca, NY 14853.

Intracellular free calcium concentrations were imaged in motile fish keratocytes, which extend broad, submicron thin, actin-rich leading lamellipodia, move rapidly in culture and tend to migrate toward the cathode when subjected to an electric field. Calcium concentrations were measured with the fluorescent indicator Indo-1. Two-photon ultraviolet excitation using a red, mode-locked, 100 femtosecond pulsed laser provided 3-dimensional submicron spatial resolution (Denk et al., 1990) and ratio imaging eliminated dye concentration and cell thickness errors. Resting calcium levels were typically 100-500 nM, with calcium concentrations lower in the lamellipodia, and higher in the cell bodies. We observed non-uniform calcium distributions within the lamella, that were correlated to cell motion; turning cells tended to pivot around slower regions in their lamellae which were higher in calcium. To study this response further we used electric fields to manipulate the cells; because cells migrate towards the cathode in constant electric fields, they are forced to turn when the direction of the field is changed. Often, but not always, the cells turned around regions that were thinner, more extended and had slightly higher calcium than the rest of the lamellipodium (usually 20 to 50 nM more).

Supported by grants from NSF(DIR8800278) and NIH(RR04224) to the Developmental Resource for Biophysical Imaging and Opto-Electronics.

W-Pos149

THE CONTROL OF DYNAMIC ARCHITECTURE OF ACTIN CORTEX AND FIBRONECTIN MATRIX BY MICROTUBULAR SYSTEM IN TRANSFORMED AND NON-TRANSFORMED CELLS. ((I.N. Kaverina)) Cancer Research Center, Russian Academy of Medical Sciences, Kashirskoye Sh., 24, Moscow 115478, Russia. (Spon. by Dr.Annemarie Weber)

The effects of two microtubule-specific drugs, *taxol* and *colcemid*, on the cytoskeleton structure and cell shape of two pairs of cultured non-transformed and ras-transformed fibroblastic cells were compared. While *colcemid* depolymerized the whole microtubular system completely, *taxol* induced decentralization of this system leading to the formation of numerous free microtubules filling the central cytoplasm.

The immunofluorescent assay showed that *taxol* induced reorganization of the pattern of microfilament bundles resulting in formation of circumferential bundles instead of straight ones. *Colcemid* treated cells acquire straight bundles, often having a criss-cross pattern. Measurements of two cell parameters, dispersion and elonigation (G.Dunn and A.Brown, *J.Cell.Sci.* (1986), 83:313-340), showed that *taxol* induces significantly larger decrease of average dispersion than *colcemid*. These results show that decentralization of microtubular system, in contrast to its complete depolymerization, leads to the transformation of a "fibroblast-like" cytoskeleton architecture to an "epithelioid" one. We suppose that microtubules in some form are essential for the development and maintenance of "epithelioid" morphology, as well as " fibroblastic" one.

The differences in actin structures, shape parameters and cell area between transformed and non-transformed fibroblasts are much lower for *taxol* and *colcemid* treated cells, then for control cultures. In *colcemid* treated cultures, but not in *taxol* treated ones, the number of fibronectin fibers in extracellular matrix increases, and the differences in fibronectin matrix of transformed and non-transformed cells disappear. The formation of extracellular matrix is though to be dependent on actin cortex tension forces. We suggest that microtubules regulate expression of the transformed-type morphology and one of the possible mechanisms of such regulation is control of actin cortex contractility.

W-Pos150

HUMAN KERATINOCYTES MIGRATE TOWARDS THE NEGATIVE POLE IN PHYSIOLOGICAL, DC ELECTRIC FIELDS. ((K.Y. Nishimura, RR. Isseroff and *R. Nuccitelli)) Department of Dermatology and *Department of Cellular and Molecular Biology, University of California, Davis CA.

Many motile cells have been observed to migrate in a directional manner when placed in a dc electric field (galvanotaxis). We have been studying the response of human keratinocytes to physiological fields ranging from 1 mV/mm to 400 mV/mm, similar to the field strengths measured in mammalian wounds. Our study was conducted to identify the threshold of the galvanotactic response, and to determine the optimal direct-current electric field strength for epithelial cell translocation and migration velocity. Human keratinocytes were exposed to various electric field strengths for a duration of two and a half hours. The threshold electric field for directed cell movement or galvanotaxis was between 5 and 10 mV/mm. With an average cell diameter of 50 μm, these cells can detect a voltage gradient as low as 0.5 mV along their width. Keratinocytes exhibit cathodally directed movement (defined by increasing mean cosine values of cellular translocation distribution) which increases with field strength between 10 and 200 mV/mm. There was no consistent change in migration velocity with different electric field strengths, however net cell displacement was maximum in electric fields of 50 mV/mm and above. Previous measurements of electric fields in skin wounds of guinea pigs lie between 100-200 mV/mm (Barker, et al. Am J Physiol. 1983. 242, R358-66). In summary, we find that human keratinocytes migrate towards the negative pole in dc electric fields that are of the same magnitude as measured in vivo.

W-Pos151

THE ASSOCIATION CONSTANT FOR GELSOLIN BINDING TO Mg-F-ACTIN IS MUCH FASTER THAN PREVIOUSLY REPORTED

((L.A. Selden [§], L.C. Gershman [§¶‡], and J.E. Estes [¶¶])) [§]Research and [‡]Medical Services, Stratton Department of Veterans Affairs Medical Center, Albany, NY 12208 and Departments of [‡]Medicine and [¶]Physiology and Cell Biology, Albany Medical College, Albany, NY 12208.

The severing activity of plasma gelsolin appears to be important for shortening of actin filaments which are released into the circulation as a result of injury. However, the rate of filament severing by gelsolin has been reported to be limited by a very slow association of gelsolin to the F-actin filament, with a rate constant of 2×10^4 $M^{-1}s^{-1}$ (Schoepper and Wegner, *J. Biol. Chem 267:*13924, 1992). We have monitored severing of pyrene labeled Mg-F-actin by gelsolin under physiologic salt conditions and, by using phalloidin in some experiments to prevent depolymerization of actin after severing, we are able to distinguish between severing and depolymerization. The decreases in pyrene-actin fluorescence on gelsolin addition were well fit by single exponentials with rate constants very similar for the samples with and without phalloidin. The observed rate constants, k_{obs}, obtained from the exponential fits were a linear function of the gelsolin concentration with a slope of 5.5×10^6 $M^{-1}s^{-1}$ and an intercept of 0.18 s^{-1}. Our interpretation of this data is that $k_{obs} = k_{+g}$[Gelsolin] + k_{-g}, where k_{+g} and k_{-g} represent the association and dissociation rate constants for gelsolin binding to the filament. If this interpretation is correct, the severing rate constant must be faster than the gelsolin association rate, which was 0.7 s^{-1} at the highest gelsolin concentration used in our experiments. Our association rate constant, k_{+g}, is nearly 200 times faster than the value reported earlier and we are not certain of the reasons for this discrepancy. (This work was supported by NIH grant GM32007-08A2 and by the Department of Veterans Affairs.)

W-Pos152

RAPID FORMATION AND SLOW DISAPPEARANCE OF Mg-F-ACTIN FILAMENTS IN THE PRESENCE OF ACTIN NUCLEATING FACTOR

((L.C. Gershman [§¶‡], L.A. Selden [§], and J.E. Estes [¶¶])) [§]Research and [‡]Medical Services, Stratton Department of Veterans Affairs Medical Center, Albany, NY 12208 and Departments of [‡]Medicine and [¶]Physiology and Cell Biology, Albany Medical College, Albany, NY 12208.

Actin Nucleating Factor (ANF) is an actin binding protein found in the leading portion of the actin peak from the final Sephacryl S-300 chromatography step of rabbit skeletal muscle purification. Previous work from our laboratory has shown that ANF is not a barbed-end capping protein; rather, it appears to enhance nucleation of actin by stabilizing nuclei or nuclear precursors (*Biophys. J. 66:*196a, 1994). We have prepared fractions enriched in ANF activity, and have tested the effects of ANF on actin polymerization by analyzing curves representing continuous polymerization time courses at varying ANF concentrations. The analysis suggests that in the presence of ANF there is rapid nucleation early in the time course, leading to formation of a large number of filaments. This rapid nucleation phase (≈ 0.1 s^{-1}) is followed by a slower ($\approx$ 0.01 s^{-1}) phase during which there is a marked reduction in the number of filaments. Experiments in which the filament number was assayed by measuring elongation rates of aliquots taken during the time course confirmed the initial rapid nucleation and subsequent slow decrease in filament number. The mechanism for the decrease in filament number may involve actin filament annealing and/or capping of the barbed filament ends by CapZ, which is also known to contaminate actin preparations. (This work was supported by NIH grant GM32007-08A2 and by the Department of Veterans Affairs).

W-Pos153

DYNAMIC LIGHT SCATTERING AND RHEOLOGICAL STUDIES OF ACTIN POLYMERIZED WITH ACTIN NUCLEATING FACTOR.

((R. Scharf[*], J. Newman[*], L.A. Selden[§], J.E. Estes[¶¶], L.C. Gershman[¶¶‡])) [*]Dept. of Physics, Union College, Schenectady, NY 12308, [§]Research and [‡]Medical Services, Dept. of Veterans Affairs Medical Center, Albany, NY 12208, and Depts. of [‡]Medicine and [¶]Physiology and Cell Biology, Albany Medical College, Albany, NY 12208.

Actin nucleating factor (ANF) is an actin-associated protein which co-purifies with actin and enhances actin nucleation. The diffusion coefficient, D, of monomeric actin samples was unaffected by the presence of ANF. Upon the addition of 100mM KCl, D drops precipitously with control actin samples and even more rapidly with ANF present. After several hundred seconds, D values of samples with and without ANF were very similar, as were the decay rates, determined using the program CONTIN. Falling ball viscometry show a reduction in low-shear viscosity in ANF-containing actin samples. Rheological measurements yield similar values for control and ANF/actin for both the elastic and loss moduli. The elastic modulus of ANF/actin significantly decreases below that of control actin as the frequency increases from 0.1 to 100 rad/sec. A similar behavior was observed at low frequency as the strain rate was increased from 1% to 100%. Overall, these results suggest that the actin polymers produced in the presence and absence of ANF are similar, although rheological data suggest that there may be some subtle differences in the polymer networks. (Supported by NSF grant MCB-9316025 (JN), NIH grant GM32007-08A2 (JE) and the Department of Veterans Affairs.

W-Pos154

DYNAMIC LIGHT SCATTERING COMPARISON OF Mg- AND Ca-ACTIN.

((Rick Scharf and Jay Newman)) Department of Physics, Union College, Schenectady, NY 12308.

The time course of polymerization and the steady-state properties of Mg- and Ca-actin solutions were characterized by dynamic light scattering under a variety of conditions. Samples of column-purified actin, at concentrations in the range 0.04 - 1 mg/ml, were polymerized as Mg- or Ca-actin in 100 mM KCl, in the absence or presence of an additional 2 mM $MgCl_2$ or $CaCl_2$. The time course of polymerization was monitored through both the mean scattered intensity and diffusion coefficient measured at an angle of 90°. Once steady-state was reached, autocorrelation function data were recorded over a range of delayed times of 1 μs to 1 s and an angular range of 20 - 90°. Results showed that although the Mg-actin samples polymerized much more rapidly than the Ca-actin samples under all conditions, other variables being the same, steady-state dynamic light scattering data showed no significant dependence on the tightly-bound divalent cation over the angular range studied. Scattered light intensities at fixed actin concentrations were highest for Mg-actin samples and lowest for Ca-actin with no excess divalent cation present. (Supported by NSF grant MCB-9316025)

W-Pos155

ACTIN POLYMERIZATION IN HUMAN NEUTROPHILS INDUCED BY FORMING A TETHER.

(Abdullatif M. Alteraifi, Doncho Zhelev and Robert M. Hochmuth) Department of Mechanical Engineering and Material Science, Duke University, Durham, NC. 27708-0300

Neutrophil migration is an important physiological and pathological activity. During migration, neutrophils exhibit polarized pseudopods, which are extensions that can create motion on substrates or engulf particles. Pseudopods are formed by rapid addition of actin polymers along the boundary of the spreading lamella. We have developed an assay whereby cells are stimulated by micropipet manipulation to form pseudopod-like structures. A latex bead coupled with CD18 antibody is used to make a point contact with a neutrophil surface. After the attachment is made between the two surfaces, a tether is formed by pulling the neutrophil away from the bead. A polymer structure expands along the tether from the cell body within 20 to 50 seconds after tether formation, depending on the chamber temperature. The rate of expansion of the actin network at the leading edge of the tether is almost constant, suggesting that the polymerization process is not limited by the diffusion of soluble actin monomers. Preliminary results show that the measured rates at 22°C and 30°C are 0.06 μm/s and 0.11 μm/s respectively. After the leading edge of the polymerized network reaches a certain length, cytoplasm starts to flow from the cell body into the expanded region, indicating a depolymerization of actin filaments at the trailing edge of the network. The rate of depolymerization is also found to be almost constant. The measured rates of depolymerization at 22°C and 30°C are 0.05 μm/s and 0.10 μm/s respectively. Both the rates of polymerization and depolymerization are nearly equal, suggesting that the whole polymerized region moves at a steady rate along the tether.

This work is supported by grant HL23728 from the NIH.

W-Pos156

EFFECTS OF ACTIN MODIFICATION IN AN ACTOMYOSIN SYSTEM WITH CONSTANT ATP CONCENTRATION.

((J. Feng and P. Dreizen))
Physiology & Biophysics, SUNY Brooklyn, Brooklyn, NY 11203.

Prochniewicz and Yanagida (1990) found that modification of actin using several cross-linking methods may result in different effects on acto-S1 ATPase and *in vitro* motility, and concluded that actin flexibility plays an important role in motility. They also examined the classical superprecipitation reaction using modified actin, but results were ambiguous. We have reinvestigated effects of actin modification in actomyosin-MgATP solution, using a phosphoenolpyruvate backup system, as compared with superprecipitation where ATP is depleted. Turbidity and phosphate production are measured simultaneously. Upon mixing rabbit skeletal myosin with unmodified actin and ATP, turbidity increases during the first 5 minutes, followed by slow decrease during the next 15 minutes. Turbidity rise is proportional with myosin concentration and ATP concentration (50 to 500 μM), and the major changes occur during constant ATPase, while ATP concentration is unchanged. The turbidity rise is not obtained with HMM or S1 under similar conditions, and presumably reflects rearrangement of actin and myosin filaments due to positional changes during cross-bridge cycling. In comparable experiments using glutaraldehyde-treated F-actin, there is little change of turbidity. The ATP hydrolysis rate is actually higher, so the difference cannot be attributed to loss of cross-bridge cycling. These preliminary findings appear to confirm Prochniewicz-Yanagida that actin flexibility plays an important role in the motility of actin and myosin filaments.

W-Pos157

BINDING OF PHOSPHATE ANALOG, BeF_x, ALTERS FUNCTIONAL CHARACTERISTICS OF SUBTILISIN-SPLIT F-ACTIN. ((T. Goodnight and E. Reisler)) Dept. of Chemistry and Biochemistry, UCLA, Los Angeles CA 90024.

In this study, we show that bound phosphate analog, BeF_x, protected subtilisin-cleaved F-actin from further tryptic digestion. Bound BeF_x also restored critical concentration of salt-induced polymerization of cleaved actin to levels similar to that of native actin. Sliding velocities in the *in vitro* motility assay were shown to be increased to levels comparable to intact actin when BeF_x was added to filaments composed of cleaved actin monomers. Additionally, BeF_x was found to improve actin's ability to protect the 50K/20K junction region on S1 from tryptic digestion. These findings indicate that the partial loss of motility and S1 ATPase activation observed in cleaved actin filaments may be due to changes in structural integrity of subdomain-2. This, in turn, may alter the interface between adjacent monomers within the actin filament or the ability of actin to form necessary binding contacts with S1.

W-Pos158

THE INTERACTION OF His40-Gln42 SITE ON ACTIN WITH SUBFRAGMENT 1 OF MYOSIN . ((E. Kim , A. Muhlrad and E. Reisler)) Dept. Chem. and Biochem. , UCLA , Los Angeles , CA 90024 .

A possible contact between the His40-Gly42 site on actin and the Asn552-His558 sequence of myosin has been suggested based on the structural model of actoS1 complex (Rayment et al. , Science 261 , 58 (1993)) . This possibility was tested by using actin labeled at its Gln41 residue with dansyl ethylenediamine (DED) .
DED modification of Gln41 on actin had no effect on actin activated ATPase activity of S1 and very little effect on motility of actin filaments . Binding of S1 to F-actin did not change the rate of F-actin crosslinking between Gln41 and Lys113 of adjacent actin units . Monoclonal antidansyl antibodies did not inhibit S1 binding to DED actin . The partial release of antibodies from DED actin by S1 is attributed to allosteric effects of S1 on actin . This results suggest only minor , if any role of His40-Gly42 site on actin in actomyosin interactions .

W-Pos159

CONFORMATIONAL DIFFERENCES IN ATP- AND ADP-BOUND G-ACTIN: A MOLECULAR DYNAMICS STUDY ((W. Wriggers[1], R. Jones[2], K. Schulten[1], and D. Keller[2])) Beckman Institute[1], UIUC, Urbana, IL 61801, Dept. of Chemistry[2], UNM, Albuquerque, NM 87131.

Starting from the consensus structure attributed to a right-handed, two-start F-actin helix (Lorenz et al., *J. Mol. Biol.* (1993) 234: 826), we have carried out four 300ps molecular dynamics simulations of G-actin, with ADP or ATP and different divalent cations (Ca, Mg) bound to the central enzymatic pocket of the protein. We employed the program X-PLOR with 12Å cutoff electrostatics and all-hydrogen representation. The nucleotides were parametrized based on existing standard data for the bond-interactions and *ab initio* calculations for the charge distributions. A primary hydration shell of explicit water molecules accounted for the protein-solvent interactions. The resulting structures show significant conformational differences, which sensitively depend on the bound substrates. In view of actin's ion-dependent ATPase activity and polymerization they can be characterized as follows: (1) The metal ion is coordinated to the β- and γ-phospates of ATP in the Ca^{++} case, similar to the actin-DNAse I complex structure (Kabsch et al., *Nature* (1990) 347: 37), whereas an unusual α-γ coordination and different sugar puckering is observed with Mg^{++}. A water molecule is found situated favorably for an inline attack on the γ-phosphate in this case. (2) With Ca^{++}, the base of ADP undergoes a rotation of 100^{o} from the initial orientation and exposes itself to the solvent. With Mg^{++}, the nucleotide is shielded from the solvent, suggesting a two state-model of ADP-bound actin consistent with chemical evidence. (3) The role of Mg^{++} to facilitate actin polymerization is supported by conformational analysis of the molecular dynamics trajectories.

W-Pos160

NUCLEOTIDE AND DIVALENT CATION FREE-ACTIN: STABILIZATION BY SUCROSE AND NUCLEOTIDE BINDING KINETICS. ((E. M. De La Cruz & T. D. Pollard)) Johns Hopkins Medical School, Baltimore, MD 21205.

We prepared nucleotide and divalent cation free actin (NDCF-actin) in buffer containing 50% sucrose (w/v). Sucrose inhibits the irreversible denaturation of actin that results from nucleotide dissociation [Kasai *et. al.* (1965) *Biochim. Biophys. Acta 94*, 494-503]. Nucleotide can be removed from ~80% of the actin. Stabilization of NDCF-actin is dependent on the sucrose concentration. The CD ellipticity (x 10^3 degree cm^2 $dmol^{-1}$) at 222 nm of NDCF-actin in 50% sucrose is -3.54. The ellipticity of denatured NDCF-actin in dilute buffer is -2.01 and that of native actin is -4.19. In 50% sucrose NDCF-actin has 1.12 and native actin has 0.5 solvent-exposed thiols. The conformation of native actin is recovered when ATP and Mg^{2+} are added. The availability of stabilized NDCF-actin permitted us to study the kinetics of nucleotide binding to actin. The observed rate constant of the reaction is linearly dependent on the concentration of εATP, a fluorescent analog of ATP. The inverse of the association rate constant is proportional to the viscosity of the solvent with an intercept near the origin as expected for a diffusion-limited reaction. The second order association rate constant for Mg^{2+}-ATP and Ca^{2+}-ATP binding to nucleotide-free actin in water at 22° C is 5 x 10^6 $M^{-1}s^{-1}$. The Smoluchowski collision rate constant for actin and ATP is calculated to be 6.5 x 10^9 M^{-1} s^{-1}, which makes the "orientation factor" 7.7 x 10^{-4}. From the ratio of the dissociation and association rate constants we calculate dissociation equilibrium constants of 1.2 x 10^{-9} M for Mg^{2+}-ATP-actin, 4.4 x 10^{-9} M for Mg^{2+}-εATP-actin, and 1.2 x 10^{-10} M for Ca^{2+}-ATP-actin.

W-Pos161

A MATHEMATICAL MODEL OF THE ACTIN FILAMENT LENGTH DISTRIBUTION PREDICTS ONLY ONE UNIQUE STEADY STATE. ((P.A. Dufort and C.J. Lumsden)) Department of Medicine, University of Toronto, Toronto, Canada, M5S 1A8. (Spon. by C.J. Lumsden)

The actin cytoskeleton and its associated regulatory proteins possess the ability to dynamically transform cytoskeletal structure and function in response to intra- and extracellular signaling events. A crucial part of this process involves rapid alterations in the distribution of actin filament lengths. We describe a mathematical model that predicts transformations of the actin filament length distribution following changes in the concentration of free polymerizable G-actin, the on and off rates of pointed- and barbed-end capping proteins, the rate of filament severing, and the rate of nucleation of new filaments. The model also differentiates between filament nucleation and severing that does and does not result in a barbed-end filament cap, allowing the effects of the sever-and-cap and nucleate-and-cap processes to be compared to their non-capping counterparts. We report results from this model predicting: (i) that once the rates of polymerization, capping, severing and nucleation are fixed, the filament length distribution is drawn toward one unique steady state; and (ii) that the addition of capping to severing and nucleating activity has a pronounced effect on both the shape and stability of the steady state. This model is the first step in our long-term goal of developing a theory describing how the activities of regulatory proteins must be orchestrated in order to transform the cytogel from loose, isotropic networks to dense, parallel bundles. Results from our study of the network to bundling transition will be used to understand how the actin cytoskeleton participates in mesangial cell hypocontractility during exposure to high glucose levels (Whiteside, C.I., *et al.* (1993) *Am. J. Pathol.* 142:1641-1653).

W-Pos162

COOPERATIVITY IN F-ACTIN: BINDING OF GELSOLIN AT THE BARBED END AFFECTS THE STRUCTURE OF THE WHOLE FILAMENT.
((E.Prochniewicz, Q.Zhang, P.Janmey*, D.D.Thomas)) University of Minnesota; *Harvard Medical School.

Gelsolin, a Ca-dependent actin-binding protein, regulates the state of assembly of actin by nucleating polymerization and fragmentation of the polymers. Two possible mechanisms of fragmentation are (a) a local effect on bonds between the neighboring monomers or (b) long-range effect on the structure of the filament. The two possibilities were tested by examining the effect of gelsolin on time-resolved absorption and phosphorescence anisotropy of F-actin labeled by erythrosin iodoacetamide at Cys 374 and analysis of the data in terms of the overall and internal rotational motions in actin filaments. Binding of gelsolin to the barbed end induced about a 10° change in the orientation of erythrosin, corresponding to conformational changes around the C-terminal of polymerized monomers, and significantly decreased torsional rigidity of the filament. This result demonstrates cooperativity within F-actin, where changes imposed at one end are propagated through intermonomer bonds on a large segment of the filament.

W-Pos163

COOPERATIVE STRUCTURAL CHANGES IN F-ACTIN. ((A. Orlova and E.H. Egelman)) Univ. of Minn. Medical School, Minneapolis, MN 55455

Much experimental evidence has existed for cooperativity within the F-actin filament. We have used electron microscopy and three-dimensional reconstruction to actually visualize cooperative changes of state that can be seen at low-resolution. The magnitude of the cooperativity, extending over tens to hundreds of subunits, as well as the size of the conformational changes, involving large displacements of mass, are surprising. One example of such cooperativity is the stabilization of tryptically-cleaved F-actin by substoichiometric amounts of phalloidin (Drewes and Faulstich, *Eur. J. Biochem.* **212**, 247-253, 1993). We can show that the tryptic cleavage of the C-terminus leads to a large loss of the connectivity between the two long-pitch helical strands, and that phalloidin induces a cooperative structural change that restores this connectivity. Further, we show that modifications of the C-terminus, including tryptic cleavage, produce large allosteric changes in F-actin. X-ray diffraction from muscle has shown changes on the actin layer lines associated with activation that appear to require myosin binding, but that precede tension and complete turning on of the thin filament (*e.g.*,Kress *et al.*, JMB **188**,325-342,1986). We suggest that some of the changes we observe in F-actin may be the same as occur in muscle, and may be important in thin filament activation.

W-Pos164

TROPOMYOSIN ROTATIONAL DYNAMICS IN THIN FILAMENTS. ((J.-c. Lo & R. D. Ludescher)) Rutgers University, Department of Food Science, New Brunswick, NJ 08903-0231

We have used phosphorescence anisotropy from erythrosin-5-iodoacetamide covalently attached to rabbit skeletal muscle tropomyosin (Tm) to characterize the molecular dynamics of Tm on the surface of F-actin. Although the probe was loosely bound to Tm, it was able to monitor the molecular dynamics of the F-actin/Tm complex on the microsecond time scale. The steady-state phosphorescence anisotropy of Tm in the complex was 0.025±0.005 at 20°C. Since the anisotropy of actin in a similar complex was 0.11±0.01, Tm may be moving independently on the filament surface. Studies of the effect of temperature and solution viscosity provided additional evidence for independent tropomyosin motions. A modified Perrin plot of 1/r versus $\tau T/\eta$ (where r is the steady-state phosphorescence anisotropy, τ is the phosphorescence lifetime, T is the absolute temperature, and η is solution viscosity) provided evidence for two distinct modes of motion for Tm on F-actin; these modes corresponded to the rotation of segments with significantly different volumes. While the volume of the fast component was comparable to that of a single tropomyosin molecule, providing evidence that Tm moves on the surface of F-actin, the volume of the slow component corresponded to only a small portion of the entire complex. (Supported by Muscular Dystrophy Association).

W-Pos165

ATOMIC FORCE MICROSCOPY OF F-ACTIN SHOWS APPARENT LEFT HANDED FILAMENTS Leda A. Chang,* Fransiska S. Franke,* Paula Flicker,† and David J. Keller*, *Department of Chemistry, University of New Mexico, Albuquerque, NM 87131, and †Department of Molecular Biology, Vanderbilt University, Nashville TN 37235

Atomic Force Microscope images of F-actin show topography that is consistent with two distinct conformations of the actin filament: one that is right handed (as expected) and one that is left handed. The left handed conformation has not been reported previously. Extensive experiments have been performed to rule out AFM imaging artifacts, and electron micrographs of unidirectionally shadowed replicas of the same samples confirm the AFM results. Experiments in which molecules were prepared for imaging in exactly the same way as in a previous publication show that under these conditions the filaments always appear right handed, as reported earlier. Hence the difference in topography is due to differences in method, and is not in conflict with earlier results. The presence or absence of phalloidin, which prevents rapid depolymerization of actin filaments, makes no difference in the apparent handedness observed by AFM or TEM. Therefore, if actin filaments are able to adopt both right and left handed conformations, they must be able to switch between the two forms without depolymerizing. Such a dramatic conformational transition in intact filaments may have important implications for actomyosin function and mechanism.

W-Pos166

MAGNETIC TWEEZERS: A NEW TOOL FOR LOCAL MEASUREMENTS OF VISCOELASTIC PARAMETERS, FORCE FIELDS AND REPTATION DYNAMICS OF SINGLE FILAMENTS WITHIN ACTIN NETWORKS. ((F. Ziemann, F. Schmidt, M. Bärmann and E. Sackmann)) Biophys. Laboratory E22, Physics Dept., Technische Universität München, D-85747 Garching, Germany.

A magnetic bead microrheometer has been designed which allows local quantitative measurements of the frequency dependence of the viscoelastic parameters and their spatial variation within entangled and cross-linked actin networks. The technique has been improved to allow evaluation of the whole range of the low frequency relaxation domain: from the terminal relaxation regime to the reptation dominated plateau to the regime determined by internal filament dynamics. By embedding non-magnetic beads as probes into the networks, the spatial variation of the strain field may be reconstructed and the range of deformations of gels in the percolation regime may be evaluated.

Selective fluorescence labelling of a fraction of the actin allows observation of the conformation changes of single filaments during the deformation of the network by embedded magnetic beads. Single filaments may be coupled to streptavidin-covered magnetic beads by labelling of a fraction of actin with biotin in order to observe the motion of these single filaments during deformation of the network by the bead. Most remarkable is the complete return of the filament into its original reptation tube after removal of the force.

W-Pos167

CHARACTERIZATION OF TWO NEBULIN CLONES FROM A MOUSE SKELETAL MUSCLE cDNA LIBRARY ((J.Q. Zhang, G.Luo, B. Paterson and R. Horowits)) NIAMS and NCI, NIH, Bethesda, MD 20892.

Nebulin is a ~900 kDa protein found in skeletal muscle. The evidence to date suggests that nebulin is an actin binding protein that may play a role in determining the length of thin filaments. As a prelude to functional studies, we are isolating and characterizing cDNA clones encoding mouse nebulin. We screened a mouse skeletal muscle cDNA library with a 1.8 kb human nebulin cDNA probe (clone λHNNS4.3 isolated by Zeviani et al. *Genomics* 2: 249-256, 1988), yielding two positive clones for further study. These two clones, labeled 4b and 7a, carry inserts of 3.5 kb and 3.0 kb respectively. In northern blots, each insert detected the same ~25 kb message from skeletal muscle as the human nebulin probe, while detecting no messages from cardiac muscle. Double stranded sequence from each end of clone 4b is consistent with the entire clone encoding one uninterrupted open reading frame. This sequence encodes stretches of 465 and 232 amino acids at the ends of clone 4b that exhibit 70 to 75% similarity to human nebulin sequence in the protein databases. Optimal alignment of the clone 4b sequence with the limited nebulin sequence in Genbank yields a 58% identity with human nebulin over 1669 bp. In addition, clone 4b is composed entirely of a ~730 bp motif that is repeated 5 times, in agreement with sequence analysis of nebulin cDNAs from other species. Sequence data from clones 7a and 4b is consistent with an 880 bp overlap between them. These data indicate that we have successfully isolated partial cDNA clones that together represent 5.6 kb of contiguous mouse nebulin sequence.

W-Pos168

cDNA CLONING OF A NEBULIN RELATED PROTEIN IN MOUSE SKELETAL MUSCLE. ((G. Luo, J. Q. Zhang, T.K. Nguyen, B. Paterson and R. Horowits)) NIAMS and NCI, NIH, Bethesda, MD 20892.

Nebulin is a ~900 kDa protein found in skeletal muscle. The evidence to date suggests that nebulin is an actin binding protein that may play a role in determining the length of thin filaments. In the course of our efforts to isolate cDNA clones encoding mouse nebulin, we discovered a novel, muscle specific message that is homologous to nebulin. We screened a mouse skeletal muscle cDNA library with a 1.8 kb human nebulin cDNA probe (clone λHNNS4.3 isolated by Zeviani et al. *Genomics* 2: 249-256, 1988), yielding a positive clone containing a 17 kb insert. Restriction mapping, Southern blot analysis, and partial sequencing indicated that this insert is a concatemer containing a 1.1 kb Bam H1 fragment that binds the human nebulin probe. Surprisingly, this piece of DNA detected a ~6 kb mRNA in northern blots of both skeletal and cardiac muscle, in contrast to the ~25 kb skeltal muscle specific message we detected using the human nebulin probe (λHNNS4.3). We subcloned the 1.1 kb Bam H1 fragment and used it to isolate a putative near-full-length cDNA clone containing a ~5.5 kb insert. From these two clones, we have assembled 1420 bp of contiguous sequence that exhibits 53% identity with human nebulin over 1103 bp. This contig contains a single uninterrupted open reading frame that encodes a stretch of 413 amino acids that are 64% similar to human nebulin sequence in the protein databases. Our results demonstrate the existence of a previously unsequenced message that encodes a protein with significant sequence similarity to nebulin, even though this protein must be several fold smaller. We propose the existence of a family of nebulin related proteins, whose functions have yet to be determined.

W-Pos169

Nebulin Assembly During Differentiation Of Avian Skeletal Muscle Cultures. ((Carole L. Moncman and Kuan Wang)) Dept. of Chemistry and Biochemistry, University of Texas at Austin, Austin TX 78712.

To examine the interactions critical for the incorporation of nebulin into the sarcomeres during muscle differentiation, we have examined the temporal pattern of nebulin assembly into the myofibrils of primary cultures of chicken skeletal muscle. Immunofluorescence microscopy was performed with antibodies to nebulin, titin, myosin, α-actinin, tropomyosin, desmin and tubulin on normal cultures. In addition these experiments were performed on cultures treated with ethyl methane sulfonate (EMS) and taxol which perturb myofibril assembly. At the onset of differentiation, we observed that nebulin expression is coordinated with most of the myofibrillar proteins; however, its incorporation into the nascent myofibrils lags behind many of the sarcomeric proteins, such as: myosin, titin, α-actinin and tropomyosin. The mature striated pattern of these proteins also precedes the development of striations with nebulin. Interestingly, mAbs raised against the amino- and carboxyl- terminal portions of nebulin differ in their staining patterns in the striated myofibrils. The amino-terminal specific Ab detected a doublet pattern of staining at all times. The carboxyl-terminal mAb labeled a singlet density containing the Z-line at early timepoints, and at later time points this staining pattern developed into a doublet density. The same temporal pattern of assembly seen in the normal cultures was observed in the EMS treated cultures, but at a much slower rate. As previously reported by others, many cells in cultures treated with the microtubule stabilizing drug taxol exhibited a decrease in the amount of stress fibers and nascent I-bands as detected with rhodamine phalloidin; however, nebulin was found associated with myofibrils in a mature striated distribution. These results suggest that nebulin assembly into the myofibril is controlled by interactions of its carboxyl-terminus in the Z-line.

W-Pos170

PURIFICATION AND CHARACTERIZATION OF NEBULIN IN THE NATIVE FORM. ((L. King)) Chang Gung Medical College, Taiwan, Republic of China

Nebulin is a massive protein (about 700-900 kDa) abundant in vertebrate skeletal muscle. Since it was not purified in the native form, most of the data available thus far have stemmed from antibodies produced against denatured preparations. We have developed procedures to purify nebulin without exposing it to denaturing conditions. After extraction with Guba-Straub solution and low salt precipitation, nebulin was separated from other major muscle proteins through a two-step dialysis process. It was first dialyzed against 50 mM sodium phosphate buffer containing 50 mM NaCl to dissolve most titin. The pellet of centrifugation was further dialyzed against 50 mM sodium phosphate buffer containing 90 mM NaCl to dissolve nebulin, followed by column chromatography. The circular dichroism spectra indicate that native nebulin and nebulin renatured from denaturant treatment have different conformations. It suggests a possible inadequacy of the information obtained from nebulin purified by denaturing methods. A preliminary co-sedimentation study suggests that each nebulin molecule binds roughly 100 actin monomers. Supported by Chang Gung Medical College and NSC (R.O.C.).

W-Pos171

IMMUNOFLUORESCENCE STUDIES CONFIRM THAT PHALLOIDIN "UNZIPS" NEBULIN UNIDIRECTIONALLY FROM POINTED ENDS OF ACTIN FILAMENTS IN RABBIT SKELETAL MYOFIBRILS. ((Xiaolei Ao & Sherwin S. Lehrer)). Boston Biomedical Research Institute, Boston MA, 02114.

A previous fluorescence microscopic study on rabbit skeletal (RS) and cardiac myofibrils indicated that phalloidin dissociates nebulin from actin filaments from the pointed ends toward the z-line in RS myofibrils (Ao & Lehrer, Biophys. J., 1994). In order to directly verify the nebulin dissociation, a polyclonal anti-nebulin IgG and fluorescent anti-goat IgG were applied to ghost RS myofibrils (myosin depleted) with and without overnight preincubation with excess phalloidin. The microscopic images of the phalloidin-free fibrils showed several fluorescent bands associated with nebulin attached to actin filaments in each half sarcomere in agreement with previous studies (Wang & Wright, J. Cell. Biol., 1988). After phalloidin preincubation, there remained only one band near the z-line. To further verify the unidirectional unzipping, we preincubated the fibrils with coumarin-phallacidin (Cou-Ph) for a short time to visualize the distribution of bound phalloidin (blue fluorescence) and then introduced antibodies to visualize the displaced nebulin (red fluorescence). As more Cou-Ph bound to actin from the pointed ends, the anti-nebulin fluorescence pattern changed and was dominated by a single broad band which moved closer to the z-line. Thus, anti-nebulin band moves unidirectionally from the pointed ends toward the z-line upon binding of phalloidin to actin, which appears to be due to the collapse of nebulin upon dissociation from actin. Incubation of ghost RS fibrils with excess Ca^{+2}-Calmodulin produced a similar collapsed immunofluorescence band pattern, indicating calmodulin dissociated nebulin from actin. We are very grateful to Dr. K. Wang for providing anti-nebulin IgG. (Supported by NSF DMB 8817581 and NIH HL 22461).

W-Pos172

IS THE ACTIN ATPASE INVOLVED IN ERYTHROCYTE GHOSTS' SURFACE FLUCTUATIONS? ((A.Krol, M.Grinfeldt, V.Malev)) Lab. Cell Physiol. Institute of Cytology, Russian Acad. Sci., St.Petersburg, Russia.

We have suggested (Biol.Mem.1993,6:701) that the spontaneous fluctuations of the erythrocyte surface are caused by the membrane skeleton dynamics. To study the role of the cytoskeleton in the human red cell membrane undulations we applied cytoskeleton-binding proteins to permeable hypotonic ghosts. S1-fragment of skeletal muscle myosin suppressed the membrane undulations, whereas G-actin solutions restored them up to the initial level. We also applied DNAseI, which complexes specifically with pointed ends of actin protofilaments in hypotonic ghosts. The obtained data show that DNAse inhibits surface undulations in the ghosts, but the effect is reversed by cytochalasin D, the drug binding to barbed ends of protofilaments. At the same time, DNase partially inhibits ATPase activity in ghosts, the effect being also reversed by cytochalasin D. This allows to think that actin ATPase is involved in erythrocyte ghosts' surface undulations.

TUBULIN AND MICROTUBULE MOTORS

W-Pos173

MINIMUM SIZE OF KINESIN HEAD DOMAINS FOR DIMERIZATION AND INTERACTION WITH TAIL DOMAINS. ((D. D. Hackney and J.M. Nagy)) Department of Biological Sciences, Carnegie Mellon University, Pittsburgh, PA 15213

A head domain of *Drosophilia* kinesin α subunit extending to amino acid position 392 is dimeric when expressed in *E. coli* and has markedly different kinetic properties from a head domain extending to position 340 that is monomeric (see Hackney, D.D. (1994) Proc. Natl. Acad. Sci. USA 91, 6865). In particular, dimeric 392 releases approximately half of it's bound ADP on association with microtubules (MTs) while monomeric 340 releases all of it's bound-ADP. We have now expressed a total of 7 kinesin head domains that terminate at positions 340, 346, 357, 365, 381, 392 and 405. At low to moderate protein concentrations 340 - 365 are monomeric while all of the larger constructs are dimeric. All three of the dimeric constructs (381, 392 and 405) release half of their bound ADP on association with MTs while all 4 of the monomeric constructs undergo complete ADP release. This consistent pattern strengthens the conclusion that half site reactivity in the presence of MTs is an intrinsic property of dimeric, but not monomeric, kinesin head domains. Using glutathione sepharose beads with a bound GSTase-fusion protein containing the tail domain (864-975), it was determined that the 365, 381, 392 and 405 heads all bound to the tails at low ionic strength, but none of the shorter heads bound. Thus the site of interaction of the tail and head that is responsible for generation of the 9S folded conformation is likely to be located around 357-365 in the same region that is also critical for dimerization. Interestingly, the pattern for recognition by the SUK4 antibody exactly matches the pattern for tail binding, indicating that the sites of tail binding and SUK4 binding are possibly overlapping.

Supported by NIH grant NS28562.

W-Pos174

THE KINESIN HEAD DOMAIN K401 IS A DIMER.. **((J.J. Correia*, S.P. Gilbert‡, M.L. Moyer‡ and K.A. Johnson‡)) *Dept. of Biochemistry, Univ. of Miss. Medical Center, Jackson, MS. 39216 and ‡Dept. of Molecular and Cell Biology, Penn. State Univ., University Park, PA. 16802.**

The bacterial expressed head domain of kinesin, K401, binds and hydrolyses ATP and promotes microtubule motility. The interpretation of microtubule binding and ATP hydrolysis rates requires a knowledge of the state of assembly of the head domain. It has routinely been assumed that head domains are monomers and that the dimerization is mediated by the stalk region. We have directly measured the state of assembly of the kinesin head domain constructs K401, K366 and K341 by sedimentation velocity and sedimentation equilibrium methods in an Optima XLA analytical ultracentrifuge. Between 1 and 20 μM K401, MW 45,105, is predominantly a dimer with a sedimentation coefficient, $S_{20,w}$, of 4.9 s. Molecular weight measurements establish the dissociation constant for dimerization at 0.189 μM ± 0.055 μM, although larger irreversible aggregates are present. The dissociation constant in the presence of ADP or AMPPNP is 0.351 μM ± 0.087 μM and 0.208 μM ± 0.058 μM respectively. K366, MW 41,110, is a monomer (measured MW 40,730 ± 1188) with an $S_{20,w}$ of 3.25 s. The smallest construct K341, MW 37,847, is also a monomer (measured MW = 37,795 ± 726) with a sedimentation coefficient, $S_{20,w}$, of 2.9 s. Thus, the dimerization domain is either between amino acid residue 367 and 401, or strongly affected by the removal of this region. **[Supported by GM41117 (J.J.C.), BIR–9216150 (J.J.C.) and GM26726 (K.J.).]**

W-Pos175

TRANSIENT ELECTRIC BIREFRINGENCE INVESTIGATIONS OF NONCLARET DISJUNCTIONAL AND KINESIN ((Buu Q. Luu[†], Don Eden[†], Daryl Zapata[#], Elena Sablin[‡], and Jon Kull[‡])) [†]San Francisco State University, [#]George Washington High School, [‡]University of California, San Francisco, San Francisco, CA

We have initiated a transient electric birefringence (TEB) investigation to compare the hydrodynamic and electrical properties of the motor domains of two cytoplasmic motor proteins: nonclaret disjunctional (ncd) and kinesin. Using a new TEB cell, the experiments were performed at 4°C in neutral PIPES buffers at ionic strengths in excess of 100 mM. Identical solutions with either added ADP and Pi or added ADP and VO_4^{-3} were compared. All solutions exhibit orientation via a permanent electric dipole moment. After 520 ns long pulses, the decay times for ncd(335-700) were independent of the field strength and yield $\tau_{20,water}$= 32.6 ns and 34.6 ns with ADP, Pi and vanadate respectively. The respective specific Kerr constants (K_{sp}) are -1.65×10^{-12} and -1.15×10^{-12} cm²/V². Vanadate appears to increase the effective size of the ncd motor, while decreasing K_{sp}. In contrast to ncd, kinesin(349) exhibits a decrease in $\tau_{20,water}$ with increasing field strength with both ADP, Pi and ADP, vanadate. However, the rotational times are also longer with added vanadate. K_{sp}= $+3.6 \times 10^{-13}$ cm²/V² for kinesin(349) with both ADP, Pi and ADP, vanadate.

(Supported in part by grants NIH 1R15-AR42751 and Research Corporation HS0367 to DE.)

W-Pos176

KINETICS OF MONOMERIC KINESIN MOTOR DOMAINS ((M.L. Moyer, S.P. Gilbert, & K.A. Johnson)) Dept. of Biochemistry & Molecular Biology, Pennsylvania State University, University Park, Pa. 16802

Steady state and presteady state kinetic methods were used to analyze two *Drosophila* kinesin constructs (K341 & K366) in comparison to K401. These each represent the kinesin motor domain containing the N-terminal 341, 366, or 401 amino acids, respectively. The quaternary structure of these proteins was determined by sedimentation velocity and sedimentation equilibrium centrifugation. K401 is predominantly a dimer at concentrations > 1 μM whereas both K366 and K341 are monomeric. Like native kinesin and K401, K341 and K366 demonstrate a low ATPase activity in the absence of microtubules, and ADP release is rate limiting during steady state turnover ($0.01 s^{-1}$ and $0.02 s^{-1}$, respectively). Microtubules activate the steady state ATPase to $140 s^{-1}$ for K341 ($K_{M,ATP}$=66 μM; $K_{0.5,MT}$=1.2 μM tubulin) and to $95 s^{-1}$ for K366 ($K_{M,ATP}$=61 μM; $K_{0.5,MT}$=4.4 μM tubulin) in comparison to K401 at $20 s^{-1}$ ($K_{M,ATP}$=60 μM; $K_{0.5,MT}$=1 μM tubulin). The rapid quench experiments for K401 showed a burst of product formation during the first turnover indicating that the rate limiting step for the MT•K401 complex occurs after ATP hydrolysis. Yet with K341, no burst of product formation was observed during the first turnover. These results suggest that for K341, the rate limiting step no longer occurs after ATP hydrolysis and the mechanism for this truncated kinesin is not representative of the longer kinesin motor domain. Presteady state experiments are in progress with K366 to elucidate its mechanism. These experiments with monomeric K366 in comparison to dimeric K401 will permit a better understanding of the mechanistic and structural basis of the processivity of kinesin in the single motor motility assays. Supported by NIH GM 26726 to KAJ and NIH 5 T32 GM08358-04 to MLM.

W-Pos177

SPIN LABELED NUCLEOTIDES BOUND TO KINESIN FAMILY MOTORS ((Nariman Naber and Roger Cooke)) Dept. of Biochem/Biophysics, and CVRI, UCSF.

We are studying the ATP binding site on the microtubule motor protein ncd, using several spin label ATP analogs, with the spin label attached to the ribose ring. All probes exhibited some degree of mobility relative to the protein when bound to ncd, which can be determined from the splitting, $2T'_{\parallel}$, between high and low field peaks. The maximum splitting obtained for ncd was $2T'_{\parallel}$ = 5.2 mTesla with the spin probe attached to the 2' position of the ribose through a two atom link. Greater mobility was obtained for labels with longer linkers. This indicates that the spin probes are undergoing restricted nanosecond rotational motion relative to the protein. When the ncd-analog complex bound to microtubules, the splitting between the high and the low field peaks increased for all of the analogs, indicating that the probe became more immobilized when ncd was bound to microtubules. We found that microtubules could be oriented by flow into capillaries using methods developed for F-actin. Some preliminary experiments show that spin-labeled nucleotides bound to ncd were partially oriented when the ncd was bound to the oriented microtubules in these samples . Supported by AR30868 & AR42895.

W-Pos178

FORCE EXERTED BY KINESIN AS IT BUCKLES A MICROTUBULE. ((F. Gittes, E. Meyhöfer, S. Baek and J. Howard)) Dept. of Physiology & Biophysics, and the Center for Boengineering, University of Washington, Seattle, WA 98195.

To determine whether kinesin motors are sensitive to the angle at which they are loaded, we measured forces and displacements generated by these motors as they bent microtubules in a modified *in vitro* gliding assay. Analysis of *large* bends allows calculation of both the magnitude and direction of the motor's force when the force is no longer parallel to the direction of movement. In previous work (Gittes et al., J. Cell Biol. 120:923; Gittes et al., Biophys J. 66:A312) we determined the bending stiffness of taxol-stabilized, rhodamine-labeled microtubules, and subsequently arranged a situation in which such microtubules are "clamped" to a glass surface along biotin-labeled seed regions near their minus ends. When a kinesin motor, fixed to the surface, attaches to a microtubule and moves towards its plus end, the microtubule will buckle if the compressive force is large enough. Shapes of buckling microtubules were digitized from video images obtained by fluorescence microscopy. In the present work, an exact (non-linearized) bending theory provided theoretical shapes that were best-fit to the observed shape in each video frame; in this way, motor force and displacement histories of entire buckling events were calculated. At the onset of an event, the motor force rose within a few tenths of a second to the critical value needed to buckle the filament (typically in the range of 4-6 pN or smaller). Over the next 1-2 sec, as the filament buckled sideways, the reaction force vector on the motor rotated and decreased in magnitude. The component of force parallel to the filament fell steadily from its initial value. The component perpendicular to the filament rose from zero, surpassed the parallel force and leveled off at roughly half of the critical buckling force. The speed of the motor was sometimes small at first, depending on the event, but typically accelerated as the elastic load dropped, reaching values consistent with unloaded gliding speeds, near 1 μm/sec. This analysis of buckling events is the first measurement of motor forces that are not wholly parallel to the direction of motion. It shows that kinesin motion is possible in the presence of a large perpendicular component of load.

W-Pos179

FORCE GENERATION IN KINESIN MEASURED IN A CENTRIFUGE MICROSCOPE BASED MOTILITY ASSAY Hall, K.W.; Cole, D.G.*; Yeh, Y.; Scholey, J.M.*; Baskin, R.J. Section of Molecular and Cellular Biology* Graduate Group in Biophysics and Section of Molecular and Cellular Biology* University of California at Davis, Davis, CA 95616

We have used a centrifuge microscope based motility assay in order to estimate forces exerted by kinesin molecules on demembranated sperm. With an improved optical system we find that our estimate of time averaged (sustained) force generated by a sea urchin egg kinesin molecule is slightly higher than we previously reported being between 0.24 pN (1.3 g/cc sperm density) and 0.49 pN (1.6 g/cc). We have considered three hypotheses as the possible basis for our results: (1.) The results are based on a lever action of the (bent) sperm axoneme that magnifies the low centrifugal force in its application to the motor protein. (2.) Variation in the force produced by a motor protein (stochastically generated?) results in a motor that works intermittently but cannot sustain a load. The centrifuge microscope, being a device that places a constant load (not velocity dependent as is drag force) on the demembranated sperm, is not measuring peak force but rather measures the (time-averaged) sustained load. The reduction in velocity observed at relatively low loads may result from transient delay (backward slipping?) of the sperm during those instances when the molecular force is less than the centrifugal force. The net result of this is a progressively slower observed velocity at increasing forces until finally the centrifugal force has been increased to the extent necessary to pull the sperm off the kinesin coated coverslip. (3.) Different force estimates reflect the use of different types of instrumentation or sources of kinesin. We have estimated the force necessary to trap sperm moving on a kinesin coated surface using a laser trap (Beckman Laser Institute, Irvine, CA). Preliminary results show that trapping forces > 2.4 pN are required, using sea urchin egg kinesin prepared as in the centrifuge microscope assay.

W-Pos180

STUDIES OF KINESIN-NUCLEOTIDE INTERMEDIATE STATES: COMPARISON TO MYOSIN. ((S.S. Rosenfeld[1,2], J. Xing[3], B. Rener[1], and H.C. Cheung[3])) Depts. Neurology[1], Cell Biology[2], and Biochemistry[3], Univ. Alabama at Birmingham, Birmingham, AL 35294

While kinesin and myosin are capable of producing ATP-dependent movement, fundamental differences may exist in the ways these two molecular motors interact with nucleotide. We have examined this by preparing two bacterially-expressed constructs--K332 and K413--derived from a clone of human kinesin (kindly provided by Dr. R. Vale, UCSF). K332 contains the first 332 residues from the N-terminus and is monomeric, while K413 contains the first 413 residues and is dimeric. We have examined the interactions of these constructs with nucleotide in the presence and absence of beryllium fluoride and vanadate, and have compared our findings to those with smooth muscle S-1. Beryllium fluoride reduces both the K_m and V_{max} of the microtubule-activated ATPase for both K332 and K413 by 5-10-fold. It likewise decreases the K_d for K332:ADP and K413:ADP binding to microtubules. Similar effects were seen in the rate of microtubule-accelerated release of mant ADP from K332. Both beryllium fluoride and vanadate *increase* the rotational correlation times of labelled K332:ADP and K413:ADP, to values seen in the absence of nucleotide, while the opposite was seen with S-1. Furthermore, the values of the correlation times for K413:nucleotide suggest that the two heads in this dimer have relatively little segmental flexibility. These results support previous conclusions that kinesin:ADP:P_i is a strongly bound state, while kinesin:ADP is weakly bound, the reverse of what is seen in myosin. However, these studies also suggest that for *both* myosin and kinesin, strongly bound states have longer rotational correlation times than weakly bound ones. The structural implications of these findings will be discussed.

W-Pos181

ENGINEERING SELF-ASSEMBLY INTO KINESIN AND NCD
((Andrew Lockhart and Robert Cross)) Marie Curie Research Institute, Oxted, Surrey RH8 OTL, England. (Spon. by M. Peckham)

Molecular motors are typically modular in design, containing a motor or head domain (ATPase and track binding functions), a stalk region and a cargo binding domain. The stalk region of myosin II allows myosin to self assemble into bipolar or side-polar filaments ranging from 1 to 5 μm in length. Using protein engineering techniques we have fused the head domains of the microtubule motor proteins kinesin and non claret disjunctional (ncd) with the stalk region of a non-muscle myosin II to create two novel fusion proteins called kynosin and clarosin, respectively.
The recombinantly expressed, purified fusion proteins assemble into filaments under physiological conditions and are enzymatically active. The filaments are able to move microtubules in motility assays at near wild type velocities (5-6 μm/ min for clarosin and 35-40 μm/ min for kynosin). We are at present optimising the conditions for filament assembly and characterising the structure of the filaments so as to define the intramolecular stagger of the filaments and the axial spacing between the projecting motor domains. The filaments are useful for several reasons. They are visible under DIC microscopy, moving along microtubules as beads. The self-assembly clamps the molecules in the filaments, defining their orientation and by copolymerising with headless myosin tails we can also control motor density on the surface of the filaments. It should be also possible to make clarosin-kynosin copolymers, thereby using each motor to apply a load to the other.

W-Pos182

SINGLE PARTICLE TRACKING : OPTIMIZING THE LOCALIZATION OF FLUORESCENCE LABELED MOLECULES.
((Emmanuel Beaurepaire and Watt W. Webb)) Applied and Engineering Physics, Cornell University, Ithaca, N.Y.14853.

Parameters limiting the precision of localizing single fluorescent particles in a sequence of digitized images (Ghosh & Webb, *Biophys. J.* 66 1301-1318, 1994) were analysed in order to optimize automated single particle tracking (SPT) experiments performed on fluorescently labelled molecules. An issue in the simultaneous localization of several diffraction-limited fluorescent molecules is the presence of a varying, unevenly distributed background. Algorithms using template matching (Cf. Gelles *& Al., Nature* 331 450-453, 1988) or spatial filter-based detection were evaluated. A well-suited procedure is to detect the particles as abrupt intensity changes in the image, and to compute a background image locally interpolated from the values measured around the particles; this image can be substracted from the original image before the localization. Other issues include the digitization characteristics of the image. Uncertainties due to pixel depth and pixel size were estimated. Control experiments show that a cooled CCD-based setup producing 12-bit images and including the above background correction enables one to track the individual trajectories of a population of fluorescent particles to precision of 10 nm or better. Portable programs operable on any workstation have been developped and will be made available.

Supported by the Developmental Resource for Biophysical Imaging and Opto-electronics funded by NSF(BIR8800278) and NIH(RR04224).

W-Pos183

THREE-DIMENSIONAL RECONSTRUCTION OF MICROTUBULES WITH AN ASSOCIATED MOTOR PROTEIN USING A BACK-PROJECTION PROCEDURE.
((H. Sosa., E. Sablin,* R.D. Vale,* and R.A. Milligan)) Dept. of Cell Biology, The Scripps Research Institute MB 25, La Jolla CA 92037. *Dept. of Pharmacology, Univ. of California San Francisco, CA 94143-0001.

We have developed a back-projection procedure to obtain the three-dimensional (3D) structure of microtubules from electron micrographs. This procedure addresses the problem of obtaining the 3D structure of microtubules without assuming that they are perfect helical structures. There is evidence indicating that the α-β tubulin dimers that constitute the microtubule are not arranged helically. This prevents the use of helical reconstruction algorithms, commonly used to obtain 3D information of filamentous protein assemblies from electron micrographs. The procedure developed by us takes advantage of the protofilament tilt present in microtubules with a number of protofilaments other than 13. Using this method we have computed 3D maps from cryo-electron-microscope images of microtubules and microtubules with the associated motor protein NCD. The tubulin subunits in end-on projections of the 3D maps are slewed given a distintive hand to the structure. The NCD motor domain bind to the tubulin dimers along a protofilament and they reinforce the slewed appearance of the structure in end-on projections.

W-Pos184

PRELIMINARY INTERPRETATION OF THE STRUCTURE OF TUBULIN
((S. G. Wolf, E. Nogales, I. A. Khan*, R. F. Ludueña*, and K. H. Downing)) Life Science Div., Lawrence Berkeley Lab., Berkeley CA 94720; *Dept. of Biochem., Univ. of Texas Health Science Ctr, San Antonio TX 78284

Using electron crystallography of zinc-induced tubulin sheets, we have obtained density maps of tubulin with a resolution of about 3.5 Å in projection, and in three dimensions to 6.5Å. Among the salient features of the projection maps are regions that show stripes at a spacing of about 4.8 Å, characteristic of β–sheets. The 3-D map shows a number of features that can be interpreted in terms of secondary structural elements. Although higher resolution is still needed to identify amino acid side chains, we can already make a number of speculative but functionally significant interpretations of these features. For example, based on the localization of the taxol binding site in projection, we have identified the β monomer and assigned a region near the protofilament interface to the N-terminus of the molecule. The location of the GTP binding site is expected to be near the N-terminus. Sequence predictions indicate that a long α-helix near the lateral and longitudinal contacts between monomers corresponds to the C-terminal region of the protein. Thus, the C-terminus is in a location that allows the known variations in its sequence to affect polymerization characteristics by modulating both inter-monomer and inter-dimer interactions. These interpretations are being tested further by imaging sheets formed with subtilisin-cleaved tubulin, which can confirm the site of the C-terminus, and by comparisons of images of isotypically purified tubulins. Previous X-ray studies (Beese et al., J. Mol. Biol. 194, 257 (1987)) identified three domains within the tubulin structure. Although the overall shape of the molecule in our map is quite different from the earlier model, we can identify regions within the map that correlate with those three domains.

W-Pos185

BENDING OF MICROTUBULES BY APPLYING CALIBRATED FORCES WITH OPTICAL TWEEZERS.
((M. W. Allersma, A. G. Z. Crowley, C. F. Schmidt)) Dept. of Physics and Biophysics Research Division, University of Michigan, Ann Arbor, MI 48109.

A single beam gradient laser trap (optical tweezers) can be used to three-dimensionally trap μm-sized dielectric partlicles under a microscope (K. Svoboda & S.M Block, Annu. Rev. Biophys. Biomol. Struct., 23, 247 (1994)). The force exerted on the trapped particle can be calibrated. We developed a dual trap scheme which allows to move and set two traps independently in the field of view of the microscope. We used this dual trap to capture and bend in vitro reconstituted microtubules (bovine brain). As "handles" we attached 0.28 μm streptavidin coated polystyrene beads (Seradyne) to microtubules that were copolymerized from biotinylated and unlabeled tubulin. Microtubules can be bent to large angles with a few piconewtons of force applied to each end.

W-Pos186

IMAGING MICROTUBULES UNDER PHYSIOLOGICAL CONDITIONS WITH ATOMIC FORCE MICROSCOPY.
((M. Fritz*, M. Radmacher*, J. P. Cleveland*, P. K. Hansma*, M. W. Allersma†, R. J. Stewart§, C. F. Schmidt†)) *Dept. of Physics, Univ. of California, Santa Barbara, CA 93106, †Dept. of Physics, Univ. of Michigan, Ann Arbor, MI 48109, §Bioengineering Dept., Univ. of Utah, Salt Lake City, UT 84112.

Atomic Force Microscopy (AFM) holds the potential to image surfaces at molecular and even atomic resolution. However, imaging of "soft" biological molecules under physiological conditions (under buffer) has been hampered by the relatively large forces (nanonewtons) applied, which tend to deform or push aside the molecules that are to be imaged. The under water tapping mode, a recently developed operation mode of the AFM, allows to image with much smaller effective forces (100s of piconewtons) (P.K. Hansma et al., Appl. Phys. Lett. 64, 1738 (1994)). In this mode, the base of the cantilever is vibrated vertically, and the damping of the response of the tip is used to measure the distance between tip and sample.
We applied this technique to image in vitro reconstituted microtubules (bovine brain) immobilized on a silane derivatized glass surface (trimethoxysilylpropyl-diethylene triamine). The images were obtained at 30 kHz drive frequency with an amplitude of about 5 nm and a scan frequency of 5 Hz. The lateral resolution was about 10 nm. Isolated microtubules could be resolved and were adhered so tightly to the substrate that repeatedly imaging with forces between 100 and 600 pN did not damage them. Interestingly, microtubules crossing over other microtubules showed very strong localized deformations around the cross-over point. This may suggest that microtubules can non-elastically adapt to a small radius of curvature.

W-Pos187

DETECTION OF CILIARY BEAT FREQUENCY AND METHACHORAL WAVE LENGTH BY TWO DIMENSIONAL FFT ANALYSIS. ((T. Nguyen and P. Verdugo)) Center for Bioengineering, University of Washington, Seattle, WA 98195.

Cilia are one of the most ubiquitous microscopic engines known in nature. They function as a paddling propeller in unicellulars, and as a fluid-transporting driver in ciliated epithelia. With the exception of high speed cinematography and high speed video, methods to detect ciliary motion present severe shortcomings and artifacts. Standard analog video imaging have aliasing problems that make it unreliable when beat frequency goes beyond 15 Hz. Laser-Doppler methods are reliable but expensive to implement. Techniques based on photodetection of the modulation of light transmitted across the beating cilia are promising as they are easy to implement and have now been well validated; however, these techniques only report changes of ciliary beating that are strictly localized to the sampling pinhole of the photodetector. Thus, if beating is not homogeneous across several cells, the sampled beat frequency does not represent the behavior of the whole population but only of the few cilia detected in the pinhole. Here, we present the development and validation of a new low-cost method that allows simultaneous monitoring of beat frequency and methachronism in clusters of 2 to 100 ciliated cells depending on the microscope magnification. This technique was implemented by focusing the image of a field of epitheliary ciliated cells, grown in primary tissue culture, on the CCD detector array of a Spectra-Source® digital video camera. The light intensity fluctuations produced by the moving cilia on a single line of 336 pixels were sampled with a 12-bit resolution at 128 samples/sec. Samples were then shifted to computer memory forming a 336x336 data-point matrix. A two dimensional Fast Fourier Transform of this matrix was processed in real time to render the spectral distribution of beat frequency across fields of 10-100 ciliated cells, with a spectral resolution of 0.25 Hz in a window of 0 to 64 Hz. These measurements demonstrate excellent correlation with data obtained by simutaneous high-speed video recordings (240 fields/sec). If beat frequency is coherent across a whole field, both phase and metachronal wave-length parameters can also be processed and displayed as a function of time and space. Our results show that beat frequency remains coherent within small clusters of cells; however, in cultured epitheliary ciliated cells, it can vary broadly in time and space among different cell clusters. Supported by NASA NAG-9-604

IMAGING I

W-Pos188

INTERPOLATED IMAGE DECONVOLUTION AND COLOCALIZATION ANALYSIS. ((E.D.W. Moore*, W. Carington, K. Fogarty, L. Lifshitz and F.S. Fay)) Mol. Med., Univ. Mass. Med. Center, Worcester MA 01655 and *Dept. of Physiol. Univ. of British Columbia, Vancouver V6T 1Z3.

The co-localization index (CI) measures the codistribution of fluorophores in dual-labelled immunohistochemical experiments. We have conducted theoretical and experimental analyses of the resolution limits of the CI using paired models of fluorescent objects distributed on a planar membrane. Analysis reveals that the registration of image pairs to the nearest pixel using fiduciary markers in the images results in a small random mis-registration of images. This effect reduces the dynamic range of the CI for two molecular species by reducing its value when they are distributed identically and increasing it when they are distributed fully complimentary. Further, the effect of the mis-registration decreases as the size of the objects increases relative to the size of the pixels. We tested the accuracy of this model by imaging beads of various sizes. The model accurately predicted the mean overlap, as well as accounting for the variation in CI with bead size. To increase the size of the objects relative to the size of the pixels, we used an interpolated image deconvolution algorithm. The powerful non-negativity constraint in the algorithm allows the data to be mathematically re-digitized, finer than the original sampling grid. An application to the distribution of the ryanodine and dihydropyridine receptors in guinea pig bladder smooth muscle reveals a high degree of overlap, with displacements of 50 nm reliably detectable.

W-Pos189

PUMP-PROBE FLUORESCENCE MICROSCOPY BY STIMULATED EMISSION FOLLOWING EXCITATION ((P. T. C. So, C. Y. Dong and E. Gratton)) Department of Physics, University of Illinois at Urbana-Champaign, Urbana, IL, 61801.

We have developed a new fluorescence microscopic time-resolved imaging technique using the pump-probe method. A first pulse laser source (pump) is focused into a diffraction limited spot to excite a fluorescent sample under study. A second laser (probe), operated at slightly different frequency, is also focused to induce stimulated emission from the sample. The difference in laser frequencies generates a low frequency cross-correlation fluorescence signal. There are two significant advantages of this new technique. First, the amplitude of the cross-correlation signal depends on the spatial integral of the intensity product of the pump and probe lasers. We concluded that the overlapping of two lasers introduces an axial sectioning effect similar to that in two-photon excitation and confocal microscopy. In other words, we expect improved spatial resolution compared to conventional fluorescence microscopy. Secondly, the low frequency signal and the corresponding harmonics give us picosecond time-resolved information at high laser repetition frequencies. Therefore, dependence on fast optical detectors to study ultra-fast phenomena is eliminated.

We have succeeded in implementing pump-probe microscopy to image model systems (latex spheres). The next step is to obtain time-resolved images of stained living cells. Microscopic images of these samples will be presented. We will also discuss the theory of this technique with an emphasis on the improvement of spatial resolution. This work is supported by the NIH (RR03155).

W-Pos190

A NEW COMBINED SYSTEM FOR RATIO FLUORESCENCE PHOTOMETRY AND DIGITAL IMAGING OF MUSCLE FIBRES ((Dietmar Uttenweiler, Claudia Veigel, Reinhold Wojciechowski, Makoto Makabe & Rainer H. A. Fink)) University of Heidelberg, II. Physiologisches Institut, Im Neuenheimer Feld 326, D-69120 Heidelberg, Germany

We have developed an integrated microscopy system combining fast dual excitation photometry and digital image analysis with high spatial resolution, based mainly on standard components. The system consists of a commercially available dual excitation photometric system (OSP-3; Olympus), an attached ICCD-camera and a frame grabber board. For synchronization of the excitation sequences and image acquisition we had to design circuitries for external triggering of the ICCD camera and the software for frame grabbing. With this integrated setup one can easily switch between the fast photometric mode (ratio frequency 100 Hz) and the imaging mode (ratio frequency 4.17 Hz). We used the system to record Fura-2 calcium images (ratio 340/380nm) which were correlated with the 25 times faster spot measurements and were analysed by means of image processing (MCID Imaging Research). In particular we studied release and uptake of calcium ions from the sarcoplasmic reticulum of isolated and permeabilized skeletal muscle fibre preparations. In addition the external trigger facility allows to combine the system with other cell physiological methods e.g. electrophysiological techniques. Such a system will also be important for cellular studies in which other fluorescence indicators are used to monitor similar time dependent and spatial alterations in cellular distributions of ions and small labeled molecules.

W-Pos191

CONSTRUCTION AND PERFORMANCE OF A RAPIDLY SWITCHING, FILTER-BASED FLUORESENCE EXCITATION SYSTEM. ((Frank T. Horrigan & Richard J. Bookman)) Dept. of Molecular & Cellular Pharmacology, Box 016189, University of Miami, Miami, FL, 33101

Here we describe a filter-based fluorescence excitation system which can switch between any of 6 interference filters in less than 1 ms and provides arbitrary dwell time at any selected wavelength. Filters are arranged in a stationary, linear array and can be easily exchanged or tilted in order to tune their center wavelengths. Two closed-loop scanning galvanometer mirrors are used to select between filter light-paths and to direct the output of the excitation system into a light guide. The dual galvanometer design provides functions such as continuously adjustable excitation intensity, shuttering of system output in ~200 μs and blanking between filter transitions without the need for neutral density filters, blocking filters, or shutters. The system is ideally suited to imaging applications since wavelengths can be switched within the vertical blanking period of a video signal and can be maintained at a selected wavelength for any number of frame times. In addition, PMT- based dual-wavelength ratio measurements can be performed at up to 500 Hz. Thus this one excitation system provides nearly ideal performance for both video-based and PMT-based fluorescence measurements. (Supported by NSF & AHA/FL)

W-Pos192

LINE SCANNING MICROSCOPY WITH TWO-PHOTON FLUORESCENCE EXCITATION. ((Jeffrey B. Guild and Watt W. Webb)) School of Applied and Engineering Physics, Cornell University, Ithaca, NY 14852

To break the imaging speed barrier imposed on laser scanning fluorescence microscopy (LSFM) by fluorophore saturation, line focusing and scanning is utilized to simultaneously illuminate many resolution volumes. We analyzed the photophysics of two-photon fluorescence excitation (TPE) in line illumination and predicted feasible three-dimensionally resolved imaging at video rates or faster. Unlike point focused TPE, the total line focused TPE fluorescence increases logarithmically with specimen thickness. This additional background fluorescence reaches twice the focal volume signal when focusing into a thickness about $100\mu m$ (1.3 NA). To achieve an equivalent fluorescence emission per resolution volume using line (l) and point (p) TPE, a line of N equivalent focal volumes requires an increase in illumination power, P, of $P_l/P_p \cong N\sqrt{t_p/t_l}$ for pixel integration time, t. Line scanning at video rates (30 images/second) and $N \sim 500$ requires a laser power of $\sim$ 600mW relative to point focused imaging at 1 image/second using $\sim$ 5mW. The additional necessary power is readily obtained with available Ti:Sapphire mode-locked lasers. We present an analysis of the axial sectioning ability, resolution, background rejection, and excitation power requirements of a TPE line scanning microscope. Experimental verification of this theory and its practical application to fluorescence imaging are currently under investigation.

Supported by the Developmental Resource for Biophysical Imaging and Opto-electronics funded by NSF(DIR8800278) and NIH(RR04224) and NIH(RO7719).

W-Pos193

THICK, CLOUDY SAMPLE FLUORESCENCE IMAGING CHARACTERISTICS: COMPARISON BETWEEN ONE AND TWO PHOTON EXCITATION. ((Warren R. Zipfel[1], Kevin C. Hodgson[1], Catharine Conley[2] and Watt W. Webb[1])) [1]Developmental Resource for Biophysical Imaging and Opto-Electronics (DRBIO), School of Applied and Engineering Physics, Cornell University, Ithaca, NY 14853. [2]Section of Genetics, Cornell University, Ithaca, NY 14853.

An important advantage of two photon excitation of fluorescence for laser scanning microscopy (TPELSM) is its greatly increased capability for imaging deep in thick samples. Longer wavelength excitation (700 - 900 nm) used in TPELSM is significantly less scattered, allowing for acquisition of high quality images in thick, cloudy samples where conventional one photon microscopy fails. A comparison of imaging between one and two photon excitation is made in a homogenous scattering sample, as well as in two thick biological samples: (1) the process of male meiosis was imaged 100 microns into a 0.5 mm thick, intact living bud from petunia and (2) calcium levels and neuron to neuron connections were imaged in rat hippocampal slices. Three dimensional reconstructions of the two biological samples are presented to demonstrate the advantages of two photon excitation in thick, highly scattering samples.

Supported by grants to DRBIO by NSF (BIR8800278), NIH (RR04224) and NIH (R07719). C. Conley was supported by an NSF predoctoral fellowship and a joint USA - Israel BARD grant.

W-Pos194

DYNAMICS AND DISTRIBUTION OF GLUCOSE-INDUCED NAD(P)H VIA TWO-PHOTON EXCITATION MICROSCOPY. ((B.D. Bennett, G. Ying, T. Jetton, M.A. Magnuson, and D.W. Piston)) Molecular Physiology and Biophysics, Vanderbilt University, Nashville, TN 37323. (Spon. A. Beth)

Glucose-induced insulin secretion involves coupling glucose catabolism to intracelluar Ca^{2+} in pancreatic β–cells. Although metabolic functionality is limited in some β–cells, when studied in isolation, video microscopy of whole islets reveals synchronous oscillation of intracellular Ca^{2+} from one islet region to the next, putatively due to intercellular communication. We are using two-photon excitation microscopy to allow dynamic NADH fluorescence measurements deep within intact islets, with 1μm depth resolution. Since autofluorescence and Indo-1 measurements are accessible via two-photon excitation microscopy we hope to define the dynamics and steady-state distribution of glucose-induced changes in redox-potential and Ca^{2+} at the cellular level. Of particular interest is whether the small population of metabolically less competent β–cells can be entrained in the Ca^{2+} oscillation syncytium. Here we begin with β–cell NAD(P)H autofluorescence to measure any regional differences in metabolic functionality within the islet. A concentrated glucose buffer was pipetted into a 30°C bath containing a basal (1 mM) glucose to give a final glucose concentration of 30 mM. After glucose addition, autofluorescence increased first in the islet periphery then advanced gradually toward the core, apparently following diffusion of the high glucose front. The islet was then fixed and immunostained for insulin and glucagon to identify β– and α–cells, respectively. We found that glucose-induced autofluorescence elevation was low in a small group of β–cells (≅10%) and were predominantly peripheral in origin. Thus, most β–cells respond to glucose and this response appears to be normally distributed. We anticipate that Ca^{2+} measurements will show whether metabolically incompetent β–cells are functionally important. Supported by the Beckman Foundation and Vanderbilt Diabetes Center.

W-Pos195

REALTIME IMAGING OF SINGLE FLUOROPHORES ON MOVING MOLECULAR MOTORS. ((I.Sase, H.Miyata, J.E.T. Corrie*, J. Craik* and K. Kinosita, Jr.)) Dept. Phys., Fac. Sci. Tech., Keio Univ., Hiyoshi, Yokohama 223, Japan; *MRC, Natl. Inst. Med. Res., Mill Hill, London NW7 1AA, U.K.

Single fluorophore imaging will open up the possibility of directly visualizing interactions among individual biomolecules, because most proteins and many ligands can be labeled with at least one fluorophore without seriously affecting their functions. Successful imaging has already been made with dry samples. Here we report on the video rate imaging of individual tetramethylrhodamine molecules carried by actin filaments sliding over myosin in an aqueous environment. The observation was made with an ordinary epifluorescence microscope after minor modifications that greatly reduced the background light (originating mainly from the microscope itself). When each actin filament carried only one or two rhodamine molecules, we observed tiny fluorescent spots running steadily at the speed of actomyosin motor until they abruptly photobleach one by one. Most of the spots could be directly judged as single fluorophores because actin filaments heavily labeled with rhodamine served as a reliable intensity standard. This work, done in aqueous environment, should have wide applicability in biophysics.

W-Pos196

TETHERED PARTICLE MOTION METHOD FOR STUDYING TRANSCRIPTIONAL ELONGATION AND TERMINATION BY A SINGLE RNA POLYMERASE MOLECULE ((Hong Yin*, Robert Landick‡, and Jeff Gelles†)) *Biophysics Program, †Department of Biochemistry, and The Center for Complex Systems, Brandeis University, Waltham, MA 02254. ‡Department of Biology, Washington University, St. Louis, MO 63130

Schafer et al. [*Nature* 352:444-448 (1991)] devised the tethered particle motion (TPM) method to directly detect the movement of single, isolated molecules of a processive nucleic acid polymerase along a template DNA molecule. In TPM studies, a particle is attached to one end of the DNA template, which is bound to a surface immobilized polymerase molecule. Time-resolved measurements of the DNA contour length between the particle and the immobilized enzyme are made by determining the magnitude of particle Brownian motion using light microscopy and digital image processing. Using specimens containing particles tethered by individual DNA molecules of known lengths, we have obtained a calibration curve relating observed Brownian motion to DNA tether length. TPM analysis on such specimens also allowed determination of the accuracy of the technique and the effect of experimental variables on measurement precision. Improved sample preparation methods now permit TPM data collection at rates sufficient for practical use of microscopic kinetics techniques to analyze *E. coli* RNA polymerase reaction mechanisms. Measurements on time-averaged single-molecule elongation rates from large numbers of individual RNA polymerase molecules reveal some kinetic heterogeneity in the surface-immobilized molecules. We are currently applying the TPM method to study the mechanism of factor-independent transcription termination.

W-Pos197

Development of a microinterferometer for kinetic tethered particle tracking: Application to protein/DNA interactions. ((J. D. B. Sutin and J. M. Beechem)) Vanderbilt Univ., Dept. of Molecular Physiology and Biophysics, Nashville, TN 37232.

Single-molecule protein-DNA interactions may be studied with particle tracking. The state of the DNA protein complex is inferred from the Brownian motion of a polystyrene bead constrained by a DNA tether to a substrate. Previous investigations have used video enhanced Nomarski differential interference contrast (DIC) microscopy to record a time sequence of images of the bead (e.g., Yin, Landich, & Gelles, 1994; Dec. *Biophys. J.*). Each image of the bead in the field is fit to a double Gaussian yielding a size parameter which correlates to the DNA length. For these fits to converge, each image must be acquired for several seconds, limiting the kinetic capabilities of this method. In order to increase the time resolution, we are currently developing a microinterferometric based method similar to that used in optical trapping (Denk & Webb, 1990; *Applied Optics* 29:2382). The measurement system consists of a Zeiss Axiovert 135 in a dual 100X 1.3NA Plan-Neofluar Pol objective/condenser configuration with standard DIC Wollaston sliders. The microscope is illuminated with a mode-locked Titanium:Sapphire laser such that two diffraction limited spots are formed in the focal plane. Detection consists of two photomultipliers operating in analog mode with appropriate analog processing. In this approach, the motion of a single bead between two orthogonally polarized beams disproportionately retards the phase of one beam relative to the other, which is measured by the ellipticity of the recombined beam. This approach expands the kinetic capabilities of the measurement at the expense of parallel acquisition of multiple tethered particles within the same field. Application of this technique for the examination of both DNA polymerase reactions and transcription factor binding to complex promoter regions will be explored.

W-Pos198

NONUNIFORM DISTRIBUTIONS OF IgE ON PLANAR MEMBRANES CHARACTERIZED BY IMAGING FLUORESCENCE CORRELATION SPECTROSCOPY ((Zhengping Huang and Nancy L. Thompson)) Department of Chemistry, University of North Carolina, Chapel Hill, NC, 27599-3299

Fluorescence correlation spectroscopy is useful for detecting and characterizing molecular clusters that are smaller than or approximately equal to optical resolution in size. Here, we report recent progress in the development of an approach in which the pixel-to-pixel fluorescence fluctuations from a single fluorescence image are spatially autocorrelated. In these measurements, tetramethylrhodamine-labelled, anti-trinitrophenyl IgE antibodies were specifically bound to substrate-supported planar membranes composed of trinitrophenylaminocaproylphosphatidylethanolamine and dipalmitoylphosphatidylcholine. The antibody-coated membranes were illuminated with the evanescent field from a totally internally reflected laser beam and the fluorescence arising from the IgE-coated membranes was recorded with a cooled CCD camera. The image was corrected for the elliptical Gaussian shape of the evanescent illumination after background subtraction. The spatial autocorrelation function of the resulting image generated two useful parameters: the extrapolated initial value, which was related to the average cluster intensity and density; and the correlation distance, which was related to the average cluster size. These parameters varied with the IgE density. The autocorrelation functions calculated from images of planar membranes containing fluorescently labelled lipids rather than labelled IgE demonstrated that the spatial nonuniformities were prominent only in the presence of IgE. In addition, unlabelled polyclonal anti-IgE enhanced the nonuniform IgE distributions. This work was supported by NIH Grant GM-37145 and by NSF Grant GER-9024028.

W-Pos199

NEW POTENTIOMETRIC DYES FOR MICROINJECTION, NEURONAL TRACING, AND INTRACELLULAR LABELLING. ((J.P. Wuskell[1], C. Fink[1], M. Wei[1], L.M. Loew[1], L.B. Cohen[2], Y. Tsau[2] and D. Zečević[2])) [1]Physiology, U. Conn. Health Center, Farmington, CT 06030; [2]Physiology, Yale U. School of Medicine, New Haven, CT 06510.

Di-4-ANEPPS and Di-8-ANEPPS are voltage-sensitive dyes which have been successfully used to map membrane potential changes in a variety of preparations. However, the physical properties of these compounds do not permit certain experiments for which optical recording of membrane potential might be otherwise highly appropriate. We have synthesized new dyes, based on the ANEP chromophore, designed to meet such specific requirements. Di-2-ANEPEQ is highly water soluble with short alkyl chains and a double positive charge. It has been microinjected into individual neurons in ganglia of the snail *Helix aspersa* to permit optical recording simultaneously from the cell body and long axonal branches. Di-12-ANEPPQ and di-8-ANEPPQ retrogradely label specific neuron types in chick spinal cord and monitor activity in motoneuron cell bodies; since up to 24 hours is required for the dye to travel up these neurons, it must bind irreversibly and persistently to the plasma membrane. Di-18:2-ANEPPS contains 2 linoleyl chains, rendering it highly soluble in soybean oil. Microinjection of this dye/oil solution results in efficient labelling of the endoplasmic reticulum, but to date voltage dependent signals have not been recorded. (Supported by USPHS grant GM35063).

W-Pos200

LOCALIZED PHOTOLYSIS OF CAGED COMPOUNDS IN THE DENDRITES OF CEREBELLAR PURKINJE CELLS. ((S.S.-H. Wang and G.J. Augustine)) Department of Neurobiology, Box 3209, Duke University Medical Center, Durham, NC 27710.

The dendrites of cerebellar Purkinje cells (PCs) are the most highly branched in the mammalian central nervous system and are a likely place for intracellular signals to be compartmentalized. It is therefore important to know how quickly and how far chemical signals spread from their site of origin. We are using an ultraviolet laser to photolyze caged compounds in a small region of a PC arbor. Whole-cell patch recordings were made from PCs in sagittal cerebellar slices from P14–21 rats while introducing caged compounds through the recording pipette. Laser UV uncaging illumination was shuttered and focused onto the specimen through an Olympus 40X water immersion objective. To determine the limits of photolysis, confocal microscopy (Noran Odyssey) was used to observe the spread of caged fluorescein dextran (cF-D; 10 kD MW) in soma and dendrites. In 10 msec, 50% of the cF-D was photolyzed in a spot 3–5 μm wide. Based on measurements of the time to peak of fluorescence signals as a function of distance, cF-D diffuses at approximately 20 $\mu m^2/s$ in the proximal dendrite, but is slowed by a factor of 3 to 10 in more distal regions. Diffusion therefore appears to be impeded in far regions of the dendritic arbor. Our next goal is to use this method to produce localized dendritic elevation of second messengers and neurotransmitters.

W-Pos201

RATIO IMAGING MEASUREMENT OF TRANS-GOLGI pH IN LIVING CELLS MICROINJECTED WITH LIPOSOME-ENTRAPPED FLUOROPHORES. ((O. Seksek. J. Biwersi and A. S. Verkman)) CVRI, UC San Francisco, CA 94143

A novel method was developed to introduce fluorescent probes selectively into the aqueous phase of the *trans*-Golgi in living cells. Normal human skin fibroblasts were microinjected with a suspension of small uniform-sized liposomes which fused with the *trans*-Golgi and delivered their fluid-phase content. Confocal microscopy showed colocalization of liposome-delivered sulforhodamine 101 (SR) with the specific lipid-phase *trans*-Golgi marker NBD-ceramide. Efficient liposome fusion required 37°C, ATP and precise liposome size, and was sensitive to NEM but not to GTPγS. To measure *trans*-Golgi pH, two fluorophores were entrapped in the same liposomes: fluorescein-sulfonate (F, pH-sensitive, pKa=6.3) and SR (pH-insensitive). This pair was chosen because of their bright fluorescence, non-overlapping spectra, and low membrane permeability. After fusion of the liposomes with the *trans*-Golgi, confocal cell images were collected by a cooled CCD-camera using a coaxial-confocal (Nipkow wheel) microscope. F/SR ratio was calculated from background-subtracted pixel intensities integrated over the *trans*-Golgi area. The dependence of *trans*-Golgi pH on F/SR was calibrated by varying pH *in vivo* using high K^+ solutions containing bafilomycin, monensin and CCCP. *Trans*-Golgi pH of the human skin fibroblasts was found to be 6.17 ± 0.02 (n = 174), with little variation over the lumen-corresponding area. Alkalinization of *trans*-Golgi occurred upon stimulation by cAMP agonists and protein kinase C activators, suggesting pH regulation in the organelle. This is the first direct measurement of *trans*-Golgi pH in living cells, and it provides an effective method to deliver fluid-phase fluorescent indicators into the secretory pathway.

W-Pos202

ENHANCEMENT OF EXOGENOUS PHOSPHOLIPASE A2 ACTIVITY BY SPECIALIZED DOMAINS FORMED UPON IGE RECEPTOR CROSSLINKING IN RBL CELLS. ((Rebecca M. Williams and Watt W. Webb*)) Depts. of Physics and *Applied & Eng. Physics, Cornell University, Ithaca, NY 14853.

Specialized domains have recently been shown to form around crosslinked IgE receptor patches in stimulated RBL cells (a mucosal mast cell line). Because phospholipase A2 (PLA2) is known from model membrane experiments to act only at lipid domain boundaries, we have examined the effect of IgE receptor crosslinking on the activity of exogenously added PLA2. In secreting cells, we measure PLA2 product formation using two-photon excited fluorescence laser scanning microscopy to provide the three-dimensional resolution and sectioning capabilities necessary for differentiating among various membranous regions within a cell. We load the cells with a UV absorbing bis-pyrenyldecanoyl phosphatidylcholine probe which undergoes a fluorescence emission shift upon PLA2 hydrolysis. Fluorescence is detected simultaneously at the two wavelengths corresponding to the excimer and monomer peaks of pyrene. With appropriate substrate concentrations, ratioed pixel values are independent of average fluorophore densities. Images reveal a three-dimensionally resolved cellular distribution of PLA2 product formation. Our results imply enhancement of the activity of exogenous PLA2 by the specialized domains formed by receptor crosslinking in these cells. These ongoing studies are particularly applicable to cells treated with a spatially polarized antigenic stimulation.

W-Pos203

ORIENTATION STUDIES OF THE OPTICAL PROBE EOSIN-5-MALEIMIDE COVALENTLY BOUND TO ERYTHROCYTE BAND 3 BY CONFOCAL POLARIZATION MICROSCOPY. ((S.M. Blackman, E.J.Hustedt, A.H Beth, & D.W. Piston)) Mol Physiol. & Biophysics, Vanderbilt Univ., Nashville, TN 37232.

Studies of the micro- to millisecond-scale rotational dynamics of integral membrane proteins have extensively utilized time-resolved optical absorption or emission anisotropy decay. According to the uniaxial rotational diffusion model, the data are fit by sums of exponential decay terms whose population-weighted preexponential factors are related to the orientation of the probe with respect to the diffusion axis. For the erythrocyte anion transporter (band 3) labeled with eosin 5-maleimide (EMA), in ghost membranes, the observed decays have been difficult to interpret using specific dynamic models. Independent constraints on probe orientation could allow resolution of multiple decay populations, if they exist, as well as more precise determinations of the rotational diffusion constants and thus the oligomeric states of the postulated populations. Such orientational information has been obtained for a variety of optical probes, by measuring steady-state absorption or emission polarization of macroscopically oriented samples. We are using a laser scanning confocal microscope to measure polarization of the steady-state fluorescence emission of EMA-band 3 in erythrocyte membranes. The data is interpreted according to a theoretical model we are developing with reference to similar work in the literature. This model is being tested on data from lipid probes whose dipoles are thought to be noncolinear and oriented roughly parallel and perpendicular to the membrane normal; early results show orientation angles can be determined by this measurement to an accuracy of ~10°. This model is being applied to polarization data from EMA-band 3 to infer probe orientation information, which may help resolve the question of multiple oligomeric populations of band 3. This model should be applicable to other systems which can be oriented, specifically to integral membrane proteins which react at a single site with a specific, bright, fluorescent probe. *Supported by Arnold & Mabel Beckman Foundation.*

W-Pos204

IN VIVO INVESTIGATIONS OF GENE TRANSCRIPTION BY CONFOCAL MICROSCOPY ((G.H. Patterson, P.A. Weil, and D.W. Piston)) Dept. of Molecular Physiology and Biophysics, Vanderbilt Univ., Nashville, TN 37232.

Investigations of gene transcription in cells by *in situ* hybridization and immunolocalization have indicated the existence of specific regions of transcriptional activity within the nucleus. However, cell viability is not maintained using these techniques, and thus "snap shots" of transcription in a single sample cannot be acquired at multiple times. We are particularly interested in the temporal evolution of the active regions, and are attempting to design a strategy to non-invasively monitor transcription events in living cells. We have begun to study the *in vivo* behavior of a key transcription factor, the TATA binding protein (TBP), in a living cell by laser scanning confocal microscopy (LSCM). Yeast TBP was fluorescently labeled with fluorescein isothiocyanate (FITC) and microinjected into the cytoplasm of HeLa cells. TBP-FITC was found to localize to the nucleus within 24 hours, and was evenly distributed throughout the nucleus except in the nucleolus, which held very little of the labeled protein. Subsequent observations (2-3 days after microinjection) of the same cells revealed that mitosis had occurred in >60% of the labeled cells, indicating that the cells were still viable after microinjection and LSCM imaging. Fluorescence observed in the daughter cells was no longer localized to the nucleus, possibly due to degradation of the TBP by cellular proteases. Gel mobility-shift assays and cuvette based fluorescence studies are currently underway in order to determine the functionality and binding kinetics of our labeled TBP compared with wild type. Supported by the Arnold and Mabel Beckman Foundation and the Vanderbilt Molecular Biophysics Training Program.

W-Pos205

OXYGEN CONCENTRATION IN LIVING CELLS. ((T. French, P.T.C. So, K. Berland, and E. Gratton)) Laboratory for Fluorescence Dynamics, Department of Physics, University of Illinois at Urbana-Champaign 61801.

We have measured molecular oxygen concentration by observing fluorescence lifetime quenching of pyrenebutyric acid. Using a scanning two-photon fluorescence microscope, we obtained three dimensional images of the oxygen concentration in living cells. The knowledge of molecular oxygen concentration within a cell is considered a fundamental property, the basis of almost every physiological and pathological process. Oxygen concentration can provide crucial information about respiration, energy transport, carcinogenesis, and freezing damage. Previous measurements (using NMR spin lattice relaxation, ESR line broadening, and fluorescence intensity quenching) all have a strong dependence on probe concentration. Since the probe concentration is not known *a priori*, the quantitative determination of the oxygen concentration is subject to calibration. Fluorescence lifetime quenching directly measures the quenching rate without regard to probe concentration. The bimolecular quenching constant relates oxygen concentration to the quenching rate. The principal factor in the bimolecular quenching constant is the diffusional rate of oxygen. Estimates for the diffusional rate of oxygen in a cell were used to calculate the oxygen concentration maps. We will present images of cells studied under various metabolic conditions to compare oxygen usage. This work was supported by National Institutes of Health grant RR03155.

W-Pos206

MEASUREMENT OF CELL WATER VOLUME CHANGES IN SINGLE CELLS USING FLUORESCENT PROBES. ((F.J. Alvarez-Leefmans, J. Altamirano and W.E. Crowe)) Depto. de Farmacología, CINVESTAV-IPN, Ap. Postal 14-740, MEXICO 07000 D.F.; Depto. de Neurobiología, Inst. Méx. de Psiquiatría, Calzada México-Xochimilco 101, MEXICO 14370, D.F. and Dept. Physiol. and Biophys. UTMB, Galveston, TX 77555-0641, U.S.A.

A non-invasive microspectrofluorimetric technique for continuous measurement of cell volume changes (< 5%) in single cells, will be described. It is based on the principle that relative cell water volume (CWV) can be measured by introducing an impermeant probe into cells and measuring its changes in concentration. If the intracellular content of the probe is constant, changes in its concentration reflect changes in CWV. We have used calcein, a derivative of fluorescein, as the probe. The fluorescence intensity of calcein is directly proportional to its concentration and independent of changes in the concentration of native intracellular ions within the physiological range. Because calcein is two to three times more fluorescent than other probes such as BCECF, and it is used at its peak excitation and emission wavelengths, it has a better signal-to noise ratio and baseline stability than the other dyes. Calcein can also be esterified allowing for cell loading and because of the possibility of reducing the intensity of the excitation light, measurements can be performed producing minimal photodynamic damage. The technique can be applied to any cell type which can be grown or affixed to a coverslip. The limits, potential applications and pitfalls of the technique are discussed. (Supported by NINDS USA Grant NS29227 and CONACyT México, Cátedra Patrimonial II, No. 920252).

W-Pos207

CELL VOLUME MEASURED BY TIR MICROFLUORIMETRY: APPLICATION TO WATER AND SOLUTE PERMEABILITIES IN TRANSFECTED CELLS. ((Javier Farinas, V. Simanek and A.S. Verkman)) Program in Biophysics, UCSF, CA 94143.

A total internal reflection (TIR) microfluorimetry method was developed to measure continuously the volume of adherent cells, and applied to measure water and solute permeabilities in transfected cells expressing water channel homologs. Cell cytosol was labeled with the membrane-impermeant, aqueous-phase fluorophore calcein. TIR microfluorimetry was utilized to quantify the fluorescence excited by the evanescent field in a very thin layer of cytosol (~150 nm) adjacent to the glass-aqueous interface. Because the amount of fluorophore in cell cytosol remains constant, the fluorescence signal should be inversely related to cell volume. For Sf-9 and LLC-PK1 cells, this prediction was confirmed for small volume changes (relative osmolality 0.67 - 1.33). To measure plasma membrane osmotic water permeability, P_f, the initial rate of osmotically-induced cell volume change was calculated from the TIR fluorescence time course. LLC-PK1 cells expressing the CHIP28 water channel showed a mercurial-sensitive, 3-fold increase in P_f compared to untransfected cells (P_f = 0.0043 cm/s , 10 °C). For measurement of plasma membrane solute permeability, the rate of volume change induced by solute gradients was measured. The glycerol permeability coefficient of Sf-9 cells expressing GLIP, a glycerol channel, was $(1.3 \pm 0.26) \times 10^{-5}$ cm/s (22 °C), greater than that in control cells $(5.8 \pm 1.4) \times 10^{-6}$ cm/s (n=4, $p < 0.05$), indicating functional expression of GLIP at the plasma membrane. Urea permeability was the same in GLIP and control cells. These results establish the TIR method for continuously measuring cell volume changes in adherent cell monolayers. The method should be applicable to the study of cell membrane water and solute permeabilities as well as cell volume regulation.

IMAGING II

W-Pos208

FIBER OPTIC-BASED EVANESCENT WAVE IMMUNOSENSORS FOR DETERMINATION OF ENVIRONMENTAL POLLUTANTS. ((R.M. Wadkins, L.C. Shriver-Lake, P.T. Charles, D.W. Conrad, and F.S. Ligler)) Center for Bio/Molecular Sci. & Engineer., Naval Research Laboratory, Washington, DC 20375. (Spon. by G. Anderson)

Detection of toxic small molecules is becoming increasingly important in the arenas of hazardous waste spill detection and remediation, and monitoring of waste storage areas. Most currently used procedures for detection of toxic material in aqueous solutions involve considerable sample processing efforts and time consuming instrumental analyses. An alternative to these detection methods is that provided by fiber optic-based immunosensors. By utilizing the specificity of antibodies produced against the analytes, concentrations can be determined in environmentally relevant ranges with minimal technical effort as compared to instrumental methods. Antibodies are immobilized on partially unclad fibers and the fibers are directly exposed to the sample. Antigen binding is detected by a change in fluorescence via a competitive assay in which fluorescently labeled antigen competes with unlabeled analyte for binding sites on the immobilized antibody. The fluorescence is monitored through evanescent wave excitation near the surface of the fiber. This evanescent wave sensing has been used to develop assays for the detection of trinitrotoluene (TNT) and polychlorinated biphenyls (PCBs) in aqueous samples. Using Cyanine 5 labeled trinitrobenzenesulfonic acid (Cy5-TNB) as a competitor, TNT can be detected as low as 10 ng/mL (8 ppb). PCBs have also been detected in the ppm range using a similar system. Our results indicate that fiber optic-based immunosensors provide a rapid, portable method for detection of environmentally hazardous materials.

W-Pos209

NEAR-FIELD SCANNING FLUORESCENCE MICROSCOPY OF A SINGLE MYOFIBRIL IN PHYSIOLOGICAL BUFFER. ((E.J. Seibel and G.H. Pollack)) Center for Bioengineering WD-12, University of Washington, Seattle, WA 98195.

We have constructed a near-field scanning fluorescence microscope to image muscle proteins under physiological conditions at super resolution (<200 nm). Our near-field microscope is configured in the transmission mode with a tapered fiber-optic probe as the illuminator and an objective lens, located underneath the sample and wet cell, as the light collector. The probe is coated with aluminum, except the very tip, which creates an aperture of 50 to 150 nm diameter for light emission. The light emitted from the probe tip remains collimated at the dimension of the aperture for a limited range, called the near-field. Raster scanning of the fluorescently-labeled sample within the near-field region of the probe generates an image that is not diffraction limited in resolution. However, fluorescent structures beyond the near-field region could be expected to degrade resolution in a thick sample. We examined this issue using the isolated myofibril (~1 μm dia) to represent a "thick" sample having a smooth surface. Actin (thin) filaments are in register throughout the cross-section of the myofibril. Filaments are fluorescently labeled at their tips using fluorescein-phalloidin. Fluorescence images obtained from these preparations show distinctly the labeled filament tips from the upper filament layers, with an apparent resolution of 50-100 nm. The exquisite sensitivity of near-field scanning microscopy to surface detail is confirmed, even in "thick" specimens imaged in transmission. Thus, the near-field scanning fluorescence microscope offers unprecedented ability to detect fine structural changes of myofibrillar proteins in physiological buffer that may accompany muscle contraction.

W-Pos210

NANOSCALE COMPLEXITY OF TRANSFERRED MONOLAYERS STUDIED BY NEAR-FIELD SCANNING OPTICAL MICROSCOPY ((Jeeseong Hwang*, Christine Bohm@, Lukas Tamm@, Eric Betzig# and Michael Edidin*)) *The Johns Hopkins University, Baltimore, MD 21209, @University of Virginia, Charlottesville, VA 22908 #AT&T bell Laboratories, Murray Hill, NJ 07974 (Spon. by M. Edidin)

We demonstrate that Near-Field Scanning Optical Microscopy (NSOM) reveals previously undiscovered nanoscale structures in liquid-condensed and solid-condensed monomolecular phospholipid monolayers with a resolution of $< \lambda/50$, where λ is the wavelength of the light. We further show that these structures and diffusion of the fluorescent lipid analogs across the phase boundaries are strongly modulated by small amounts of dopants such as 1 mole % of cholesterol and the ganglioside GM_1 which are also observed to modulate domain shapes of phospholipid monolayers in the fluid/solid coexistence region.

W-Pos211

PROBES FOR A SCANNING NEAR FIELD INFRARED MICROSCOPE BASED ON FREE ELECTRON LASER AND SYNCHROTRON RADIATION. ((Mi Kyung Hong and Shyamsunder Erramilli)) Physics department, Princeton University, Princeton NJ 08544.

Infrared spectroscopy is one of the most sensitive forms of spectroscopy used in Biological Physics. However, the use of infrared microscopy combined with spectroscopy has been somewhat limited by the poor spatial resolution set by the long infrared wavelengths (~ 10 μ). If recent breakthroughs in visible near field microscopy can be extended to the infrared region of the spectrum, one can use the intrinsic strong infared absorption of biomolecules to provide images with a contrast as high as 10^4, without any form of staining. Highly collimated high brightness infrared beams produced by the Stanford Free Electron Laser and synchrotron radiation produced at Brookhaven are used in combination with novel probes based on tapered chalcogenide glass fibers, and tapered hollow glass capillaries coated on the inside with metal to show that a transmitted efficiency of 1 part in 10^6 is obtained, more than enough for near field infrared imaging and spectroscopy. Applications of the new microscope to imaging biological membranes in order to elucidate the mechanism of anesthetic action are proposed.

Support from the National Science Foundation and the Office of Naval Research is gratefully acknowledged.

W-Pos212

SURFACE IMAGING AND 3D OPTICAL SECTIONING WITH A HYBRID SCANNING FORCE AND DIC LIGHT MICROSCOPE. ((A. Stemmer)) Marine Biological Laboratory, Woods Hole, MA 02543.

Scanning force and optical microscopy are mutually complementary techniques, the former being primarily surface sensitive while the latter rather volume oriented. Their combination into a single hybrid instrument provides a unique platform to study how cell surface properties determine, or are affected by, the three-dimensional dynamic organization inside the living cell. I report here results obtained with a hybrid scanning force and light microscope which can acquire thin optical sections in non-confocal, high-NA, video-enhanced differential interference contrast (DIC), polarization and fluorescence while the force microscope is in place and operating. DIC combined with optical sectioning is particularly useful to visualize the dynamic finestructure in the 3D cytoarchitecture of living cells while fluorescence imaging provides complementary, site-specific information owing to its exceptional power in locating labelled structures. The force microscope adds direct, nanometer-scale, tactile access to topography and force-related biophysical properties of the cell surface. Taken together, the optical and force microscope data are likely to further our understanding of the close relationship between anatomy and physiology on the single cell level. (Supported in parts by a Swiss National Science Foundation Fellowship and research grants R37 GM31617 from NIH and MCB-8908169 from NSF (both to Dr. Shinya Inoué)).

W-Pos213

SCANNING FORCE MICROSCOPIC STUDY OF CHROMATIN STRUCTURE IN LOW SALT CONDITIONS. ((G. Yang, S. Leuba, K. van Holde, J. Zlatanova, and C. Bustamante)) Institute of Molec. Bio. and Howard Hughes Medical Institute, Univ. of Oregon, Eugene, OR 97403. Dept. of Biochem. and Biophys. Oregon State Univ., Corvallis, OR 97331. (Spons. by W. A. Baase)

The structures of chromatin fibers in low salt conditions have not been unambiguously determined. Electron microscopy studies typically showed "beads-on-a-string" or "open zig-zag" structures. We used the Scanning Force Microscope (SFM), which can operate under less damaging conditions, to study the structures of chicken erythrocyte chromatin fibers in low salt concentrations. The chromatin fibers were deposited on mica and glass surfaces and imaged in air. SFM images of unfixed fibers revealed irregular, three-dimensional structures. Upon glutaraldehyde fixation, very similar structures were observed. The extended "beads-on-a-string" fibers were seen only in chromatin depleted of the linker histones H1 and H5. To establish the relationship between the SFM image of a chromatin fiber and its structure in solution, computer simulation was used to elucidate the effects of fiber deposition, tip convolution and tip compression. A molecular model of chromatin was first generated based on a set of parameters concerning the linker rigidity, excluded volume effects, surface relationships between the histone octamer and its associated DNA, and the linker length variability. The disk-shaped nucleosomes and the linker DNA of the model chromatin fiber were then projected onto a surface without changing their relative orientations. The effects of finite tip dimensions on the SFM images were then simulated. The similarity between the simulated and experimental images shows that the chromatin structures revealed by SFM are a reflection of that in solution.

W-Pos214

HIGH RESOLUTION SFM IMAGES OF COLLAGEN FIBERS.AND SMALL DERMATAN SULFATE PROTEOGLYCAN Seema Singh,* Sean Quigley,† Kathryn G. Vogel† and David J. Keller*,.*Department of Chemistry and †Department of Biology, University of New Mexico, Albuquerque, NM 87131.

In a collagen fiber individual collagen molecules are gathered in a parallel array with a 67 nm axial shift that give rise to the characteristic banding pattern observed by electron microscopy. This 67 nm periodic banding pattern and the twisted microfibrillar organization of the fibers have been visualized by Atomic Force Microscopy (AFM). The process of collagen fiber formation was followed by stopping polymerization at 1, 25 and 40 minutes. At 1 minute the AFM images show a fibrillar aggregate with no structure; at 25 minutes, the fibrils have widths ranging from 53 to 175 nm and clearly show the 67 nm periodicity. At 40 minutes (upon completion of fiber formation) the AFM images shows fibrils with the same periodicity, but with width ranging from 120 to 300 nm. There is evidence that the gap regions of the bands are important local binding sites for proteoglycans. As a step toward investigating the collagen-proteoglycan interaction, small dermatan sulfate proteoglycan (decorin) from cultured bovine tendon fibroblast was deposited on mica and imaged by SFM. The images show a globular protein head and a tail of approximately 70 nm. Subsequent analysis will examine collagen fiber formation in the presence of decorin and molecular level interaction of collagen fibers with decorin and biglycan.

W-Pos215

A NOVEL FORCE PROBE FOR TESTING MOLECULAR ADHESION AND STRUCTURE AT SOFT INTERFACES ((K. Ritchie, R. Merkel, and E. Evans)) Dept. of Physics, University of British Columbia, Vancouver, Canada, V6T 1Z1

In probing structure and molecular attachments at soft biological interfaces, forces are expected to range downwards from levels set by strong covalent bonds (~ 1 nN) to weak non-covalent bonds produced by van der Waals interactions (~ 10 pN). Moreover, even weaker forces may arise when surface polymers or membrane structures are displaced, *i. e.* ~ 0.1 pN or less. Motivated by high resolution techniques like the surface force apparatus (SFA) and the atomic force microscope (AFM), we have developed an ultrasensitive-tunable force probe for the purpose of testing macromolecular interactions and structure at soft interfaces. In the design, the classic mechanical spring of the SFA or microfabricated cantilever of an AFM is replaced by a biomembrane capsule (e. g. a human red blood cell or lipid vesicle) pressurized by micropipet suction. As a surface probe, a latex microsphere is biochemically *glued* to the capsule membrane. The stiffness of the transducer is the membrane tension which can be controlled from levels 1000 fold less than the softest AFM cantilever in use today upward over a four order of magnitude range while in use. Combined with high resolution optical and piezo-electric techniques, this assembly can be used to measure and apply forces in the sub pico-Newton to nano-Newton range at a resolution (±5 nm) comparable to the roughness scale of biological interfaces. Results from prototypical experiments on tissue culture cells demonstrate tests of submicroscopic rigidity, cytoskeletal activity, and strength of molecular attachments at cell interfaces.

W-Pos216

FIRST CHARACTERIZATION OF ATTRACTIVE SURFACE FORCES DUE TO ORDERED WATER BY ATOMIC FORCE MEASUREMENTS ((K.Schilcher, W.Baumgartner, P.Hinterdorfer, H.Schindler)) Institute for Biophysics, University of Linz, Austria

Force-distance curves were measured with a NANOSCOPE III in aqueous solutions between Si tips (~10 nm radius) and two types of substrates ((100)Si surface or freshly cleaved mica) with lever force constants (k) between 0.02 to 2 N/m. Continuous "trace-retrace" cycles showed large long-ranged attractive forces. During "trace" the tip jumped to the substrate at distances (z_{on}) depending on the k value. During "retrace" tip and substrate stayed in contact up to a disruptive force (F_{off}). In water (buffered to pH 7) F_{off} values were 13 nN (mica) and 5 nN (Si). A plot of z_{on} and F_{off} values for different k values showed that the attractive force decays exponentially with separation (z), according to $F(z) = F(0)\exp(-z/\lambda)$. The decay length ($\lambda$) was 5.2 nm for Si and 0.4 nm for mica. This force is attributed to ordered surface water. The OH-groups at Si and mica surfaces are arranged like OH-groups in ice, forcing surface water into spatially fixed hydrogen bonding. Tip-substrate approach reduces the amount of surface water, thus lowering total free energy, leading to attraction which decays exponentially due to exponential decay of ordering. Additions of salt abolished this attractive force with an EC_{50} value of ion concentration (c) of 24±2 mM, independent of using NaCl, KCl, CsCl, $CaCl_2$ or $MgCl_2$. All data well fitted the relation $\lambda(c) = \lambda/(1+c/EC_{50})$. The EC_{50} value found is actually the concentration where, in average, one ion is expected to be found between tip and substrate reducing effectively surface water ordering due to its own hydration shell. Interestingly, at 500 mM salt, the F_{off} data were quantized with the smallest residual force value of 35 pN. This is likely to reflect either single or smallest clusters of hydrogen bonding. Such forces should be considered to occur between membranes and proteins in distinction to hydrophobic, electrostatic and hydration forces. (Supported by the Austrian Research Funds, project S66/07).

W-Pos217

SCANNING TUNNELING MICROSCOPY STUDIES OF FREEZE-DRIED METAL-COATED BACTERIOPHAGE Φ 29 CONNECTOR BIDIMENSIONAL CRYSTALS.
((M.Vélez, G.Rubio, N.Agrait, J.L.Carrascosa* and S.Vieira)) Universidad Autónoma de Madrid y *Centro Nacional de Biotecnología , Cantoblanco, Madrid 28049, SPAIN.

Scanning tunneling microscopy of metal-coated specimens is a useful tool for the three dimensional study of proteins. It gives a very good signal to noise ratio and direct height information of the structures. This complements the information contained in the transmission electron micrographs, which are two dimensional projections of the objects. We describe a variation of the freeze-drying metal coating procedure that allows us to image with the STM the inner side of the metal replica, previously in contact with the protein molecules. We then use this preparation procedure to study two dimensional crystals of the bacteriophage Φ 29 connector, a system that has been thoroughly characterized using different electron microscopy techniques. A three dimensional reconstruction of the connector has been obtained from tilted images of negatively stained tetragonal ordered aggregates (Carazo et. al. 1986, J.Mol.Biol.,192, 853-867). More recently a higher resolution study of thin crystals of Φ 29 connectors in ice has been undertaken using low dose microscopy and diffraction, confirming the main structural features up to 0.9 nm resolution (Valpuesta et.al., 1994, J.Mol.Biol., 240(4),281-287). We now provide topographical information of the crystal surface with a lateral resolution limited by the size of the metal coating grains (2±1 nm diameter) and a vertical resolution of 0.2 nm also imposed by the corrugation of the metal coating. Individual connectors are clearly distinguished and the height difference between two neighboring connectors is measured to be 1 ± 0.2 nm. The high signal to noise ratio obtained in STM images allows the study of individual crystals, to measure their thickness and to analyze the protein orientation in the different layers of multilayered aggregates.

W-Pos218

SCANNING ION-CONDUCTANCE MICROSCOPY OF ULTRA-SOFT SAMPLES: CELL SURFACES AND NARROW PORES. ((Y.E. Korchev, M. Milovanovich[1], C.W. Pitt[1] and C.L. Bashford)) Div. Biochemistry, St. George's Hosp. Med. Sch., London SW17 0RE & [1] Dept. Electronic & Electrical Engineering, University College London.

When a conventional glass microelectrode approaches either hard or soft surfaces ion current (to a reference electrode in the bath) depends on the surface-electrode separation in an approximately linear fashion and with submicron resolution. The ion current, in either ac or dc protocols, can be used in the feedback control loop of a scanning probe microscope to reveal the topography of very soft samples without damaging them. We have successfully imaged living cells - mouse melanocytes, human fibroblasts and rabbit erythrocytes - and microporous, plastic filters using this approach under conditions where the vertical displacement of the tip exceeds 30μm. Images obtained before and after treatment of cells with pore-forming toxins reveal the damage induced at the single cell level. In microporous filters conditions which modulate ionic current through the pores do so with no obvious change in pore topography.

We are grateful to Dr. D.C. Bennett for providing melanocytes and to the Engineering and Physical Science Research Council for financial support.

W-Pos219

LOCATING CALCIUM IN MEMBRANES WITH X-RAY STANDING WAVES ((J. Wang and M. Caffrey)) Chemistry Dept., The Ohio State University, Columbus, OH 43210.

While the biochemical functions ascribed to calcium are many and varied, investigations of same are often limited by a paucity of techniques available for its direct measurement in natural and model systems. Thus, indirect studies concerned with calcium typically resort to replacing it with a spectroscopically active ion such as a lanthanide or to complexing it with a bulky fluorophor. In this study, we show that synchrotron radiation-based x-ray standing waves (XSW) can be used to monitor directly and with atomic resolution the location of calcium in the profile structure of a model membrane under ambient conditions. Specifically, the position of an atomically thin layer of calcium suspended in an arachidate (C20:0) bilayer above one and two bilayers of ω-tricosenoic acid (ω-TA, C23:1) on a gold mirror has been determined. The distance between the calcium layer and the mirror surface increases by 53 Å from an initial value of 114 Å when the number of intervening ω-TA bilayers is changed from one to two. This new capability has far reaching implications for biological structure-function studies involving calcium at surfaces and interfaces and in thin films. The membrane topology of proteins such as phospholipase A_2, protein kinase c and the oxygen evolving complex should now yield to study by allowing us to focus on the intrinsic calcium which, in this application, doubles as a structural benchmark.

Supported by NIH DK45295

W-Pos220

X-RAY STANDING WAVES AS PROBES OF SURFACE STRUCTURE: EFFECTS OF INCIDENT BEAM ENERGY ((S. Kirchner, J. Wang, Z. Yin and M. Caffrey)) Chemistry Dept., The Ohio State University, Columbus, OH 43210.

The x-ray standing wave (XSW) technique is emerging as a powerful tool for investigating the distribution of specific elements in organic thin films and at surfaces. In the course of our work on Langmuir-Blodgett films, the question arose as to the sensitivity of the structure measurement to the energy of the x-ray beam used to generate the XSWs under conditions of total external reflection. A high sensitivity would require a revised experimental protocol for such measurements particularly in systems containing more than one type of probe or reporter atom. The question was addressed in two ways. First, in a theoretical study, the optical properties of the system were examined to identify possible energy-dependent components such as surface roughness. The analysis shows that provided surface roughness is small its contribution can be accounted for satisfactorily by the simple Debye-Waller model. The second approach to the question was experimental. Thus, a series of XSW measurements were made on LB films of manganese arachidate (C20:0) on a gold mirror surface at three incident x-ray beam energies in the 7 keV to 11.2 keV range. The x-ray fluorescence data showed no obvious dependence on incident x-ray energy. These results demonstrate that the contribution of surface roughness to the x-ray fluorescence yield profile is minimal under these conditions and that the XSW measurement is not incident beam energy dependent in the range studied.

Supported by NIH DK 45295.

W-Pos221

FLASH CONTACT X-RAY IMAGE OF LIVING ALGA *chlamydomonas reinhardi* ((T. Majima, H. Shimizu, T. Tomie, K. Miura, M. Yamada, T. Kanayama, R. Cotton, A. D. Stead and T. Ford)) Electrotechnical Laboratory, Tsukuba, JAPAN and London University, U. K. (Spon. by H. Matsumura)

The x-ray images of unicellular alga *chlamydomonas reinhardi* in water were obtained by flash contact x-ray microscopy. The readout of x-ray image relief on an x-ray resist by an AFM gives us the quantitative information on mass density distribution of specimens (T. Tomie et al, Science 252, 691(1991)). The subcellular structures of basal part of flagella and chloroplasts were visible in the x-ray image. The image also showed the existence of a low density envelope structure around the cell body. Such a structure was not observed in the electron microscopy observation of specimens fixed by glutalaldehyde (R. Kamiya and G. B. J. Witman, Cell Biol., 98, 97(1984)). These results demonstrate that the x-ray microscopy can be powerful for the observation of living materials.

W-Pos222

KINETICS AND FIDELITY OF E. COLI DNA POLYMERASE III HOLOENZYME

((L. B. Bloom[1], M. R. Otto[2], Z. Kelman[3], M. O'Donnell[3], J. M. Beechem[2], and M. F. Goodman[1])) [1]Dept. of Biological Sciences, USC, Los Angeles, CA, [2]Dept. of Molecular Physiology and Biophysics, Vanderbilt Univ., Nashville, TN, [3]Dept. of Microbiology, Cornell Univ., New York, NY

E. coli DNA polymerase III (pol III) holoenzyme is responsible for replication of the *E. coli* genome. The holoenzyme is composed of at least 10 different subunits which can be divided into smaller units. The pol III core is composed of three subunits: α, 5'→3'polymerase, ε, 3'→5' exonuclease and θ. Pol III core alone is capable of DNA synthesis but with a low processivity of about 10-20 nucleotides per binding event. Accessory proteins, β and γ complex, interact with the core polymerase and increase its processivity to greater than 8000 nucleotides in a single binding event. While the kinetics and fidelity of synthesis by α , αε, and core have been studied, little work has been done to address the effects of the accessory proteins, β and γ complex, on the fidelity of DNA synthesis. We have defined a "minimal" primer/template system which supports processive synthesis on a synthetic primer/template of defined sequence. Primer/template requirements for processive synthesis will be discussed. The availability of a synthetic primer/template system allows us to design primer/templates of specific sequences to measure the effects of local DNA sequence context on the fidelity of synthesis by pol III in the presence and absence of accessory proteins. Using this minimal primer/template system, we will discuss the effects of processivity on the misincorporation frequencies of pol III core alone and in the presence of the accessory proteins at selected primer/template sites. Using the same minimal primer/template system with an extrinsic fluorescent label, we will discuss the interactions and dynamics of the individual subunits in the holoenzyme complex with DNA and the kinetics of assembly of a complex with DNA.

W-Pos223

CALORIMETRIC ANALYSIS OF λ cI REPRESSOR BINDING TO DNA OPERATOR SITES. ((E. Merabet and G. Ackers)) Dept. of Biochemistry and Molecular Biophysics, Washington University School of Medicine, St. Louis, MO 63110.

The enthalpies of cI repressor binding to bacteriophage λ right operator DNA sites have been measured using Isothermal Titration Calorimetry. The association of wild type cI with synthetic operator DNA (21bp) containing specific sequences O_R1, O_R2, or O_R3 is characterized by large negative enthalpies, in agreement with van't Hoff results obtained by quantitative footprint titrations (Koblan, K.S., & Ackers, G.K. (1992) *Biochemistry* 31, 57-65). By comparison, non-specific binding yields aproximately zero enthalpy. The large negative enthalpies of interaction cause the net thermodynamic driving force for cI repressor-DNA association to be enthalpic in the physiological temperature range. Extrapolation of the enthalpy-entropy compensation plot shows that, for O_R1, $\Delta H=0$ at T_H= -26.0 °C. Measurements of the heat of binding cI to synthetic DNA fragments containing combinations of multiple specific sites (O_R1, O_R2, and O_R3) show that the enthalpies are not additive, suggesting a contribution from cooperative interactions between repressor dimers bound to adjacent sites. However, comparison of the results of wild type and GD147, a mutant containing a single amino acid change (Gly to Asp) in the C-terminal domain of cI repressor and defective in cooperative interactions (Beckett et al. (1993) *Biochemistry* 32, 9073-9079), indicates that dimer-dimer contacts account for only a fraction of the non-additivity of the enthalpies. Conformational changes of the DNA and/or the protein may contribute significantly to this increase in enthalpy. Additionally, we examined the importance of the consensus "half-site" to the recognition process. The refined co-crystal structure of the N-terminal domain suggests that the binding of cI dimer to O_L1 is asymmetric (Beamer, L.J. and Pabo, C.O. (1991) *J. Mol. Biol.* 227, 177-196). Our results indicate that cI does not bind to the consensus half-site alone, and that association with a symmetrical site in which both halves are consensus is characterized by a weaker binding and a much smaller enthalpy than the one obtained for the cI-O_R1 association. These results support the idea that repressor-operator recognition cannot be explained in terms of a simple recognition code. (Supported by NIH grant GM 39343)

W-Pos224

O_R1 DYNAMICS AND λ *cI* REPRESSOR BINDING: TIME-RESOLVED FLUORESCENCE ANISOTROPY DECAY USING 2-AMINOPURINE

((J.B.A. Ross,[1] B. Wolf,[1] D.F. Senear,[2] and W.R. Laws[1])) [1]Biochem. Dept., Mount Sinai School of Medicine, New York, NY 10029 & [2]Dept. Molecular Biology and Biochem., University of California, Irvine, CA 92717.

Cooperative binding of λ *cI* repressor to the right operator (O_R) of the bacteriophage λ is a paradigm for regulation of initiation of transcription. Protein dimers bind to three adjacent operator sites in O_R. Dimers also self-associate to higher oligomers, including octamer. The protein self-association has sufficient free energy to account for the observed cooperativity (Senear et al., (1993) *Biochemistry 32*, 6179-6189). Since octamer can bind four O_R1 21-mers, octamer must bind to the three DNA sites simultaneously with a free energy change that is less than the sum of the free energy changes for dimer binding to each site separately. To help understand the contributions to cooperativity that could arise from structural rearrangements of the DNA, we have examined the dynamics of the O_R1 21-mer in the presence and absence of repressor by using time-resolved fluorescence anisotropy. The two 5' adenines were replaced with 2-aminopurine to serve as fluorescence probes. In the absence of protein, the oligo exhibits three rotational correlation times, reflecting the 5' segmental motions and the high asymmetry of the DNA. The protein-oligo complex has two correlation times, reflecting the 5' segmental motions and the global motion of the complex, now dominated by the protein. Supported by NIH Grants GM-39750 (J.B.A.R.) and GM-41465 (D.F.S.).

W-Pos225

CHARACTERIZATION OF THE BINARY AND TERNARY COMPLEXES OF YEAST GCN4 AND TBP WITH DNA: A TIME-RESOLVED FLUORESCENCE STUDY. ((Matthew H. Wilson, Gina M. Perez-Howard, P.A. Weil, J.M. Beechem)) Vanderbilt University, Dept. of Molecular Physiology & Biophysics, Nashville, TN.

A fluorescence based assay system is being developed to examine the protein-protein/protein-DNA interactions involved in the activation of transcription. As a simple model, we are utilizing a small double-stranded DNA fragment which contains both a concensus GCN4 and TATA binding protein (TBP) binding site: 5'-CCTATGACTCATCCGGATCCGGTATAAAAGGCC-3'. Preliminary characterization of the photophysical properties of the single tryptophan in the activation domain of GCN4 has revealed concentration dependent oligomerization in the absence of DNA. The observed time resolved anisotropy reveal a large decrease in the rotational correlation time of GCN4 over the concentration range of 20→0.3μM. It was found that the single tryptophan in GCN4 located in a region of the protein which has not been structurally characterized was sensitive to DNA binding, as observed by a red-shift in the steady-state emission spectrum. Experiments were also performed using the acridine homodimer (AHD) intercalating dye, which binds with high specificity to repetitive T-A sequences (hence the TATA-box). It was found that stoichiometric binding isotherms could be obtained with our model DNA sequence. The fluorescence intensity of this dye increased upon binding of GCN4 at the upstream site. The origin of this change in quantum yield is not known. At higher GCN4 concentrations (mole ratio of GCN4/DNA = 8), the GCN4 drove AHD off the DNA. Experiments are underway which examine (both kinetically and time-resolved) the effect of pre-bound TBP on the interaction of GCN4 with this DNA fragment.

W-Pos226

Characterization of the Interaction with TATA Box DNA by Single Tryptophan Containing Mutants of TATA Binding Protein (TBP): A Time-Resolved Fluorescence Study. ((Gina M. Perez-Howard, D. Poon, P.A. Weil, J.M. Beechem)) Vanderbilt University, Dept. of Molecular Physiology & Biophysics, Nashville, TN.

TBP specifically binds the TATA box of Eucaryotic genes just upstream from the start site, and is a crucial element which allows assembly of those elements needed for transcription by RNAP II. It has now been found that TBP is essential for RNAP I and RNAP III also. TBP binds in the minor groove and radically bends DNA upon interaction. A spectroscopic characterization of the DNA binding and solution properties of wild type *S. cerevisea* TBP was previously done using the intrinsic (W26) tryptophan on the amino terminal (non-DNA binding) region of the protein. This data revealed that wild-type TBP exists in solution as a multimer and then dissociates into a monomer upon binding DNA (Perez-Howard et. al., submitted). In order to further investigate this binding process, single tryptophan mutants of TBP, where the native tyrosines have been replaced (one at a time) for tryptophans, have been developed. All of these Y→W mutants were found to be viable in yeast (with the native TBP gene eliminated), indicating that these mutant TBP's were functional. We are currently examining the TBP mutant Y195W (W26Y). This tryptophan is located on the concave surface of TBP, which interacts with TATA box DNA. Time resolved experiments of the free mutant TBP in solution have shown associative type anisotropy decays. The recovered rotational correlation time(s) are consistent with the results obtained from *wt* TBP, indicating higher oligomeric TBP states in the absence of DNA. Additional experiments utilizing fluorescent TATA DNA (5' Rhodamine-X labeled) allow both binding and stopped-flow kinetic experiments to be performed at extremely low concentrations (pM-nM). At sub-stoichiometric TBP concentrations, simple 1:1 TBP/DNA complexes are found. However, at higher TBP/DNA ratios, additional complex assembly processes can be observed.

W-Pos227

EFFECTS OF DNA AND PROTEIN STRUCTURE ON THE BINDING OF DNA TO THE POLYMERASE AND EXONUCLEASE DOMAINS OF KLENOW FRAGMENT.

((D. P. Millar and T.E. Carver)) Department of Molecular Biology, The Scripps Research Institute, La Jolla, CA 92037. (Spon. by Peter Wright)

The 68 kD Klenow fragment of DNA polymerase I can be used to examine the molecular mechanisms involved in DNA replication fidelity. The enzyme contains a 3'-5' exonuclease domain that proofreads polymerase errors by selectively removing misincorporated nucleotides from the DNA primer terminus. The polymerase domain may also contribute to fidelity by suppressing mutagenic errors that distort DNA upstream from the primer terminus, such as frameshift errors. To analyze the structural factors that influence binding of DNA to each domain of the enzyme, we have directly measured partitioning of fluorescently-labeled DNA between the polymerase and exonuclease sites using time-resolved fluorescence spectroscopy. We have examined a series of defined oligonucleotide primer/templates containing internal base mismatches, A-tract kinks and bulged nucleotides to assess the effect of structural distortions of DNA on enzyme binding. Internal mismatches located up to four base pairs from the DNA terminus appear to inhibit binding at the polymerase site. Duplexes containing A-tract kinks or bulged nucleotides close to the primer terminus also exhibit a diminished tendency to bind at the polymerase site. These results suggest a mechanism whereby the enzyme can suppress frameshift errors in addition to proofreading misincorporated bases. In addition, we have also analyzed how specific amino acid residues within the enzyme influence DNA binding. Supported by NIH grant GM44060 and NRSA fellowship GM15729.

W-Poe228

NEW METHODS FOR TIME-RESOLVED "FOOTPRINTING"

((B. Sclavi, M. R. Chance, M. Brenowitz)). Department of Physiology & Biophysics and Department of Biochemistry, Albert Einstein College of Medicine, Bronx, NY 10461.

We are developing two new nuclease protection "footprinting" methods that can be used to study DNA-protein interactions on millisecond timescales. Both methods are based on the production of hydroxyl radicals, which are used to cleave the DNA. The first method is based on the radiolysis of water by x-rays where a high flux, white, x-ray beam at the National Syncrotron Light Source is used to irradiate the samples. We have shown that adequate cutting of DNA for a footprint experiment can be obtained with a beam exposure equivalent to 12 ms. The second method is based on the photolysis of methylcobalamin in the presence of hydrogen peroxide. The products of this photolysis reaction are Co(II), methyl radicals and hydroxyl radicals. Both of these methods can now be used as fast, practical ways of obtaining DNA-protein footprints, with results that are very similar to those obtained by Fenton chemistry. These methods have been validated by examining footprints of both Lac and Gal repressors. Both of these methods can potentially be used to study macromolecular interactions and folding on millisecond timescales.

This research is supported by NSF MCB-9410748 and NIH grants RR-01633 and GM-51506.

W-Poe229

NOVEL SPECTROSCOPIC ANALYSIS OF THE TAT PROTEIN - TAR RNA INTERACTION.

((Ting Xiang, Max Diem, and Dixie J. Goss)) Chemistry Department, Hunter College, City University of New York, NY, NY 10021

The Tat (trans-activator) protein from (HIV-1) is a potent activator of HIV transcription and is essential for HIV replication. A short peptide (9 amino acids) that contains the basic region of the HIV Tat protein binds specifically to an RNA stem loop structure, ΔTAR, which is a shortened form of the native TAR (trans-acting response element). Here we report Circular Dichroism (CD) measurements and the first vibrational CD (VCD) measurements of the tat-peptide, the ΔTAR region and their 1:1 complex. These studies give detailed structural information about the tat-TAR interaction indicating that the Tat-peptide is not unordered as previously described. Calculations suggest that the Tat-peptide is probably an extended left-handed helix with a slightly higher twist than beta sheet. CD and VCD both indicate conformational changes upon the specific binding of Tat-peptide with ΔTAR RNA. Modeling studies of this interaction show peptide binding at the junction of the double-stranded stem and the loop region. Several potential H bonds are identified.

W-Poe230

LENTIVIRAL NUCLEOCAPSID PROTEIN INDUCES LARGE CHANGES IN THE CIRCULAR DICHROISM SPECTRA OF POLY(rA).

((P.W. Sims, C.A. Gelfand, B. Woodson, R. Montelaro, L. Ehrlich, C. Carter, and J.E. Jentoft.)) Case Western Reserve Univ., Univ. of Pittsburgh, and State Univ. of New York at Stony Brook.

The retroviral nucleocapsid protein (NC) has several important roles in the viral life cycle that are presumably related to its nucleic acid binding properties. Lentiviral NCs from equine infectious anemia virus (EIAV) and human immunodeficiency virus type 1 (HIV-1) are able to induce remarkably complex changes in the circular dichroism (CD) spectra of poly(rA). Under stoichiometric binding conditions and at molar ratios of NC to poly(rA) up to 0.2, the bands of both positive and negative ellipticity in the CD spectrum of poly(rA) decrease in amplitude, a change that is attributed to the base unstacking of the poly(rA). Furthermore, the spectra have an isosbestic point at 253nm that is consistent with a simple binding event. However, as the molar ratio of NC to poly(rA) is increased above 0.2, a salt dependent second binding state is induced, and this state is characterized by a further decrease in the amplitudes, shifts in the wavelengths of the bands of both the positive and negative ellipticities, and the loss of the isosbestic point. Significantly, the EIAV gag polyprotein can perturb the CD spectra of the poly(rA) in the same manner as the mature EIAV NC. We suspect that the biological role of the lentiviral NCs are related to their ability to induce large changes in the nucleic acid structure upon complexation, a property that has not been explicitly recognized as an attribute of these proteins.

This poster is a contribution of the Protein Group at Case Western Reserve University.

W-Poe231

ESCHERICHIA COLI PRIMARY REPLICATIVE HELICASE DnaB PROTEIN. OLIGOMERIC STRUCTURE AND INTERACTIONS WITH ssDNA.

((Wlodzimierz Bujalowski, Ug-Sung Kim, and Maria J. Jezewska)), Department of Human Biological Chemistry and Genetics, The University of Texas Medical Branch at Galveston, Galveston, Texas 77555-0653

The oligomeric structure of the *E. coli* primary replicative helicase DnaB protein and ssDNA binding properties, in relation to the protein's functions, have been characterized. Sedimentation equilibrium, sedimentation velocity, and ligand binding studies show that, in solutions containing magnesium ions, the DnaB helicase exists as a stable hexamer in a large protein concentration range ($\sim 10^{-7}$ - 10^{-5} M, hexamer). The hexamer has a nonspherical shape and, when modeled as a prolate ellipsoid of revolution, has an axial ratio of a/b = 2.6 ± 0.6. In the absence of Mg^{2+}, DnaB protein forms a trimer which, at low protein concentrations, dissociates into monomers. The analysis of the ratio of the sedimentation coefficients of the DnaB hexamer and monomer indicates that elongated DnaB protomers aggregate with cyclic symmetry with the protomers being in a plane about a six-fold rotational axis. The functions of the DnaB protein *in vivo* are related to its ability to interact with ss and dsDNA under ATP control. The obtained results show that only ribonucleotide triphosphates act as very specific, positive allosteric effectors, inducing a conformational change in the protein which leads to its dramatically increased affinity for ssDNA. There is a significant heterogeneity among ssDNA binding sites, indicating strong asymmetry in the protein-nucleic acid complex. This functional, and possibly structural, asymmetry is strongly amplified in the presence of ATP nonhydrolyzable analogs. The implications of the studied interactions for the DnaB helicase functioning in the replication of *E. coli* DNA is discussed.

W-Poe232

CHARACTERIZATION OF THE SINGLE-STRANDED DNA-BINDING (SSB) PROTEIN ENCODED BY THE RK2 PLASMID

((J. R. Casas-Finet, O. S. Jovanovic, and D. H. Figurski)) Structural Biochemistry Program, PRI/DynCorp, NCI-FCRDC, Frederick, MD 21702, and Department of Microbiology, Columbia University, New York, NY 10032. (Spon. by J. R. Casas-Finet)

Studies from several laboratories have revealed a family of closely related bacterial and plasmid single-stranded DNA-binding (SSB) proteins, of which the SSBs of *E. coli* and the F plasmid are best characterized. We have identified a unique family of SSBs expressed by Inc P α and β plasmids that share *ca.* 30% identity with the *E. coli* SSB protein. These SSBs have a molecular mass (13 kDa) and primary sequence similar to that of the DNA-binding domain of *E. coli* SSB but lack its variable C-terminal region. We have previously shown that the IncP α plasmid RK2 *ssb* gene can complement an *E. coli ssb-1* mutant. The RK2 *ssb* gene was cloned into a pET16b expression vector, and RK2 SSB was found to constitute *ca.* 50% of the cellular protein after induction. The recombinant protein was purified by centrifugation and affinity chromatography on a ssDNA-agarose column. RK2 SSB eluted at high salt (2.5 M KCl) to give a preparation that was 95% pure and contained both monomeric and tetrameric forms. The DNA binding activity of the purified protein was verified by a gel shift assay using an 81-base partially random oligonucleotide. SDS-PAGE and Western blot analysis using polyclonal rabbit antibody raised against purified protein showed that the tetrameric form dissociated into dimers and monomers after boiling. No cross-reactivity against *E. coli* SSB was observed for the RK2 SSB antibody. RK2 SSB had a CD spectrum with a band of negative ellipticity peaking at 216 nm, typical of β structure. Its overall fluorescence emission was maximal at 343 nm, whereas Trp photoselection resulted in maximum emission at 347 nm. Together with a blue-shifted excitation maximum of 276.5 nm, these results suggest a solvent-exposed environment for the single Trp residue of RK2 SSB and a significant Tyr to Trp energy transfer at the singlet level. Spectral deconvolution points to a significant contribution of the Tyr population to the overall emission. Binding of RK2 SSB to single-stranded nucleic acids resulted in large quenching of its integrated emission with minor effects in band position or linewidth (e. g., 43% quenching and 2 nm blue-shift for poly(dA)). The extent of quenching was dependent on the particular lattice, and was reversed at high [NaCl]. Binding stoichiometry (11 nucleotide bases/SSB monomer at [NaCl] > 0.3 M) was dependent on salt concentration, as seen for *E. coli* SSB.

W-Poe233

SINGLE-STRANDED DNA BINDING DOMAIN OF RECA PROTEIN: CONFORMATIONAL CHANGES IN BOTH THE DNA BINDING PEPTIDES AND SINGLE-STRANDED DNA UPON COMPLEX FORMATION

((Lijiang Wang, Oleg N. Voloshin, & R. Daniel Camerini-Otero)) Genetics & Biochemistry Branch, NIDDK, NIH, Bethesda, MD 20892.

The E.coli RecA protein plays a key role in both general recombination and DNA repair. Biochemical studies have shown that in vitro RecA protein has a number of enzymatic activities. In all these reactions RecA first must bind to single-stranded DNA (ssDNA). Recently, we have shown that a 20 amino acid peptide derived from RecA protein is a ssDNA binding region of RecA protein (R.Gardner, O.Voloshin & R.D. Camerini-Otero, submitted for publication). Five amino acids in the sequence of this peptide are highly conserved among prokaryotic recombinases and their eukaryotic homologs. To elicit the importance of these residues for DNA binding, several synthetic peptides were prepared. Filter binding and potassium permanganate modification experiments have shown that an aromatic amino acid in the middle and the conserved residues at the ends of the peptide are required for binding. Upon binding, peptides, like the whole RecA protein, unstack bases in ssDNA but not in duplex DNA. Though at low concentrations all the peptides have a similar random-like structure as indicated by their CD spectra, the DNA binding peptides change to a unique ordered structure upon binding. The possible binding site size, the conformation of the ordered structure, and the correlation of binding to the conformational change will be discussed.

W-Pos234

A CRYSTALLOGRAPHIC STRUCTURAL ANALYSIS OF THE INTERACTIONS BETWEEN THE CATABOLITE GENE ACTIVATOR PROTEIN AND ITS DNA BINDING SITE AT 2.5Å RESOLUTION. ((G. N Parkinson. R. H. Ebright. and H. M. Berman.)) Dept. of Chemistry and Waksman Institute, Rutgers University, Piscataway N.J. 08855-0939

Catabolite gene activator protein (CAP), a sequence-specific, helix-turn-helix DNA binding protein, regulates transcription in *Escherichia Coli.* in response to elevated intercellular levels of c-AMP, its allosteric effector. The structure of the CAP-DNA complex at 3.0Å has been previously reported[1]. The structure contained a DNA fragment with a gaps in the phosphate backbone important for CAP-DNA interactions. With the use of a high energy synchrotron radiation source and by using a DNA fragment without the missing sites of interaction we were able to collect and refine the CAP-DNA complex to 2.5Å resolution. The resolution and quality of data permits the unambiguous identification of amino acid-base pair H-bonded contacts and water-mediated contacts in the CAP-DNA complex. With the inclusion of the missing phosphates all predicted protein-DNA interactions can now be observed. Results show that the expected contact points are in agreement with those predicted on genetic and biochemical evidence. Ser179, Thr182 and the amino backbone group of 179 are contacting the phosphate group at position 9. Important water mediated contacts are observed between the recognition helix F and DNA bases in the major groove. The guanidinium group of Arg185 uses waters between G7 N-7, and G9 N-7 as well as a direct contact to T8 O-4.

1 Schultz S., C., (1991). Science, **253**, 1001-1007.

This research is supported by a grant from the NIH (GM 21589-19)

W-Pos235

THREE DIMENSIONAL STRUCTURES OF THE NK-2 HOMEODOMAIN PROTEIN IN THE FREE AND DNA-BOUND STATES BY NMR. ((D. H. H. Tsao, J. M. Gruschus, L.-H. Wang, M. Nirenberg and J. A. Ferretti)) NHLBI, NIH, Bethesda, MD 20892-0380.

The homeodomain is approximately a 60 amino acid residue segment present in eukaryotic transcription regulators. It is believed that it regulates transcription by binding to sequence-specific DNA. The NK-2 homeodomain protein, from *Drosophila melanogaster*, is expressed in part of the central nervous system during early embryonic development. The three dimensional structure of the free NK-2 homeodomain protein was determined by 2D and 3D NMR methods, together with molecular modeling. The protein belongs to the helix-turn-helix family of DNA-binding proteins. Upon binding NK-2 to a consensus DNA sequence that contains AAGTG as the central core,the DNA recognition helix elongates from 11 to 19 residues. The ability of the recognition helix to bind specific DNA bases is related to both its sequence and structure. The structures of the free and bound NK-2 protein will be presented and compared.

W-Pos236

DNA RECOGNITION BY HOMEODOMAINS: INVESTIGATION OF THE NK-2 HOMEODOMAIN ((J. M. Gruschus, D. H. H. Tsao, L.-H. Wang, M. Nirenberg and J. A. Ferretti)) NHLBI, NIH, Bethesda, MD 20892-0380.

Homeodomain proteins contain the helix-turn-helix motif and bind to specific DNA sequences. Many homeodomain containing proteins regulate gene expression during embryonic development of eukaryotes. The NK-2 homeodomain is involved in the development of the central nervous system in *Drosophila* embryos. A model structure is presented for the DNA/NK2 complex. The structure was obtained using both experimental data, 3D heteronuclear NMR and methylation/ethylation binding interference studies, and structural homology modeling with a related DNA/homeodomain complex. The interactions at the DNA-protein interface and the mechanism for sequence specific binding are examined and compared with other DNA/homeodomain complexes whose structures are known. The DNA-protein contacts in the major groove are presented in detail, and the highly variable residue 54 of the homeodomain is shown to play a primary role in the sequence specificity.

W-Pos237

STRUCTURAL DETERMINATION OF THE RNA-BINDING DOMAIN OF RHO PROTEIN. ((T.J. Allison, D.M. Briercheck, G.S. Rule)) University of Virginia, Charlottesville, VA 22908.

Rho is a protein required for the release of nascent RNA transcripts from rho-dependent transcription complexes in both gram-negative and gram-positive bacteria. *E. coli* rho protein is a hexamer of identical 47kDa subunits and appears to function by coupling an RNA-DNA helicase activity to an RNA-dependent ATPase activity. *In vitro*, rho binds single stranded DNA and RNA, but shows preferential activation of helicase activity by cytidine-containing oligoribonucleotides. Rho is a member of a large family of proteins that show homology in an 80 amino acid RNA-binding domain.

The 130 residue RNA binding domain (RBD130) of rho has been expressed to sufficient levels for multidimensional NMR experiments. 2D-HSQC $^{1}H/^{15}N$ NMR spectra have been obtained in the presence and absence of $(dC)_{10}$. These spectra show that while many chemical shift perturbations occur, the core structure does not change upon binding. Residue- and sequence-specific assignments are being obtained from $^{13}C/^{15}N$ labeled protein using a variety of triple resonance techniques. RBD130 crystals have been grown which are monoclinic, of space group $P2_1$, and contain one monomer per asymmetric subunit. These crystals show strong uniform diffraction to 2.0Å. Two isomorphous heavy atom derivatives (Pt and Hg) have also been obtained.

W-Pos238

EXCHANGE RATES OF *L*-TRYPTOPHAN WITH TRP-REPRESSOR AND THE AV77 MUTANT DETERMINED BY NMR. ((T. H. Schmitt; Z. Zheng and O. Jardetzky)) Stanford Magnetic Resonance Laboratory, Stanford University, CA 94305-5055.

The Trp-Repressor of *Escherichia coli* is a protein responsible for the regulation of tryptophan biosynthesis. The symmetric dimeric protein binds two molecules of the corepressor tryptophan to form a holorepressor complex with high affinity for specific DNA operons in *E. coli.* The mutation $Ala^{77} \rightarrow Val^{77}$ transforms the protein into a superrepressor, that binds DNA with comparable affinity of the wild type, either in the presence or in the absence of L-tryptophan. On the other hand, the binding of L-tryptophan to the protein seems not to be affected in a large extent. In the present work, the exchange rates of *L*-tryptophan with Trp-Repressor and the AV77 mutant were calculated from the chemical shifts of *L*-tryptophan in the 1D NMR spectrum as a function of protein concentration and temperature. The exchange rates at 313 K for L-tryptophan and the wild type Trp-Repressor and for the AV77 mutant were found to be approximately 55 Hz and 65 Hz, respectively. The similarity of the results suggests that the $Ala^{77} \rightarrow Val^{77}$ mutation does not affect significantly the binding of *L*-tryptophan to the protein. A precise determination of the exchange rates will be performed by line shape analysis of the NMR spectra.

Supported by: NIH grant # GM33385. T.H.S. is recipient of a Brazilian fellowship from FAPESP (grant # 93/4719-4).

W-Pos239

Using ESR to probe peptide/DNA specific interactions ((Thaddeus S. Block, Glenn L. Millhauser)) University of California, Department of Chemistry and Biochemistry, Santa Cruz, CA 95064.

Polypeptide/DNA interactions have been studied by a multitude of biochemical techniques of varying sensitivities. Many standard techniques such as DNAse footprinting and gel mobility shifts register only tightly bound polypeptide/DNA complexes, where less stable complexes can be missed. In this work, subtle peptide/DNA specific interactions are being probed using ESR spectroscopy.

To study the peptide/DNA interactions, we are using a previously known DNA binding peptide; a truncated version of the GCN4 protein (Peter S. Kim, 1992). The natural protein binds the CRE DNA element as a leucine zipper dimer. We have modeled this dimerization with a C-terminal cysteine disulfide linkage (Peter S. Kim, 1992). Various nitroxide spin labels have been incorporated into regions of the 18 amino acid DNA binding peptide. Thus, motional dynamics can be followed with ESR spectroscopy as the peptides "tumble" in solution alone, with specific DNA oligomers present (CRE site), and with non-specific DNA oligomers present.

W-Pos240

BINDING OF PROTEINS AND SMALL MOLECULES TO DNA JUNCTIONS. ((S.A. Winkle, I. Gonzalez, R. Gonzalez, V. Obeso, V. Palau-Ramsauer, S. Reinhardt and R.D. Sheardy)) Chemistry Departments, Florida International University, Miami, FL 33199 and Seton Hall University, South Orange, NJ, 07079.

The presence of (CG)n segments enhances cleavage rates for restriction enzymes recognizing neighboring sites. The presence of TCTTG or TGTTG segments similarly enhance restriction enzyme cleavage rates and these sequences serve as preferred binding sites for carcinogens such as 4-nitroquinoline-1-oxide or N-acetoxy-N-acetyl-2-aminofluorene. The presence of these sequence motifs create potential junctions at the junctures of these sequences with adjoining sequences. Gel mobility studies and kinetic assays suggest that the enhanced cleavage rates arise from binding of restriction enzymes at the (CG)n or T(C/G)TTG motifs. Gel mobility studies and restriction enzyme inhibition assays suggest that T7 RNA polymerase, Klenow fragment and DNA polymerase may also target these sequences for preferred binding. Restriction enzyme inhibition studies suggest that actinomycin D and alkylaminoanthraquinone derivatives also target (CG)n junctions while tris(phenanthroline)ruthenium (II) binds neither to the (CG)n segment nor to the junctions. Implications of these results for protein-DNA interactions will be discussed. (This work supported by PHS MBRS GM 08205-09 (SAW))

W-Pos241

SOLUTION STRUCTURE AND DYNAMICS OF THE MINOR GROOVE BINDING DRUG SN-6999 COMPLEXED WITH d(GGGAAAAACGG)·d(CCGTTTTTCCC). ((J.M. Rydzewski, J.A. Smith, W. Leupin, and W.J. Chazin)) Department of Molecular Biology, The Scripps Research Institute, La Jolla, CA 92037. (Sponsored by J. A. Tainer)

A number of antitumor drugs and other ligands that bind reversibly to DNA serve as excellent models for the study of the physical, thermodynamic and kinetic parameters characteristic of recognition of the minor groove of duplex DNA. SN-6999 is a member of the family of bis(quaternary ammonium) heterocycles which have been shown to possess potent antitumor activity. NMR spectroscopy is being used to carry out a detailed study of the interactions between SN-6999 and an A-tract DNA duplex with the sequence designed to produce a narrow minor groove width and maximize the van der Waals complementarity of the drug and DNA. Complete ^{1}H NMR resonance assignments have been made and 31 intermolecular contacts have been unequivocally assigned. The drug binds primarily in the $d(A)_5 \cdot d(T)_5$ region, and in contrast to previous studies, with a preferred orientation along the DNA axis. Strong interactions are found to extend one residue in the 3′ direction along each strand to C_9 and C_{20}. Doubling of numerous drug and DNA resonances of the 1:1 complex observed at 1 °C indicates slow exchange between a major and minor binding mode and permitting the calculation of kinetic and thermodynamic binding parameters. A high resolution three dimensional solution structure of the major binding mode of the complex is being determined using NMR spectroscopy and restrained molecular dynamics calculations starting from a series of randomized drug and DNA structures. The results are being analyzed to identify the elements responsible for the unique binding orientation of SN-6999 in this complex, and the factors which determine the DNA sequence preferences of this class of antitumor agents.

W-Pos242

INTERACTION OF BIS-NETROPSIN ANALOGUES TO DNA OLIGOMERS ((K. Alessi[1], L. A. Marky[1], M. P. Singh[2], B. Plouvier[2], and J. W. Lown[2])) [1]Department of Chemistry, New York University, New York, New York; and [2]Department of Chemistry, University of Alberta, Edmonton, Alberta, Canada.

In an effort to study phasing, isohelicity, true bidentate vs "operational" bidentate binding, we used a combination of calorimetric and spectroscopic techniques to thermodynamically characterize: i) the helix-coil transition of two isomeric deoxyoligonucleotides with sequences: $[d(CGA_4T_4CG)]_2$ and $[d(CGT_4A_4CG)]_2$, and ii) the interaction of each oligomer with enantiomeric bis-lexitropins: (-)-(1R,2R)-bis(netropsin)-1,2-cyclopropanedicarboxamide and (+)-(1S,2S)-bis(netropsin)-1,2-cyclopropanedicarboxamide, referred to as "R" and "S" respectively. We determine standard thermodynamic profiles ($\Delta G°$, ΔH and ΔS). Melting experiments, as a function of strand concentration and salt concentration, show that the $[d(CGA_4T_4CG)]_2$ duplex is thermally more stable by 3°C. This corresponds to a more favorable $\Delta\Delta G°$ of -2 kcal/mol resulting from a differential compensation of a favorable enthalpy, $\Delta\Delta H$ = -13 kcal/mol, with an unfavorable entropy, $\Delta(T\Delta S)$ = -11 kcal/mol. This type of compensation may be explained in terms of differences in the overall hydration state of the oligomers. The analysis of the titration calorimetry binding isotherms, for the association of R and S to each oligomer, yielded stoichiometries of 2 ligands per duplex, average K_b's of ~2 x 10^5, endothermic heats of 0.3 to 3.9 kcal/mol, and favorable entropy contributions ($T\Delta S$) of 7.1-11 kcal/mol. The R ligand binds slightly better ($\Delta\Delta G°_b$ = -0.4 kcal/mol) to the $[d(CGT_4A_4CG)]_2$ duplex in enthalpy driven reactions ($\Delta\Delta H_b$ = -2.9 kcal/mol). The overall results may be interpreted in terms of the interaction of only one half of each ligand with the minor groove while the other half is exposed to solvent. Supported by Grant GM-42223 from the NIH (L.A.M) and The Natural Sciences and Engineering Research Council of Canada (J.W.L).

W-Pos243

GCMC THERMODYNAMIC ANALYSIS OF EFFECTS OF SALT CONCENTRATION ON THE BINDING OF AN OLIGOCATION (L^{8+}) TO POLYMERIC DNA ((J.P. Bond*, M.C. Olmsted#, C.F. Anderson*, and M.T. Record, Jr.*‡)) Departments of Chemistry* and Biochemistry‡ University of Wisconsin-Madison, Madison, WI. 53706 and #University of Colorado, Health Sciences Center, Department of Biochemistry, Biophysics and Genetics, 4200 E. 9th Avenue, Denver, CO 80262

The effects of salt activity ($a_\pm$) on equilibrium concentration quotients (K_{obs}) characterizing the binding of an oligocationic ligand to a polymeric nucleic acid can be expressed under typical experimental conditions as

$$S_aK_{obs} \equiv (\partial \ln K_{obs}/\partial \ln a_\pm)_{T,P,m_\pm \to 0} = \Delta(|Z_J| + 2\Gamma_{32J})$$

where the molar preferential interaction coefficient for each reactant or product species J having Z_J charges is defined $\Gamma_{32J} \equiv (\partial C_3/\partial C_{2J})_{\mu_1,\mu_3,T}$; and Δ denotes a stoichiometrically weighted difference of terms pertaining to the product and reactant species (Anderson and Record, 1993; *J. Phys. Chem.* **97**, 7116-7126). Here we evaluate S_aK_{obs} theoretically using the appropriate set of three Γ_{32J} determined by GCMC simulation for primitive models of solutions containing excess uniunivalent salt at activities in the experimental range $1.76 \le a_\pm \le 200$ mM. Values of Γ_{32J} are computed to describe the thermodynamic effects of salt interactions with i) an oligocation L^{8+}, ii) polymeric double stranded (ds) or single stranded (ss) DNA, or iii) a complex of L^{8+} with polymeric DNA. In agreement with experiments our calculations predict that S_aK_{obs} for the binding of L^{8+} to polymeric ssDNA or dsDNA is relatively constant over the range of salt activities studied. The predicted value of S_aK_{obs} for binding of the octacation to ssDNA at $a_\pm$ = 50 – 200 mM is close to that reported by Mascotti and Lohman,1990 (Proc. Natl. Acad. Sci. USA 87, 3142) for the binding of an oligolysine to ssDNA at the corresponding salt concentration.

W-Pos244

CALCULATION OF DRUG BINDING CONSTANT IN DRUG-DNA COMPLEXES. ((Y.Z. Chen and E.W. Prohofsky)) Department of Physics, Purdue University, West Lafayette, IN 47907-1396.

Drugs bind to DNA molecules by a variety of interactions. We have developed a statistical approach, using microscopic structure and established force fields, to calculate the dynamics of the disruption of these interactions leading to the drug dissociation. The calculated dissociation probability can be converted to give the equilibrium drug binding constant. Our calculated binding constant for an intercalating drug – daunomycin and a minor groove binding drug – netropsin are in fair agreement with observations. The temperature dependence of the binding constant at premelting temperatures is found to obey the van't Hoff relation in agreement with experiments. Our approach can also be used to study the effect of drug binding on the dynamical stability of the base pairs at the binding site. We find that the opening probability of certain base pairs at the binding site are decreased by orders of magnitude. The significant increase in the dynamical stability of the drug bound base pairs results in the shift in the melting temperature of the drug-bound helix in agreement with observations.

Y.Z. Chen and E.W. Prohofsky, *Biophys. J. 66*, 820 (1994).

W-Pos245

INTERACTIONS BETWEEN A DNA LIGAND AND THROMBIN. ((H. V. Hsieh, J. B. Pitner, G. P. Vonk, and D. P. Malinowski)) Becton Dickinson Research Center, 21 Davis Drive, Research Triangle Park, NC 27709-2016.

Nucleic acid ligands that bind specifically to target molecules may be isolated from large pools of random nucleic acid oligomers using an iterative selection procedure (Tuerk et al., (1992) *PNAS* 89: 6988). Previous work employing a selection procedure has found a family of thrombin-binding single stranded DNA ligands with a consensus sequence of 5′-GGTTGGTGTGGTTGG-3 (Bock et al., (1992) *Nature* 355: 564). In this poster, fluorescence polarization and surface plasmon resonance competition experiments were used to measure the equilibrium constant between thrombin and the fluorescently-labelled DNA consensus sequence. The equilibrium constants determined from these techniques were in agreement ($K_d \approx$ 1 to 6 nM), and were comparable to the equilibrium constant calculated from the apparent kinetic rates of thrombin and the consensus sequence measured by surface plasmon resonance (Ciolkowski et al., manuscript submitted; BIAcore Application Note 305).

W-Pos246

THERMODYNAMIC COMPLEXES OF DNA WITH FOLDED AND UNFOLDED HISTONE H_1 AT THE PRESENCE OF SURFACTANTS.

"A.A.Moosavi - Movahedi, F. Tasht - Zarin" Institute of Biochemistry & Biophysics, University of Tehran, Tehran, Iran.

Interaction between DNA and H_1 investigated in the presence and absence of sodium n- dodecyl sulphate (SDS) and dodecyl trimethyl ammonium bromide (DTAB) at various temperatures in 2.5 mM phosphate buffer, pH 6.4 by UV - spectrophotometer, equilibrium dialysis, titration and temperature scanning spectroscopy.

The presence of 1.33 mM SDS caused the H_1 folded and contact more with DNA. The unfolded state of H_1 caused less interaction with DNA.

Using binding data in the terms of Wyman theoretical model to calculate free energy and enthalpy of interaction comparing with enthalpy of interaction which is obtained from Pace model.

The thermodynamic parameters and precipitation percent of DNA - H_1 complexes indicate the folded H_1 - DNA causing higher energy of interaction and more precipitation than native H_1 - DNA complexes.

W-Pos247

OSMOTIC SENSITIVITY OF EcoRI BINDING. ((N.Yu. Sidorova, V.A. Parsegian and D.C. Rau*)) LSB/DCRT and OD/NIDDK*, NIH, Bethesda, MD 20892

It has been known for a long time that osmolytes like sucrose, betaine and glycerol favor star-activity of restriction enzymes. It was shown recently [C.R.Robinson and S.G.Sligar, *Biochem.*, 1994, **33**, 3787-3793)] that increased digestion by EcoRI restriction nuclease at star sites in the presence of osmolytes is correlated with decreased water activity. Results seem to indicate some loss in specificity of restriction enzyme. Could this be interpreted as a loss of specificity of EcoRI-DNA binding under conditions of osmotic stress? Enzymatic reaction is a complicated system which combines binding and cutting steps. We have investigated binding specificity of EcoRI (in the absence of required Mg^{2+} co-factor) as a function of osmotic stress. To avoid problems which arise when measuring absolute binding constants, we used a competition assay which lets us measure relative changes in binding constants. Using the gel-shift assay and different DNA competitors we show that the ratio of specific to non-specific EcoRI binding constants increases in the presence of neutral osmolytes. The enzyme as a binding protein does not lose its specificity. On the contrary, osmolytes promote specific binding over non-specific. Preliminary results show about 20-30 more water molecules are released during specific complex formation versus non-specific binding of EcoRI to poly(dI-dC)·poly(dI-dC) polymer.

W-Pos248

OSMOTIC MECHANISM OF CHROMATIN UNFOLDING DUE TO HISTONE REMOVAL. ((J.Y. Ostashevsky)) SUNY-HSCB, Brooklyn, NY 11203.

The NaCl (0.1-2.0 M) dependence of chromatin loop size for fixed V79 nucleoids stained with very low concentrations of ethidium (E) bromide or propidium (P) iodide was monitored directly with fluorescent microscope image analysis and indirectly with flow cytometry 90° light scattering. Both methods showed a slight increase in loop size in 0.2-0.7 M NaCl and a large increase in 0.7-1.2 M NaCl due to removal of histone H1 and H2A/H2B dimers, respectively. No change in loop size was seen in 1.2-2.0 M NaCl, where H3/H4 tetramers dissociate from DNA. It follows from the salt-dependence of E/P fluorescence for chromatin and dehistonized nucleoids that removal of each H1 and H2A/H2B dimer is respectively accompanied by binding of 0.5 and 2.0 Na^+ ions to DNA, and removal of each H3/H4 tetramer is accompanied by the release of 1.0 Na^+ ions from DNA. We suggest that the osmotic pressure of Na^+ counter ions bound to DNA plays the major role in the histone-removal-induced changes in chromatin loop size. The loop expansion due to removal of H2A/H2B dimers seems to be a cause -- not a consequence -- of chromatin unfolding. Otherwise, it is not clear, why removal of H2A/H2B dimers (each of which contacts only 20 bp of the 160 bp per nucleosome) has such a large effect on chromatin unfolding, while removal of H3/H4 tetramers (which releases the remaining 120 bp) does not change loop size. This mechanism is consistent with the depletion of H2A/H2B dimers in transcribed chromatin reported in the literature. Supported by NIH grant RO1 GM 43374.

W-Pos249

BINDING ETHIDIUM AND PROPIDIUM TO CHROMATIN AND EFFECT OF BOUND DYES ON NUCLEOID LOOP SIZE. ((J.Y. Ostashevsky and S. Rozenblyum)) SUNY-HSCB, Brooklyn, NY 11203. (Spon. by C.S. Lange)

Binding of ethidium (E) and propidium (P) to chromatin (CN) and dehistonized (DN) nucleoids prepared from fixed V79 cells and effect of E/P binding on the size of nucleoid loops in 0.1-2.0 M NaCl were monitored with flow cytometry fluorescence and 90° light scattering, and with fluorescent microscope image analysis. Both dyes enhance dissociation of histone H1 and core histones from nucleosomal DNA. This process results in the following features of E/P binding to CN: 1) dye binding becomes time-dependent; 2) removal of each type of histone starts at lower NaCl concentrations than in absence of dyes; 3) E/P binding constants for CN in 0.6-2.0 M NaCl become greater than those for DN; 4) E/P binding to CN in 0.6-1.0 M NaCl is accompanied by the binding of Na^+ ions to DNA; at other NaCl concentrations release of Na^+ from DNA occurs. E/P binding to DN is similar to that for free DNA in solution, releasing 0.9 and 1.3 Na^+ ions per bound E and P molecule, respectively. Dependence of CN loop size on E/P concentration in 0.7-1.5 M NaCl (range of H2A/H2B dimer removal) is bell shaped shortly after preparation. The dependence curves for CN the next day, and at any time for DN, are flat at low dye concentrations and then decrease at high concentrations. We suggest that the major cause of this dependence is changes in the osmotic pressure of Na^+ counter ions bound to DNA. At low dye concentrations, the dye-accelerated removal of H2A/H2B dimers leads to the binding of Na^+ ions to DNA, their osmotic pressure increases, and loops expand reaching their maximal size with time. At high dye concentrations no H2A/H2B histones remain, dye binding releases Na^+ ions, their osmotic pressure decreases, and the loops shrink. Supported by NIH grant RO1 GM 43374.

W-Pos250

SEQUENCE PREFERENCE OF MOUSE H1° THAT HAS BEEN EXPRESSED IN *E. COLI* CELLS. ((D. Su and S. E. Wellman)) Dept. of Pharmacology, Univ. MS Med. Center, Jackson, MS 39216-4505.

The mouse histone H1° has been expressed in and purified from *E. coli* cells. To make the expression construct we amplified the mouse H1° coding sequence, using primers that added restriction sites. To add the restriction site at the 5'-end of the DNA, we added an extra codon, which would result in the addition of an alanine just after the methionine at the amino-terminus of the protein. We inserted the amplified DNA into the pET-11d expression vector. The identity of the construct was confirmed by sequencing the DNA. The protein was expressed in BL21(DE3)pLysS cells. Expression of the target protein was induced by treatment of the cells with isopropyl-β-D-thiogalactopyranoside (IPTG). The H1° was extracted in 5% $HClO_4$ and purified using reverse-phase HPLC. We examined the effects on thermal denaturation of a 214-base-pair DNA fragment of addition of the expressed H1° protein. The protein bound preferentially to one region of the DNA fragment, a region that is relatively GC-rich. This result indicates that the H1° is not totally non-specific, but rather binds with some sequence preference to DNA.

W-Pos251

DESCRIBING THE SUBNUCLEAR DISTRIBUTION OF TOPOISOMERASE I WITH TEXTURE ANALYSIS. ((R.M. Wadkins, S.D. Baker, M.K. Danks, and P.J. Houghton)) Dept. Mol. Pharmacol., St. Jude Children's Research Hospital, Memphis, TN 38101. (Spon. by M. Garner)

Recent reports in the literature on the effectiveness of certain antitumor drugs have revealed that the cellular distribution of the proteins targetted by these drugs is altered in drug-resistant cell lines. To understand how this altered distribution affects the function of the cell and the toxicity of therapeutic compounds, it is necessary to develop a methodology to describe subcellular distribution of antigens. Texture analysis of digitized images directly lends itself to characterization of the distributions of pixel grey-values within a given spatial sampling, such as that obtained with fluorescently immunostained cells. To characterize the distribution of the nuclear protein human topoisomerase I (topo I), the cellular target of the camptothecin drugs, we have applied the method of run length texture descriptors to the analysis of a variety of cell lines that have been immunostained to determine topo I localization. The staining reveals that topo I is primarily associated with the nucleoli in each line. However, when the distributions are compared by MANOVA multivariate analysis of run length statistics, each cell line is shown to have a characteristic staining pattern that segregates it from the other lines. Principal component analysis has been used to determine which of the computed texture descriptors are most effective in describing the staining. We thus show that run length analyses are useful in describing the subcellular localization of topo I and have the potential to be used for other cellular antigens.

W-Pos252

MOLECULAR DYNAMICS STUDY OF NUCLEAR HORMONE RECEPTOR DNA BINDING.

((T.C. Bishop and K. Schulten)) Beckman Institute, UIUC, Urbana, IL 61801.

Molecular dynamics simulations are utilized to investigate the effect that nuclear hormone receptor proteins may have on DNA conformation upon binding. For this purpose simulations of the DNA binding domain of the glucocorticoid receptor (GR-DBD) dimer complexed with a consensus and a non-consensus response element have been conducted. A simulation of the uncomplexed consensus response element has also been conducted as a control. The structures used for the simulations are based on the crystal structure of the GR-DBD complexed with a non-consensus DNA segment (Luisi et al. (1991) **Nature 352**, 497-505). Each of the structures simulated has been solvated with an ellipsoidal shell of water, so that the total number of atoms for each protein-DNA system is approximately 13,500. Energy minimization, equilibration and dynamics have been conducted for each system. Analysis of the protein-protein and protein-DNA interactions reveal that interaction with a consensus DNA sequence is more favorable, as expected. Significant, protein-DNA interactions involving the amino acids gly458, ser459 and phe463 and protein-protein interactions involving the amino acid arg488 were observed in the simulations which were not reported earlier (Numbering based on rat-GR). DNA helical parameters have also been evaluated from the simulations and indicate that the dimer induces a bent, approximately 35°, and underwound conformation, approximately 11.2 bp/turn.

BILAYERS/BINDING

W-Pos253

A MITOCHONDRIAL PRESEQUENCE IN PHOSPHOLIPID BILAYERS: THE TOPOLOGY AND ENERGETICS OF BINDING.

((T. E. Thorgeirsson, Y. G. Yu, and Y.-K. Shin)) Department of Chemistry and Lawrence Berkeley Laboratory, University of California, Berkeley, CA 94720.

Cysteine-substituted variants of a 25-residue peptide derived from the presequence for subunit IV of yeast cytochrome c oxidase were synthesized and modified with a nitroxide spin label. The immersion depth and orientation of the peptide in phospholipid bilayers was studied using Electron Paramagnetic Resonance (EPR) collisional relaxation methods. The data suggest that the presequence is located at the interface of the head-group and acyl-chain regions such that the hydrophobic side chains are solvated by the acyl chains but the charges located at the surface of the bilayer. The equilibrium partitioning of the spin labeled peptides into negatively charged lipid vesicles was also studied using EPR. The apparent partition constant is found to be an explicit function of the membrane surface potential (Ψ) calculated from Gouy-Chapman-Stern theory. At low Ψ (< 0.5 RT/F) the partition equilibrium is described by the linear dependence of the transfer free energy ΔG^{el} on Ψ with the slope equal to the full charge of the peptide, but deviations from the ideal limiting behavior are observed at high Ψ.

W-Pos254

BINDING AND LOCALIZATION OF DIPYRIDAMOLE MOLECULES IN IONIC MICELLES: EFFECT OF MICELLE AND DRUG CHARGES.

((Christiane P.F.Borges, Iourii E.Borissevitch and Marcel Tabak)). Instituto de Quimica de Sao Carlos-USP, Cx.Postal 369, 13560-970, Sao Carlos-SP, Brasil.

Interaction of the coronary vasodilator dipyridamole (DIP) with micelles of cationic (CTAC), anionic (SDS) and zwitterionic (HPS and LPC) has been studied by fluorescence spectroscopy. Difference in quantum yields for the neutral and charged (protonated) drug allows to determine the pK_a, pK_a shift and ΔpK_a due to interaction with micelles. Change of fluorescence emission upon binding allows to obtain the association constants (K_b) of both protonated and neutral forms of the drug. K_b for the neutral form in all types of micelles are in the range $(1\text{-}7)*10^3$. For protonated DIP K_b decreases for CTAC, HPS and LPC due to electrostatic repulsion between the protonated DIP molecule and positive charges of micelles. For SDS K_b increases due to attraction of the drug to negative charges at the micelle surface.The localization of DIP in micelles was investigated using fluorescence quenching by acrylamide, iodide and quenchers with known localization in the micelle (TEMPO and spin labeled 5-doxyl and 12-doxyl stearic acids). The DIP molecules in both protonated and nonprotonated forms are localized in the micelles near the region which separates their polar and nonpolar parts, so that its polarizable heteroaromatic cycle is placed close to the polar part and the nonpolar substituents are included in the hydrophobic interior of the micelle. The electrostatic interaction between the protonated DIP molecules and the micelle charges either moves DIP into the micelle interior (for cationic and zwitterionic micelles) or draws it closer to the micelle surface (for the anionic one).

Support: CNPq, FINEP and FAPESP.

W-Pos255

BILAYER AND OCTANOL PARTITIONING OF A COMPLETE SET OF HYDROPHOBIC HOST-GUEST PENTAPEPTIDES.

((William C. Wimley and Stephen H. White)) Department of Physiology and Biophysics, University of California, Irvine, 92717-4560.

A proper hydrophobicity scale is of fundamental importance for understanding protein folding in membranes. We therefore synthesized a set of 20 host-guest peptides of the form AcWLXLL, where X is any of the natural amino acids, and measured the partitioning of each (25°C, pH 7.0) into phosphatidylcholine bilayers and into octanol in order to measure such a scale. These data provide (1) a complete interfacial hydrophobicity scale[1] for bilayer partitioning of peptides and (2) a water-octanol hydrophobicity scale for the amino acids in the context of a peptide rather than a model amino acid. The X-residue contributions to the free energy of water-octanol partitioning for the pentapeptides are very similar to those measured by Fauchere and Pliska for N-acetyl amino acid amides[2]. Relative to the glycine pentapeptide, the contribution of the other amino acids to the free energy of bilayer partitioning fall into 5 broad categories: ***asp*** and ***glu*** are very unfavorable (+1-2 kcal/mol); ***asn***, ***gln***, ***pro***, ***lys***, and ***arg*** are slightly unfavorable (~+0.4 kcal/mol); ***ala***, ***ser***, ***thr***, ***his***, and ***val*** are equal to glycine (± 0.2 kcal/mol); ***met***, ***leu***, and ***ile*** are slightly more favorable (~-0.4 kcal/mol); and the aromatic amino acids, ***tyr***, ***phe*** and ***trp***, are much more favorable (-1-2 kcal/mol). Except for the acidic and aromatic amino acids, the octanol and bilayer free energy contributions are not strongly related to each other in a simple way. The apparent cost of burying polar side chains in the bilayer interface is small, and the contribution of the aliphatic side chains is also smaller than it is for octanol partitioning. Although the hydrophobic effect must play a central role in the bilayer partitioning of peptides, these results indicate that the "bilayer effect" contribution is significant and that the bilayer interface is not well modeled by bulk solvents such as octanol. Supported by NIH (GM 46823).

[1]Jacobs, RE and White, SH (1989) *Biochemistry* **28**:3421-3437
[2]Fauchere J and Pliska V (1983) *Eur J Med Chem* **18**:369-375.

W-Pos256

DETERMINATION OF 1:1 AND 1:2 DIVALENT CATION TO PS BINDING PARAMETERS FROM ELECTROPHORESIS DATA

((Suren A. Tatulian)) Dept. of Mol. Physiology and Biol. Physics, University of Virginia School of Medicine, Box 449, Charlottesville, VA 22908

Electrostatic considerations predict that the binding of divalent cations to singly charged acidic lipids is likely to proceed with a 1:2 ion-to-lipid stoichiometry, but the fact that divalent cations at ~ 0.1 M concentrations reverse the sign of the negative surface potential of membranes provides evidence for 1:1 stoichiometry. In this work, analytic expressions are obtained for 1:1 and 1:2 binding constants and for the fractions of corresponding complexes based on extensions of the Gouy-Chapman-Stern theory and of Cohen-Cohen theory (Cohen, J.A., Cohen, M., 1981, Biophys. J. 36, 623). This approach relies on the ion concentration and the slope of the surface potential vs concentration curve at the charge reversal point. Application of this theory to previously published electrophoresis data on PS vesicles (McLaughlin, S., Mulrine, N., Gresalfi, T., Vaio, G., McLaughlin, A., 1981, J. Gen. Physiol. 77, 445), varying the thickness of the shearing layer (δ) from 0 to 2 Å, showed that a) the 1:1 binding constants (K_{11}) do not depend on δ and are similar to those determined in the original paper; b) the 1:2 binding constants are extremely sensitive to δ: K_{12} ≈ 25, 85, 110, 190 M^{-1} at δ = 0 and 2, 3, 5, 10 M^{-1} at δ = 2 Å for Mg^{2+}, Ca^{2+}, Sr^{2+}, Ba^{2+}, respectively; c) the fraction of 1:2 complexes also dramatically depends on δ: θ ≈ 0.60, 0.73, 0.74, 0.77 at δ = 0 and 0.22, 0.21, 0.26, 0.32 at δ = 2 Å for the above sequence of ions. These results imply that the thickness of the shearing layer is a critical parameter for which the exact value is required to gain information on the ion binding mechanism from electrophoresis data. The present theory may be applied to experimental results on surface potential vs concentration curves obtained by other methods.

W-Pos257

ADSORPTION AND ADHESION AT VESICLE SURFACES: THE INFLUENCE OF GRAFTED POLYMER ON AVIDIN-BIOTIN BINDING AND TESTS OF RECEPTOR-MEDIATED ADHESION (Doris A. Noppl and David Needham) Department of Mechanical Engineering and Materials Science, Duke University, Durham, NC 27705

Receptor-mediated adhesion is a very important process in biology. Many scientists have focused on both theoretical and experimental aspects of cell adhesion. However most theories consider simplified model systems that can only partly be applied to living cells. In order to create a model system that is more closely related to the documented theoretical models, specific adhesion was studied between lipid vesicles via avidin-biotin receptors. Micropipette techniques were used to examine the adhesion between individual vesicles that were otherwise non-adherent due to the co-incorporation of polyethyleneglycol lipids (PEG-lipids). In this way it was shown that certain characteristics of specific adhesion, e.g., spreading behavior, receptor accumulation and the influence of surface grafted polymer, can be explained thoroughly by mechanic and thermodynamic principles in the absence of cell metabolism. By measuring the spreading energy of the confined receptors in the contact zone the rate of accumulation of receptors in the zone was determined. Therefore it was possible to estimate the diffusion coefficient of avidin bound to biotinylated lipids in a lipid membrane to be on the same order of the lipid diffusion coefficient of 10^{-8} cm^2/s.

In the adsorption experiments the binding of avidin to biotinylated vesicles with incorporated PEG^{750}-lipid (M_W 750 g/mol) was characterized. Fluorescently labeled avidin, epifluorescence microscopy and image processing methods were used to quantify the amount of avidin bound to a biotinylated vesicle during incubation in avidin solution. The influence of incubation time and PEG-lipid concentration was determined. 2 mol% PEG-lipid reduced the binding rate to 50% of control (no PEG lipid). The results suggest that the additional surface pressure of PEG provides an energy barrier to binding while diffusion of avidin to the surface is largely responsible for the time dependence.

W-Pos258

SYNTHESIS AND STABILITY CONSTANT OF THE COPPER COMPLEX OF AN AZAMACROCYCLE SURFACTANT. ((Dhananjay B. Puranik[b], Alok Singh*[a], Kenneth M. Jones[b,c], Eddie L. Chang,*[a])) [a]Naval Research Laboratory, Washington D.C. 20375, U.S.A., [b]Department of Biochemistry and Molecular Biology, Georgetown University, Washington D.C. 20007.

We are interested in the effects of metal chelation on mixed surfactant systems. For this purpose, the 1-hexadecyl-1,4,8,11-tetraazacyclotetra- decane (N-cetyl cyclam) surfactant and its copper(II) complex were prepared. The choice of cyclam as the parent metal chelating moiety was based on the highly stable metal complexes cyclam forms. However, there have been no reported values for the protonation and stability constants of the N-alkylated cyclams. We have titrated the tetrahydrochloride of N-cetyl cyclam with NaOH both in the absence and presence of Cu(II) ions. Titration-curve data were used to determine analytically the protonation and stability constants of the lipid. The results were checked with HYPERQUAD, a program designed for calculating equilibrium constants in solution. The dispersive properties of N-cetyl cyclam were also studied.

W-Pos259

INTERACTIONS OF LIPOSOMES WITH NOVEL FREE RADICAL SCAVENGERS. ((C.S. Randall and H.-Y. Cheng)) SmithKline Beecham Pharmaceuticals, King of Prussia, PA 19406

Carvedilol, a new vasodilator and ß-adrenoreceptor blocker, has recently been shown to be a potent inhibitor of lipid peroxidation, apparently by acting as a scavenger of free radicals. This property, which has been linked to the drug's carbazole moiety, is distinct from other ß-blockers and may contribute to carvedilol's unique cardioprotective effects. To probe the relationship between antioxidant activity, drug structure, and cell membrane permeability, fluorescence spectroscopy and differential scanning calorimetry (DSC) were applied using liposomes as model membrane systems. Carvedilol fluorescence was markedly shifted to lower wavelength in the presence of liposomes and also less sensitive to quenching agents, suggestive of a more hydrophobic environment. In DSC studies, carvedilol and structurally related analogs exhibited characteristic concentration-dependent perturbing effects on liposome thermal behavior, consistent with increased membrane fluidization involving the polar head groups of the liposome as well as the interior hydrophobic portion. The degree of association is sensitive to drug structure; the carbazole moiety is important, but may not be the sole determinant for optimal membrane interaction.

W-Pos260

FABRICATION OF VECTORIALLY ORIENTED CYTOCHROME OXIDASE MONOLAYERS TETHERED TO INORGANIC SUBSTRATES. ((J.A. Chupa, J.P. McCauley, Jr., R.M. Strongin, A.B. Smith, III, J.K. Blasie*; L.J. Peticolas and J.C. Bean**)) *Department of Chemistry, University of Pennsylvania, Philadelphia, PA 19104 and ** AT&T Bell Laboratories, Murray Hill, NJ 07974. (Spon. by J.A. Chupa)

We have developed a systematic methodology for constructing model membrane systems which possess the asymmetry of vectorially oriented membrane proteins inherent in natural membranes. Bifunctional organic chain molecules in the form of self-assembled monolayers (SAMs) are utilized to tether both soluble and detergent solubilized membrane proteins to the surface of Ge/Si multilayer substrates. The periodic nature of these substrates enable novel interferometry and holography techniques to be employed to determine the profile structure of the tethered protein monolayer. The utility of these methods has been demonstrated previously for a peripheral and an integral membrane protein whose three-dimensional structures were independently known to atomic resolution (Chupa *et al.*, 1994, *Biophys. J.* 67:336). We have extended this approach to the integral membrane protein, cytochrome oxidase, whose three-dimensional structure is currently known to only ~20 Å resolution. Structural studies confirmed the formation of a vectorially oriented single monolayer of protein tethered to the surface of an amine-terminated SAM. In addition, optical absorption measurements were consistent with the x-ray diffraction results indicating the reversible formation of a densely packed single monolayer of fully functional protein on the surface of the SAM. This work precedes more detailed future structural studies employing polarized x-ray spectroscopy and resonance x-ray diffraction of the protein's redox centers.

W-Pos261

MODULATION OF MEMBRANE ADHESION BY SPECIFIC AND NONSPECIFIC INTERACTIONS. ((T. J. Feder, G. Weissmüller, B. Žekš and E. Sackmann)) Biophys. Laboratory E22, Physics Dept., Technische Universität München, D-85747 Garching, Germany.

Nonspecific and specific adhesion of phospholipid membranes to solid surfaces is investigated. We use giant phospholipid vesicles as cell models, and control the strength and specificity of the membrane-substrate interaction using biofunctionalized surfaces, and by varying conditions such as the buffer, temperature, and osmolarity. Neutral phospholipid membranes (DMPC, EggPC) exhibit fairly strong nonspecific adhesion to avidin surfaces. They adhere, but do not burst, and finger-like spreading, similar to some cell motions, is observed. For specific adhesion, we incorporate various biotinylated lipids into the vesicles, and coat the surface with streptavidin. Strong adhesion, with localized contact sites, is observed. The interaction is investigated as a function of ligand-receptor concentration and affinity. We observe the contact dynamics, and reconstruct cross-sectional profiles using reflection interference contrast microscopy, which exploits thin film interference and allows for sensitive measurement of sample-substrate separation distances.

W-Pos262

THE EFFECTS OF BERYLLIUM ON THE ELECTROSTATIC AND THERMODYNAMIC PROPERTIES OF THE LIPID MEMBRANES ((Yu.A.Ermakov, A.Z.Averbach, V.I.Lobyshev)), A.N.Frumkin Institute of Electrochemistry RAS, Leninsky pr.31, Moscow 117071, Russia

Adsorption of Be at the lipid membranes was studied by the method of the inner membranous field compensation sensitive to total boundary potential changes and applied to planar lipid membranes (BLM), and by electrophoretic measurements sensitive to surface component of this potential. Both methods show the similar potential changes corresponding to Be association constant about two orders higher than for Mg. Zeta potentials of DPPC liposomes below phase transition temperature are more positive than above and give the association constant about 20 times higher. This fact disagrees with potential changes of opposite sign observed at phase transition of planar BLM from DPPC. The separation of lipids between two pools was observed by differential scanning calorymetry in the presence of Be. One pool has the ethalpy proportional to surface area occupied by cation and the phase transition temperature depending on its concentration. Data obtained in heavy and normal water solutions reveals the clear isotopic effect. It support the idea that the cation adsorption is accompanied by rehydration processes and some structural changes at the membrane surface.

W-Pos263

POLYCATION ADSORPTION ON THE SURFACE OF LIPID MEMBRANES STUDIED BY ELECTROKINETIC AND THERMODYNAMIC METHODS ((Yu.A.Ermakov, A.A.Yaroslavov, A.A.Efimova)) A.N.Frumkin Institute of Electrochemistry RAS, Moscow State University, Moscow, Russia

Quasi-elastic light scattering spectroscopy and differential scanning calorimetry of liposomes and techniques of planar lipid membranes were applied to study the role of structural factors in surface electrostatic and thermodynamic effects induced by adsorption of charged synthetic polycations. There are some evidence obtained about the separation of acid and zwitterionic components in lipid mixture in the presence of large polycations. As it follows from zeta-potential and particle size measurements in liposome suspension and from different procedures of boundary potential measurements in planar bilayers the adsorption of macromolecules is irreversible depending on the presence of acid lipids and on the phase state of lipid bilayers. Some speculations on the structure of lipid/polymer complexes were made.

W-Pos264

EFFECTS OF PEG ON LIPID MONO-AND BILAYERS

((M. Winterhalter, H. Bürner, M. Käsbauer, C. Andersen, D.D. Lasic and R. Benz)) Biotechnologie, Am Hubland, D-97 074 Würzburg, Germany.

We investigated the effect of polyethylene glycol (PEG) on lipid mono-and bilayers. The PEG was either added to the aqueous solution or was covalently bonded to lipids. In a first series we measured the surface pressure and surface potential of lipid monolayers in presence of various amounts of PEG either applied on the surface or dissolved in the aqueous subphase. These results were compared with experiments using covalently bonded PEG. It was found that both experiments yielded similar results. Furthermore PEG is surface active and buildt in the air/water interface up to surface pressures of about 10 mN/m. At larger surface pressures the PEG is squeezed out. Depending on the lipid PEG shows an ordering effect. In a second series of experiments we measured the influence of PEG on the transport properties. We used the translocation of lipophilic ions to probe the effect of PEG on the intrinsic potential barrier. In a third series we revisited the influence of PEG on the fusion properties of liposomes.

* this work was supported by grants of the DFG

W-Pos265

ADSORPTION OF 9-AMINOACRIDINE TO CHROMATOPHORE MEMBRANES AND MODELLING OF THE PROBE RESPONSE TO ARTIFICIALLY INDUCED TRANSMEBRANE ΔpH. ((R.Casadio and S. Di Bernardo)) Lab. of Biophysics, Dept. of Biology, University of Bologna, I-40126 Bologna, Italy.

Adsorption of the fluorescent probe 9-aminoacridine onto photosynthetic chromatophores is determined at equilibrium with a microdialyzer at low (.005 M) and high (.150 M) ionic strengths and at different pH values in the range from 5.5 to 8.5. It is found that the probe-membrane interaction can be described by a single sigmoid function of the Hill type provided that electrostatic effects are accounted for with the Gouy-Chapman theory for the diffusive double layer. Two different surface charge densities for the chromatophore membrane are consistent with the data: about 0.5 and 1.3×10^{-3} $e^-/Å^2$ in the region of acidic and alkaline pH values, respectively. By considering equilibrium distribution of the amine in the presence of a ΔpH, modelling of the experimental relationship between artificially induced ΔpHs of known extents and the observed quenching of fluorescence is obtained when the free probe concentration in the inner and outer bulk compartments is evaluated from the adsorption isotherms determined at the different pH values.

W-Pos266

SORPTION OF UN-IONIZED AND IONIZED PENTACHLOROPHENOL TO EGG-PC BILAYER. A COMPARISON WITH OCTANOL-WATER PARTITION. ((Shanru Wang and Pavel Smejtek)) Dept. of Physics and Environmental Sciences and Resources Doctoral Program, Portland State University, Portland, Oregon 97207

Octanol-water partition coefficients, K_{ow}, play important role in understanding and predicting distribution of toxic chemicals in environment. K_{ow} has been used to characterize the distribution of toxics in biota, sediments, and soils. Pentachlorophenol (PCP) is a highly potent and hard-to-degrade uncoupler used as wood preservitive and as herbicide. Its $K_{ow} = 1.3 \times 10^5$ and $pK_a = 4.85$. We have studied sorption of un-ionized and ionized PCP between egg-PC membranes and water by measuring aqueous concentration of PCP in the presence and absence of liposomes and ζ-potential of liposomes. We show that the distribution isotherms for both species of PCP can be described by Langmuir-Stern-Grahame model. From the fit of the model to the data we obtained the linear partition coefficients, β_m and the membrane adsorption site area, P_s. The volume partition coefficient $\gamma_m = 2\beta_m/t$ (t = thickness of membrane core) can be compared to K_{ow}.

While partition into octanol and sorption into lipid membrane are similar for un-ionized species, the sorption of ionized species to mebrane is about 500 times greater than predicted from K_{ow}.

Supported in part by NIH (ES0502) and by NSF (CTS-9316026).

PCP	Un-ionized	Ionized
β_m, (μm)	550	30
γ_m	290,000	16,000
P_s, (nm^2)	0.6	3.5
K_{ow}	130,000	30

W-Pos267

ADSORPTION OF RUTHENIUM RED TO PHOSPHOLIPID BILAYERS. ((D. Völker and P. Smejtek)) Dept. of Physics, Portland State University, Portland, Oregon 97207

In addition to its staining properties, Ruthenium Red (RR), is a potent modulator of membrane activity due to its affinity to numerous Ca^{+2}-binding proteins. In aqueous solutions RR is present as an hexavalent cation

$$[(NH_3)_5 Ru^{III}-O-(NH_3)_4 Ru^{IV}-O-Ru^{III}(NH_3)_5]^{+6}$$

We have studied adsorption of RR to liposomes by means of spectrophotometric assays. Five freez-and-thaw cycles to achieve equilibration of RR and ultracentrifugation for the removal of liposomes from the suspension. We present RR distribution isotherms (pH = 7.3) for PC/PS, PC/PI and PC/PG liposomes as a function of surface charge density (lipid ratios 20:1, 10:1, 5:1) and lipid concentration in the suspension (0.3, 3 and 10 mg/ml). The distribution isotherms can be reproduced with Langmuir-Stern-Grahame adsorption model. Within the framework of this model RR behaves as a cation with effective charge $q_m < 6$. q_{eff} was found to be a function of membrane surface charge density. q_{eff} was highest ($\approx 5.2 \pm 1$) for liposomes with lowest charge density. q_{eff} was lowest ($\approx 3.2 \pm 0.1$) for the highest charge density. The intrinsic adsorption constant (for 10:1 membranes) of RR, K_m, and q_{eff} are given in the Table. These results make it possible to estimate RR binding to lipid matrix of biomembranes.

	PC:PS	PC:PI	PC:PG
q_{eff}, (e)	4.1 ± 0.4	4.0 ± 0.3	3.9 ± 0.2
K_m, (M^{-1})	2.2 ± 1.1	0.66 ± 0.2	0.80 ± 0.2